Structural Changes Accompanying Intramolecular Electron Transfer: Focus on Twisted Intramolecular Charge-Transfer States and Structures

Zbigniew R. Grabowski*,† and Krystyna Rotkiewicz†,‡

Institute of Physical Chemistry, Polish Academy of Sciences, Warsaw, Poland, and Institute of Chemistry, Akademia Świętokrzyska, Chęcińska 5, 25-020 Kielce, Poland

Wolfgang Rettig*

Institute of Chemistry, Humboldt University, Brook-Taylor-Strasse 2, D-12489 Berlin, Germany

Received June 20, 2001

Contents

* To whom correspondence should be addressed. E-mail: Z.R.G., zrgrab@ichf.edu.pl; W.R., rettig@chemie.hu-berlin.de.
† Polish Academy of Sciences.
‡ Akademia Świętokrzyska.

10.1021/cr940745l CCC: $44.00
Published on Web 09/17/2003

I. Introduction

A. Object and Scope of the Review

Electron-transfer (ET) reactions, between separate molecules (intermolecular) or between distinct re-

Zbigniew Ryszard Grabowski was born 1927 (original prewar name Ryszard Abrahamer). Under the German occupation he was self-taught while in hiding. He took part in the Warsaw uprising in 1944, and was then enjailed in Nazi prisons and camps. From 1945 to 1950, he studied chemistry at Warsaw University; he spent 1947–1962 in research and teaching, obtaining his Ph.D. in 1955 with Prof. Wiktor Kemula, and then in the Institute of Physical Chemisty, Polish Academy of Science, as full professor and head of the Photochemistry & Spectroscopy Department. He studied as a post-doc with A. N. Frumkin in Moscow and as a Rockefeller Fellow with Th. Förster in Stuttgart. He is a cofounder of the College of Science in Warsaw, 1993. He retired in 1998, and now works part-time in research. He was married in 1953 to Anna, who is now also a professor of physical chemistry. He has two children, Urszula, an artist-paintress, and Jan, a historian at the University of Ottawa. His early research was in electrode kinetics and stereochemistry of electrode processes. He discovered the electric field strength effects on the mechanisms of electrode reactions. He paid special attention to reactive intermediates: free radicals and uncommon tautomers, and their reactivities in electron and proton transfers. In cooperation with J. Koszewski (electronics) and J. Jasny (optics), he developed a series of new instruments for time-resolved spectroscopy. A major part of his activity was devoted to investigation of luminescence, structures, kinetics, and reactivities of polyatomic organic molecules in their electronically excited states. He studied acid–base equilibria in excited states and general spectral thermodynamic (and extra-thermodynamic) rules as applied to the excited-state reactions (*generalized Förster cycles*). He recognized (with K. Rotkiewicz) the dual fluorescence of some flexible donor–acceptor molecules as connected with structural changes in their charge-transfer states. He coined the term of the TICT excited states. An interest in chemical evolution led him to the study of reactions which seem to occur in the interstellar matter: the photochemistry of cyanoacetylenes. In 1971–1972, he was an Overseas Fellow of the Churchill College, Cambridge. He was an invited professor in 1958 at the University of Moscow, in 1986 at the Universités Romandes en Suisse (Fribourg, Lausanne), Université Paris Sud, Orsay; in 1987 at the Université de Bordeaux I, Talence; in 1988 at the Institute for Molecular Science, Okazaki; in 1989 at Kathol. Universiteit Leuven; in 1976 as the Theodor Förster Memorial Lecturer, European Photochemistry Association. In 1980 he received the Marie Skłodowska-Curie Award, Polish Academy of Sciences; in 1990 the J. Śniadecki medal, Polish Chemistry Society; in 1992 the A. Jurzykowski Foundation (New York) Award for Chemistry; in 1993 Dr. h.c., University de Fribourg (Suisse); in 1994 the Polish Science Foundation Annual Award in Science; in 1997 the Medal of the Institute of Physical Chemistry, Polish Academy of Sciences. He is an elected member of the German Academy of Sciences "Leopoldina"; Learned Society of Warsaw; Polish Academy of Sciences (1983; election for 6 years not accepted by the communist authorities, for political reasons). He is an honorary member of the Polish Chemistry Society. From 1980 to 1990, he was a member of the "Solidarity" trade union, active also when it was illegal. He was a cofounder in 1980 of the Society for the Advancement of Sciences and Arts (independent Polish assocation of scholars, 1982–1989 delegalized); from 1980to 1992 he was chairman of the Council, and from 1992to 1995 he was president of the Society. He is a member of the European Photochemistry Association, the Holocaust Children Association, and the Association of Jewish Combattants of Second Word War. He is a long-term member of the editorial boards of the popular scientific journal *Problemy*, *Chemical Physics Letters*, *Journal of Luminescence*, *Nouveau Journal de Chimie* (*New Journal of Chemistry*), and *Journal of Fluorescence*.

Krystyna Rotkiewicz (born in 1936 in Warsaw, maiden name Suchocka) studied chemistry from 1953 to 1959 at the Technical University in Warsaw. She obtained her Ph.D. in 1968, under the supervision of Prof. Z. R. Grabowski. She was a fellow of the Alexander von Humboldt Foundation 1970–1971 at the Max Planck Institute of Biophysical Chemistry in Goettingen; in 1977 (one month) at the Institute of Physical Chemistry, University of Mainz; in 1982–1983 (three months) at the Institute of Organic Chemistry, Technical University, Aachen; in 1990 (one month) in the Institute of Physical and Theoretical Chemistry, Technical University, Berlin. Since 1968, she has been an associate professor at Institute of Physical Chemistry, Polish Academy of Sciences, and since 1994 she has been a university professor (since 2001 full professor) and head of the Chemical Physics Department, Pedagogical University in Kielce (since 2000 new name: Świętokrzyska Academy). She is married to Piotr Rotkiewicz and has two sons, Wojciech, a biologist, and Marcin, a journalist. She started her research with syntheses of aromatic amines, dyes, and studies on water pollution. Her Ph.D. thesis focused on the excited states of aromatic amines. In Goettingen she studied the solvent isotope effect in 4-(*N*,*N*-dimethylamino)benzonitrile (DMABN); these studies were continued later in Warsaw and led, in cooperation with Prof. Z. R. Grabowski, to distinguishing a new class of CT states, the TICT excited states. Her current interests include the photoinduced electron tarnsfer in large π-electronic electron donor–acceptor systems, photochemistry of aromatic amines (identification of amine carbene), and supramolecular complexes of aromatic compounds. She has been in cooperation with the Institute of Theoretical Chemistry and Radiation Chemistry, University of Vienna, since 1979; with the Institute of Physical and Theoretical Chemistry, Technical University Berlin, 1983–1990; with the Institute of Chemistry, Humboldt University, Berlin, since 1990; and with the Research Institute for Extreme Materials, University of Osaka and the Institute of Technology in Kyoto, 1994–2000. She is a member of the Polish Chemistry Society, European Photochemistry Assocation, Societas Humboldtiana Polonorum; since 1980 "Solidarity" trade union (1981–1989 illegal; chairman of "Solidarity" in the Institute of Physical Chemistry, 1991–1994). She is the recipient of awards from the Secretary of the Polish Academy of Sciences in 1975 and 1979, and in 1997 the Silver Cross of Merit.

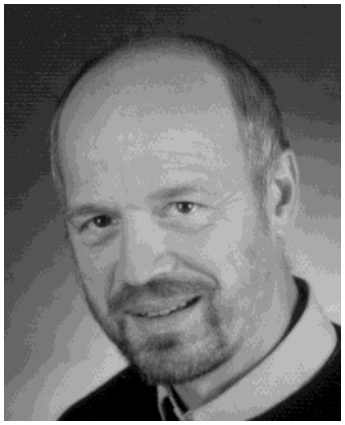

Wolfgang Rettig (born 1947, married, two children) studied chemistry in Stuttgart, Paris, and Basel, where he got his Ph.D. in photochemistry in 1976, under the guidance of Prof. J. Wirz. He was a post-doc in Reading, England, studying gas-phase kinetics with Prof. H. M. Frey. He worked in research and teaching at the Technical University Berlin (1977–1993) as a group leader and associate professor since 1988. He worked with Prof. E. Lippert on the dual fluorescence of acceptor anilines, especially with time-resolved fluorescence using synchrotron radiation. His work widened the field of compounds with anomalous fluorescence properies linked with intramolecular twisting. Since 1993, he has been full professor in Physical Chemistry at the Humboldt University Berlin. He spent research stays in Nottingham, England (1987), Göttingen (1988), Jerusalem (1999), and Bordeaux (1999), which were aimed at enlarging the range of methods applied to this subject (supersonic jet, picosecond time-resolved absorption and fluorescence, high-pressure studies). His research interests include mechanisms of photochemical primary processes (electron and proton transfer; trans–cis and valence isomerizations; visual process); ultrafast fluorescence and absorption spectroscopy; solvation of excited states; quantum-chemical modeling of photoreactions; fluorescence probes for biology, medicine, and analytical chemistry; and fluorescence polymer probing. He is a fellow of the Cusanuswerk and the Deutscher Akademischer Austauschdienst (1972–1976), and a Heisenberg-fellow (1984–1989). He received the Grammaticakis-Neumann prize in photochemistry in 1990 (Swiss Society for Photochemistry and Photophysics), and an honorary medal of the Institute of Physical Chemistry of the Polish Academy of Sciences, Warsaw (1996). He served as chairman of the 5th International Conference on Methods and Applications of Fluorescence Spectroscopy, Berlin, 1997. He is a member of the editorial boards of *Journal of Fluorescence* and *Photochemical Photobiological Sciences*. He is a member of the Gesellschaft Deutscher Chemiker, Deutsche Bunsen-Gesellschaft, European Photochemistry Association, and Society of Fluorescence.

gions within the molecule (intramolecular), are some of the most frequently encountered photochemical primary processes. In such inter- or intramolecular processes, the reaction product is usually called a charge-transfer (CT) state, or an intramolecular CT state (ICT) or exciplex (note that all these terms are widely abused in the literature, applied to any state with somewhat increased dipole moment). The photoinitiated ET processes and the CT states play a fundamental role in photosynthesis in plants, and in numerous existing or conceived applications, e.g., in the molecular devices of future technologies. The interest focused on these excited states is therefore both cognitive and applied.

True ICT states often differ markedly from the parent ground states in their molecular structure (i.e., in both electronic structure and molecular geometry), provided the rigidity of the molecular skeleton is not too high. Initially, the structure of the excited molecules was identified mainly from experimental evidence. Subsequently, theory complemented the experiment and often went beyond it. The results, however, are often ambiguous and give rise to numerous controversies.

The aim of this review is to summarize, on the background of other types of ICT states, the experimental and theoretical findings concerning the excited-state structures of the much discussed compounds in which the electron donor (D**)** and the electron acceptor (A) moieties are linked by a formally single bond: the D−A molecules. In this case, the freedom to adapt the molecular geometry to a new electron density distribution is limited as compared to an *intermolecular* ET. Thirty years ago we formulated a structural hypothesis,[1] which came to be known as the twisted intramolecular charge transfer (TICT) model.[2,3] After the first general overview of the field,[4] the rapidly growing volume of literature has been extensively reviewed several times, with respect to

both the diversity of the compounds displaying similar behavior[5] and the physical phenomena involved.[6] Over the years, much new evidence and several mutually controversial hypotheses and quantum-chemical calculations[7−10] have been published. The TICT phenomena were found in, and the corresponding concepts applied to, many very different areas of pure and applied science. Along with well-substantiated papers, numerous other articles were published which attempted to assign very diverse findings to the TICT process. Further reviews have been published[11−13] covering, inter alia, the kinetic aspect of the phenomena. Since there is already a rich list of literature[14] far exceeding 1000 papers (prior to the beginning of the year 2002), it appears worthwhile to present an overview, mainly of those studies which contributed to the structural aspects of the CT excited states. Such a review is timely, as the discussion seemingly approaches its end with the insight recently gained into the excited-state structures and processes (the literature referred to mainly covers the period until the end of 2002).

A major part of this review (sections II−IX) concerns the most discussed compound, **1**, and its close derivatives and analogues (usually with only a single aromatic ring). The much broader class of biaromatic D−A molecules, with very different and often larger donor or acceptor units, is presented more concisely and only for some exemplary families of compounds (section XI). Sections XII (Charge Transfer Triplet State) and XIII (Conclusions and Open Questions) encompass both of the two main groups of compounds. The following section contains a glossary of abbreviations. A concise summary of the nearly 300 formulas mentioned in the text is available as Supporting Information, for easy reference.

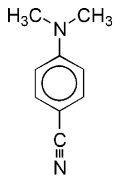

1

B. Excited-State Reactivity in Electron Transfer

Molecules in their excited states are characterized by the wave function, Ψ_e, which is different from that of the ground state, Ψ_g, and thus they differ in their electron density distributions. In his pioneering work on electronic spectra of molecules, Th. Förster[15] anticipated the high dipole moments of the excited states of otherwise (in their ground state) weakly polar molecules. He described a polar molecule (e.g., **1**, the molecule to be discussed at length in this review) by the superposition of two wave functions, that of a "normal" structure, Ψ_N, and that of a highly polar quinoid structure, Ψ_Q (eq 1, Scheme 1). Fun-

$$\Psi_g = c_N\Psi_N + c_Q\Psi_Q \qquad \Psi_e = c_Q\Psi_N - c_N\Psi_Q \quad (1)$$

damental changes in the electron density distribution have major consequences, e.g., for the acid−base properties and for other types of reactivities of the excited chemical species. Also, molecules in their electronically excited states quite generally display increased reactivities with respect to electron transfer, both as reducing agents (at least one electron in a high-energy orbital) and as oxidants (excitation of an electron generates a low-energy vacancy) (Figure 1). Therefore, electron-transfer (ET) reactions are the type most generally observed for excited species.

Being as a rule very fast, these reactions usually compete with radiative deactivation processes. Let us consider the case in which both reaction partners, D and A, are built into one molecule but barely interact (Figure 2). If an electron transfer from D to A is energetically feasible in the excited state, the product of such an intramolecular ET reaction is a charge-separated species, $D^+\cdots A^-$. Its electronic struc-

Scheme 1. Mesomeric Structures of Benzene Para-Substituted with a Donor and an Acceptor: (a) the "Normal" and (b) the Highly Dipolar Quinoid Canonical Structures[a]

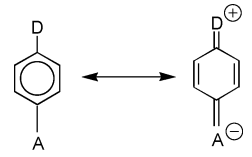

a **b**

[a] In an excited state, a reversal of the polarity contributions was expected; see eq 1.[16]

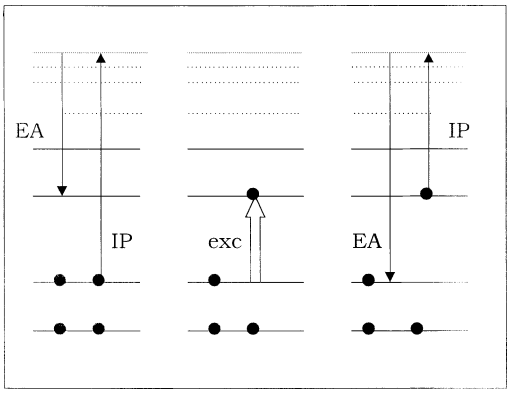

Figure 1. Simple orbital scheme of the processes involved: IP, ionization potential; EA, electron affinity; exc, excitation. Left, ground state; middle, excitation; right, excited state.

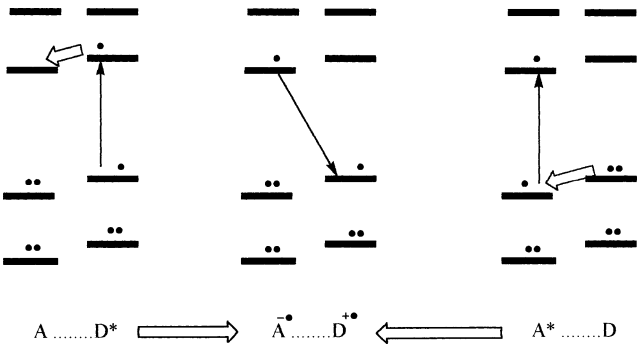

Figure 2. Scheme of the photoinduced electron transfer between nearly non-interacting D and A. On excitation of either D or A, the same CT state is formed; its fluorescence — a radiative ET — is indicated by the arrow in the middle.

ture corresponds to the *ground state* of the free radical ion pair of opposite charges, consisting of a radical cation D^+ and radical anion A^-. We shall call it the *pure electron-transfer* (ET) state, as defined by its zero-order wave function:

$$\Psi_{CT} = \Psi_{D^+}\Psi_{A^-} \quad (2)$$

A relaxation process, accompanying or following the electron transfer, adapts the molecular structure, and often the structure of the environment as well, to the new electron density distribution and to the new intra- and intermolecular interactions. Among so-called "bichromophoric" systems, there are many which have a rather rigid system of bonds, e.g., **2**,[17] **3**, and **4**.[18] The change of the *electronic* structure, and the reorganization of the adjacent solvent layers, does not appear to be accompanied by any major modifications of their *molecular* structure.

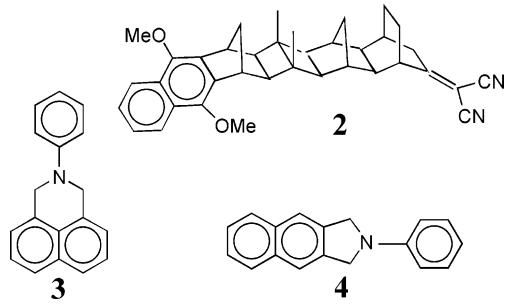

In the cases **2**−**4**, the distance of the separated charges and the presence of saturated ("insulating") bridges seem to be responsible for the near-noninteraction of the D^+ and A^- subsystems. In contrast, for more or less flexible D−A molecules, several often opposing forces determine the resulting structure of the excited state. The structural changes occurring in the CT states can be roughly divided into

(i) those arising from the one-electron oxidation of D, and the one-electron reduction of A, as reported briefly in the next section; and

(ii) those appearing in the mutual conformation of D^+ and A^- when compared to the parent D−A molecule, as reported in the subsequent sections.

C. Structural Changes Due to One-Electron Gain or Loss

Molecules usually undergo significant modifications of their structure when losing or gaining an electron. In small molecules, the changes of the structure upon one-electron oxidation or reduction are more prominent and easier to detect. These changes in the donor or acceptor moiety, e.g., pyramidalization or planarization, linearization, or bending, etc., often determine the structural relaxations of the CT excited states that are presently being reviewed. In an excellent but little known series of early papers by Walsh,[19] a very simple set of rules, based on elementary molecular orbital (MO) theory and qualitative deduction, were formulated. Walsh's rules can be used as a useful predictive tool in cases in which no experimental or theoretical data are

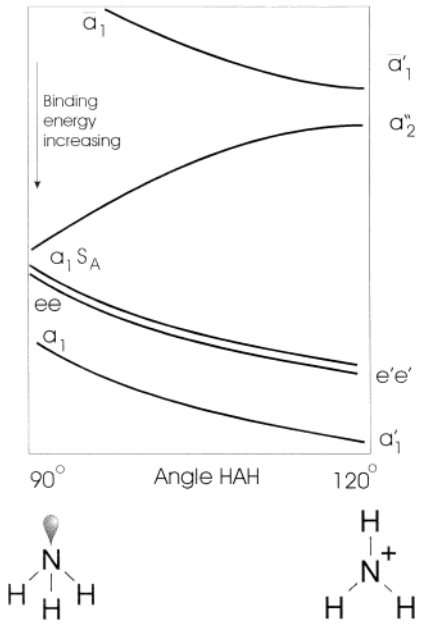

Figure 3. Walsh's rules for the AH_3 molecules[19d] applied to NH_3. Eight valence electrons occupy the four lowest orbitals: the three lowest (σ_{N-H}) tend to stabilize the planar (D_{3h}) structure, and the fourth (the lone pair, σ_A), strongly stabilizes the pyramidal structure, C_{3v}. Loss of one electron from this orbital favors the planarity of the radical cation $^{\bullet}NH_3^+$. Reproduced with permission from ref 19d. Copyright 1953 The Royal Society of Chemistry.

available. We shall not present the rules here and will limit ourselves to a few examples chosen from frequently encountered donor and acceptor groups.

The electron donors most frequently discussed in the present review are the aliphatic amines. The simplest of them, NH_3, is pyramidal in the ground state and is planar as the positive radical ion, changing the hybridization from sp^3 to sp^2 (Figure 3).[19d,20] Simple aliphatic amines behave similarly, e.g., $N(CH_3)_3$.[21] Even in the case of a cage amine with a rather rigid structure, like azabicyclooctane (ABCO), the structure of the positive radical ion can be approximated from the spectrum to that of the Rydberg excited state. The pyramidal arrangement of the bonds around the bridgehead nitrogen is considerably flattened in the lowest excited Rydberg state.[22] The flattening of amines on ionization is very important for the further discussion of the CT states.

Hydrazines, bent and twisted by about 90° in the neutral parent molecule, tend to coplanarity when oxidized to the radical monocation due to the formation of a three-electron bond (vide infra), which stabilizes the cation and prevents the twist.[22]

Certain molecular structures become unstable when ionized, and some bonds can be broken (Scheme 2).[23] Bond cleavage is also observed upon one-electron reduction, such as in numerous halogen derivatives or esters.[24] Such profound modifications of the molecular structure may also appear in the *intramolecular* CT excited states and deserve to be studied.

An important and peculiar class is presented by those radical cations which form an intramolecular three-electron bond. For example, some aliphatic diamines, after a single ionization, undergo a struc-

Scheme 2. Examples of Strained Ring Cleavage on Ionization in Some Three-Membered (5,[25] 7[26]) or Four-Membered Cycles (6[27])[a]

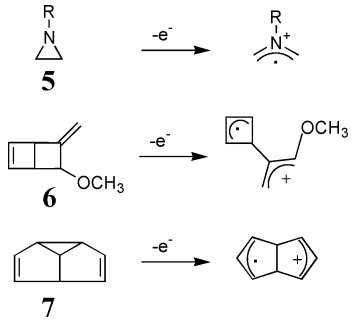

[a] Adapted with permission from ref 23. Copyright 1991 Kluwer Academic Publ.

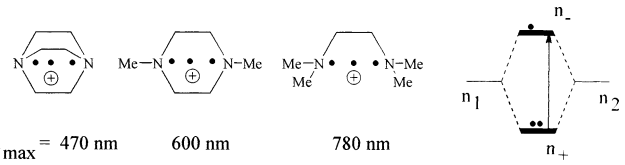

Figure 4. Radical cations of 1,3-diamines are often stabilized by a three-electron bond. Two interacting degenerate n_N orbitals (n_1 , n_2) split and form the doubly occupied n_+ and the singly occupied n_- orbitals (mixed, in fact, with the interacting σ orbitals), which is accompanied by a structural relaxation. Upon relaxation, the splitting increases and the lowest optical transition ($n_- \leftarrow n_+$) becomes stronger and shifts to shorter wavelengths.

tural relaxation to a new conformation stabilized by a three-electron bond,[28] manifested also by an absorption band in the visible range (Figure 4).[29−31]

The three-electron bond corresponds to either a *through-space* or a *through-bond* interaction of the *n*-orbitals. A thorough theoretical and experimental study of the cation radical **9**[32] led to the conclusion that its relaxed structure is mainly stabilized by through-bond interaction. This is in accord with the strengthening of the interaction and the blue shift of the absorption band in the visible due to the increasing number of ethylene bridges linking the two N atoms in **8**, **9**, and **10** (cf. Figure 4). The relaxed

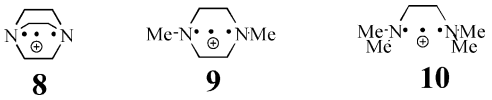

structure of the radical cation **9** is not yet definitely known. Instead of a boat structure with a minimal N−N distance, as expected for the through-space interaction, the through-bond mechanism favors a chair structure as the most stable conformation. In this particular case, the methyl substituents are in axial positions with the spin and charge delocalized between the two equivalent N atoms.[32,33] Three-electron bonds between two S atoms are especially stable.[34,35]

According to the Walsh rules but with a number of reported exceptions, for a one-electron reduction to a negative radical ion, the structural impact of one excess electron is most often similar to that for one-electron excitation. In both cases, usually the same orbital is singly occupied.[19a]

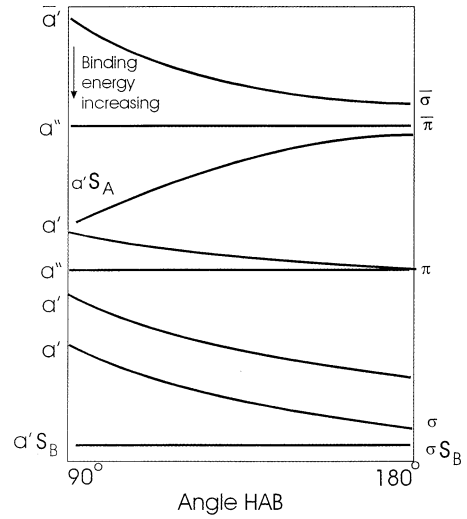

Figure 5. HCN, with its 10 valence electrons occupying the five lowest orbitals, is linear. Excitation or population by one electron of the sixth orbital, π_g* (a′S_A), bends the molecule.[19c] Reproduced with permission from ref 19c. Copyright 1953 The Royal Society of Chemistry.

The linear molecule HCN is bent in several of its lowest excited states as the lowest unoccupied MO strongly destabilizes the linearity.[19c] The same orbital becomes occupied upon one-electron reduction (Figure 5). The following early predictions are all supported by ample spectroscopic evidence.[36]

Acetylene, being isoelectronic to HCN with its 10 valence electrons, is linear in the ground state but should be bent when in an excited state or as a negative radical ion with 11 electrons.[19c] The lowest excited state is indeed trans-bent, in accord with the Walsh rules.[37]

Ethylene, planar in its ground state, becomes twisted by 90° in the lowest excited states and slightly pyramidal around each of the C atoms.[19i,38] The twisted excited singlet,[39] *resp.* triplet,[40] is the transition state in the cis−trans isomerizations and photoisomerization of the ethylene derivatives. From the same general rules, a twisted structure is expected for the ethylene anion radical, which is consistent with the mechanisms of catalysis of the thermal cis−trans isomerization. Similar structural changes are also expected wherever the positive or negative *charge becomes localized* within such a group in an intramolecular CT state.

D. Flexible Molecules

To approach qualitatively the structure of the lowest CT state of a polyatomic molecule which has some internal conformational flexibility,[41,42] it is good to start from a conformation with nearly non-interacting D^+ and A^- units, as depicted in Figure 2. To state this more precisely, *non-interacting* means having a zero or negligible overlap of the MOs of both moieties, either due to *symmetry*, by orthogonality of their π-electronic systems, or by a sufficient *distance* between the D and A. The forces exerted on such a *zero-order ET state* can be roughly divided into three components:

Scheme 3[a]

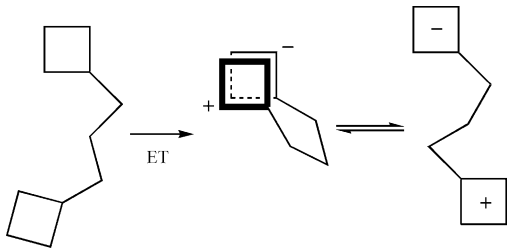

[a] In low-polarity solvents, flexibly linked D···A molecules turn, after an ET, into compact sandwich exciplexes ($^{+}$D||A^{-}). In highly polar solvents, along with (or from) such intramolecular sandwich exciplexes, flexibly linked solvated radical ions of opposite charge are formed ("stretched" intramolecular exciplexes, $^{+}$D^^A^{-}).[46,47]

(i) The *Coulombic attraction* exerts what is called a "*harpooning effect*".[43] Wherever possible, the oppositely charged radical ions tend to come close together, as in the flexibly linked exciplexes.[44−46] Such an approach is often impeded by steric effects, or by stabilization of a highly dipolar conformation in high-polarity solvents (Scheme 3). Considerable electrostatically driven conformational changes are reported, even for apparently rigid or semirigid molecules.[48,49]

(ii) *Intramolecular interactions* between the excited states in general lead to deviations from the *zero-order* geometry, as they are increasing with growing orbital overlap. Interactions with upper states depress the energy of the real CT state, whereas those involving the ground state elevate it. Detailed analysis of the effects of orbital interactions have been published; see, for example, the classical paper by Beens and Weller.[50] The inclusion of these interactions, as inferred from the modern theories of electron transfer and from the band shape of the radiative ET transitions, is shown in section X.

(iii) *Interactions with the medium*, in particular with the polar solvent, stabilize the highly polar CT state with respect to the other less polar states or conformations involved. Therefore, the structure approaches more closely the zero-order ET state in highly polar media (Scheme 3). Specific interactions, most commonly those with protic solvents tending to form hydrogen bonds, affect the molecular structure in a molecule-specific way.

It is important to note that photoinitiated processes are not the only means for populating the excited CT states. They can also be efficiently populated in an ET reaction between the radical cation and the radical anion. This can be chemically generated[51] or formed in electrode processes.[52] The reaction, e.g., A−D^{+} + A^{-}−D → (A−D)* + A−D, is detected by the emission of *electro-chemiluminescence*.[53−56] Numerous examples of chemically generated ICT states have been reported for several series of singly bonded aromatic donors and acceptors, provided certain electrochemical and chemical conditions are fulfilled.[55−61] A chemical generation of the ICT states should also be possible in certain cases in which the photoinduced reaction is too slow to occur during the lifetime of the precursor excited state. Currently, however, no such cases have been described.

II. Singly Bonded D–A Molecules and the Case of DMABN

A. Dual Fluorescence and Lippert's Explanation

If linked by a single bond, the D^{+} and A^{-} subsystems have a very limited degree of freedom. Internal rotation around the central bond, as in large-amplitude torsional motion or *twist*, seems to be the *first choice* vibrational mode for a relaxation involving a change in the electronic structure of the excited state, although it is not the only one involved. Along with the twist angle, the distance changes between D^{+} and A^{-}, i.e., the central bond length. In the coplanar conformation, strong conjugation (the quinoid structure, like in **1b**) augments the central bond order and contracts the bond. In the 90° twisted conformation, the decoupled D^{+} and A^{-} moieties are linked by a single bond, but its length may be somewhat reduced, as compared to a typical single bond length, due to the Coulombic attraction of the opposite charges. Also, each of the charged subsystems may deviate, due to different interactions, from the geometry and electronic structure characteristic for the separate radical ion species, D^{+} or A^{-}.

The first clearly recognized and most discussed example of this class was 4-(*N*,*N*-dimethylamino)-benzonitrile (DMABN, **1**).[62] DMABN has been discovered as an amazing molecule that, in the absence of any excited-state reaction familiar at that time, emits two fluorescence bands. The two bands strongly depended on solvent polarity and temperature.[63,64] In nonpolar solvents, only one fluorescence band appears, originating from the $^{1}L_b$ ($^{1}B_2$) state,[65] and later called by different authors *B fluorescence* (F_B), *normal fluorescence* (F_N), or *locally excited fluorescence* (LE). In polar solvents, a further long-wavelength fluorescence band grows in relative intensity, while the intensity of the first band decreases with increasing polarity of the medium.

Initial investigations concerning the anomalous fluorescence of DMABN described the most characteristic features of the phenomenon: Lippert et al.[63] discovered that the dual fluorescence depends strongly on the solvent polarity and on the temperature. Solvent polarity exerts its influence in the form of a strong solvatochromic shift of the F_A band (Figures 6, 7, and 17) and an increasing ratio of intensities, F_A/F_B (see, e.g., Figure 6). The ratio varies in a characteristic manner, indicating a thermally activated process at low temperatures, reaching a maximum with increasing temperature, and then diminishing with the excited-state equilibration in the *high-temperature*, or *thermodynamic* regime, vide infra.

On the basis of the solvatochromic shift (Figure 7), Lippert determined the dipole moment of the long-wavelength-emitting excited state of **1** to be $\mu_A^* \approx 23$ D.[63] The long-wavelength emission was assigned to the second excited singlet state, $^{1}L_a$, which is more polar than $^{1}L_b$ and presumably approaching a highly dipolar quinoid structure. The Lippert−Mataga solvent polarity function[16,67−69] is

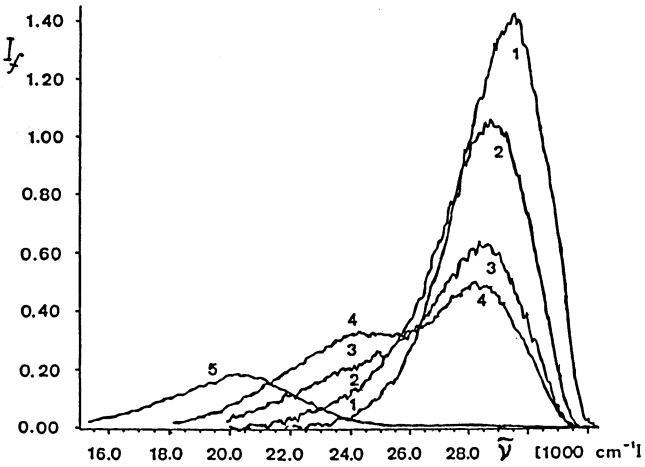

Figure 6. Fluorescence spectra of DMABN (**1**) in several solvents: (1) *n*-hexane, (2) dibutyl ether, (3) diethyl ether, (4) butyl chloride, and (5) acetonitrile. Excitation intensity was constant. In the solvents of medium polarity, two bands are clearly seen; in acetonitrile the high-energy band is quite small. Reproduced with permission from ref 66. Copyright 1992 The Indian Academy of Sciences.

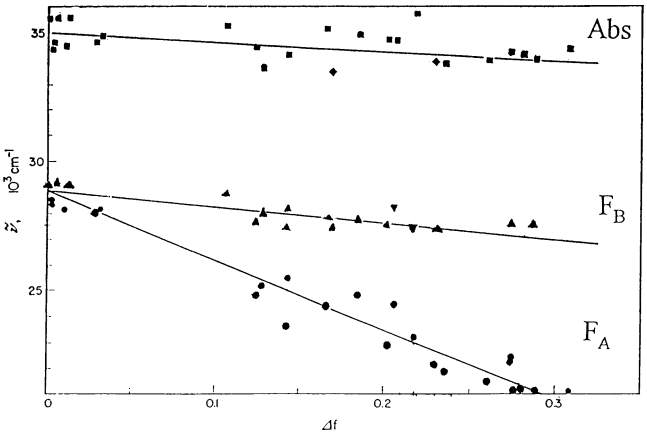

Figure 7. Solvatochromy: solvent effect on the spectral position of the absorption maximum, ^1L_a, and of the two fluorescence bands, F_B and F_A, of **1**. (Adapted with the kind permission of Prof. E. Lippert.) The Lippert−Mataga solvent polarity function[16,67−69] is shown in eq 3.

$$\Delta f = \frac{\epsilon - 1}{2\epsilon + 1} - \frac{n^2 - 1}{2n^2 + 1} \qquad (3)$$

With the polar solvent reorientation, an inversion of states turns ^1L_a into the lowest excited state, within the lifetime of the excited state (Figure 8). Therefore, the two emissions are usually called fluorescences B (or F_B) and A (F_A). The long-wavelength-emitting state (A*) is characterized by its very large dipole moment. The temperature dependence of the interconversion of the emitting states is more complex, but in a broad range it can be interpreted as corresponding to a thermally activated and solvent-polarity-assisted intramolecular reaction, B* → A*.[63,70]

The Lippert hypothesis lasted over a decade until new experimental evidence compelled several authors to seek interpretations that differed from the original. Starting from the early 1970s, the number of hypotheses rapidly grew, along with the accumulating experimental data and theoretical calculations. Soon,

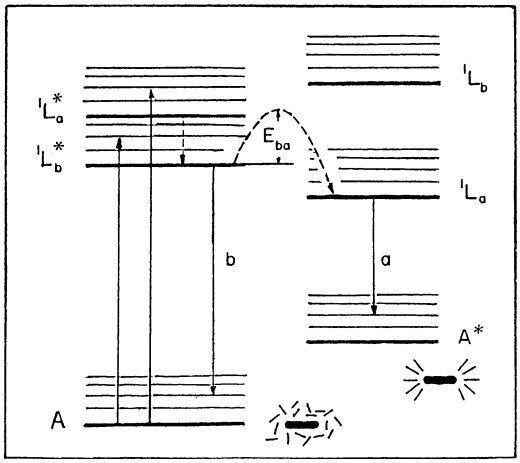

Figure 8. Lippert's scheme of the inversion of states of different polarity. In the polar solvent, the orientational relaxation of the solvent shell leads to an avoided level crossing (potential barrier E_{ba}). After relaxation, the more polar state, ^1L_a, becomes the lowest excited singlet (fluorescent) state.[63] Reproduced with the kind permission of Prof. E. Lippert.

it became evident that not only DMABN exhibited the dual fluorescence CT phenomenon; it was also common among other flexible D−A molecules. The vivid discussions and controversial views which have lasted for 30 years, and are only now seemingly reaching final conclusions, have contributed to the understanding of the structures and reactivities of the electronically excited molecules.

B. Main Hypotheses

Many hypotheses were formulated in competition with the simple and initially convincing explanation given by Lippert et al.[63] on the $^1L_b \rightarrow {}^1L_a$ inversion of states. We shall mention those which assign the origin of the new fluorescence band in DMABN to an excimer, to a protonated species, to an exciplex with the solvent, or to an intramolecular structural change — by a 90° twist of the amino group (TICT), by a pseudo-Jahn−Teller (PJT) distortion, by a rehybridization (pyramidalization, inversion, wagging) of the amino group (WICT), by a rehybridization (bending) of the cyano group (RICT), or by the planarization of the molecule in the CT state (PICT). These will be very briefly presented below, before the main body of the experimental findings, their interpretations, and the theoretical calculations. Afterward, the arguments for and against these different views will be collected and summarized.

1. Emission from an Excimer[71−74]

The hypothesis failed after finding that, with thoroughly purified samples, for a broad concentration range, the intensity ratio of both bands was independent of the concentration of DMABN.[1,75,76]

Excimers of **1** or related compounds (e.g., **11**) are indeed formed but only at high concentration, when an association reaction becomes possible for kinetic reasons: $k_r[\text{DMABN}] \geq 1/\tau_f$. As expected for excimers, their dipole moment is small (if any — it depends on mutual orientation), and the position of the respective fluorescence band is virtually *solvent-polarity-inde-*

pendent over the whole accessible range of solvent polarities,[77] which definitely disproves the excimer hypothesis. Additional evidence is provided by the

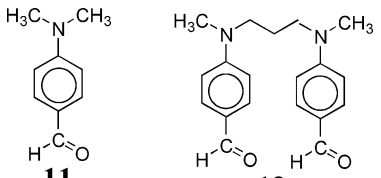

11 **12**

study of the flexibly linked three-methylene-bridged aldehyde analogue of DMABN, **12**.[77] It emits three fluorescence bands: F_B, F_A, and the almost polarity-independent excimer band (the latter indicating that no CT state is involved in this excimer). Related ground-state dimers (or higher aggregates) are preferentially formed in nonpolar solvents at low temperatures[76−80] and have no relation to the F_A emission, although sometimes they exhibit a strongly red-shifted fluorescence.

2. Proton Transfer[81] and Hydrogen Bonding[82,83]

Kosower and Dodiuk[81] ascribed the long-wavelength emission to a protonated species (cation), **13**. The excited-state proton-transfer hypothesis did not receive acceptance, as it did not explain the dual fluorescence of **1** in aprotic polar solvents. Later, even Kosower did not continue to support this point of view.[84,85]

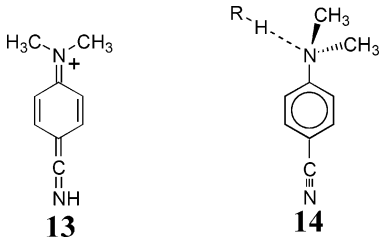

13 **14**

The ground-state H-bonding was described by Cazeau-Dubroca et al. as the major (or even the only) cause of the TICT state formation: the tetragonal arrangement of bonds in the complex (**14**) should constitute, on breaking the H-bond in the excited state, a precondition for the twist.[83,86−89]

3. Exciplexes with the Solvent[90,91]

As the addition of a polar solvent to a nonpolar one caused a marked quenching of the fluorescence of **1** coupled with the appearance of a new band, F_A, Chandross suggested the formation of 1:1 (and possibly also higher) specific, stoichiometric exciplexes of the excited DMABN with small polar molecules of the solvent. He stressed the fairly general behavior of that type in various intermolecular exciplexes and correlated the solvent−solute interaction with the dipole moment of the solvent molecule. Later, on the basis of new experiments,[92] he tended toward the TICT hypothesis (vide infra). The Chandross hypothesis[91] was revitalized and substantiated by Varma and his students.[7,93,94] In alkane solutions of **1**, on addition of a polar solvent P, the F_B fluorescence is quenched while F_A grows, as shown by the linearity

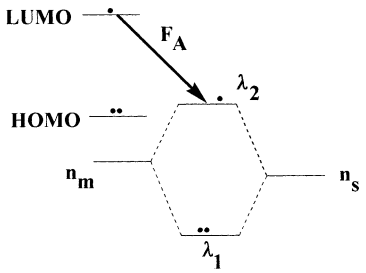

Figure 9. Scheme of terms in the exciplex with the solvent, as proposed by Varma et al.[93] Lone pairs of the solute molecule, n_m, and of the solvent, n_s, interact, which results in a splitting (λ_1, λ_2). Reproduced with permission from ref 93. Copyright 1983 The Royal Society of Chemistry.

Table 1. Fluorescence Anisotropies[a] in Glycerol Solutions: $\lambda_{excitation}$ Close to the Maximum of the First Absorption Band and $\lambda_{measurement}$ Close to the Maximum of the Given Emission Band (from the Data of Ref 1)

	compd	
	15	**17**
F_B	0.26	0.33
F_A	0.28	0.29

[a] Anisotropy $R \equiv (I_{\parallel} - I_{\perp})/(I_{\parallel} + 2I_{\perp})$, where $I_{\parallel}$ and $I_{\perp}$ are the emission intensities at mutually parallel, *resp*. perpendicular, polarization of the excitation and emission beam.[183]

of the intensity ratio plots, $F_A/F_B = k[P]$, indicating a formation of 1:1 exciplexes (for alternative interpretations, see section III.A.1). On the basis of ample evidence of measurements in mixed solvents, they concluded that the solvent effect is due not to dielectric polarization but to specific interactions. These were ascribed to a σ-type exciplex bonding of the n_N electrons of **1** with the lone pairs of the solvent molecule (Figure 9). Such an exciplex, primarily with the planar DMABN species, undergoes a structural relaxation resulting in a more stable n,n-type exciplex, with one electron from the *n*-orbital localized on the twisted amino group. Description of this specific solute−solvent interaction as a three-electron bond to the solvent lone pair was also suggested by Wang.[95] Later, the group of Varma, continuing to support the exciplex hypothesis, withdrew from the concept of an intermediate planar exciplex.[96]

4. Intramolecular Twist (TICT)[1,70]

The study of the dual fluorescence of DMABN and its derivatives **15**−**17** revealed that the fluorescence anisotropy in glycerol solutions, instead of being of opposite sign as predicted by Lippert's explanation, was positive *in both bands* (Table 1);[97] and the two isomers behaved very differently in the same solvent (ether): **15** exhibited dual fluorescence, with a dominant F_B band, whereas **16** emitted almost exclusively the F_A fluorescence. The evidence was tentatively interpreted in terms of a steric effect: the methyl substituent in the position ortho to the $-NMe_2$ group sterically hinders the coplanar (quinoid) structure. This disfavored the assignment of F_A to the coplanar quinoid structure, of the type **b** in the Scheme 1 (section I.A). A new hypothesis involving an intramolecular structural change was formulated,[1] with the

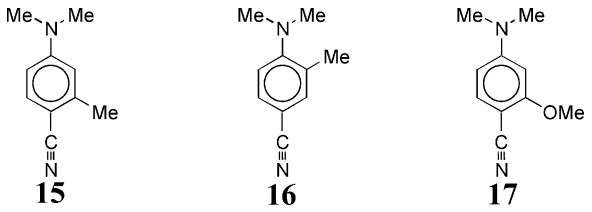

15 **16** **17**

F_B band assigned to an approximately coplanar structure and F_A to a CT excited-state conformation with a highly twisted NMe_2 group, possibly perpendicular to the aromatic ring (A*, Figure 10). A full

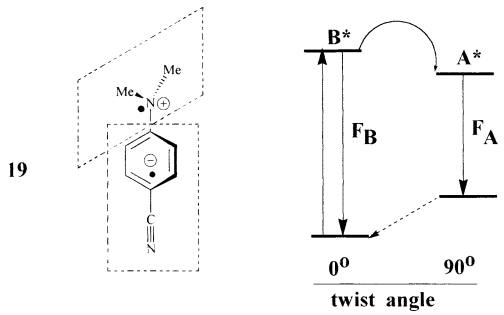

Figure 10. TICT model of DMABN. A* represents the pair of mutually orthogonal radical ions, linked by a single bond. In the scheme of terms, in the ground state the 90° twist corresponds to the top of a potential barrier to internal rotation. The barrier between the B* and A* states reflects the thermal effects on the kinetics, originally thought to correspond to an avoided state crossing.[4]

ET can appear in such an orthogonal conformation, because the system is decoupled with a zero overlap of the orbitals involved.

After finding similarities in the behavior of numerous other D−A compounds, structurally different from **1**, the rotamerism accompanying the intramolecular separation of charges was assumed to be a rather widespread phenomenon. The term *twisted intramolecular charge-transfer* state was coined, abbreviated TICT (Figure 11).[2−4]

Figure 11. Model of a TICT excited state for a D−A molecule.

5. Pseudo-Jahn–Teller Effect: Rehybridization of the Donor

A different approach was suggested by Zachariasse and co-workers.[8,98,99] They noticed some evidence that was apparently incompatible with the TICT hypothesis. The F_A emission of **1** and the typical bimodal fluorescence kinetics appear not only in polar media but also in toluene solutions, where no dielectric relaxation of the solvent is expected.[98] A dual emission in alkanes as solvents was reported for some analogues of DMABN, e.g., the ester **32**,[100] and a trace of F_A was detected even in **1**.[101,102] Zachariasse et al. found a correlation between the efficiency of the CT state formation and the $^1L_a-^1L_b$ energy gap (in absorption) and postulated that the proximity of these two electronic states favors the CT state. These phenomena are ascribed − in rather general terms − to the *pseudo-Jahn−Teller* (PJT) distortion of the molecular structure. The PJT coupling of ^1L_a and ^1L_b states via the inversion mode (rehybridization) of the amino group is assumed to lead to a pyramidal geometry in the ICT state[8,99] (in an early version of their hypothesis; however, see below for the modification to the PICT model, and section III.E.1.a for an alternative explanation of the effect of the $^1L_a-^1L_b$ energy gap). The donor rehybridization model is sometimes called *wagging ICT* (WICT).

6. Rehybridization of the Acceptor (RICT)

Aside from the amino group, another site of a structural change in the molecule of DMABN could be in the cyano substituent. Already in the first paper re-examining Lippert's explanation in terms of a conformational change,[1] it was stated that, "it is not clear whether the orientation of the −CN group deviates from axiality, as may be the case in the excited state according to Walsh".[19c] In fact, an anomaly in the Stark splitting in rotational spectra of benzonitrile vapor led Lombardi to suggest a nonspectroscopic state to be close to the 0−0 transition of the first π,π^* absorption band.[103] Later, Lewis and Holman,[104] with semiempirical INDO/S calculations, identified this perturbing state of benzonitrile as corresponding to the structure with the bent cyano group (C−C−N angle ≈ 123°), in analogy to the excited states of HCN and alkyl nitriles (cf. section I.C). Analogous calculations for **1** indicated the presence of such a state with the bent −CN group (**18**) and with nearly the same energy as that of the calculated TICT state; its properties (too small dipole moment, polarization of the transition) indicated, however, that the bent state is not the one responsible for the F_A fluorescence.[104]

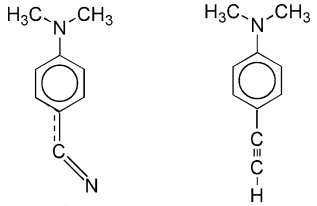

18 **19**

The experimental finding by Mordziński of the perturbation of the molecular supercooled jet spectra of benzonitrile and tolunitrile by a low-lying CT state[105] revived the discussion. Advanced ab initio calculations (HF, CIS, CASSCF, and CASPT2) indicated that the low-lying, strongly polar excited state of **1**, with the −C≡N group bent (**18**), is a possible F_A emitter.[9] In a subsequent paper, the same authors[10] compared **1** with the isoelectronic analogue, **19**. In both cases, there appear two series of highly polar states with structures different from those of the ground states: one, corresponding to the TICT model, with the rotated amino group and a C_{2v} symmetry, and the other with the −C≡N group, *resp.* the −C≡CH group, bent, belonging to the C_s symmetry point group. For the latter structure, the term *rehybridization by intramolecular CT* (RICT) was suggested. The RICT state had a somewhat higher energy than the TICT state in **1**, but markedly lower in **19**, and so the prediction was that **19** should emit

a CT fluorescence not only in polar solvents, but probably also under isolated molecule conditions in a molecular jet.[10] Later, the authors of this hypothesis admitted that the reaction coordinate is better described by of the twist angle, although they claimed that the lowest excited-state energy of the CT state (in the free molecule) corresponds to a twist angle $\theta \approx 60°$.[106]

Soon, experiments revealed that **19** does not exhibit dual fluorescence, and its only emission is from a "locally excited" π,π^* state, independent of the polarity of the solvent, and with a single-exponential decay.[107] On the other hand, a more recent experimental study of **19** concluded that a CT state is populated in polar solvents, but without observable emission, due to a very efficient internal conversion.[108]

Thus, the RICT hypothesis was very seriously shaken. Ironically enough, after this long discussion in a multitude of papers, it was recently found that the anomaly in the jet spectra of benzonitrile or tolunitrile[105] disappears at higher resolution than that previously used.[109] Moreover, the RICT hypothesis would not help to explain ample evidence on analogues of **1** in which the −CN group is replaced by such substituent as −CHO, $-COCH_3$, −COOR, or $-CONR_2$, or those in which the whole benzonitrile acceptor is replaced by the pyridine or pyrimidine ring (vide infra).

7. Planarization of the Molecule (PICT)

Stepwise, Zachariasse[110] redefined his model of the structural change in **1**,[111,112] calling it *planar intramolecular CT* (PICT).[201] Tacitly abandoning his previous pyramidalization and PJT distortion hypotheses (section 5, above) as not decisive for the structure of the CT state, or rather leaving its importance for the reaction path open for discussion, he returned to an idea close to Lippert's original hypothesis (Figure 9): the S_2 state (^1L_a) is transformed into an S_1 state (^1L_a, CT). Upon the state reversal, the highly dipolar planar quinoid structure is formed (like **b** in Scheme 1).

The forbidden character of the F_A radiative transition is assigned to the CT electronic structure (though it is not clear where the donor and acceptor units are localized in the quinoid structure, and why this forbidden character does not appear in the $^1L_a \leftarrow {}^1A_1$ absorption). The PICT model seems not to be able to explain the steric effects or the behavior of the rigid model compounds (vide infra, section III.A.2).

III. Fluorescence Spectroscopy

A. Solvent Effects and the Model Compounds

1. Solvent Effects on the Spectra

The long-wavelength F_A fluorescence of **1**, as with all typical CT emissions, undergoes a strong red-shift with an increase of the polarity of the solvent (cf. Figures 6 and 7 and Figures 14, 15, and 17 below). A controversy arose whether the different solvents exert *specific* or *nonspecific* effects. The question of specificity or nonspecificity of interactions drew the attention of many authors. On one hand, the solvatochromic plots satisfactorily correlated with the emission maxima as approximately linearly dependent on the solvent polarity functions of various forms,[63,113,114] contradicting the explanation based on *specific* solute−solvent interactions. On the other hand, in some cases, exceptions from the correlation appear in strongly hydrogen-bonding protic solvents, e.g., alcohols or water.[81,115,116] Also, a multiparameter regression analysis[117] according to Kamlet and Taft[118] indicated that, along with the general interactions (polarity + polarizability), hydrogen bonding affects the energy level of the CT state emitting the F_A fluorescence.[119,120] The hydrogen-bonding effects are referred to below, in section IV.C.

Two findings[7] strongly support the specific interactions, i.e., the exciplex model:

(i) The ratio F_A/F_B in mixed solvents seems not to depend on the macroscopic dielectric permittivity; in various mixed solvents of the same (low) dielectric constant, F_A/F_B depends on the nature and concentration of the added polar cosolvent.

(ii) In alkane solutions, the F_B emission is quenched and F_A grows on addition of a polar solvent P. The intensity ratio is a linear function of [P]: $F_A/F_B = k[P]$, which seems to indicate the formation of a 1:1 exciplex as responsible for the F_A emission.

The first observation can be tentatively explained by the preferential solvation of the solute dipole in hexane solution by the polar cosolvent added in small amounts. The polarity of the local environment of the solute would be very different from that of the bulk solution. Nevertheless, some specific solute−solvent interactions almost certainly influence the wavelength of the F_A fluorescence, at least in some of the analogues of **1**.[121]

With respect to the second point, the stoichiometric ratio of solute to solvent was carefully studied in numerous molecular jet experiments with contradictory conclusions (vide infra, section V); the 1:1 or 1:2 clusters seem to play an important role in the appearance of a red-shifted fluorescence, but only in hydrogen-bonded complexes.[122,123] In the case of polar aprotic acetonitrile, at least five molecules of ACN are needed.[124]

There is much less convincing evidence for the solutions. On addition of ethanol to a hexane solution of **17**,[125] the stepwise behavior of the lifetimes, measured at different wavelengths of the fluorescence, indicates that along with the bare molecule (in hexane) there appear several different complexes with ethanol, emitting at longer wavelengths (Figure 12).

It seems that − in contrast to the situation in most other polar *aprotic* solvents − in alcohols DMABN and its analogues really form specific hydrogen-bonded stoichiometric complexes in the excited state, not only 1:1, but also with several solvent molecules (with a possible special role of ethanol tetramers?[125]). Other pieces of evidence in favor of the hydrogen-bonded excited states are discussed in section IV.C.

With regard to the linear plots of the intensity ratio, F_A/F_B, as a function of the concentration of the polar solvent in the binary solvent mixtures, such a

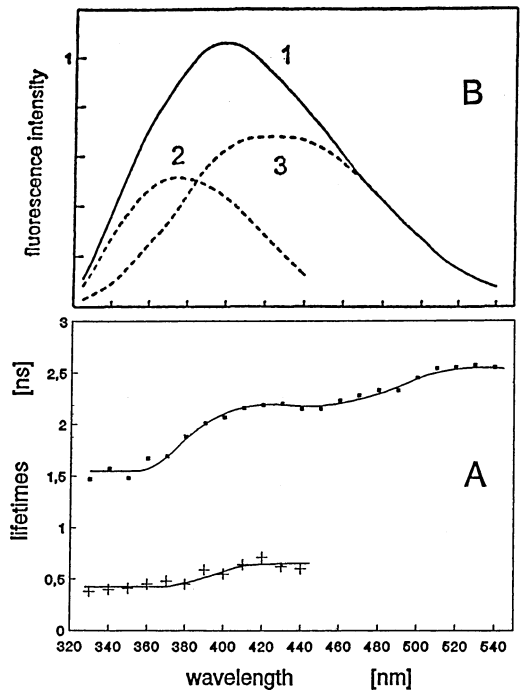

Figure 12. Stepwise complexation of **16** in 0.176 M ethanol in *n*-hexane, from the analysis of biexponential fluorescence decays. (A) Long and short lifetimes as a function of emission wavelength. (B) (1) Stationary fluorescence spectrum, lifetime-associated fluorescence spectra; (2) fast decay, identical to the stationary spectrum of **17** in *n*-hexane; (3) long lifetimes. Reproduced with permission from ref 125. Copyright 1996 Elsevier Science.

linear plot is only exceptionally observed in the full concentration range (Figure 13, top); in most cases it is found only in a limited range (Figure 13, bottom).

Such a linear relation as in Figure 13 can be expressed by eq 4:

$$R \equiv F_A/F_B = a + b[P] \qquad (4)$$

where P denotes the polar cosolvent. This could reflect either an equilibrium or the kinetics of the reaction $B^* + P \rightarrow$ *exciplex*. However, what seems not to have been previously noticed is that eq 4 cannot be derived simply for either of these cases, as the addition of a polar to a nonpolar solvent changes the dielectric properties of the medium, and the constancy of an equilibrium constant or a reaction rate coefficient is lost.

The observed type of a linear relation (eq 4) can be derived, however, without assuming the formation of any stoichiometric exciplexes, on the basis of the CT fluorescence shift with the changing composition (and polarity) of the solvent mixture, e.g, as in Figure 14.

Growing solvent polarity stabilizes the CT state, modifying both the equilibrium constant and the rate of any ET reaction (Figure 15). Denoting the corresponding changes by δ, we can assume $\delta\Delta S_o \approx 0$, at least in nonassociated solvents (or, $T\delta\Delta S_o \ll \delta\Delta H_o$). The ET occurs in the Marcus normal region, i.e., within the validity range of the linear free energy relations:

$$\Delta H^{\#\prime} - \Delta H^{\#} \equiv \delta(\Delta H^{\#}) \approx \alpha(\delta\Delta H_o) \qquad (5)$$

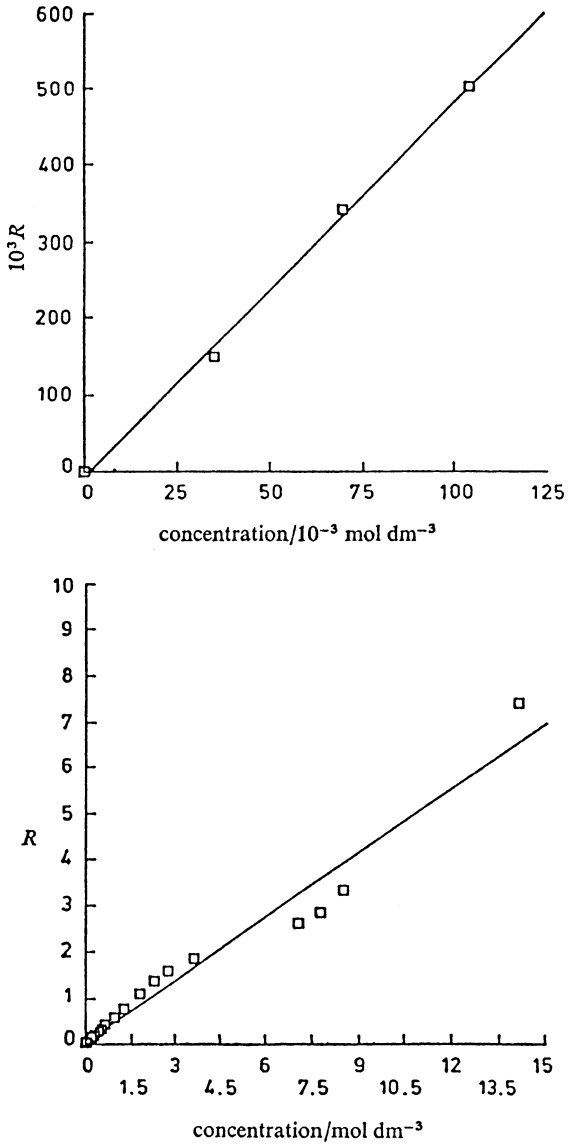

Figure 13. Intensity ratio $R \equiv F_A/F_B$ for **1** as a function of the concentration of the polar component, in binary solvent mixtures. Top, in CHX + CF_3CH_2OH; bottom, in CHX + C_2H_5CN. Adapted with permission from ref 7. Copyright 1980 The Royal Society of Chemistry.

Typically, e.g., in the Brønsted relationship, $\alpha \approx {}^1/_2$. The intrinsic probe — the shift of the fluorescence band — serves as a good measure of solvation. At least in some cases (Figure 14), the shift can be described as

$$\delta\tilde{\nu}_f = \gamma \ln [P] \qquad (6)$$

From the data in Figure 14, $\gamma = -617$ cm^{-1}. The shift in the emission maximum has its origin only partially in the stabilization of the excited CT state, $\delta\Delta H_o$, and partially in the rising level (destabilization) of the FC ground state (Figure 15, eq 7):

$$(\tilde{\nu}_i' - \tilde{\nu}_i) \equiv \delta\tilde{\nu}_i \approx \beta(\delta\Delta H_o) \qquad (7)$$

If both components contribute to a similar extent,[127] $\beta \approx 2$. Substituting eqs 5−7 into the relations linking the equilibria with ΔH_o or the rates with $\Delta H^{\#}$, we arrive at eqs 8 and 9, respectively:

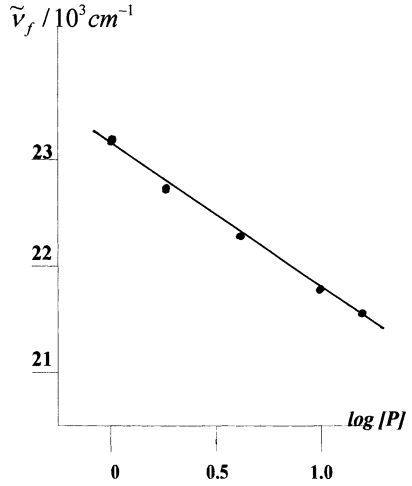

Figure 14. Maximum of the CT fluorescence of **1** in the binary solvent mixtures of cyclohexane + ethanol. Figure courtesy of Dr. K. H. Grellmann, unpublished results.

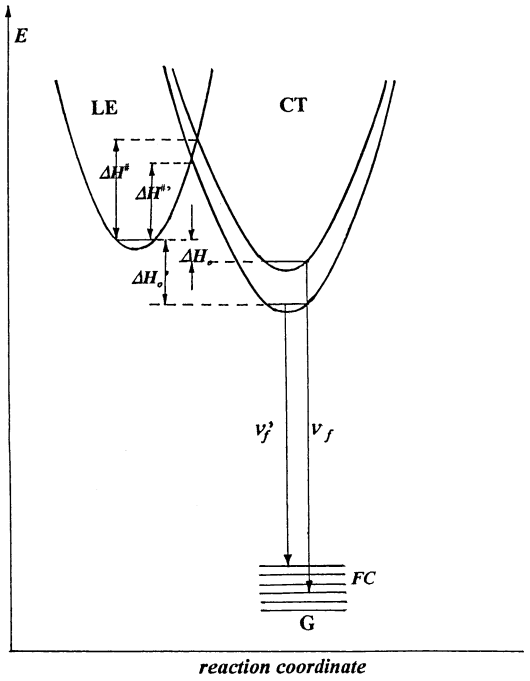

Figure 15. Schematic of the effect of the polarity of the medium on the rate and equilibrium of the ET reaction. A polarity increase (e.g., a larger content of the polar component P in a binary solvent mixture) approximately does not affect the LE state, and the stabilization of the CT state is denoted by the changed values (primed): $\Delta H_o'$, $\Delta H^{\#\prime}$, $\tilde{\nu}_i'$. The Franck−Condon (FC) ground-state level, determined mainly by the destabilization energy of the solvated solute,[126] increases with the polarity of the medium.

$$\delta \ln K \approx -\delta(\Delta H_o/RT) \approx -(\gamma/\beta RT)\delta \ln [P] \quad (8)$$

$$\delta \ln k \approx -\delta\Delta H^{\#}/RT \approx -\alpha(\delta\Delta H_o/RT) \approx -(\alpha\gamma/\beta RT)\, \delta \ln [P] \quad (9)$$

Substituting the most probable values of α and β as mentioned above, and γ from Figure 14, we obtain for the equilibrium, at $T = 293$ K,

$$\delta \ln K \approx 1.5(\delta \ln [P]) \quad (10)$$

and for the kinetics of the ET process

$$\delta \ln k \approx 0.75(\delta \ln [P]) \quad (11)$$

In each case, the exponential coefficient ($K \sim [P]^{1.5}$, $k \sim [P]^{0.75}$) is not far from unity. It is understandable why the relation (4) is often observed only in a limited range of the concentration [P], because of the approximate character of these relations.

Taking into account that, in the molecular supercooled jets, CT emission is not observed in the 1:1 van der Waals complexes of DMABN with aprotic polar molecules, while it appears in larger solute−solvent clusters (1:5 for DMABN with ACN),[124] still another alternative explanation arises. In a mixed nonpolar (N) and polar (P) solvent, the surrounding of **1** will be a distribution of "clusters" **1**:P_p:N_n, where the total coordination number $p + n$ depends on the molecular sizes of solute and solvent, and the cluster size distribution depends only on [P], on the dipole moments, and on specific interactions between the partners. It can be assumed that, like in the jets, only the clusters with $p \geq r$ are reactive,[128] and in most cases $r > 1$. The key point is that only *one* additional polar solvent molecule P transforms a nonreactive cluster ($r - 1$) into a reactive one. This transformation can occur either (a) in the excited state, as a solvent shell reorganization with the rate constant depending linearly on [P] but also related to solvent viscosity (translational diffusion), or (b) in the ground state, where the equilibrated cluster distribution will generally depend on [P] in a more complicated way. If, however, $r \gg 1$, the concentration of *reactive* clusters will also be linearly related to [P] for low concentrations of P. The condition $r \gg 1$ is fulfilled for **1**.[124]

Summarizing, the approximately linear quenching relation (4) can appear even in the absence of specific 1:1 solute−solvent clusters.

2. Steric Effects and Model Compounds

Not only DMABN exhibits a dual fluorescence of that type, but also its numerous derivatives and analogous compounds, with modified donor or acceptor groups in the benzene ring. It was an early observation that the same $-CH_3$ substituent, in the position ortho or meta to the $-NMe_2$ group of **1**, exerts very different effects[1] (section II.B.4) (see Figure 17).

To check a possible role of the steric effect, a series of model compounds were synthesized, with the dialkylamino group structurally fixed nearly coplanar to the ring (**20**), or strongly sterically hindered (**21**), or rigidly fixed in a position perpendicular to the aromatic ring (**22**). The results (Figures 16 and 17) were explicit. While the compounds with a possible rotational freedom around the benzene−amine bond — **1** (DMABN), **15**, **17**,[1] **23** (PYRBN), and **24** (PIPBN)[129] — exhibit a dual fluorescence, those with fixed rigid structure emit only one band: in the case of coplanar **20** (MIN, CMI), this band is very similar to the F_B fluorescence of DMABN;[130,131] in the rigidly perpendicular **22** (CBQ), it is similar to the F_A band.[4,132]

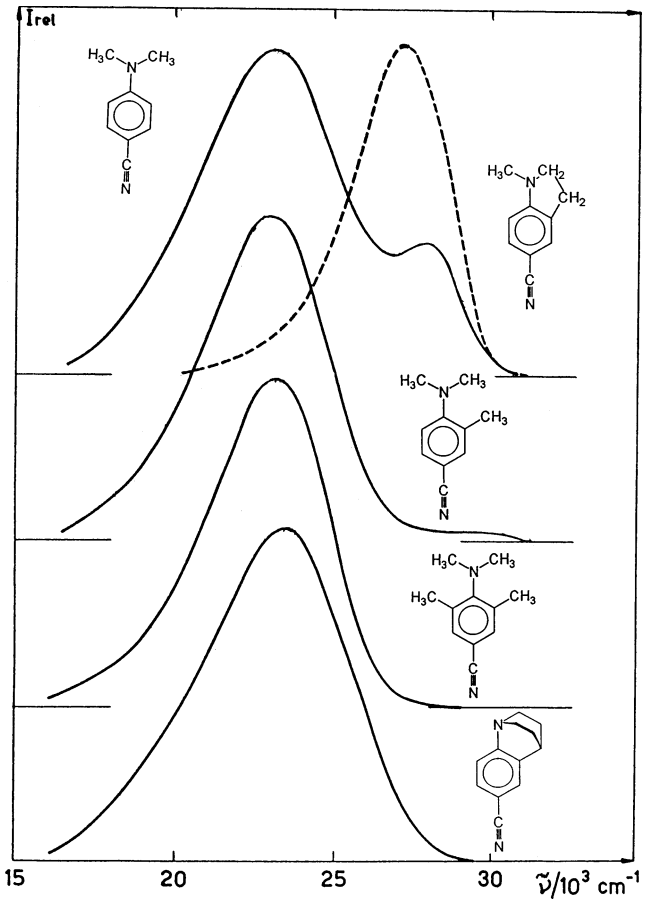

Figure 16. Fluorescence spectra of **1** and the model compounds **20**, **21**, **16**, and **22** in CH_2Cl_2 at room temperature. Adapted with permission from ref 3.

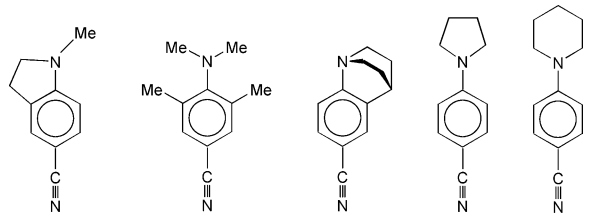

20 **21** **22** **23** **24**

The similarity is especially noticeable on comparing the solvatochromic shifts in solvents of widely different polarities (Figure 17). While there is nearly no shift (F_B only) in the emission of **20**, compounds **1** and **15** exhibit two bands, and compounds **21** and **22** emit only (and **16**, *almost* only) one band, F_A, which shifts strongly, about 5000−6000 cm^{-1} between the two solvents considered. The cases of the sterically hindered but not rigid compounds **16** and **21** (TMABN) are, however, not quite clear: usually only one fluorescence band is observed, but when alkanes were used as solvents the band has an unusual width (Figure 17, Table 2). Also, **22** has an unusually broad fluorescence band ($\Delta\tilde{\nu} \approx 6000$ cm^{-1})[132−134] in alkanes (cf. section III.D on emission anisotropy)

The CT emission of **21** was observed also in the gas phase,[135] its CT character being confirmed by the high dipole moment of the emitting state.[136] In very different solvents (nonpolar, polar, aprotic, protic), at temperatures below 80 K, a weak, *short-wavelength* second fluorescence band of **21** appears

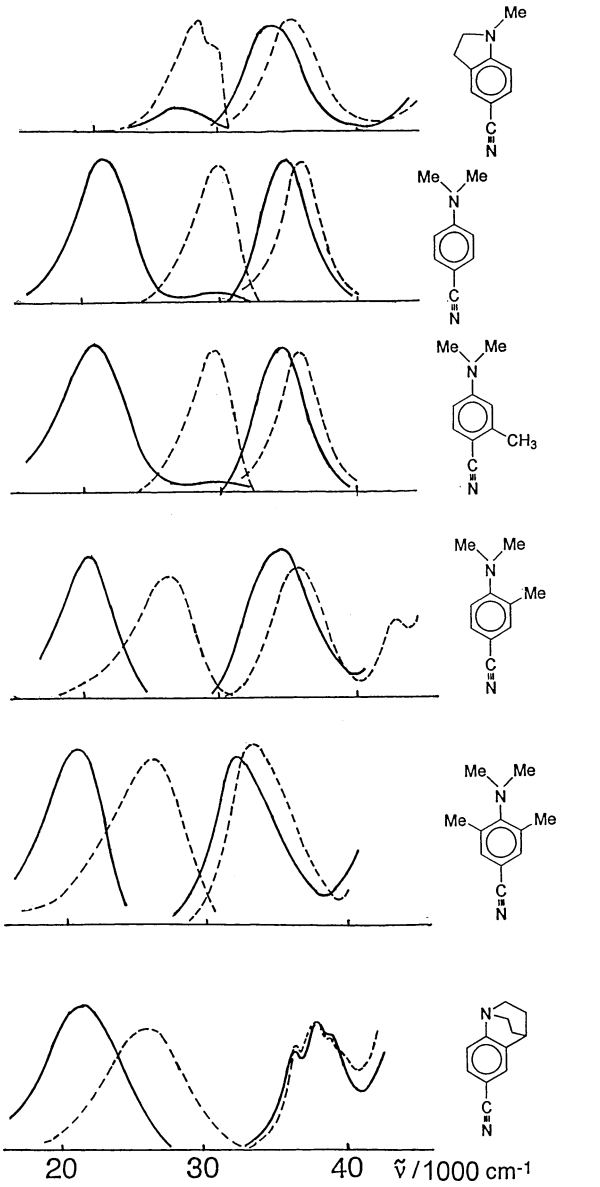

Figure 17. Absorption and fluorescence spectra of DMABN and several model compounds: (top to bottom) **20**, **1**, **15**, **16**, **21**, and **22**. Dashed lines, in nonpolar *n*-hexane; solid lines, in highly polar acetonitrile (in the case of **20**, exceptionally, in ethanol). Reproduced with permission from ref 134. Copyright 1999 Elsevier Science.

($\lambda_{max} \approx 350$ nm) at excitation energies ≥2000 cm^{-1} *above* the onset of the absorption. It was interpreted as an emission from a π,π^* excited state, modified by strong steric hindrance (**21** has the $-NMe_2$ group twisted by ∼60° vs the ring plane in the ground-state structure[137,166]) to a shallow minimum (Figure 18).[135] Remarkably, the observation and the interpretation were reproduced in the study of **21** in the supercooled molecular jet, where the CT emission appears at $\lambda \approx$ 380 nm and the π,π^* emission at $\lambda \approx 340$ nm.[138]

The comparison of the LIF spectra of DMABN and its *pretwisted*[140] derivatives, **16** and **21**, under jet-cooled conditions, with those in thermalized vapor or in condensed phases (Table 2, Figure 19) reveals that **16** behaves somewhat peculiarly. Its LIF spectrum is strongly reminiscent of **1** in nonpolar solvents: it is markedly narrower and blue-shifted as compared to the LIF fluorescence of **21** in the jet, but in the

Table 2. Fluorescence of DMABN and Its *Pretwisted* Derivatives in the Supercooled Molecular Jet As Compared to Other Environments[a]

compd	environment	ν_f^{max} (cm^{-1})	$\Delta\nu_{1/2}$ (cm^{-1})
1	*n*-hexane	29 100	3600
	ethanol glass	29 100	3000
	vapor	28 500[d]	
	LIF,[b] jet	30 500	~3000
16	*n*-hexane	27 800	5800
	ethanol glass, 77 K	25 500	
	LIF, jet	29 600	~4500
21	*n*-hexane	26 000−26 900	5800
	vapor[c]	26 000	6200
	LIF, jet	25 500	~9000
42	*n*-hexane	26 050[e]	
	vapor	26 500[d]	

[a] Data evaluated from ref 139 unless otherwise stated. [b] LIF, laser-induced fluorescence. [c] Reference 135. [d] Reference 196. [e] Reference 170.

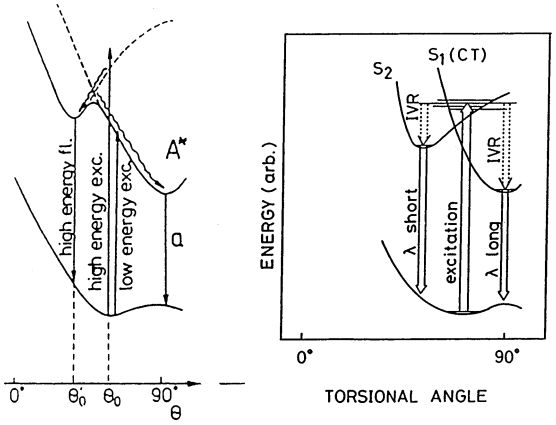

Figure 18. Schemes explaining the photophysical behavior of **21** in solutions[135] (left) or in the supercooled molecular jet[138] (right). The strong steric effect of the two ortho-methyl groups locates the energy minimum in the ground state at ~60° twist of the $-NMe_2$ group vs the ring; the lowest excitation is already to a CT potential hypersurface. Higher energy excitation populates a shallow trap of the less polar π,π^* state with a minimum energy twist angle $\theta < 60°$. Reproduced with permission from refs 135 and 138. Copyright 1982 and 1987 Elsevier Science.

condensed phase it shifts to the red, even in a rigid solvent at 3.5 K.[139] The red shift and the remarkable broadening of the fluorescence spectrum in hexane are accompanied by a strongly polar character (TICT?) of the emitting state.[116] This suggests that the intermolecular interactions, even with a nonrelaxing rigid solvent, diminish the inner energy barrier or facilitate the intramolecular vibrational redistribution (IVR), catalyzing the population of the CT state. It seems that the emission of **16** is from a primary excited state of the bare molecule in a vacuum but from a CT state in the condensed (even nonpolar) phase.

The luminescence spectra of the model compounds exemplify the effect of the substituents sterically hindering the coplanarity of the $-NR_2$ group with the ring, as depicted in Figure 20.

3. Bandwidths

The F_B and F_A emission bands differ in their nature, F_B corresponding to a typical π,π^* transition,

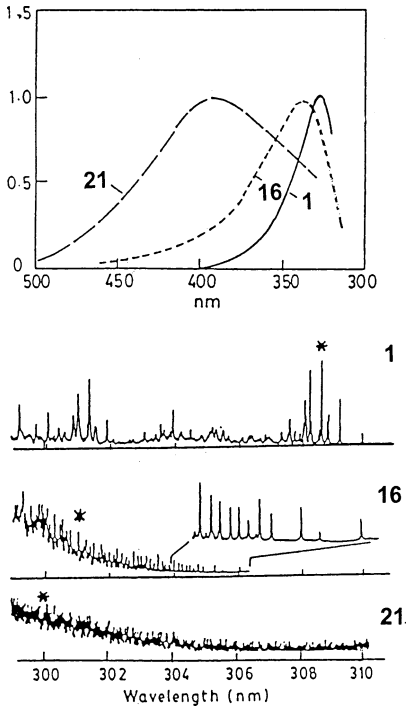

Figure 19. Laser-induced fluorescence (LIF) spectra of **1**, **16**, and **21** in the supercooled molecular jet. Top, dispersed emission spectra; bottom, the corresponding excitation spectra (monitored at $\lambda = 340$ nm for **1** and **16**, and at $\lambda = 400$ nm for **21**). The excitation of the dispersed fluorescence is marked by the asterisk. Adapted with permission from ref 139. Copyright 1992 Indian Academy of Sciences.

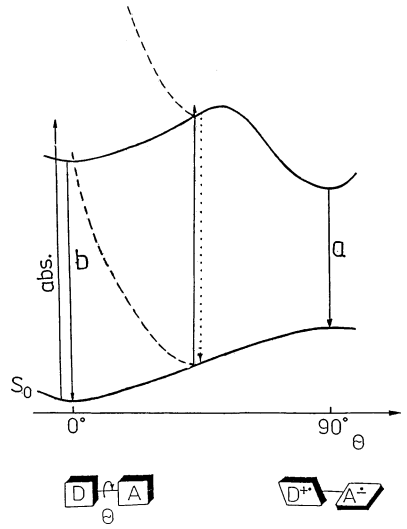

Figure 20. Simplified scheme (in accordance with the TICT model) of the effect of steric interactions in the derivatives of **1**. Potential cross section along the torsional coordinate θ, in the S_0 and S_1 states, in the absence of steric interaction (solid curves) and with a substituent sterically hindering the coplanarity of the amino group with the ring, e.g., an ortho-methyl group (dashed curves). With the shift of the potential minimum to larger twist angles θ, the barrier in the excited state diminishes.

delocalized over the whole conjugated π-electronic system,[141] and F_A representing a typical CT fluorescence, a radiative back-ET transition,[142] i.e., occurring in the inverted Marcus region.[143] A quantitative theoretical description of the radiative electron transfer (in absorption or in emission) was given in the key paper by Marcus,[144] often referred to in the

discussions below (sections X and XI). According to the theory, the bandwidth $\Delta\tilde{\nu}_{1/2}$ of a radiative ET band should grow with the polarity of the solvent (as is indeed often observed[144,145]), approximately as

$$\Delta\tilde{\nu}_{1/2} \sim 2kT\lambda_o + \lambda_i hc\tilde{\nu}_i \qquad (12)$$

where the *solvent* and low-energy modes reorganization energy λ_o is expected to rise linearly with the solvent polarity function, while the *inner* reorganization energy λ_i is connected with the average high-frequency modes, $\tilde{\nu}_i$. Both λ_i and $\tilde{\nu}_i$ are usually considered as solvent-polarity-independent. It is therefore astonishing that the CT fluorescence (F_A) of DMABN does not show any clear dependence on the polarity of the medium. The emissions of the model compounds for a TICT fluorescence, **21** or **22**, show even some tendency toward narrowing of the band in the polar solvents (e.g., Figure 17; see also ref 8). The emitting CT excited state seems not to change its electronic structure with the polarity of the solvent. If the most probable twist angle in the CT state were nearly constant, irrespective of the solvent (e.g., $\theta \approx 90°$ in a TICT state), it would not be clear which factors could be *decreasing* with the rise of the polarity of the medium, to compensate the unquestionable rise of λ_o in eq 12. Both $\tilde{\nu}_i$ and λ_i should be rather constant.[146] It may be that, with increasing solvent polarity, the population distribution around the equilibrium position (e.g., around the twist angle $\theta = 90°$, Figure 25) gets narrower, and consequently the bandwidth does as well.

4. Isoemissive Points

In the binary mixed solvents, nonpolar + polar, in some cases well-defined *isoemissive points* are observed which are not yet understood. They are usually observed only in a limited range of concentrations of polar solvent, e.g., in the case of **1**, **21**, or **22** in hexane + ethanol or methanol added,[125,147] i.e., always with an alcohol as the polar cosolvent. The sterically hindered **21** exhibits, however, quite evident isoemissive points also in the whole concentration range of other solvent mixtures, such as *n*-hexane + CH_2Cl_2 or *n*-butyl chloride (Figure 21).

These data are interpreted by Varma and his team in terms of two emissive species with a *parent−daughter* relationship, as one of the proofs for the formation of the exciplexes with a polar solvent[147] (or even with a nonpolar but aromatic one, like benzene[149]). The evidence for and against this interpretation is discussed in sections II.B.3 and III.A.1. In the case of **21**, in which only one fluorescence band is observed (the CT band)[150] with a solvent-independent transition dipole moment (Table 5), only one excited species seems to emit in all solvents, and a parent−daughter relationship is not reported.

Classical conditions for the occurrence of an isoemissive point were formulated for monomer−excimer systems as a function of temperature.[151,152] *Mutatis mutandis*, one can adapt them to the case of *any* excited-state reaction Y* → Z* (in particular, it may be also an equilibrium Y* ⇄ Z*) as a function

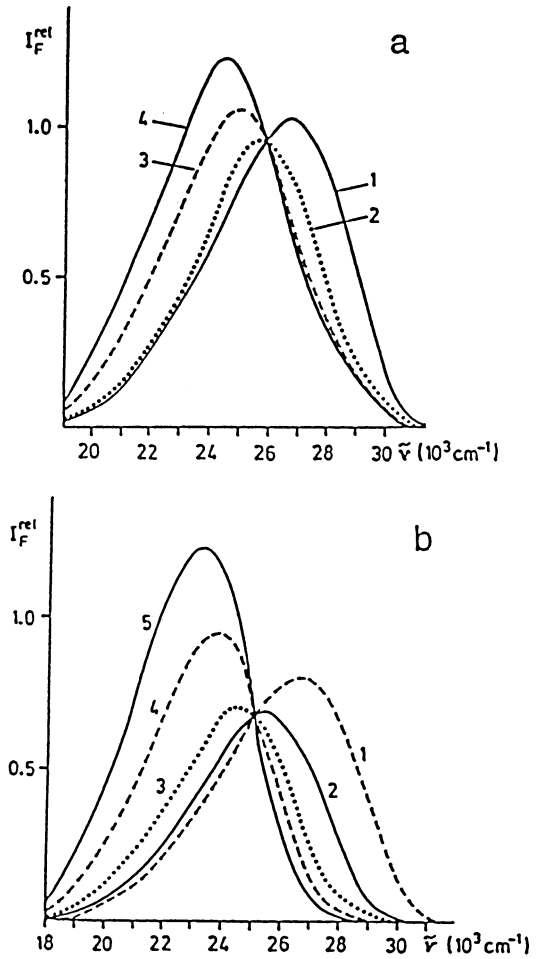

Figure 21. Isoemissive points. Fluorescence spectra of 1×10^{-4} M **21** in *n*-hexane + *n*-butyl chloride binary mixtures: (a) in (1) 0, (2) 20, (3) 50, and (4) 100 vol % C_4H_9Cl; (b) in *n*-hexane + CH_2Cl_2 mixtures containing (1) 0, (2) 10, (3) 30, (4) 60, and (5) 100 vol % CH_2Cl_2. Reproduced with permission from refs 148 and 139. Copyright 1986 Elsevier Science and 1992 The Indian Academy of Sciences.

of any parameter X which affects the concentrations [Y*] and [Z*]. X may be the temperature, pressure, composition of the solvent, and even — with certain restrictions — time. If the measurements are done at a constant excitation rate, i.e., if the absorption at λ_{exc} does not depend on X, an isoemissive point would be observed if the following conditions hold:

(i) The emission spectra of Y* and Z* markedly differ (by more than the mean of their $\Delta\tilde{\nu}_{1/2}$), but partially overlap, and their shapes and spectral positions are *independent of the variable X*.

(ii) The *inner* quantum efficiency $k_f/(k_f + k_{nr})$ of each emission does not change with changing X.

(iii) $d[Y^*]/dX = -d[Z^*]/dX$, i.e., there exists a parent−daughter relationship (in equilibrium or irreversible kinetics).

Here, these conditions are obviously *not met*: the two component bands have neither constant spectral shapes ($\Delta\tilde{\nu}_{1/2}$ changes) nor constant spectral positions (there are large red shifts with increasing polarity of the medium). The inner quantum efficiencies are also not constant: the quantum yield ϕ_f of **21** in mixed solvents changes nonlinearly, not even monotonically (e.g., Figure 21). An extremum is found for the *nonradiative* rate, k_{nr}, in an intermediate range

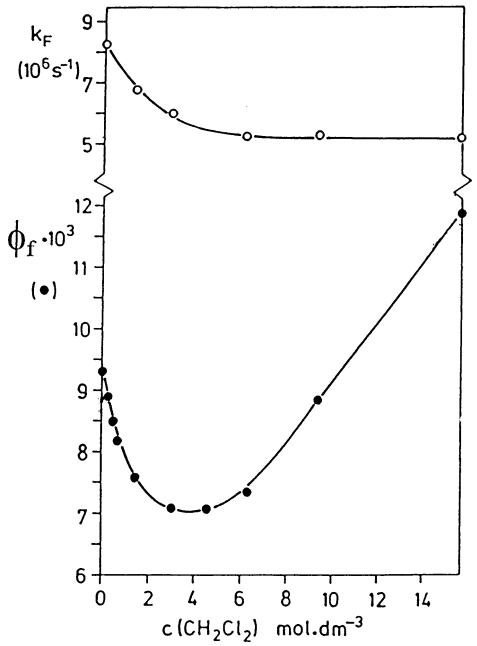

Figure 22. Fluorescence of 1×10^{-4} M **21** in *n*-hexane + CH_2Cl_2 binary mixtures, $T = 21$ °C. Radiative rates, k_f, and quantum yields, ϕ_f. Reproduced with permission from ref 153. Copyright 1987 Elsevier Science.

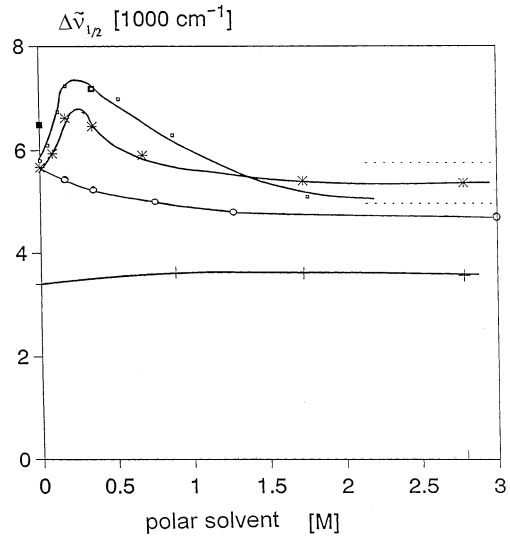

Figure 23. Fluorescence bandwidths ($\Delta\tilde{\nu}_{1/2}$) in binary mixed solvents, *n*-hexane + a polar solvent: □, **16**; +, **20**; ∗, **21** with ethanol added as polar solvent; ○, **21** with CH_2Cl_2 added.

of concentrations. A maximum of k_{nr} has also been observed in mixed solvents for the CT state of **1**.[153] Thus, the occurrence of an isoemissive point would result from an accidental mutual compensation of several factors. Therefore, probably, the isoemissive points are usually observed for this group of compounds only in a limited concentration range of the solvents. Important evidence for the existence or nonexistence of *two emitting excited species* is given by the bandwidths ($\Delta\tilde{\nu}_{1/2}$). Whenever two emitting species coexist and their maxima are not too distant, a plot of $\Delta\tilde{\nu}_{1/2}$ versus the variable X will exhibit a maximum. In Figure 23, the *pretwisted* compounds **16** and **21**, which emit only the F_A fluorescence, exhibit clear maxima in hexane + EtOH mixtures. In the same solvents, the rigidly flat **20**, emitting only the F_B fluorescence, has a constant $\Delta\tilde{\nu}_{1/2}$ value. Complex formation of the CT states of **16** and **21** with EtOH is therefore supported by the maxima in Figure 23.

The origin of the isoemissive point in the case of **21** (Figure 21) is still an open question. However, the absence of any extrema on the full width at half-maximum (fwhm) plot in the mixture hexane + CH_2Cl_2 (along with the constancy of the transition dipole moment in emission, Table 5) is evidence *against* exciplex formation, at least in aprotic polar solvents.

Somewhat different are the cases in which the molecule emits a dual fluorescence. Then, it would be less astounding to observe an isoemissive point, as the above conditions (ii) and (iii) are often fulfilled; one can, however, expect a solvatochromic shift of the CT emission, against condition (i). Such an isoemissive point is reported for the molecule **25** in methylcyclohexane + ACN mixtures.[154]

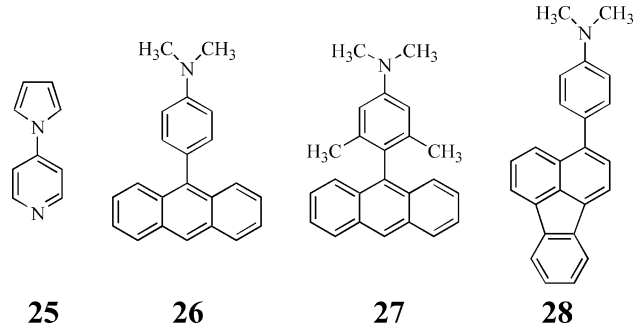

25 **26** **27** **28**

In summary, the appearance of isoemissive points in the fluorescence spectra of some analogues of **1** in mixed solvents remains mysterious. In rhodamine dye lactones, which are quite different CT systems, isoemissive points were observed as well, although the conditions usually accepted as necessary for the appearance of an isoemissive point were also violated by the solvent shift of the spectra.[155−157]

B. Dipole Moments

To check the charge separation inferred for DMABN and the related molecules in the excited state, the excited-state dipole moments were theoretically calculated and measured experimentally. The latter is most frequently done by measuring the solvatochromism,[127] either from the solvent polarity effect on the Stokes' shift,[16,67,68]

$$hc(\tilde{\nu}_{abs} - \tilde{\nu}_{flu}) = hc(\tilde{\nu}^{o}_{abs} - \tilde{\nu}^{o}_{flu}) + \frac{2(\vec{\mu}_e - \vec{\mu}_g)^2}{a_o^3}\left[\frac{\epsilon - 1}{2\epsilon + 1} - \frac{n^2 - 1}{2n^2 + 1}\right] \quad (13)$$

or from the fluorescence shift alone (eq 14), which is advisable if the absorption and emission transitions have different orbital origins. The latter is usually the case for the CT emission of molecules with dual fluorescence.

Table 3. Experimental Values of the Dipole Moments (in Debye Units, 1 D = 3.34 × 10^{-30} C·m) of the Excited State of DMABN and Some of Its Derivatives[a]

compd	μ_G	μ^{FC} [b]	μ_B^{eq}	μ_{CT}^{eq}
1	(4.5)[A,c]	14.9[A,h]	11.4[S,h]	(23)[S,m]
	6.2[D,c]	12.6[A,j]	10.0[T,k]	12.6[S,n]
	6.1[D,A,d,e]	11.0[A,c]	5.7[E,h]	17.3[S,o]
	6.6[D,l]	13.0[S,h]	9.1[C,i]	18[S,u]
			9.7[C,l]	19.5[T,k]
				16.5[E,h]
				14−15[C,i]
				16.1[C,l]
16	(2.9)[A,c]	11.9[A,c]		15.5[E,e]
	5.1[D,c]			
21	(2.8)[A,c]	14.5[A,c]		11.8[E,s,t]
	4.5[D,c]	10−11.5[S,q]		15−18[T,p]
	4.5−4.8[F,f]			12−14.5[E,e,h,s]
				14.8[C,i]
22	4.0[F,f]	11.4[S,h]		13−15[S,r]
	3.9[A,g]			12.3[S,h]
23			6.1[E,e]	17.0[E,h]
24			6.1[E,e]	17.2[E,h]
20	6.2[F,f]		6.0[E,e]	
42				16−18[S,v]
29			6.2[E,h]	
30	6.7[D,l]		7.2[E,h]	16.4[E,h]
				17.3[C,l]
32			6.5[E,h]	13.5[E,h]
33			5.7[E,h]	
35				15.9[E,e]
39				17.4[C,l]
40	6.7[D,l]			17.4[C,l]

[a] Key to subscripts and superscripts: G, ground state; B, primary excited state; FC, Franck−Condon state (reached in absorption); eq, equilibrated excited state (fluorescent state); CT, the A* (TICT) excited state; D, dielectric measurement; S, solvatochromy; T, thermochromy; E, electrooptical method in emission; A, electrooptical method in absorption; C, transient dielectric loss or time-resolved microwave conductivity; F, electric field anisotropy. Methodically less reliable values are in parentheses. [b] Corresponding to the main (^1L_a-type) absorption maximum in UV. [c] Sinha, H. K.; Muralidharan, S.; Yates, K. *Can. J. Chem.* **1992**, *70*, 1932. [d] Baumann, W. *Z. Naturforsch.* **1981**, *36a*, 868. [e] Reference 12. [f] Reference 191. [g] Reference 581. [h] Reference 116. [i] Reference 96. [j] Reference 158. [k] Suppan, P. *J. Luminesc.* **1985**, *33*, 29. [l] In dioxane.[99] [m] Reference 63. [n] Reference 7. [o] Reference 161. [p] Reference 137. [q] Reference 135. [r] Reference 132. [s] Reference 136. [t] In the gas phase. [u] Reference 114. [v] Reference 170.

$$hc\,\tilde{\nu}_{flu} = hc\,\tilde{\nu}^{o}_{flu} - \frac{2\vec{\mu}_e(\vec{\mu}_e - \vec{\mu}_g)}{a_o^3}\left[\frac{\epsilon - 1}{2\epsilon + 1} - \frac{1}{2}\left(\frac{n^2 - 1}{2n^2 + 1}\right)\right] \quad (14)$$

In these equations, the superscript "o" indicates the absence of a solvent (free molecule), μ_g and μ_e are the ground- and excited-state dipole moments, a_o is the radius of the Onsager cavity, ϵ is the static dielectric constant, and n is the optical refractivity index of the solvent. The approximation used (rigid point dipole in the center of a spherical Onsager cavity) neglects the polarizability of the solute.

Other measurement techniques exploit the electrochromism,[158,159] thermochromism,[160,161] time-resolved dielectric loss (TRDL),[162] or time-resolved microwave conductivity (TRMC).[163] Some selected experimental values are given in Table 3. The scattered data for the CT state of **1** center around 13−17 D (i.e., (45−55) × 10^{-30} C·m), which corresponds to a state with a full electron transfer from the amino N atom roughly to the center of the aromatic ring (Figure 24). The somewhat lower values of μ_{CT} for **22** compared to **1** may result from the nonaxial symmetry of **22**, as well as from the nonplanarity (pyramidal bonds arrangement around N^+) of the cage amine skeleton (cf. section I.C). Some data (anisotropy of the emission, absorption coefficient of **22**) hint at an admixture of a $^1\pi,\pi^*$ state lying close to the CT (here, the n,π^*) state.[164] In the case of the sterically hindered derivatives **16** and **35**, the dipole moments measured with the integral electrooptical emission method (IEOEM) indicate a less polar emitting component (B*) in nonpolar solvents. The measured excited-state dipole moment value μ^* changes with the polarity of the solvent from 11.7 D in heptane to 15 ± 0.7 D in medium-polarity solvents ($\epsilon > 5$).[165]

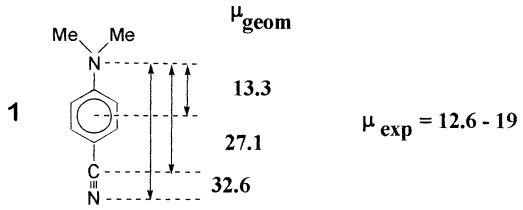

Figure 24. Dipole moment (in debye units) of the CT excited state of **1** (DMABN): μ_{exp} as compared to the values μ_{geom} corresponding to the full one-electron transfer from the amino nitrogen to several positions in the molecule (at the ground-state geometry; bond lengths from the crystal structure,[166] bond angles from the CAS calculation[167]).

There are several comprehensive reviews on the excited-state dipole moments of DMABN and analogous D−A compounds.[116,165,168] The results, especially on comparing the dipole moments of DMABN and its sterically hindered or rigid derivatives (Table 3), are interpreted as follows:

(i) The experimental results are scattered, but are independent of the method of measurement.

(ii) There is practically a full separation of charges in the emitting CT state, in agreement with numerous theoretical calculations for the decoupled $D^{\bullet+}$ and $A^{\bullet-}$.

(iii) The dipole moments μ_{CT}^{eq} are approximately solvent-independent in weakly or strongly polar media, which means that the polarizability effects in the charge-separated structure seem to be small. The values for the sterically crowded compounds[169] are somewhat lower in nonpolar solvents, probably due to a broader angular probability distribution (the *atomic polarizability* effect[116]).

C. Radiative Rates and Transition Moments

1. Quantum Yields and Radiationless Deactivation Processes

The fluorescence quantum yield of the primary excited state of DMABN in nonpolar hydrocarbon solvents is reported to be $\phi_B = 0.27$,[94] $\phi_B \geq 0.2$,[153] or $\phi_B = 0.18$.[170] With increasing polarity of the solvents, the quantum yield of F_B drops by 2 orders of magnitude because a new and faster depopulation channel—that of the excited-state ICT reaction — is being switched on.

Table 4. Exemplary Radiative Rates, k_{f_A}, of the CT Fluorescence of DMABN and Some Analogues[a]

molecule	solvent	$k_{f_A}/10^6\ s^{-1}$ ($T = 298$ K)	ϵ_1/cm^{-1}	$k^o_{f_A}/10^6\ s^{-1}$ upper limit	refs
1	BuCl	13	161	6.2	171,172
30	BuCl	14	140	7.1	171,172
45	ACN	5.4			133
23	BuCl	10	324	2.3	171,172
24	BuCl	16	160	7.7	171,172
36	BuCl	12	288	3.2	171,172
21	PrOH	5.1	250	1.4	70,135
22	ether	7			190
	ACN	3			
42	HEX	9	(130)	6	170
70	BN	14	590	1.3	*b*
26	MTHF	53	130	20	4,236
27	MTHF	7.3	120	3.0	4,236
62	toluene		350		225

[a] For the temperature dependence (eq 15), ϵ_1 and the upper limit for $k^o_{f_A}$ (value of k_f measured at the lowest temperature) are indicated. [b] Recalculated from: Dobkowski, J.; Karpiuk, J. In *Kinetyka Nieklasyczna*; Grabowski, Z. R., Karpiuk, J., Eds.; Inst. Phys. Chem., Polish Acad. Sci.: Warsaw, 1989; p 102.

A decrease of the quantum yield is observed in numerous protic solvents, especially in the more strongly proton-donating ones (cf. Figure 56). The strongest quenching occurs in water (cf. section IV.C).[114]

2. k_{f_A} Values and the Temperature Dependence of k_{f_A}

The radiative rates of the F_A band, k_{f_A}, in **1** and its analogues are low, indicating a forbidden optical transition. Especially interesting is the observed dependence of k_{f_A} on temperature (Table 4): the ϕ_A values, instead of being independent of temperature (see section VI.A, Figure 68), evidently rise with temperature (e.g., Figure 66). The experimentally determined emission rates seem to be activated processes, with small activation energies of a few hundred cm^{-1}.

The thermal activation is linked with the strongly forbidden character of the emission from the zero vibrational level of the TICT state. At increased temperatures, the thermal population should lead to a more allowed emission from higher, non-totally symmetric vibrational levels vibronically mixed with other electronic states (cf. the scheme in Figure 67).[4,70,129,171] Let the residual emission from the zero vibrational level be described as $k^o_{f_A}$. The temperature dependence of the emission rate k_{f_A} will then be described by eq 15,

$$k_{f_A}(T) = k^o_{f_A} + k^\infty_{f_A} \exp[-\epsilon_1/k_B T] \qquad (15)$$

where ϵ_1 means a vibronic quantum of the emissive vibronic level (Figure 25). According to the model represented in Figure 25, the effective emission rate is $k_{f_A} = \int k_{f_A}(\theta) n(\theta)\, d\theta$, with $n(\theta)$ being the angular distribution function.

Introduction of k_{f_A} as the third *temperature-dependent* rate to the set of eqs 19−21 (section VI.A.2) results in the emergence of additional inflection points on the log ϕ vs $1/T$ plots. This agrees with most studied cases of systems analogous to DMABN.[70,172]

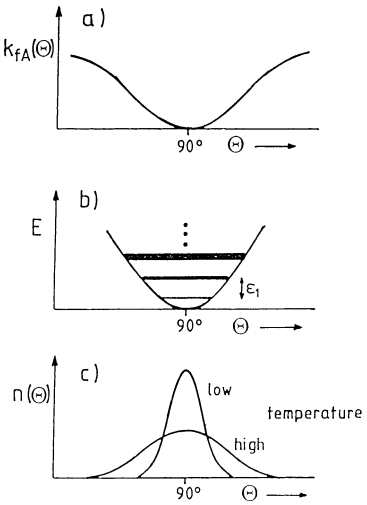

Figure 25. TICT model. (a) Radiative rate k_{f_A} as a function of the twist angle θ around $\theta = 90°$, where the transition is forbidden for the zero overlap twisted conformation (and in the case of **1** also symmetry-forbidden, $A_2 \rightarrow A_1$ in the C_{2v} point group). (b) Non-totally symmetric vibrational levels around $\theta = 90°$ (the thickness of the levels symbolizes the increased transition moment in emission). As ϵ_1 is comparable to kT at room temperature, the population of the excited vibrational levels is not negligible. (c) The (classical) angular population distribution function. Reproduced with permission from ref 172. Copyright 1991 American Chemical Society.

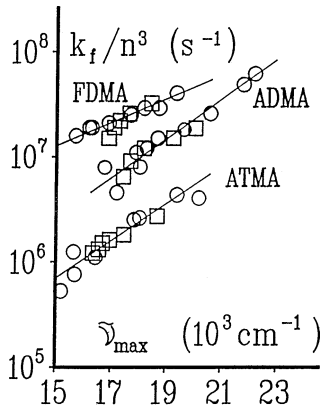

Figure 26. Plots of the fluorescence transition rate ($k_f \sim M^2_{f,CT}$) of **26** (ADMA), **27** (ATMA), and **28** (FDMA) vs polarity of the medium, expressed by the spectral position of the CT emission maximum: ○, in solvents of different polarity, at a constant room temperature; □, in one solvent (MTHF) at different temperatures, in the range 153−298 K. Reproduced with permission from ref 145. Copyright 1993 Elsevier Science.

The characteristic feature of these diagrams is the negative slope of the log ϕ_A vs $1/T$ plots, $d(\log \phi_A)/d(1/T) = -\epsilon_1/k$. From the simpler model, eq 20, and the diagram in Figure 68, is predicted a zero slope above the temperature T_2. In fact, relation (15) seems to hold in those cases in which a transition, otherwise strongly forbidden due to symmetry or due to lack of overlap, gains intensity in a non-totally symmetric (e.g., torsional) vibration. This relates not only to the A−D molecules but also to numerous sandwich exciplexes.[172]

The values of ϵ_1 are found in the range between 100 and 600 cm^{-1} and appear to be more characteristic of the emitting molecule than of the solvent. In

Table 5. Transition Dipole Moments, $M_{A,G}$ (in D), of the CT Fluorescence of 1, 22,[134] and 21[135,148] in Various Solvents

solvent	ϵ^a	$M_{A,G}$ 1	22	21
n-hexane			0.66	0.74
cyclohexane	2.06		0.64	
isooctane	1.95		0.66	
benzene	2.28		0.56	
di-*n*-butyl ether	3.06		0.68	
tert-butyl methyl ether	4.4		0.76	
diethyl ether	7.6		0.74	
tetrahydrofuran	7	1.2	0.71	
n-butyl chloride	7.0		0.68	0.79
1,1,1-trichloroethane	9		0.64	
1,2-dichloroethane	28.6	1.18	0.65	
dichloromethane	36.5	1.17	0.59	0.7
propionitrile	36.7	0.89	0.68	
acetonitrile	38.8	1.12	0.63	
dimethylformamide	36.7	1.03	0.57	
n-decanol		1.26	0.57	
n-hexanol		1.28		
n-pentanol	13.9	1.18	0.6	
n-butanol	17.8	1.23	0.66	
n-propanol	20.1	1.2	0.69	0.72
ethanol	24.3	1.17	0.66	
methanol	32.1	1.22	0.67	
2,2,2-trifluoroethanol		1.11	0.63	

[a] Dielectric constant of the solvent.

the case of **26** (ADMA) and several other D−A molecules with large aromatic moieties (discussed below, section XI.A), characterized by the lowest ϵ_1 values (about 100 cm^{-1}), it has been shown that the apparent thermal activation of k_{f_A} is due to the *changes of polarity* of the solvent with the temperature (see Figure 26).[145] This does not apply to **1** and its close (usually monocyclic) analogues, as their CT transition probabilities are independent of the solvent polarity (see the next section and Table 5).

3. Transition Dipole Moments

The best quantitative measure of the transition probability is the transition moment, usually in the electric dipole approximation:

$$\vec{M}_{CT} = \langle \Psi_{CT} | \hat{\mu} | \Psi_G \rangle \qquad (16)$$

It can be derived from the emission data:

$$|\vec{M}_f|^2 = \frac{3h}{64\pi^4 \tilde{\nu}_f^{\,3} n^3} k_f \qquad (17)$$

The transition dipole moments of the CT (F_A) emissions of **1**, **22** (a model compound for the TICT state), and the sterically hindered **21** appear to be virtually independent of the solvent polarity (Table 5). This is clearly different from the case with the numerous larger D−A molecules such as **26** and its acridyl analogues (cf. section XI).[145,172]

Thus, the observed temperature effect on the transition moment may be either direct (thermal activation) or indirect, by changing the solvent polarity, which influences the molecular and electronic structure (the polarity of fluid solvents generally increases with lowering of the temperature, and the CT bands undergo a red shift). An indirect temperature effect, by changing the solvent polarity, is observed for some large D−A molecules (Figure 26).[145] In the case of DMABN and its close analogues, however, the transition dipole of the F_A emission evidently does *not* depend on the polarity of the medium (Table 5).[173] Thus, the observed temperature effect (Table 6) is due to thermal activation. It can be explained within the TICT hypothesis as a broadening of the angular distribution of the excited-state population around the 90° twist angle (Figure 25). At lower temperatures, when the distribution gets narrower, the transition becomes more strongly forbidden.

Table 6. Transition Dipole Moment, $M_{A,G}$ (in D), of the F_A Emission of 1 in *n*-Butyl Chloride as a Function of Temperature[172] and of the Fluorescence of 21 in *n*-Propanol (Evaluated from Ref 135)

	$M_{A,G}$ at 293 K	at 250 K	at 222 K	at 200 K	at 193 K	at 182 K	at 167 K	at 154 K
1	1.11	1.08	1.04	0.99		0.95	0.89	0.84
21	0.72				0.45			0.4

D. Fluorescence Anisotropy

1. Sequence of States

The lowest two (π,π^*) excited states in benzene and its monosubstituted derivatives are the ^1L_b (the lowest) and the ^1L_a states, in Platt's nomenclature,[174] the corresponding transitions being mutually perpendicularly polarized. In the series of donor−acceptor para-disubstituted benzenes, the ^1L_a state is much more red-shifted than ^1L_b with increasing donor and acceptor strength. They become degenerate somewhere close to DMABN, and their order is reversed with still stronger substituents (Figure 27).[63,64,70]

The polarization spectra of **1** in frozen solutions close to the 0−0 transition are opposite in sign to

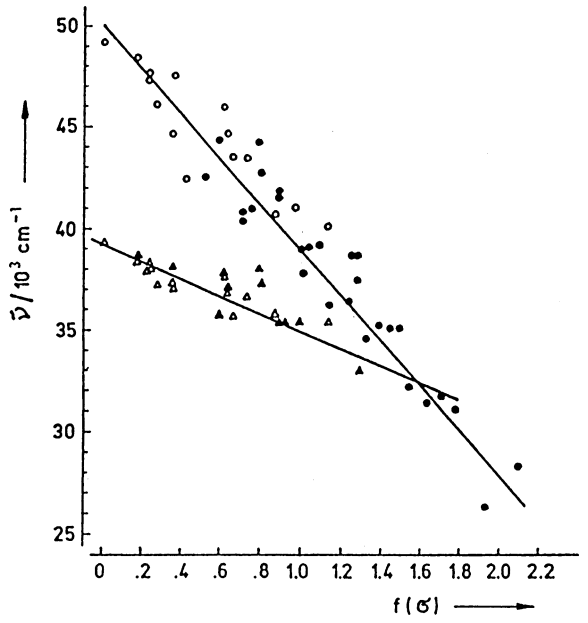

Figure 27. $^1L_a \leftarrow G$ (○,●) and $^1L_b \leftarrow G$ (△,▲) absorption maxima of the monosubstituted (○,△) and para-disubstituted (●,▲) benzenes as a function of the Hammett substituent constants, $f(\sigma)$, defined in the endnote.[175−177] For **1**, $f(\sigma) \approx 1.6$.[178] Adapted with permission from ref 70.

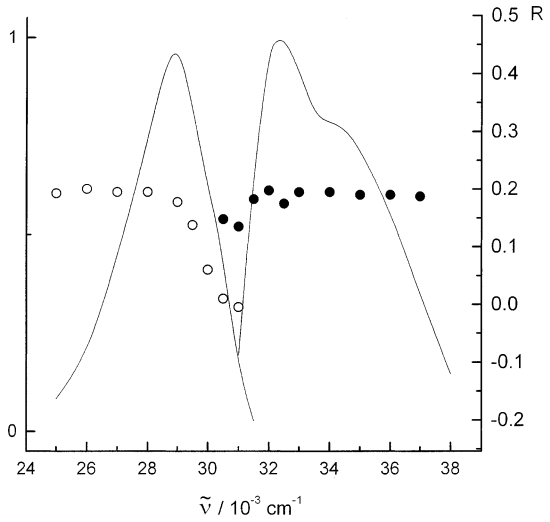

Figure 28. Spectra of **1** in *n*-propanol at $T = 103$ K. Solid curves, corrected fluorescence (left) and excitation spectra (right); open points, fluorescence anisotropy, excited at 32 500 cm^{-1}; full points, excitation anisotropy, monitored at 29 000 cm^{-1}.[182] [Anisotropy $R \equiv 2P/(3 - P)$.[183]]

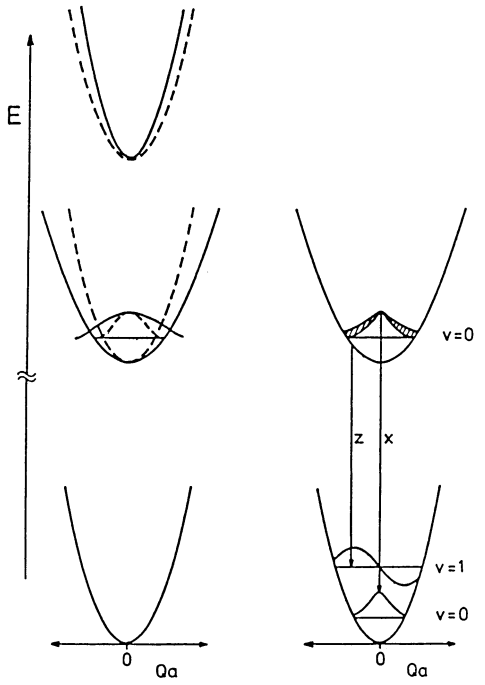

Figure 29. Scheme of the effect of a weak coupling of two crude Born−Oppenheimer states (dashed curves) along a non-totally symmetric coordinate Q_a, e.g., the torsional coordinate in the TICT model. The vibronic admixture of the upper state to the fluorescent state wave function is indicated by the shadowed area. Adapted with permission from ref 181. Copyright 1984 American Chemical Society.

those at at the emission (or absorption) maximum.[64] Examination of the fluorescence anisotropy spectrum (e.g., Figure 28) indicates that the F_B fluorescence originates in the ^1L_b state, with the emission being polarized in the molecular plane and perpendicular to the long axis. The anisotropy R is negative close to the 0−0 transition. Toward the band maximum, it becomes positive and reaches a plateau ($R \approx +0.2$). This low anisotropy value can be interpreted by the Herzberg−Teller coupling mechanism[179−181] in terms of a vibronic mixing, borrowing the intensity in the axial direction from the somewhat higher lying and more intense transition to the ^1L_a state (as in Figures 25 and 29).

The model compound for the *planar* structure of the F_B-emitting state of DMABN, **20**, possesses an anisotropy spectrum which is very similar to that of **1** in rigid solvents.[70,131] In the compounds in which ^1L_b is the lowest excited state, but the Herzberg−Teller coupling to the somewhat higher lying ^1L_a is active, the anisotropy values do not exceed $R \approx +0.2$ (**16**, **20**,[70] **29**,[181] **30**[184]). Fluorescence of dialkylanilines para-substituted with acceptors stronger than the −CN group (e.g., **43**,[70] **30**, **31**, **32**,[185] or **74**[100]) reveals strongly positive anisotropies ($R \approx +0.3-+0.4$), indicating that the ^1L_a-type state is the lowest excited singlet. In the case of **33**, the solvent dependence of the anisotropy of F_B is interpreted as a strong coupling of the two nearly degenerate ^1L_a- and ^1L_b-type states.[181]

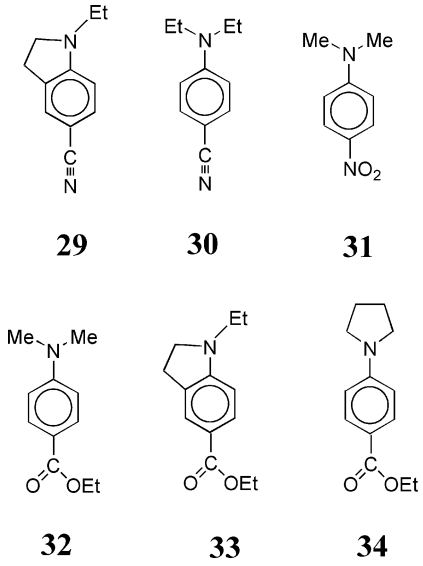

29 **30** **31**

32 **33** **34**

2. CT Emission

The highly positive anisotropy of *both* fluorescence bands of **1** and of some of its derivatives in glycerol[1] (see above, Table 1) was important for inspiring the TICT model. Still more information is contained in the polarized fluorescence spectra in strongly cooled (but still liquid) ethanol[185,186] (Figure 30), or in the more recent polarized spectra in glycerol (Figure 31). From Figures 30 and 31, one can infer that (i) the low-energy CT emission band, F_A, has a pronounced positive anisotropy ($r \approx 0.3$), i.e., its transition moment is oriented along the main molecular axis (the excitation is to ^1L_a); (ii) the anisotropy of F_A is markedly higher than that of F_B. In these measurements, the temperature (or viscosity) already allows the reaction B* → A* to proceed to a noticeable extent, but the external quenching and the rotational depolarization are still negligible.

The explanation of the observation $R(F_A) > R(F_B)$ is evident. The molecules are excited to the ^1L_a state (polarization in the long axis) and emit the F_B fluorescence from a Herzberg−Teller mixed state, whereas after the ET process (in the absence of

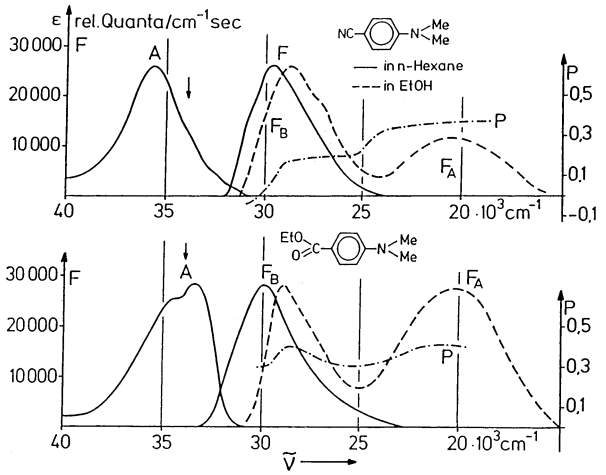

Figure 30. Absorption (A) and fluorescence (F) spectra of **1** and **32** ($c = 5 \times 10^{-6}$ M) in *n*-hexane at room temperature (solid lines). Same in ethanol at $T = 140$ K, $c = 1 \times 10^{-4}$ M (dashed), together with the degree of polarization (P) of the dual fluorescence (dash−dot). Arrows ↓ indicate the excitation wavenumber for the measurements of P.[6,185] Reproduced with permission from VCH Publishers.

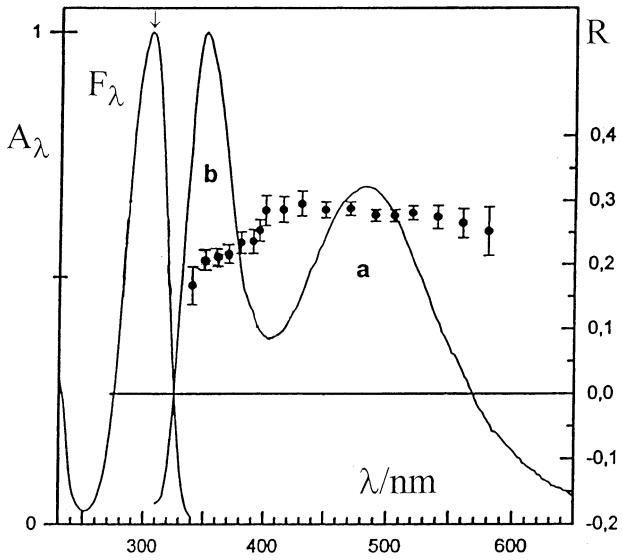

Figure 31. Absorption, fluorescence, and emission anisotropy spectra of the dual fluorescence of **1** in glycerol, $T = 295$ K. The arrow ↓ indicates the excitation wavelength. Adapted with permission from ref 187.

rotational depolarization) the transition moment regains its original orientation.

It should be noted that, in less viscous solutions than those in Figures 30 and 31, the longer-lived A* state (under nonequilibrium conditions) is much more liable to an external quenching reaction than B*.

Every hypothesis has to explain the results on anisotropy, i.e., the symmetry of the ICT state. Within the TICT model, for example, the fluorescence to the (twisted) ground state is forbidden by symmetry, because in the C_{2v} point group the TICT state belongs to the A_2 representation, but more generally due to the lack of overlap between the orthogonal orbitals p_y(N) and π_x*(ring). Deviation from orthogonality, by torsional motion of the approximately flat amino group, lowers the symmetry to C_2. The transition $A_2 \rightarrow A_1$ turns into $A \rightarrow A$ and is no longer symmetry-forbidden; the transition moment increases with growing overlap and is directed along the molecular axis *z*.

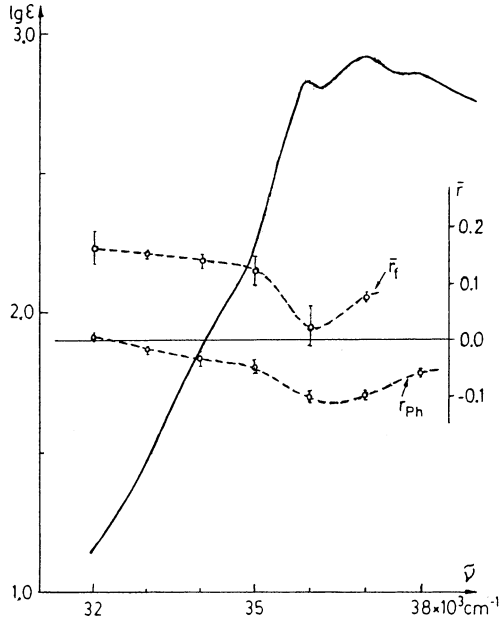

Figure 32. 6-Cyanobenzquinuclidine **22**. Dashed curves, fluorescence excitation anisotropy (r_f) and phosphorescence excitation anisotropy (r_{ph}) in MTHF, $T = 150$ K; solid curve, absorption spectrum in MTHF at room temperature. Reproduced with permission from ref 132. Copyright 1980 Elsevier Science.

If the symmetry of the molecule is lower, as in numerous derivatives of **1** (e.g., **15** or **17**), the TICT state belongs to the C_s point group, the plane of symmetry being that of the ring. In such a case, the TICT emission (A″ → A′) is no longer symmetry-forbidden, and it should be polarized perpendicularly to the aromatic ring.[1,188] It is still, however, forbidden due to the lack of overlap. With a torsional motion, even the plane of symmetry disappears, and in the C_1 symmetry point group it is the direction of the radiative electron transfer which determines the orientation of the transition dipole moment in emission from the CT state.

Time-resolved studies of DMABN fluorescence anisotropy in several fluid solvents[189] resulted in finding the initial values $R(t \rightarrow 0)$ for the F_B band up to +0.13 (in accord with the Herzberg−Teller mixing, as described above), except for glycerol, with $R(t \rightarrow 0) = +0.25$. For the F_A band, $R(t \rightarrow 0)$ is found in the range from +0.2 to +0.25, again except for glycerol which has a higher value, +0.34. While the results for F_B indicate indeed the vibronic coupling of the two lowest $^1\pi,\pi^*$ states, those for F_A are tentatively interpreted in terms of a fast torsional motion (below the time resolution of the instrument), disturbing the initial photoselection. This fast motion may also be understood as the result of intramolecular distortions in the course of the ET process. The exceptional results in glycerol solutions need further insight.

One of the model compounds, **22**, has an anisotropy spectrum[132] which is difficult to explain (Figure 32). The phosphorescence (spectrally identical to that of benzonitrile) is polarized out-of-plane. There is a depolarization or slightly positive anisotropy of the fluorescence excitation in the region of the local π,π^*

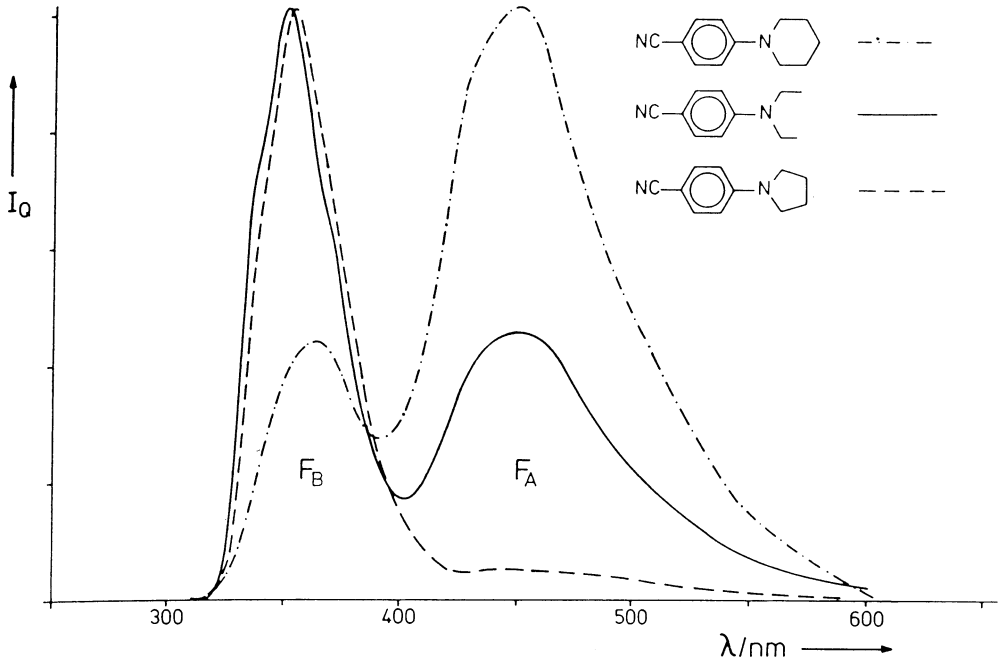

Figure 33. Corrected and normalized fluorescence spectra of **23**, **24**, and **30** in *n*-butyl chloride, $T = 155$ K (in the kinetic regime, cf. eqs 22, Figure 68, in section VI.A.2). Reproduced with permission from ref 171. Copyright 1980 Elsevier Science.

excitation and a moderately positive anisotropy of the long-wavelength n,π^* excitation. The transition dipole of the CT fluorescence evidently has an out-of-plane component (A″ → A′) and another in the direction of the ET.[132] These conclusions find unexpected support in the X-ray crystallographic study of **22**,[190] with the deviation of the molecule from C_s symmetry, which has previously been assumed from the molecular formula. Any deviation from C_s symmetry (including the *out-of-plane* vibrations) would mix the pure ET state (^{1}n,π^*) with the local $^1\pi,\pi^*$ state. The rather high molar absorptivity coefficient in the first (CT) absorption band of **22** ($\log \epsilon \approx 2$, in ACN solution[132]) seems to indicate, indeed, a vibronic mixing with the nearby local $^1\pi,\pi^*$ state bearing a transition moment. This conclusion is supported by quantum-chemical calculations with the DFT method.[164]

Another experimental method, electric field-induced anisotropy spectroscopy, permitted Baumann et al.[191] to correlate the anisotropy spectra with the direction of the permanent dipole moment of the ground or excited state. In the case of **20**, the planar model compound for the B* state of **1**, and in the cases of **21** and **22**, which served as model compounds for the TICT emission, the results verified the data and conclusions reported above.

E. Closely Analogous Compounds

With the growing interest in the peculiar properties of excited DMABN, many new compounds were specially synthesized to gain further insight into the photochemical behavior of D−A molecules with various donors D and/or acceptors A. The papers on such compounds, studied quite independently of their analogies with **1**, are briefly reported in this section. Only the D−A molecules with one benzene (or pyridine, pyrimidine) ring are described here; those with two aromatic rings, or with polycyclic systems, are presented by some examples in section XI.

1. Aliphatic Amine Donors

a. Tertiary Amines. The $-NMe_2$ donor in DMABN can be replaced by another aliphatic or alicyclic amino group. If there are no steric restrictions to internal rotation, most of these compounds reproduce the characteristic features of **1** — the dual fluorescence and the CT character of the relaxed excited state — with only some quantitative differences in rates, energies, etc. Compounds **23** and **24**[171] can serve as examples: both compounds reveal dual fluorescence, but the CT band is relatively much more intense in **24** (Figure 33), though for the larger, six-membered ring, one could intuitively expect a slow-down of the structural relaxation (via inner rotation to a TICT state) as compared to that for **23**.

The higher F_A/F_B intensity ratio in **36** vs **23** also seems to contradict the twist mechanism, in view of the more voluminous donor group in **36**. The larger rate of the B* → A* process in the case of **36** can result, however, from the effect of steric hindrance of the methyl groups (*pretwist*) (cf. Figure 20). In the case of **24**, it was additionally ascribed to the greater flexibility of the six-membered piperidino ring as compared to the rather stiff pyrrolidino ring in **23**, which should play an important role in the hydrodynamic mechanism of the rotational motion.

A real effect of the size of the rotating donor can be seen for the comparison of the same ring as in **37**, but with additional methyl substituents farther away from the benzonitrile ring, **38** (Figure 34). In this case, the size of the rotor slows the process (the effect is observed in the *kinetic* regime, $T < T_1$; cf. section VI.A.2), but the fluorescence spectra of both compounds are identical in the *thermodynamic* (*equilibrium*) regime at $T > T_1$ ($T_1 = 183$ K for **37**, ~200 K for **38** in BuCl[171,192]).

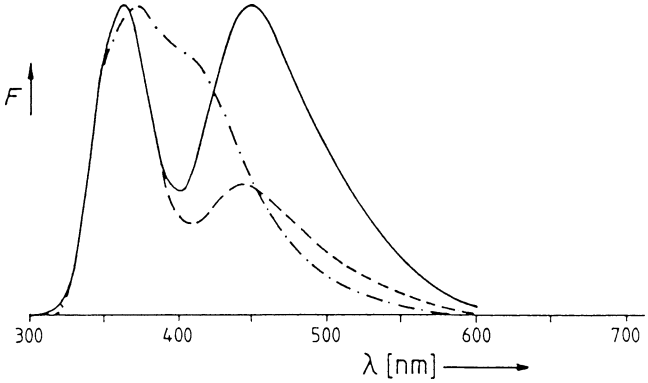

Figure 34. Dual fluorescence of the pair of hydrodynamically differing compounds, **37** (solid curve) and **38** (dashed curve), about 10^{-5} M, in BuCl, $T = 138$ K (in the kinetic regime). At $T = 298$ K, in the excited-state equilibrium regime, both compounds exhibit the same spectra (dash−dot curve).[193] Reproduced with permission from ref 5. Copyright 1986 VCH Publishers.

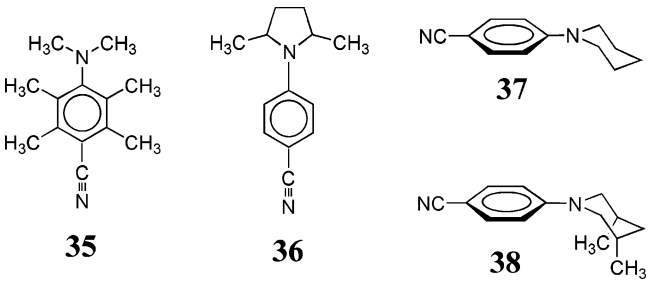

A different picture is emerging from the results obtained by Zachariasse et al. in their research on the DMABN analogues with longer chains at the amino nitrogen (**30**, **39**, **40**; Figure 35).[99,111] Within the TICT model, one could expect that the bulky donor groups would rotate more slowly, which is usually not the case;[194] in the low-polarity solvents the forward rate is as high as or higher than that for **1**.[99] Moreover, a remarkable preference for the CT emission in higher dialkyl homologues of DMABN is noticed.[99] The stationary spectra (Figure 35), with the F_A/F_B ratio growing with the length of the alkyl chain, correspond (in the low- or medium-polarity solvents studied) to the excited-state equilibria. The hydrodynamic friction has no influence on the equilibrium, as in the case of **37** and **38** above, and entropic factors may be responsible for the increased F_A contribution in the compounds with long alkyl chains.

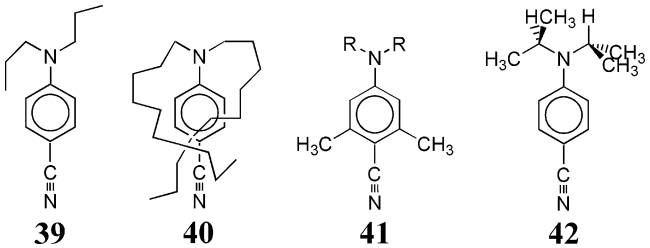

One of the derivatives of **1**, **42** with the bulky isopropyl alkyl groups, has been extensively studied.[170,195] In alkanes as solvents, and apparently even in the vapor phase[196] and in the crystal,[195] **42** emits predominantly the CT fluorescence, though with only a small overall yield. As determined from the solva-

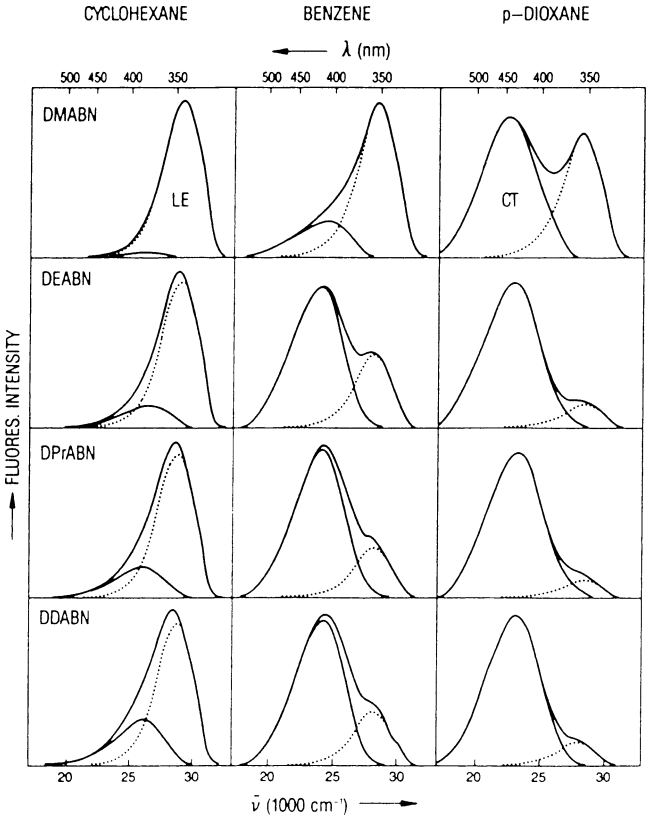

Figure 35. Fluorescence spectra of the molecules with increasing chain length in the $-NR_2$ group: **1** (DMABN), **30** (DEABN), **39** (DPrABN), and **40** (DDABN) in three solvents. The F_A (CT) and F_B (LE) dual fluorescence bands are separated by taking the single fluorescence band of **51** (vide infra) as a standard for the F_B (LE) emissions in the whole series. Reproduced with permisison from ref 99. Copyright 1992 American Chemical Society.

tochromy, $\mu^*_{CT} = 16 \pm 1$ or 18 ± 1 D (using two different evaluation methods). The CT emission band in *n*-hexane has a maximum at 26 050 cm^{-1}. The formation of the CT state in hexane is practically irreversible, i.e., in the kinetic range, (cf. section VI.A), and the deactivation of the CT state occurs mainly nonradiatively with a quantum yield close to 1, via ISC. The kinetics of the B* → A* reaction in hexane at 25 °C correspond to the rate constant $k = 3.4 \times 10^{11}$ s^{-1} ($E_a = 5.7$ kJ mol^{-1}, $k^\infty = 3.5 \times 10^{12}$ s^{-1}).

The lower activation energy of the CT process in **42** vs **1** is ascribed by the authors, in terms of the PICT hypothesis,[110] to a smaller energetic separation $^1L_a - ^1L_b$, and to a somewhat reduced pyramidalization of the bonds around the amino N atom.[170] They note a marked twist of the $-NR_2$ group in the ground-state structure (average ~14°). This *pretwist*, in terms of the TICT hypothesis, can facilitate the CT state formation (compare sections III.A and VI.E).

The authors[99] interpreted the preference for the CT state in the case of large dialkylamino groups as due to an increasing pyramidalization of the bonds around the amino N atom, with no twist. The group of Zachariasse[111] then reported a thorough analysis of the photophysical kinetics and thermodynamics of the series **1**, **30**, **39**, and **41** (R = Me, Et, Pr) in toluene. They stated an increase of the ET rate with

rising volume of the substituents to be related with an increasing preexponential factor (i.e., with a rising activation entropy $\Delta S^{\#}$), not fully counterbalanced by a growth of the activation energy.

The ab initio calculations[106] demonstrate that the pyramidalization of the amino nitrogen in **1** (the wagging coordinate) has a negligible effect on the energy of the excited CT state and on its dipole moment, and it does not couple the two excited π,π^* states.

To explain the phenomena, planar structures of both B* and A* states are assumed,[133,197] with the amino nitrogen inversion as a promoting mode and a strong electronic coupling between D and A in the A* state. Several groups tried to test this hypothesis. The photophysics of DMABN in toluene was assigned by the Varma group to an exciplex formation with the aromatic solvent.[149] The large alkyl effect was studied for a keto analogue of DMABN, **43** (DMAA), in the form of its dioctylamino derivative **44**, and was

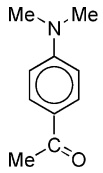

43

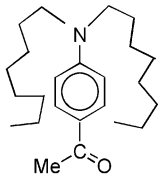

44

found[198] not to contradict the energy terms of the TICT model if the increase of the molecular volume (and/or the ground-state barrier height change[199]) was taken into account. This, of course, also holds for the corresponding DMABN derivatives. Moreover, it is shown that, for symmetry reasons (in the C_{2v} symmetry point group in a coplanar conformation, or in C_s in the case of a pyramidal $-NMe_2$ group), the inversion mode alone cannot mix the ^1L_a and ^1L_b states in DMABN.[198]

Quantum-theoretical calculations at different levels of sophistication did not find evidence for any CT state resulting from the rehybridization of the amino group[9,167,199,200] (except for a high-energy state with pyramidal amino group, thermally unavailable from S_1[199]). Later, Zachariasse et al.,[110,133,201] reporting considerable evidence, formulated the conditions for the appearance of dual fluorescence in **1** and its close analogues as follows:

− a sufficiently small energy gap between the two vibronically interacting lowest excited states, ^1L_b and ^1L_a (CT), leading to a PJT coupling;

− a not too high energy required for rehybridization of the pyramidal amino N atom to a planar structure of the final CT state. A strong coupling between the positively and negatively charged parts of the molecule in a planar (quinoid) conformation, similar to the Scheme 1b, is assumed for the CT state.

A tacitly assumed but very important condition is furthermore that the state of lower polarity (^1L_b-type state) is S_1, such that the energy gap to the highly polar S_2 state could be reduced in polar solvents. This condition is not fulfilled for **43**, **44**, and many further derivatives with a strong acceptor group, where the highly polar ^1L_a-type state is S_1, and which should therefore show in polar solvents a decreasing intensity of the CT band, according to the PJT mechanism. The opposite is observed in the experiment.[202−205]

Parusel and Köhler[206] calculated, using the DFT/MRCI method, the effects of alkyl length and alkyl branching on the excited ICT states of **1**, **30**, **39**, and **42**, and compared their gas-phase theoretical results with the solution data of Zachariasse et al.,[8,99,170] trying to find the factors privileging the CT form with growing alkyl length. They calculated the energy gap $\Delta E(S_2-S_1) \approx 0.3$ eV for **1**, **30**, and **39**. In the case of **42**, it is reduced to 0.08 eV, and this compound is markedly *pretwisted*. The results are rather confusing: they imply[206] that the relaxation of the ICT state within this group of compounds cannot be explained by one single mechanism but that, depending on the compound considered, two different mechanisms lead to the stabilization of the excited CT state. The CT excited state of **42** can be stabilized only by twisting, i.e., by forming a TICT state; also in **1** the TICT state is energetically more stable than the PICT state, whereas the TICT state is less favorable for **30** and **39**. In the latter molecules, therefore, excited-state relaxation would occur toward planarity. In all these compounds, the TICT states should have nearly the same dipole moments, ∼17 D, while the PICT or the ground-state-optimized ICT values are calculated at about 13−14 D. The observation contradicts the theoretical prediction: the dipole moments measured under comparable conditions (e.g., in the same laboratory, with the same method) of the CT states are close one to another, 16−18 D (cf. Table 3), which hints at a common equilibrium ICT state conformation in all of these compounds.

The thermodynamic discussion of the effect of alkyl size[111,133,197] on the excited-state equilibria (see Table 10) seems to need an extension. In the standard expression, $-RT \ln K = \Delta G° = \Delta H° - T\Delta S°$, the entropy change $\Delta S°$ of a CT state formation is usually *negative* (as for the charge separations, or ionic dissociation processes, mainly due to the polarization of the medium). Inspection of the published thermodynamic data[111] shows that the shift in the CT equilibria upon increasing the molecular volume is in most cases due to the less negative reaction entropies (for the polarization of the medium $\Delta S° \sim a^{-3}$)[127] rather than to a decrease of the reaction enthalpies, $\Delta H°$.

From the data reported by Schuddeboom et al.,[99] we note that the dipole moments of the CT state practically do not differ between DMABN, **1**, and its dodecyl analogue, **40**, and the CT emission energy is even higher in **40** than in **1**. In such a case, the equilibrium constants increase with the length of the alkyl chain due to the thermodynamic effects of the increasing molecular volume. This seems to be supported by the spectra of the dimethyl derivatives substituted in the ring, **41** (R = Me, Et, Pr),[111,197] in the excited-state equilibrium regime (Figure 36). As compared to the parent compounds (upper row in Figure 36), the ring-methylated compounds exhibit a higher F_A/F_B ratio, despite a somewhat more negative reduction potential of the acceptor moiety (hence, the CT bands are somewhat blue-shifted).

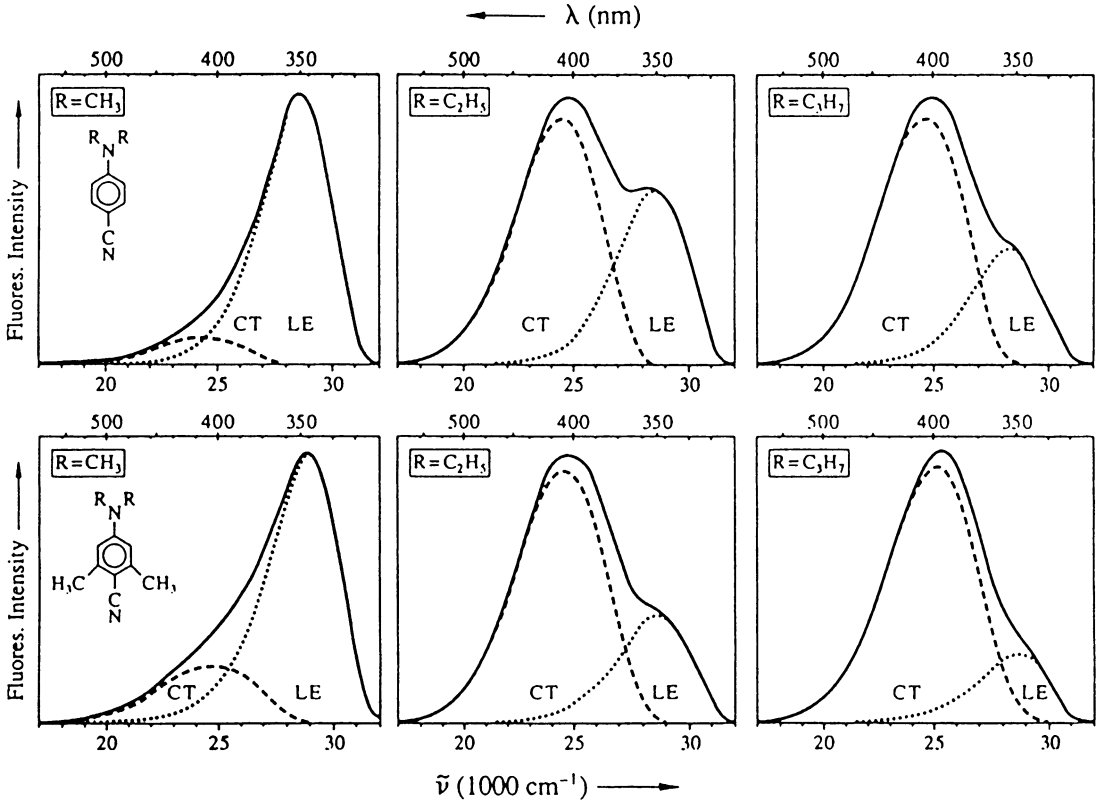

Figure 36. Fluorescence spectra of **1**, **30**, and **39** (upper row), compared to the series of ring-substituted dimethyl derivatives, **41** (R = Me, Et, Pr), in toluene, $T = 298$ K. The F_A (CT) and F_B (LE) bands are separated by taking the only fluorescence band of **51** (vide infra) as a standard for the F_B (LE) emissions in the whole series. Reproduced with permission from ref 133. Copyright 1996 Elsevier Science.

Another interesting series of compounds which initiated a vivid discussion contain the alicyclic derivatives of DMABN, with the three- to eight-membered cyclic amine donor: **23**, **24**, **45**−**50** (Figure 37).[197] **45** does not emit any CT fluorescence, and the

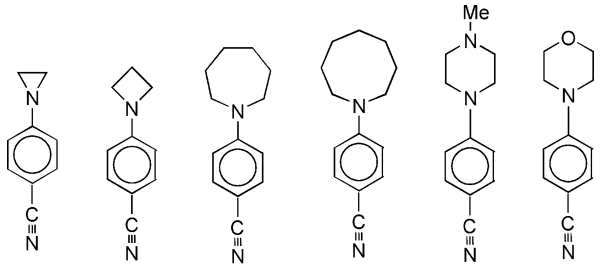

quantum yield of its LE fluorescence is the lowest of the whole series. The low yield may be explainable by the instability of the radical cation of **5** (cf. Scheme 2). **46** in low-polarity solvents exhibits the LE emission only (Figure 37), but in acetonitrile a dual fluorescence is observed (Table 10). The remaining members of the series efficiently undergo the excited-state ET reaction analogously to **1**, which was correlated with the pyramidality of the amino nitrogen atom.[111,133,197]

The properties of the series of N-heterocyclic derivatives of **1**, **45**, **46**, **23**, **24**, and **47** (P3C−P7C) were also calculated by the DFT/MRCI method.[207] In the case of **45**, the strong pyramidalization excludes both a PICT and a TICT relaxation. For other members of the series, the results shown do not seem to support the PICT model: there is no correlation between the energy gap $\Delta E(S_2-S_1)$ and the ease of the ICT state formation. With an exception for **23** as compared to **24**, the energetic preference for the TICT state (but not for the PICT state) increases with increasing ring size. The calculated dipole moments of the TICT states (17−18 D) are considerably higher than those of the PICT states (13−14 D) and consistent with the experimental ones (16−18 D,[133] Table 3).

Similarly to many other CT systems, the fluorescence maxima of numerous D−A compounds, structurally widely different, correlate well with the difference of the half-wave potentials, $E_o^{ox}(D) - E_o^{red}(A)$, in a given solvent (taking, of course, the Coulombic stabilization of the CT state and the destabilization of the FC ground state into account).[126] Then, it was surprisingly reported[197] that, in the long series of *p*-amino derivatives with the same acceptor, benzonitrile, and with widely different aliphatic or alicyclic amines as donor moieties, the energy of the CT emission does not correlate with the oxidation (or ionization) potentials of the donor (Figure 38a). This has been interpreted as evidence for a *strong coupling* of the D^+ and A^- subunits (contrary to the TICT hypothesis of a negligible overlap). The following question remained, however, mysterious and unexplained: How, in any arbitrary model, could the energy of a CT transition be very well correlated with the *acceptor* reduction potential *only*?

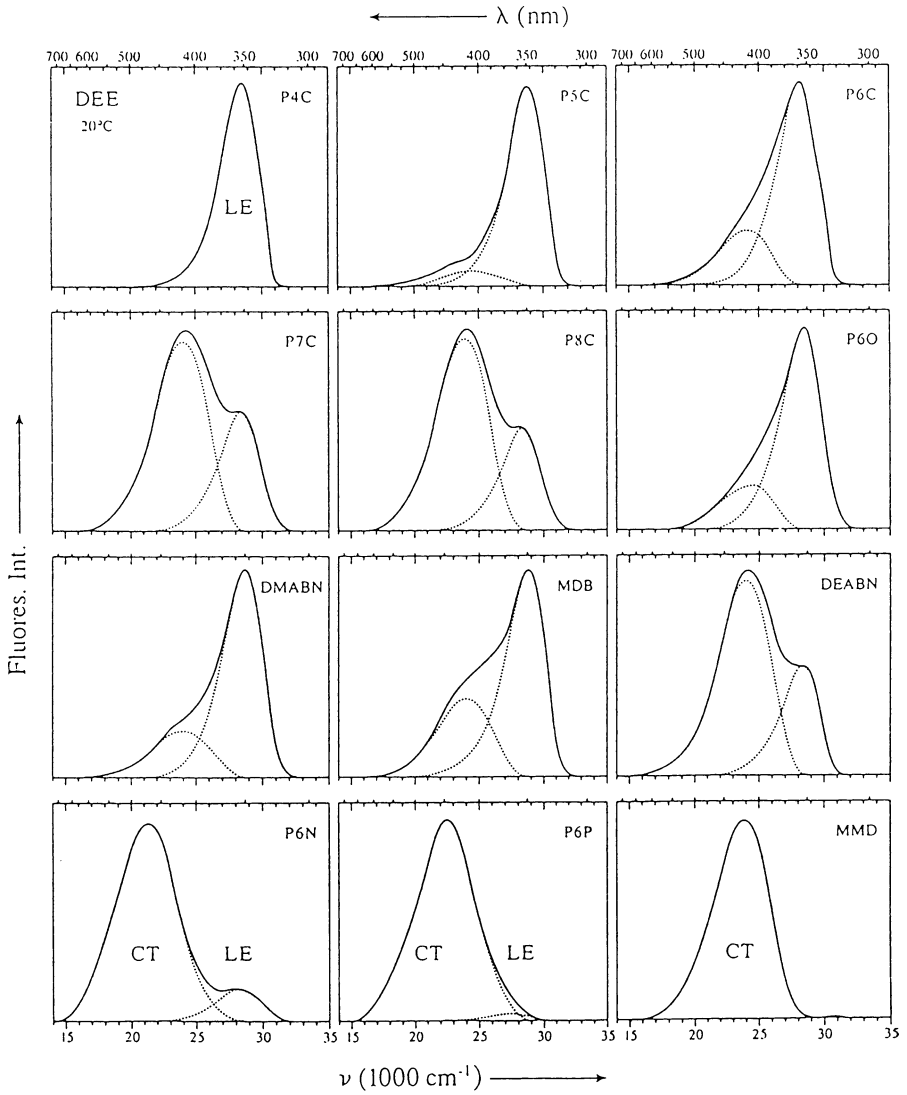

Figure 37. Fluorescence spectra in diethyl ether, T = 293 K. Upper row (from the left): **46** (P4C), **23** (P5C), **24** (P6C). Second row: **47** (P7C), **48** (P8C), **50** (P6O). Third row: **1** (DMABN), **41** (R = CH_3, MDB), **30** (DEABN). Bottom row: **49** (P6N), *N*-phenyl (instead of N-Me) derivative of **49** (P6P), **21** (MMD). Separation of bands as in Figures 35 and 36. Reproduced with permission from ref 197. Copyright 1995 Koninklijke Nederlandse Chemische Vereniging.

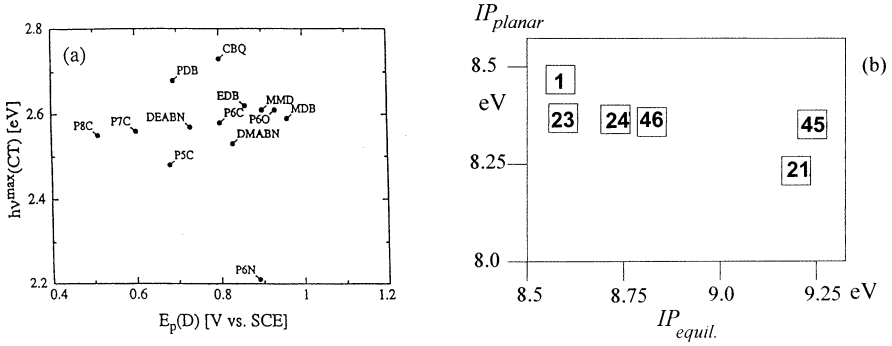

Figure 38. Donor oxidation potentials and CT fluorescence (F_A) in a series of amines, analogues of **1**. (a) Energy $h\nu_{max}$(CT) of a series of 4-aminobenzonitriles in acetonitrile, T = 293 K, vs the peak oxidation potential, E_p(D), of the *N*-methyl derivative of the donor moiety. Compounds: P8C, **48**; P7C, **47**; P5C, **23**; PDB, **41** (with R = propyl); DEABN, **30**; CBQ, **22**; P6C, **24**; DMABN, **1**; EDB, **41** (with R = ethyl); MMD, **21**; P6O, **50**; MDB, **41** (with R = methyl); P6N, **49**. Reproduced with permission from ref 197. Copyright 1995 Koninklijke Nederlandse Chemische Vereniging. (b) Ionization potentials calculated for the *planar* structures of the donor for several D−A molecules, (IP_{planar}), vs those calculated for the optimized (pyramidal) structures, (IP_{equil}). Numerical data from ref 202.

There were two remarkable points in Figure 38a, deviating from the average $h\nu_{max} \cong 2.55-2.60$ eV by more than 0.1 eV: CBQ (**22**) and P6N (**49**). Due to its rather rigid cage structure, cyanobenzquinuclidine **22** ($h\nu_{max}$ = 2.73 eV) *cannot attain the planar structure (sp^2) around the bridgehead N atom*, to fully stabilize the amino radical cations (section I.B, Figure 3). The other compound, **49** ($h\nu_{max} \leq 2.21$ eV), is an

example for the effect of a three-electron bond formation, stabilizing the radical cation in a relaxed structure (which in this case probably has a nonplanar conformation around either of the two N atoms involved[32]), as described in section I.B and in Figure 4. Strong stabilization of the emitting CT state of **49** is possible in the *twisted* structure of the excited molecule. There, both N atoms become nearly equivalent as in aliphatic amines; both n orbitals are degenerate. This is different in a *coplanar* structure (one N atom is aliphatic, the other one is coupled to the aromatic ring; the n orbitals are widely distant energetically, hence the splitting by three-electron bond formation and the corresponding energetic stabilization of the system would be small). Noteworthy is the case of another derivative of piperazine, **54**, not indicated in Figure 38a but reported in ref 197. Its emitting CT state is also stabilized ($h\nu_{max}$ = 2.29 eV), though less than in **49**. Here, in **54**, the conditions are opposite. If the D−A system were *coplanar*, both N atoms would be coupled to aromatic rings, the n orbitals nearly degenerate, and the splitting higher than in the *coplanar* **49**. In the *twisted* structure, one of the N atoms should be decoupled, but the other one remains coupled to the phenyl ring; the n orbitals would be nondegenerate and the splitting smaller than in the *twisted* **49**, in accord with the experiment. All that seems to hint at a *twisted* emitting structure, which hitherto remained unnoticed.[133,197]

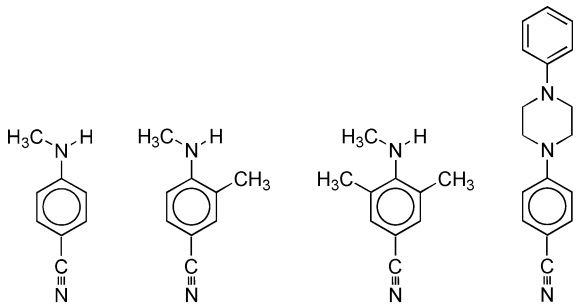

51 **52** **53** **54**

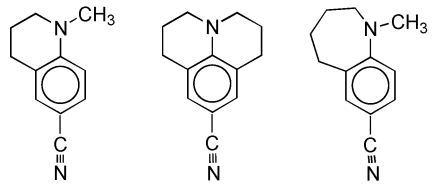

55 **56** **57**

Obviously, the (irreversible) E_p^{ox}(D) values (Figure 38a) or the literature data on the (vertical) ionization potentials are related to the more or less pyramidal equilibrium structures of the nonionized aliphatic amines. These data do not adequately describe the CT fluorescence of the D−A molecules, if the amine radical cations acquire a planar configuration of bonds around the N atom in the CT state. It is shown[202] that the ionization potentials of tertiary amines, calculated with the AM1 Hamiltonian for the planar configuration, *are very little dependent* on the equilibrium IP values (Figure 38b).[208] This finding[202] seems to clarify the situation: the emission from the CT state with an amino donor moiety having an sp^2 N atom to the Franck−Condon ground state of the same configuration may be apparently little dependent on the IP of the corresponding (tertiary) amines.

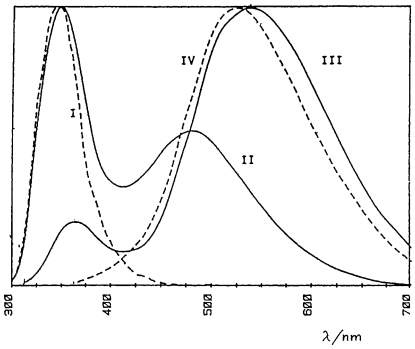

Figure 39. Dual fluorescence of a secondary amine: corrected and normalized emission spectra of **51** (I) and **52** (II), as compared to **1** (III) and **21** (IV) in aqueous solution. Reproduced with permission from ref 211. Copyright 1992 Elsevier Science.

The derivatives of **1** which are *rigidized* with respect to the twist around the $N_{amino}-C_{benzonitrile\ ring}$ bond, e.g., **20**, **29**, **55**, and **56**, emit only the F_B fluorescence.[93,94,130,131,133,181,209,210]

The situation is different for the somewhat more flexible seven-membered ring in the case of **57**, where dual fluorescence with a CT emission clearly appears.[8,92,133] The dipole moment of the CT state has not been reported.

b. Secondary Amines. Although the thermodynamical conditions for the appearance of a CT fluorescence are fulfilled for many secondary aromatic amines, i.e., with a monoalkylamino group as donor and an aromatic acceptor, such an emission has been found, until now, only in the case of (*N*-monomethylamino)benzonitriles with methyl(s) in the ortho position: **52** (MMABN)[211] and **53**[8] in polar solvents (Figure 39).

Surprisingly, the parent compound **51** (MABN) does not show any dual fluorescence under the same conditions (Figure 39), though energetically it would be allowed.[98] The most conceivable explanation for the different behavior of **51** and **52** seems not to be the steric effect of the methyl group, but rather a difference in the barrier height for the TICT formation, resulting from the different energy separation between ^1L_a and ^1L_b states in the two molecules (Figure 40).[211−213] This corresponds to an alternative explanation of the role of the energy gap between ^1L_a and ^1L_b reported and discussed by Zachariasse et al.[8,98,99] in terms of the PJT effect. In the present explanation, this empirical energy gap relationship is interpreted in terms of the torsional motion, with the twist angle θ as the reaction coordinate. The lowering of the barrier in the case of the more stable excited conformer anti of **52** vs **51** is estimated as ∼2 kcal/mol.[211]

The compound with two neighboring methyl groups, **53**, in which the steric effect is strong and the ^1L_a and ^1L_b energy gap is still lower than that in **52**, also exhibits dual fluorescence, with the F_A band being much more pronounced[8] than that in **52**.

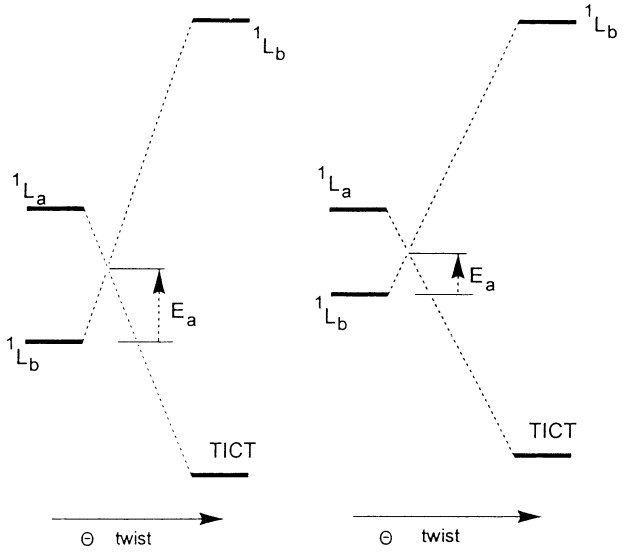

51 **52**

Figure 40. Correlation diagram of excited states for the planar and twisted forms of secondary amines **51** and **52**. Reproduced with permission from ref 211. Copyright 1992 Elsevier Science.

The efficient nonradiative deactivation of the secondary amine **53** was studied in hydrocarbon solvents.[214] **53** emits a dual fluorescence in polar solvents[8] (closely related to the case of **52**[211]), whereas in nonpolar solvents an efficient nonradiative process is assigned to a thermally activated internal conversion (IC) to the ground state. The *pretwist* of the $-NHCH_3$ group in **53** is considered as one of the main factors accelerating the IC.[214] An enhancement of IC in alkane solution was also observed when the acceptor strength was increased (**46** with fluoro substitution on the benzene ring).[215]

The difference between the positions of the maxima of CT fluorescence of **1** and **52** in H_2O (0.25 eV) is close to the difference of ionization potentials (IP_{equil}) of the secondary and tertiary amines[216] In the ester series, secondary amines, even with a long alkyl chain (vide infra, **78**: R_1 = H, R_2 = decyl, R_3 = Et), emit the F_B band only.[217]

c. Symmetric "Double Molecule". The symmetric "*double molecule*" **58**, called sometimes in the literature (misleadingly) a "*dimer of DMABN*",[218,219] is found to emit two fluorescence bands, very similar to F_B and F_A of **1**.[220,221] The molecular structure of **58** in the crystal has been compared to that of **1**.[219]

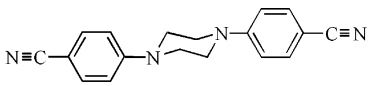

58

The molecule is centrosymmetric, with the ground-state structure different as compared to **1**: the benzonitrile rings are twisted by 18°, and the bonds around the amino N atoms form a flattened pyramid. The $N_{amino}-C_{phenyl}$ bond length increases from 1.360 Å in **1** to 1.389 Å in **58**, because of a weaker coupling. The nonzero twist angle is also observed in the smaller piperidino derivative **24**[209] and is connected with a steric interaction of the ortho-H atoms between the two rings (HH distance ~2 Å). The absorption and fluorescence spectra of both compounds are very similar, but in aprotic polar solvents (BuCl, ACN) the CT emission of **58** is somewhat shifted to lower energies as compared to that of **1**, and the ratios Φ_A/Φ_B are higher. It is clear that a symmetry breaking occurs in the excited state, and the CT state of the A−D−D−A molecule **58** can be described as $A^-{-}D^+{-}D{-}A$. The symmetry breaking is explained by the close vicinity of the two orbitals of **58**, LUMO and LUMO−1 (Figure 41).

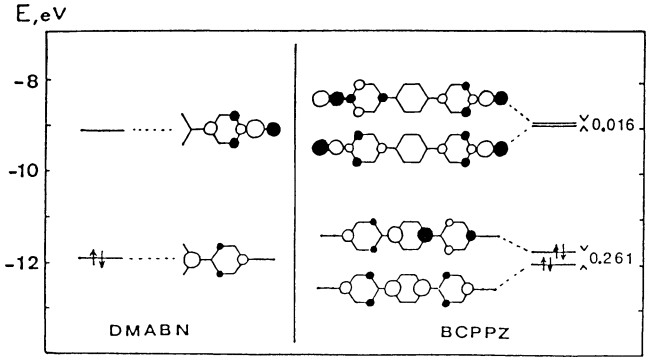

Figure 41. Orbital energies in **1** (DMABN) and **58** (BCPPZ) from extended Hückel calculations. Reproduced with permission from ref 219. Copyright 1993 Elsevier Science.

The dipole moment of the CT state of **58**, measured by time-resolved microwave conductivity, was first reported as $\mu^* \approx 24$ D,[218] later corrected to $\mu^* \approx 10$ D.[222] The measured μ^* value is interpreted as a sum of that of the CT *subunit* $A^-{-}D^+$ (~17 D) and the oppositely oriented dipole moment of the much less polar D−A subunit (the latter estimated to be ~6.6 D, as in the ground state of **1**). It is suggested that a resonance exchange between the CT and the "*nonpolar*" halves of the molecule[220] occurs, on the basis of the microwave conductivity data, with a period of about 20 ps.[222]

The relatively high value for the "CT half", $\mu^* \approx 17$ D,[221] and the higher stabilization of the CT state in polar media, despite a much larger Onsager cavity of **58** than that of **1**, indicate that the dipole moment change upon ET is probably *higher* in **58**. It can be rationalized in terms of a three-electron bond in the piperazine ring (see above, section III.E.1, discussion of the molecule **49** and **54**), which somewhat extends the separation distance of the charges in **49** and in **58**.

An important piece of evidence for the structure of excited molecules is the transient absorption spectrum of the given excited state. The (nanosecond) transient absorption spectrum of **58**, in ACN or in THF, reveals a maximum at 390 nm and a broad, weak band with a maximum around 520−560 nm.[219,221] The first one is observed also in **1** and is characteristic of the benzonitrile radical anion (cf. section IV.A). The long-wavelength band seems to correspond to the piperazine radical cation moiety with a three-electron bond (cf. section I.B, Figure 4). The molecule **58** has been studied in the search for fast molecular switches,[220] in particular its complexes

Scheme 4

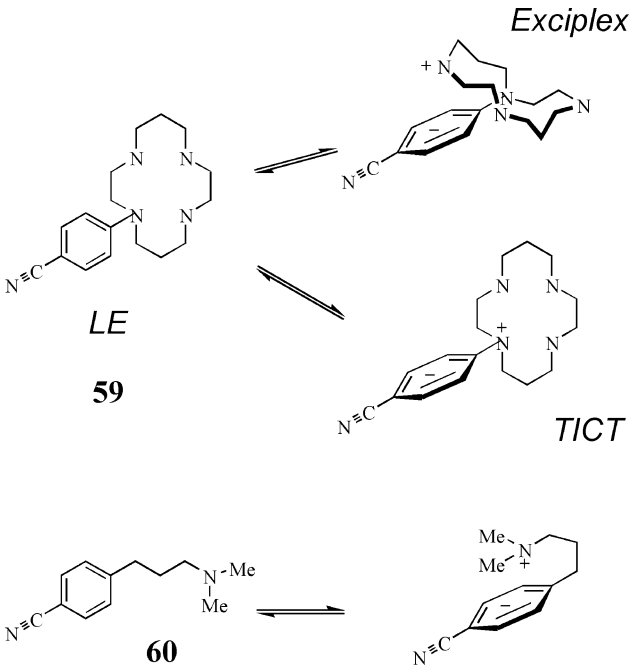

with Ru^{II} and Ru^{III} (Ru being coordinated to the cyano N atoms; cf. section IV.C).

d. Macrocycles. If the amino nitrogen atom of DMABN is a part of a macrocyclic system, e.g., as in the cases of **59**, **61**, and **62**, one observes more complex ground- and excited-state chemistry, which is discussed here only briefly. **59** emits *three* fluorescence bands:[223] one of them, F_B (LE), has a practically solvent-independent spectral position, whereas the other two strongly overlapping bands undergo a solvatochromic shift to a different extent. One of them behaves similarly to the F_A band of **1** and is assigned to a TICT emission. Between them spectrally is the third band, which is assigned to an intramolecular exciplex (Scheme 4) on the basis of a smaller solvatochromic shift than CT, and a similarity to the emission of the intramolecular exciplex of **60**.[224] With increasing polarity of the solvent, the TICT emission grows at the cost of not only F_B but also the exciplex fluorescence.[223] The dipole moment of the TICT state is larger than that of the exciplex.

Two crown ether derivatives of **1** are reported which change their structure, as the crown ethers do, on complexation: **61** (DMABN-crown-4) and **62** (DMABN-crown-5). [225] Both molecules emit two fluorescence bands. CT emission is observed even in nonpolar alkane solvents. The dipole moments of the CT state are close to that of **1**, about 13.5−15 D. The CT band is, however, more pronounced and shifted to lower energies (more in the case of **62**) as compared to **1**. In this respect, **61** and **62** are similar to the DMABN derivatives with long aliphatic chains, e.g., **39** and **40**.

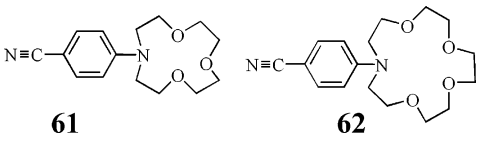

Upon complex formation with Ca^{2+}, the F_B/F_A intensity ratio grows and both bands shift to higher energies, F_B much less than F_A. Evidently, the lone pair of the amino N atom is involved in the complex formation, and the partial (in the B* state) or full electron transfer from this N atom (in the TICT state) destabilizes the excited complex in comparison to the ground state.[226,227] The data reported, including the temperature effects in the kinetics and the thermal activation of k_{f_A} ($\epsilon_1 = 360$ cm^{-1}), are interpreted as supporting the TICT nature of the CT state.[225]

2. Various Substituents on the Ring

It was noticed very early that the *dual fluorescence* characteristic of **1** does not appear in its meta isomer, **64**. Compound **64** emits only *one* fluorescence band, which shifts to the red in polar solvents, but considerably less than for **1**.[8,92,98,202,228] Also in supercooled molecular jet experiments, the van der Waals complexes of the meta isomer with a single polar molecule exhibit a different behavior with respect to line widths, congestion, and lifetime compared to the corresponding complexes of the para isomer.[229] This is tentatively connected with a dynamic coupling of the emitting excited state with another (CT?) state only in *p*-DMABN, as it seemed to be supported by solvation studies in clusters.[230] Neither the DMABN isomers, **64** and **65**, nor the dicyano derivative, **66**, reveals a dual fluorescence: all of them, despite having a reduction potential of the acceptor moiety the same as or less negative than that of **1**, emit in a variety of solvents only one *aniline*-like fluorescence band (analogous to F_B), and its decay is single-exponential.[8,98] An explanation is found in a larger $^1L_a-{}^1L_b$ energy gap as compared to that observed with **1**. In a comparative study of the spectra and photophysical properties of meta and para isomers with several different substituents,[202] it was noted that all the meta isomers have red-shifted spectra in both absorption and F_B fluorescence. The absence of the CT band in **64** can then be readily accounted for using the TICT model. Even if the TICT state of **64** were of the same energy as that of **1** (it is expected to be slightly higher in energy due to reduced Coulomb stabilization[231]), the thermodynamic driving force for the transformation from B* to A* will be considerably reduced in **64**. This has been substantiated by quantum-chemical calculations.[232]

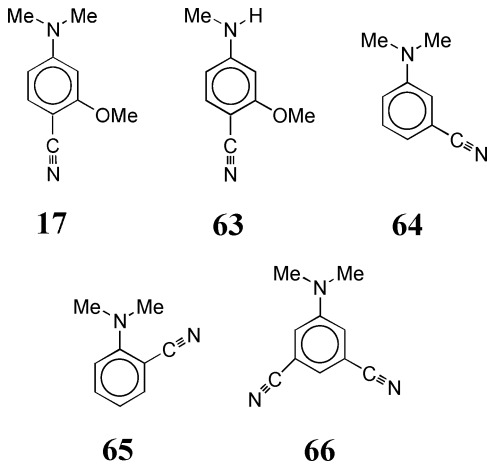

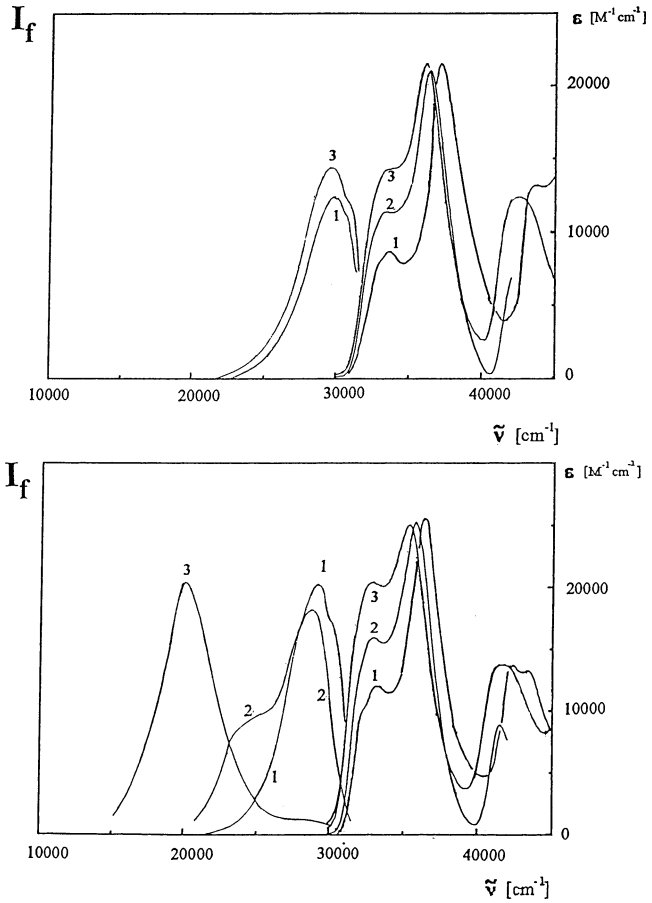

Figure 42. Absorption and fluorescence spectra of the methoxy-substituted DMABN, **17** (bottom), and its monomethylamino analogue, the secondary amine **63** (top). Solvents: (1) *n*-hexane, (2) diethyl ether, and (3) acetonitrile.

Ring-substituted 2,6-dimethyl derivatives of 4-(*N*,*N*-dialkylamino)benzonitriles give rise to a preference for the F_A fluorescence with growing alkyl length.[111] The methyl ring substitution shifts the CT emission to higher energies, though less than expected thermodynamically.[111] The data on the energetics of the cyano derivatives **64** and **66** were also analyzed, indicating a discrepancy between the simple theory of the electronically decoupled CT states and the experiment.[111] The factors which depend on the molecular volume, especially the noticeable differences in the destabilization energies of the FC ground state,[126] seem to have been neglected in deriving this conclusion.

The question of different CT reactivities of positional isomers, with unchanged reduction *resp*. oxidation potentials of the acceptor and donor moieties, linked with the electronic structures and symmetries of the orbitals and states involved, is not clear; it is discussed, inter alia, in sections XI.A.7 and XIII.B.

One of the derivatives of **1** which was first synthesized and studied, **17**, reveals a luminescence which is very much like that of **1** (cf. Figure 66): dual fluorescence and similar spectral positions of the emission maxima.[1,70] The lower symmetry (C_s, and even this is lost with a twist of the amino group) and an additional donor substituent (−OMe) apparently play minor roles in this case. The monomethylamino analogue, **63**, emits only one fluorescence band, which is slightly structured, solvent-independent, and only slightly blue-shifted as compared to the F_B band of **17** (Figure 42).[233]

The absorption spectra of both compounds are characterized by two close-lying bands, whereby the solvent-induced vibronic coupling changes the ratio of band intensities, the long-wavelength one is growing in intensity, and that at shorter wavelengths decreases with solvent polarity[1,233] (Figure 42) or with the concentration of electrolyte ($LiClO_4$) added.[79] The anisotropy of excitation is positive and nearly constant across both absorption bands.[70]

Dual fluorescence is also reported for the *p*-(*N*,*N*-dimethylamino)benzenesulfonate ion, **67**, though only in aqueous solvents. In H_2O, the fluorescence bands at 365 and 475 nm behave kinetically, and with respect to solvatochromy, as an LE and a CT band, respectively. The authors ascribe the CT state to an amino-twisted (TICT) structure.[234]

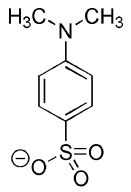

67

3. Carbonyl Derivatives

Dual fluorescence has been reported for several *p*-carbonyl derivatives of *N*,*N*-dimethylaniline (**11**, **43**),[4,70,77,78,235−237] but again not for their meta isomers.[235] The dual fluorescence of these compounds was very similar to that of **1**, except in nonpolar solvents. For these compounds, the S_1 state is of $^1n,\pi^*$ nature, deactivating very fast to the $^3\pi,\pi^*$ state (intense phosphorescence only).[77,78,238,239] As expected for the state sequence,[70,185] the fluorescence anisotropies of these carbonyl compounds in frozen propanol are high, $R \approx +0.35$, close to the 0−0 transition, which indicates that the state reached in absorption is identical with the emitting state. ^1L_a is the lowest excited state in this case, responsible for the F_B emission. No vibronic mixing is observed in the fluorescent state. Another characteristic feature of the low-temperature spectra is the difference between the fluorescence and phosphorescence excitation spectra: fluorescence excitation is shifted somewhat to lower energies, and phosphorescence excitation is shifted by 1000−2000 cm^{-1} to higher energies with respect to the absorption spectrum. Similar effects were reported, inter alia, for several other *p*-D,A-disubstituted benzenes if an effective ISC channel opened somewhat above the 0,0 level of the S_1 state.[240,241]

The reaction times for B* → A*, as estimated from the stationary spectra and low-temperature lifetimes in an irreversible reaction approximation, were found to be a few picoseconds for both **68** and **43** in *n*-propanol.[78] Application of the method of strong fluorescence quenching by O_2 revealed a reversibility

of the excited-state ET reaction of **43** in ACN, with a forward reaction time of about 1.1 ps and an equilibrium constant $K \approx 128$.[237] Later, true picosecond time-resolved methods allowed the reaction rates to be determined more directly for a series of compounds, resulting in the detection of bimodal kinetics with the establishment of an excited-state equilibrium in medium-polarity solvents.[242,243] In the case of

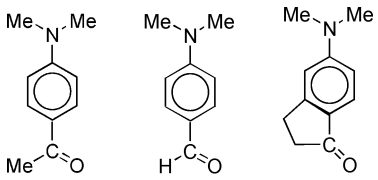

43 **68** **69**

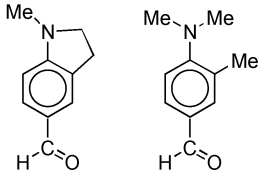

70 **71**

the carbonyl derivatives, the TICT hypothesis offered alternative pathways, as two flexible bonds could be twisted (Scheme 5).

Scheme 5

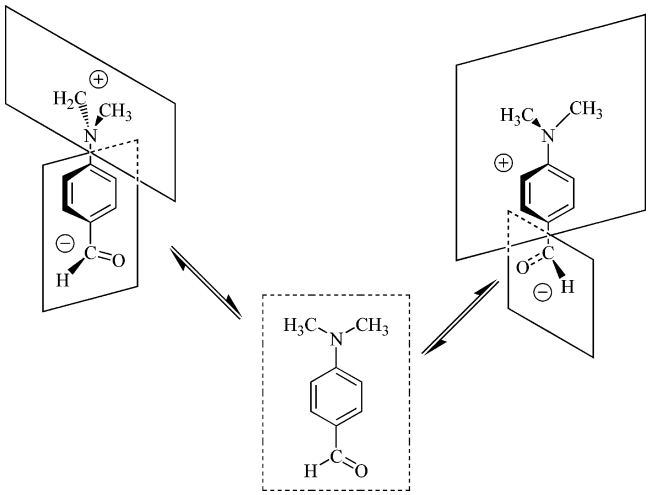

INDO/s calculations[78] indicated that rotation of the $-NR_2$ group would be energetically much more favorable (even with inclusion of the solvation effect, although the *−CHO twisted* state should have a markedly larger dipole moment). Most informative was, however, a systematic experimental study and comparison of a series of suitably *tailored* model compounds:[244,245] **43** and **68** (with the possibility of internal rotation of each of the substituents), **69** (>C=O group fixed coplanar with the aromatic ring), **70** (amino group fixed in the same way), and **71** (with the sterically hindered amino group) (Figure 43).

Similarly to the case with DMABN and its model compounds (Figure 16), the compound with the amino group kept rigid, **70**, emits *only* the F_B fluorescence, while the sterically hindered *o*-methyl derivative, **71**,

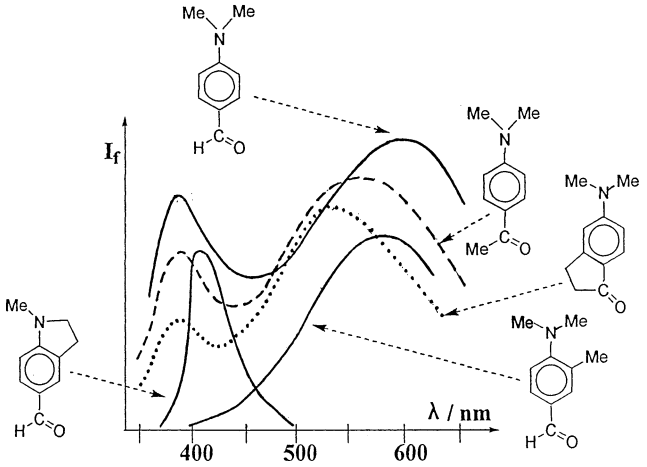

Figure 43. Fluorescence spectra of carbonyl derivatives **43**, **68**−**71** in acetonitrile. Spectra of **43**, **68**−**70** adapted with permission from ref 245; spectrum of **71**, previously unpublished, by courtesy of Dr. J. Dobkowski.

presents only the F_A band; the other compounds emit both fluorescence bands in polar solvents. Analogous, complementary evidence is given by the transient absorption spectra of the excited states of these compounds (see below, section IV.A.2).[142,246]

Both sets of experimental results are, in our opinion, in accord with the TICT hypothesis. Moreover, they are not explicable in terms of the competitive hypotheses: any PJT effects[8,99] would be quite different in these carbonyl derivatives as compared to those in **1**, as the sequence of the low-lying excited states differs radically: due to the ^1L_a -type state being the lower one, any state coupling should *decrease* and not increase with growing solvent polarity. Moreover, the lack of the −C≡N substituent disproves the rehybridization of this acceptor group[9,10] as a cause of the dual fluorescence phenomenon. The AM1 theoretical calculations, including the solvation effects, support the TICT model as a common behavior of both **1** and **68** (Figure 44).[199]

4. Acids and Esters

Dual fluorescence of *p*-(dimethylamino)benzoic acid **72** and its ester **73** appears in polar solvents. The fluorescence of the acid **72** is additionally complicated by the protolytic dissociation in some solvents.[235] Therefore, we focus our attention on the esters. The photophysical behavior of these esters appears closely analogous to that of **1** (solvatochromy of the F_A band, solvent polarity effects on the intensity ratio F_A/F_B, changes of band intensities as a function of temperature). An important difference from **1** and **68** exists in the sequence of states in absorption, as depicted in Figure 45. As the B* state is of ^1L_a type in the esters,[5,181] no vibronic mixing is observed in the F_B emission (cf. Figure 30). In the carbonyl compounds, too (above, section III.E.3), the ^1L_a state is below ^1L_b, as testified by the anisotropy spectra,[70] but in the low-polarity solvents the lowest-lying $^1n,\pi^*$ state quenches the fluorescence via fast ISC: $^1n,\pi^* \rightarrow {}^3\pi,\pi^*$. This is different from the observations with the esters that show sizable fluorescence yields *even in nonpolar solvents*, often with dual fluorescence.[5,100,202] This is especially evident at lower temperatures if

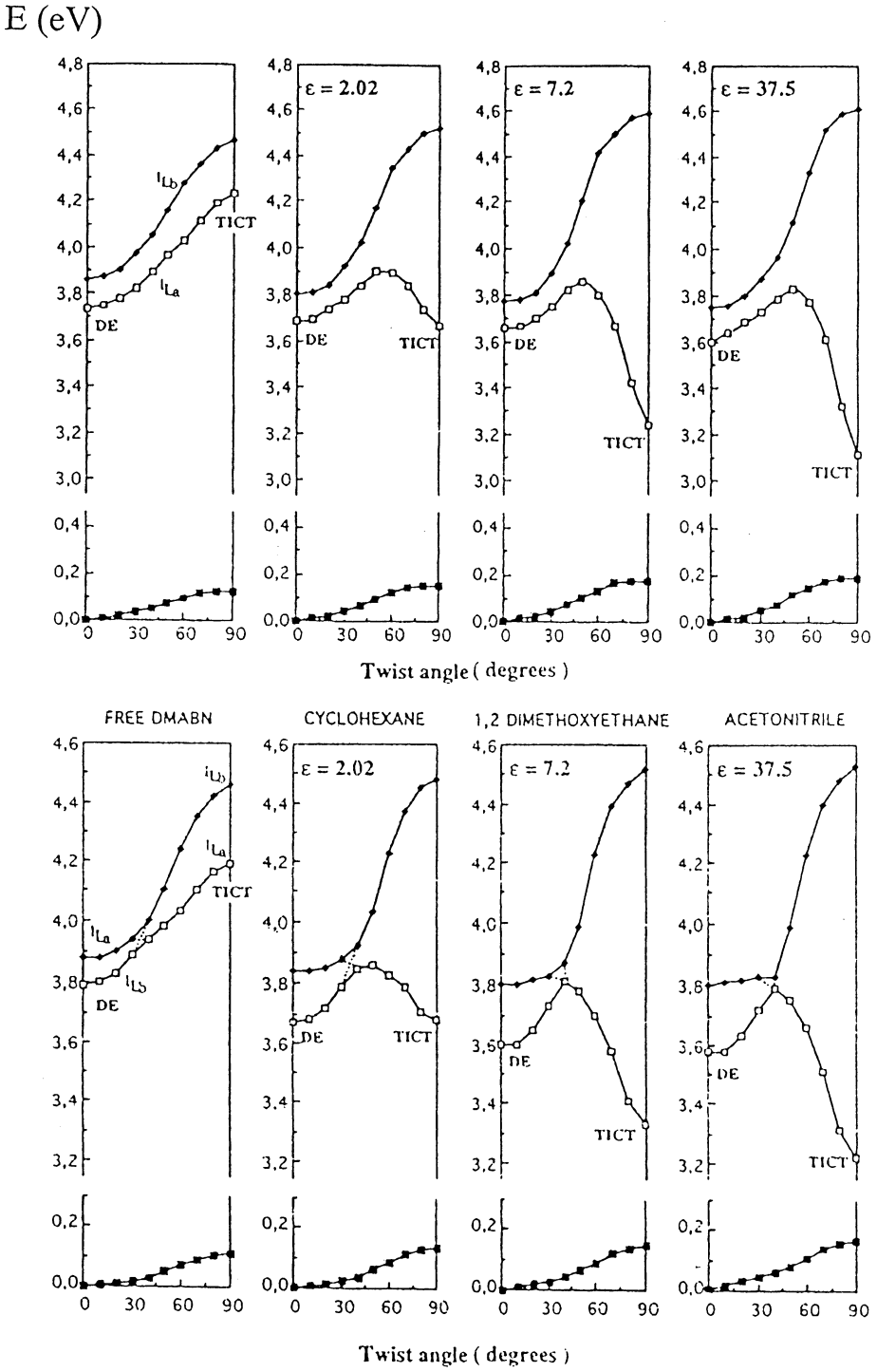

Figure 44. Energy levels of the ground state and of the two lowest excited $^1\pi,\pi^*$ states of **68** (above) and **1** (below) as functions of the twist angle θ in the gas phase and in several solvents of increasing polarity. Calculated with the AM1/"solvaton" model.[247] From the left: free molecule; cyclohexane (ϵ = 2.02); 1,2-dimethoxyethane (ϵ = 7.2); acetonitrile (ϵ = 37.5). Adapted with permission from ref 199. Copyright 1995 American Chemical Society.

the amino group may be somewhat *pretwisted* already in the ground state (e.g., **74** or **75**, cf. Figure 46). The broadening of the F_B emission band of **74** was interpreted as a contribution of a CT fluorescence present even in the gas phase.[248,249]

It is noteworthy that the inversion of ^1L_b- and ^1L_a-type states does not inhibit the dual fluorescence in the carbonyl and carboxy derivatives, though it could be expected on the basis of the PJT hypothesis (see sections II.B.5 and III.E.3, above).

Even the properties of the only observed (mainly F_B) emission band of **32** in alkanes imply a dual fluorescence behavior. The band half-width is measurably increased as compared to that at low temperatures, or to that of **1**, indicating a contribution of a fraction of a CT band which is merged with the F_B band. The band broadening has been verified by several independent groups.[5,250,251] However, already in the case of **73**, doubts have been raised as to the origin of the F_A band. In the case of **72** and **73**, it has

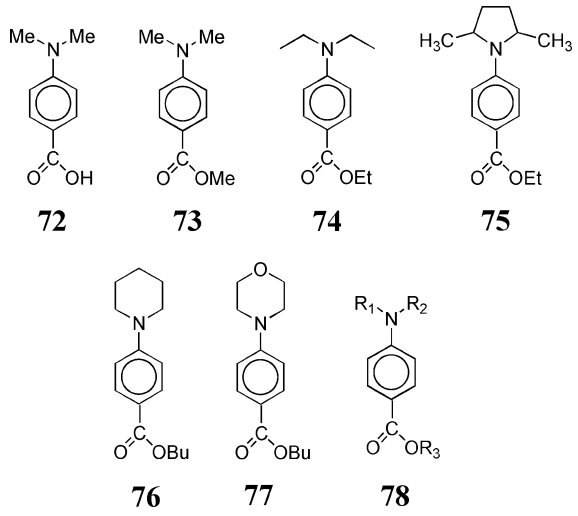

been noticed that the intensity ratio F_A/F_B depends somewhat on the excitation wavelength (in contrast to **1**), i.e., that the two bands have different excitation spectra; the effect was tentatively ascribed to rotameric conformers.[235] In supercritical CHF_3 as solvent, the excitation spectra for the two bands of **32** also differ slightly.[252]

The dual fluorescence of **32** and **73** in alkanes is claimed not to be reproducible.[250,251] From studies in the supercooled molecular jet, the authors ascribed the red-shifted emission band observed there to an excited dimer (vide infra, section V), and upon checking the fluorescence of **32** in pentane solution, they found an excimer emission ($\lambda_{max} \approx 410$ nm) at sufficiently high concentrations of the solute, 10^{-3}–10^{-2} M.[250] Other authors found an excited dimer as the main component of F_A, even in acetonitrile at very low concentrations of **73**, 10^{-6} M.[253,254]

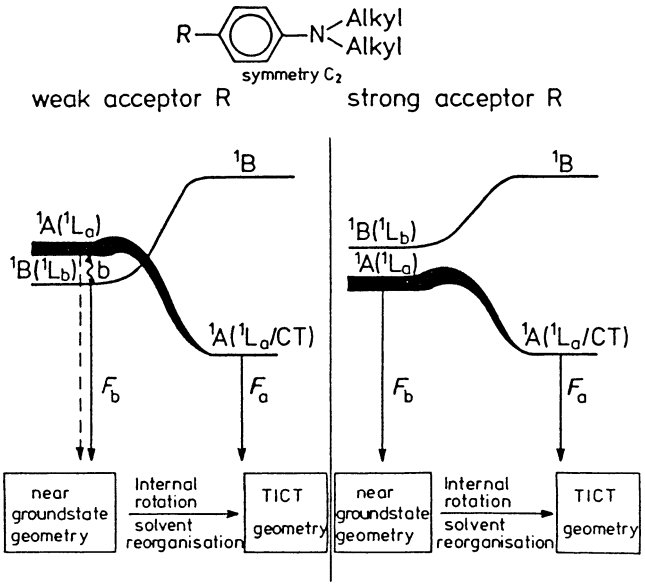

Figure 45. Schematic presentation of the substituent effect on the sequence of states and on the photophysics of *N*,*N*-dialkylanilines with an acceptor group in the para position. Line thickness represents the probability of the radiative transition. −CN belongs to the "weak" and −COOR and −CHO − to the "strong" acceptors (cf. Figure 27). Adapted with permission from ref 185. Copyright 1979 VCH Publishers.

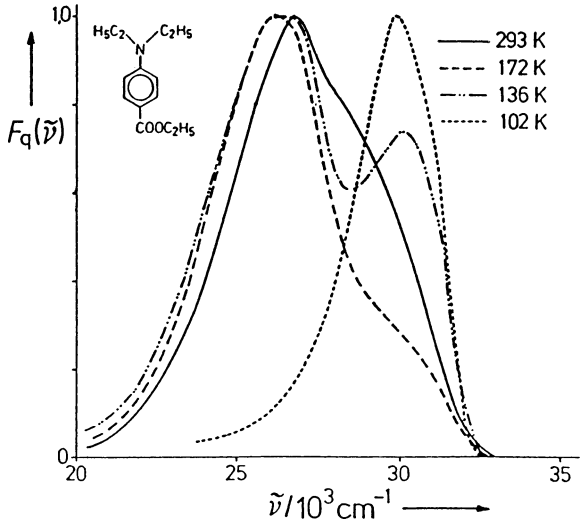

Figure 46. Dual fluorescence (corrected and normalized) of 5×10^{-6} M **74** in MCH + methylcyclopentane (1:1) at the temperatures indicated. Adapted with permission from ref 100. Copyright 1981 VCH Publishers.

Esters with long alkyl chains, e.g., **78** ($R_1 = R_2 =$ Me; $R_3 =$ hexadecyl), are likewise reported to form excimers in various organic solvents + H_2O mixtures. In ethyl acetate, e.g., addition of H_2O quenches the F_A fluorescence (~480 nm), giving rise to an excimer emission (~420 nm).[255] These findings are reported either for high concentrations of the esters or, in the case of aggregation in the ground state, in a saturated solution. The data reported earlier[100] related to very dilute solutions and were independent of concentration in that range (Figure 46).

A thorough study[217] of a large number of various esters **78** , including those with long-chain alkyls in the R_1, R_2, or R_3 position, fully supported the existence of two emission bands of all these compounds (except a secondary amine) in MCH. In addition to the F_B band ($\lambda_{max} \approx 350$ nm, usually only a shoulder), the long-wavelength band ($\lambda_{max} \approx 390$ nm) is predominant at 193 K. In benzene solution at 295 K, the F_A band shifts to ~420 nm and is relatively smaller for the compounds with R_1 or $R_2 =$ Me than for all other derivatives **78**. Starting from ethyl, the size of the alkyls did not regularly influence the ratio F_A/F_B (in contrast to the observations with the derivatives of DMABN[99]). This behavior of the compounds **78** was interpreted in terms of three emitting states, including a specific exciplex with benzene.[217]

Alternatively, it is explained in terms of TICT state formation. The steric effects producing a pretwisted ground-state conformation, or the thermodynamic effects connected with the rising molecular volume (cf. above, section III.E.1.a), seem to play an important role. It is similar to that observed in the other families of D−A compounds emitting dual fluorescence. The indoline derivative with the amino group fixed in the plane of the ring, **33**, emits only one band in all solvents, F_B,[100,181] analogously to **20**, **29**, and **56** in the series of nitriles, or to **70** among the carbonyl derivatives.

It is noted that **32** in *chlorinated solvents* reveals higher emission energies and higher activation energies of the ET processes (in both directions) than in

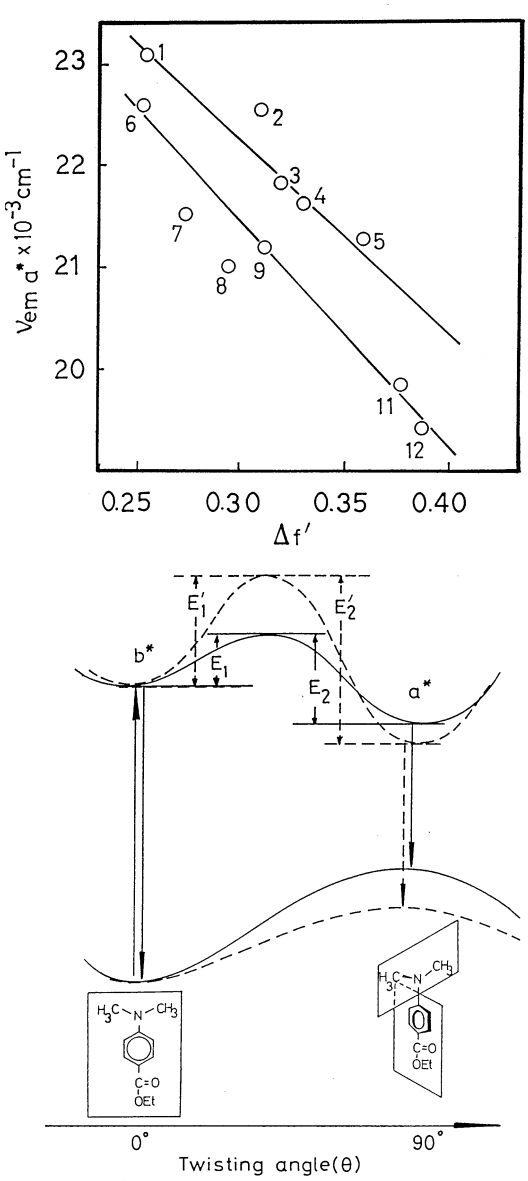

Figure 47. (Top) Solvatochromic plot of the TICT fluorescence of **32** in chlorinated (1−5) and other solvents (6−11). Solvents: (1) $CHCl_3$, (2) BuCl, (3) CH_2Cl_2, (4) 1,2-dichloroethane, (5) di(chloroethyl) ether, (6) diethyl ether, (7) butyl acetate, (8) ethyl acetate, (9) THF, (10) butyronitrile, and (11) ACN. (Bottom) Schematic sketch of the solvent effect on the energy diagram. Solid lines, normal solvents; dashed lines, chlorinated solvents. Adapted with permission from ref 121. Copyright 1990 American Chemical Society.

other solvents.[121] From the difference in solvatochromic plots, it is inferred that the dipole moment μ_A^* in these solvents is lower than that in the other ones (Figure 47), which is ascribed to specific donor−acceptor interactions, different in the ground and excited state. It is mentioned[121] that for several other molecules, anomalies in chlorinated solvents were reported but not interpreted by the respective authors.

(Dialkylamino)benzoates are widely used in polymer research as probes for microviscosity, both in polymers and in polymer solutions.[256−260] Several butyl esters, e.g., **76** and **77**, were used to follow the course of polymerization by the ratio F_A/F_B.[261]

p-(Dialkylamino)salicylic acids and their esters exhibit *triple* fluorescence, whereby one of the bands is assigned to intramolecular proton transfer and the other band is assigned to CT emission. In the esters with the −OH group replaced by −OMe, only the latter reaction is possible. The assignments are supported by the solvent effects and by the transient absorption spectra.[262−264]

5. Pyridines and Pyrimidines

Another family of compounds exhibiting dual fluorescence, similar to DMABN and its analogues described in the preceding sections, also possesses a dialkylamino group as the donor but a pyrimidine or pyridine ring as the acceptor. First, dual fluorescence of **79** was observed, though only in a highly polar solvent, EtOH. In the isomeric symmetric pyrimidine derivatives, the 2- or 5-(dimethylamino)pyrimidines, no dual fluorescence was found. In the case of **80**, only one band was observed in *all* solvents, namely that corresponding to the excited state with a high dipole moment.[265] From the solvatochromic shifts vs the Bilot−Kawski polarity function,[266] the *increase* of the dipole moment in the excited state was found as $\Delta\mu^* = 5.6$ D for **79** in most solvents (F_B), while for **80** $\Delta\mu^* = 11.2$ D (F_A) was determined.[265]

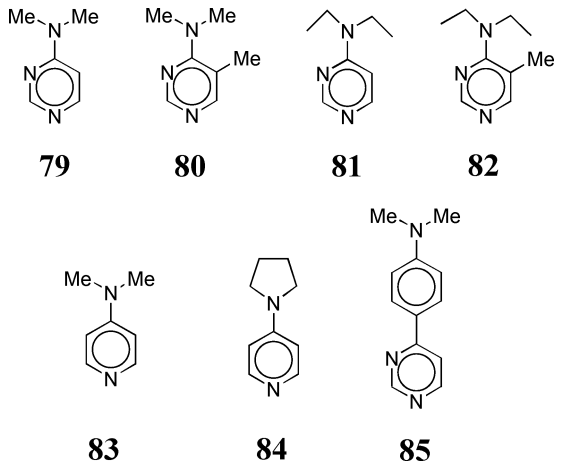

Both fluorescence bands of **79** had indentical excitation spectra. Later, from the solvatochromy of **80**, a dipole moment $\mu_{CT} \approx 13.6$ D was determined.[267] It was shown[268] that, in the case of **79**, even the highly polar solvents do not give rise to the F_A band when they are *aprotic*, such as ACN. In **81**, however, the F_A band clearly appears (Figure 48) in these solvents as well as in alcohols.

Clearly, the H-bonding with the protic solvents promoted the appearance of the F_A band. The protonated or *N*-methylated (in position 1) cations of **79** or **80** did not fluoresce. Therefore, the 1:1 complexes with Zn^{2+} were investigated, and they exhibited the F_A band, shifted to considerably lower energies (Figure 48). These observations imply an enhancement of the acceptor properties of the pyrimidine ring − by hydrogen bonding to the alcohol or by coordination to Zn^{2+} − as the decisive factor in the appearance of the CT fluorescence band in **79**. In the case of **81**, the F_A band appears more easily in polar

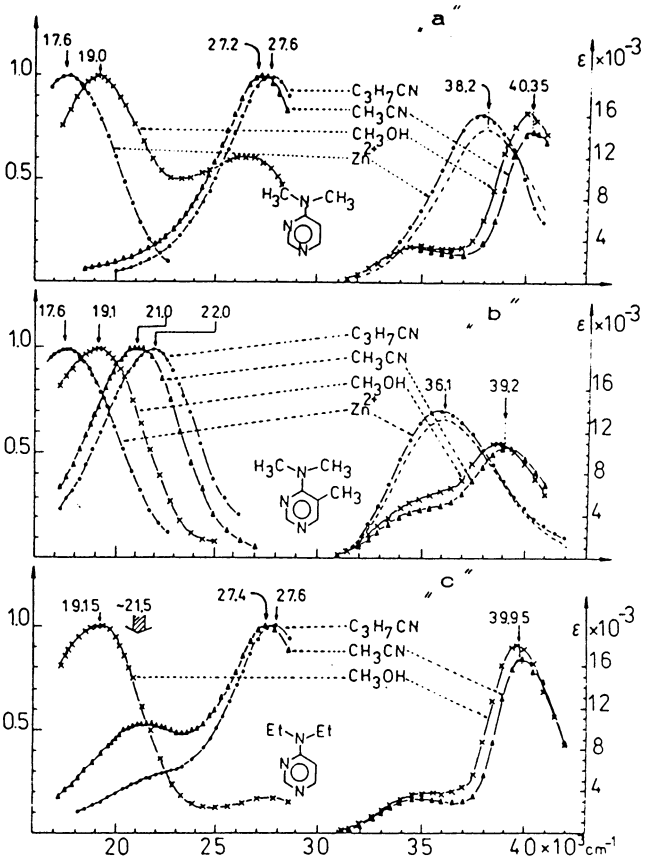

Figure 48. Absorption and fluorescence spectra of (a) **79**, (b) **80**, and (c) **81** in several solvents, and of the 1:1 complexes of **79**, *resp*. **80**, with Zn^{2+} in ACN. The absorption spectra of these complexes nearly match the spectra of the *N*-methylated cations of **79** or **80**, respectively (dashed curves). Reproduced with permission from ref 268. Copyright 1989 American Chemical Society.

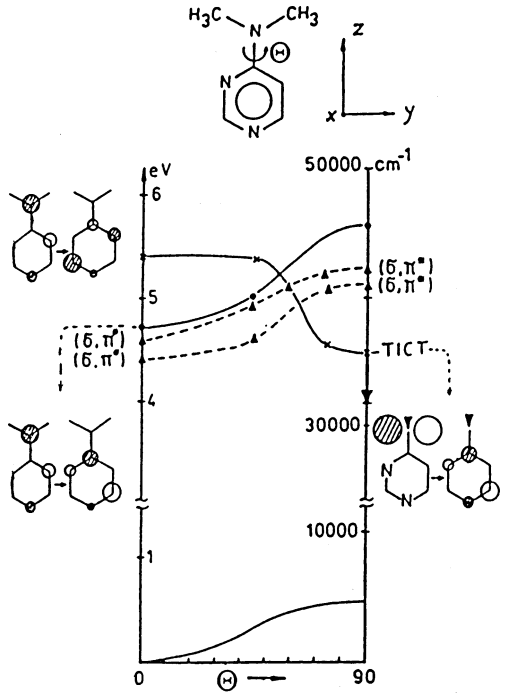

Figure 49. Lower electronic states of **79** calculated by the INDO/S method, for several angles of twist θ around the ring−NMe_2 bond. For the ground-state barrier to internal rotation, 0.6 eV was taken.[269] The dominant configurations of the two lowest-lying π,π^* states ($\theta = 0°$) and of the TICT state ($\theta = 90°$) are shown. The energies of the two $\sigma\pi^*$ states are probably not reliable in this method. The arrow on the right vertical axis marks an estimate of the solvent stabilization in ACN solution. Reproduced with permission from ref 268. Copyright 1989 American Chemical Society.

aprotic solvents, recalling the comparison of **1** and its ethyl analogue, **30**.

The analogy goes further: steric hindrance in the ortho position, i.e., *pretwisting* the amino group, gives rise to the CT fluorescence as the only band in **80**, and very similarly in **82.** The implied assignment of the emitting CT state to a TICT state is also corroborated by semiempirical quantum-mechanical calculations (Figure 49).

One important feature of the TICT model is that the transition in emission is strongly forbidden; this leads to the prediction of a *decline* of the transition dipole moment between absorption and fluorescence. In the case of **80**, these transition dipole moments are 2 D in absorption and 0.7 D in emission (opposite, e.g., to the behavior of 4-(*N*,*N*-dimethylanilino)-pyrimidine **85**, which does not acquire a TICT conformation, with both values practically equal to each other).[267]

Picosecond kinetic measurements indicated that the two emissions of **80** in butyronitrile exhibit a parent−daughter bimodal relationship, establishing the equilibrium within 18 ps. In propanol, the fluorescence kinetics of **79** are very different: a fast multiexponential decay of F_B (very strong quenching is observed in various *protic solvents*) is followed by a common decay at later times (equilibrium). Most probably, of the several possible H-bonded species (there are three different N atoms, i.e., three possible sites of H-bonding in the molecule), only one undergoes the ET reaction; the other sites lead to fast quenching, possibly by a H^+ transfer with formation of a nonfluorescent cation.[270]

The sterically hindered compounds, **80** and **82** — in contrast to the parent compounds **79** and **81** — emit a distinct long-wavelength (presumably CT) fluorescence, even in molecular jets, when clustered with MeOH molecules.[271,272]

The pyridine analogue, **83**, also emits two fluorescence bands[267] (easier than **79**, also in aprotic polar solvents), the bands being independent of the excitation wavelength or concentration (in the range 10^{-6}–10^{-3} M). The dipole moment determined from the solvatochromy of **83** is $\mu \approx 13$ D. In protic solvents, strong quenching reduces the emission below the detection limits; only one ground-state H-bonded complex is observed, at the ring N atom.[266]

In contrast to the interpretation of the H-bonding as described above,[267,268,271,272] Cazeau-Dubroca et al. assign the ground-state hydrogen bonding of **83** not to the ring nitrogen, but to the amino group.[89] The tetragonal ground-state H-bonded amino group should be a precondition for TICT state formation (cf. section II.B.2). These authors ascribe the dual fluorescence in aprotic solvents only to the presence of water (in contrast to other reports[267]). In another laboratory,[154,273] the absorption and dual fluorescence of **84**, evidently implying H-bonding, were interpreted in terms of two types of exciplexes. The twisting hy-

Scheme 6[a]

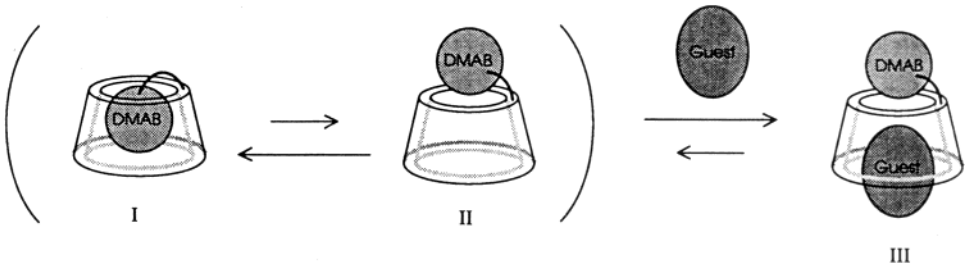

[a] In aqueous solution, **89** is preferentially in the intramolecularly complexed form (**I**) with the *p*-(dimethylamino)benzamide (DMAB) moiety in the interior of the CD ring. Addition of a guest molecule forms the guest:CD complex (**III**) via the open form (**II**), where the DMAB moiety is more exposed to water. Reproduced with permission from ref 279. Copyright 1993 American Chemical Society.

pothesis is experimentally supported by a recent comparison of **83** with sterically hindered derivatives (analogues of **16** and **21**):[274] the red-shifted band of the dual fluorescence increases in relative importance for the pretwisted compounds.

6. Amides

Derivatives of DMABN with the amido group replacing the cyano group exhibit an interesting possibility to vary the acceptor strength of the substituent while retaining the same *class* of the para acceptor substituent. Thus, the primary amide **86** has red-shifted absorption spectra as compared to the tertiary amide **87** because the alkylation reduces the acceptor strength.[275] Both amides exhibit dual fluorescence in polar solvents, although with rather low quantum yields, presumably due to a close-lying n,π^* state. As expected for a substituent with a higher acceptor strength, **86** shows the CT band shifted to the red and more intense as compared to that of **87**. Thus, modification of the acceptor produces the effects expected for a CT emission.[276] In **87**, the alkyls can be replaced by an ion-complexing crown ether, as in **88**. Here, the macrocycle is situated in the acceptor site. One can contrast it to the corresponding crown derivative of DMABN, **62**, in which the macrocycle is in the donor moiety of the TICT molecule. Upon complexation, e.g., with Ca^{2+} (Figure 50), the behaviors of these two fluorescence probes are opposite: Ca^{2+} binds to the electron-rich nitrogen in the crown and, in the case of **62**, diminishes the effective donor strength, while in the complex the acceptor strength increases in **88**. As a consequence, upon complexation, the CT band shifts to the blue and loses relative intensity for **62**, while it shifts to the red and gains relative intensity for **88** (Figure 50b).[277,278]

A step further toward supramolecular photochemistry has been possible with amides still more functionalized than **88**, namely including a β-cyclodextrin ring with a large molecular cavity, as in **89**.[279] In aqueous solution, the CT band of DMABN derivatives is generally strongly quenched due to specific protic solvent interactions (cf. section IV.C.1), so that mainly the F_B fluorescence is observed. This is different if the molecule is included in the interior of a cyclodextrin (CD) ring. The size of the CD cavity seems to be optimal in the case of β-CD for such an intramolecular inclusion complex to be formed by folding the molecule **89**. A strong CT emission band

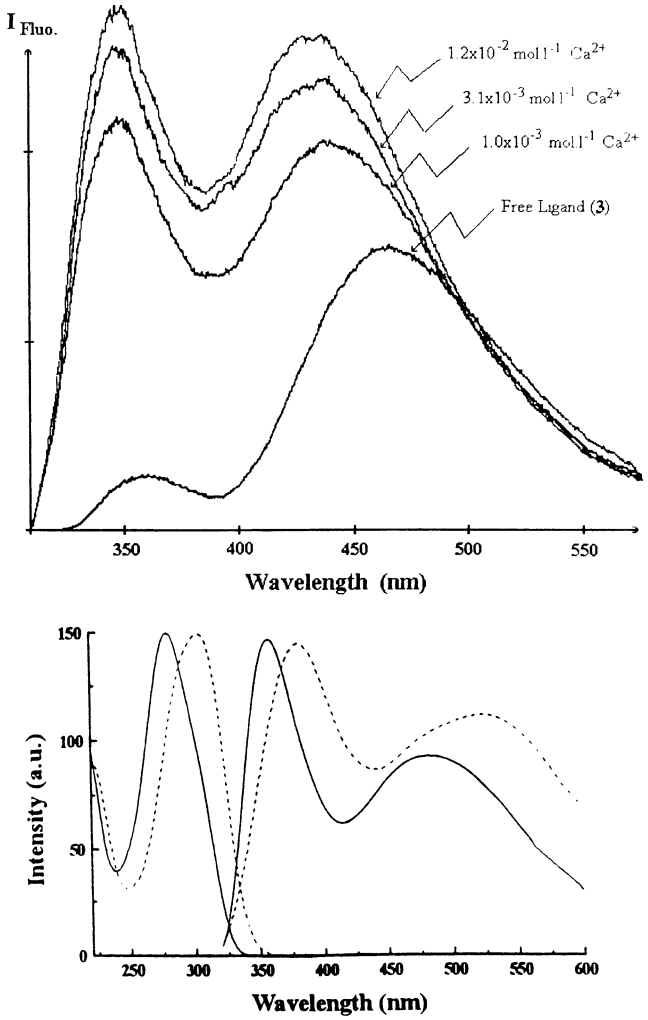

Figure 50. Effect of Ca^{2+} addition (ca. 10^{-3} M) on the dual fluorescence of (a, top) **62**[225] and (b, bottom) **88**[277] in ACN at room temperature. The uncomplexed molecule is denoted in (a) as free ligand; in (b) it is represented by the solid curves. Note the blue shift of the CT band in (a) and its red shift in (b) on addition of Ca^{2+}.

is observed for **89**, even in aqueous solution. If another compound, with a large affinity for β-CD, is added to the solution, it will displace the *p*-(dimethylamino)benzamide moiety from the β-CD ring, with a corresponding drop in the relative intensity of the CT fluorescence band. In this way, fluorescent sensors of molecular recognition can be developed (Scheme 6). Some applications in the spectroscopic determination of binding constants of β-CD to alcohols such as cyclooctanol, 1-adamantanol, l-borneol,

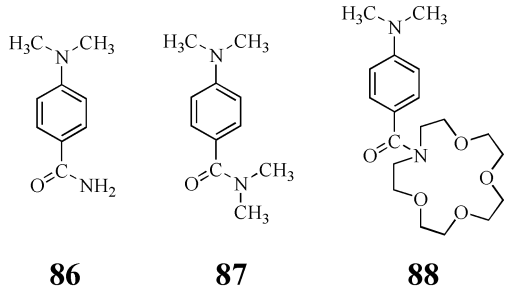

86 87 88

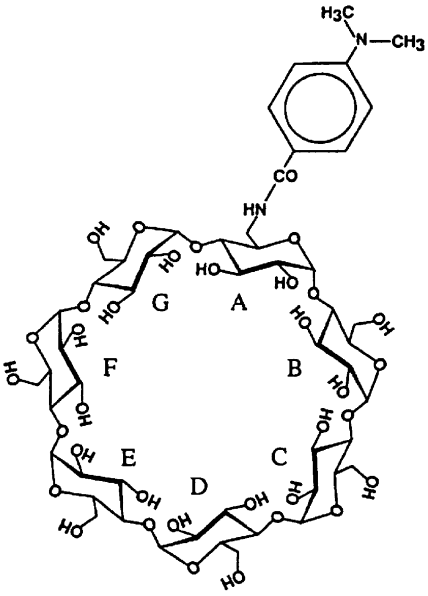

89

l-menthol, etc., and also in protein binding, have been demonstrated.[279,280]

The amide **90** forms a complex with Cu^{II} extremely slowly (a few days). In contrast to the macrocyclic amide **88**, in which complexation with Ca^{2+} favors the CT fluorescence band, in this complex (its structure is represented schematically below) the CT emission is totally quenched and the LE fluorescence is enhanced by a factor of 17. Evidently, the excited-state ICT process is inhibited. This, along with a blue shift in absorption, indicates that upon such type of coordination to Cu^{2+}, the electron acceptor strength of the amide group is weakened.[278]

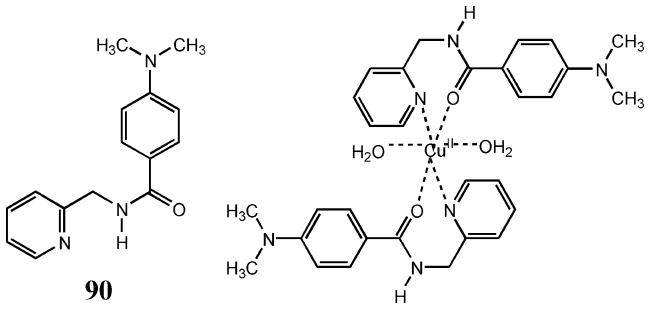

90

7. Nitro Derivatives

p-Nitro-*N*,*N*-dimethylaniline, **91**, emits a fluorescence only at low temperatures, at about 22 000 cm^{-1}. It is structured and has only a small Stokes' shift, whereas the value expected for a TICT state is estimated to be about 11 000−12 000 cm^{-1}.[242] The model compounds **92**−**96**, except the nonfluorescent **93** (with a highly twisted and thus decoupled nitro group), also emit at low temperatures only.[242]

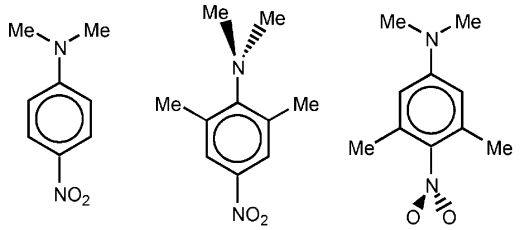

91 92 93

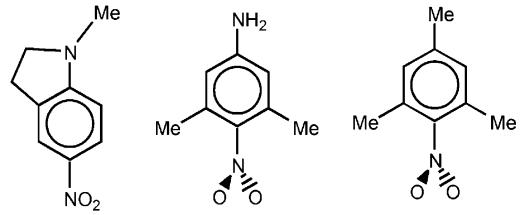

94 95 96

The thermally activated quenching starts in *n*-propanol at temperatures exceeding 100−110 K. The activation energies are lower than that of the viscous flow of the solvent or those of the typical CT state formation in propanol. INDO/S calculations indicate a high dipole moment of the lowest $^1\pi,\pi^*$ state (^1L_a type) of **91**, which excludes the preferential stabilization by solvation of any TICT state (with the $-NMe_2$ or $-NO_2$ group twisted).[242] In the planar conformation, excited **91** should acquire a highly dipolar, quinoid structure (similar to Scheme 1b). It is noteworthy, however, that the model compound with the sterically hindered $-NMe_2$ group, **92**, has a broad, unstructured fluorescence band and a considerable Stokes' shift (~6500 cm^{-1}, twice as much as the other two compounds).[242]

In their study of the effect of an electric field on the absorption spectra, Sinha and Yates[281,282] have shown that all three compounds, **91**−**93**, have high dipole moments in their FC states reached in absorption, the highest one ($\mu^*_{FC} \approx 15.5$ D) in **92** with a strongly pretwisted NMe_2 group, which makes a relaxation to a TICT state probable. The much higher excited-state dipole moment of **95** ($\mu^*_{FC} \approx 22.5$ D), measured in the same way, is close to the value calculated for a TICT state, indicating a practically full CT excitation,[282] as in the case of nitromesitylene, **96**.[281] The authors stress the important role of a *minimum overlap* of the substituent and ring orbitals in the CT states in this group of compounds. The lack of any CT emissions (maybe except for **92**) is due to an efficient ISC, and probably to a very fast deactivation of an unusually low-lying TICT state.[242]

IV. Transient Spectra, Structure, and Reactivity

A. Transient Electronic Absorption Spectra

Good insight into the structure of the CT states is gained from their transient (time-resolved) absorp-

Scheme 7. Relaxation of the Excited Tetraphenylethylene to Its CT State

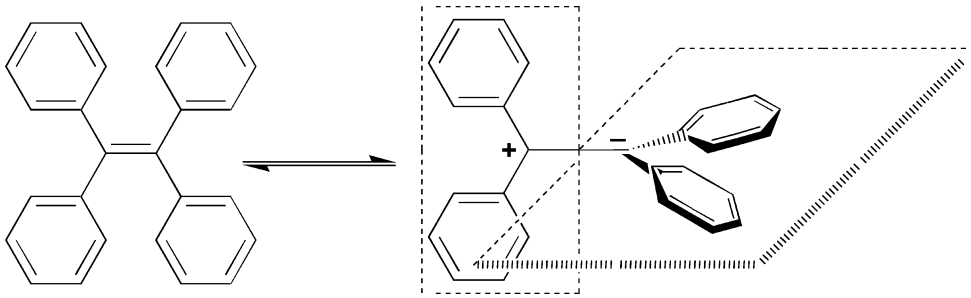

tion spectra. In the case of a full electron transfer, i.e., at a negligible orbital overlap, a unit charge will be localized on D^+, and the other one on A^-. The absorption spectrum of such a CT state should correspond to the sum of the spectra of the component subsystems (local chromophores): the radical anion A^- and the radical cation D^+. If there is, however, any interaction between them (apart from the Coulombic attraction), the observed transient absorption spectra would deviate more or less from such additivity, the maxima would be shifted, or new bands would appear. A few cases are described to exemplify the rule.

Intramolecular exciplexes are formed in the excited state of the compounds $(CH_3)_2N-\phi-(CH_2)_n-$pyrene (P_n). Transient absorption spectra, in the visible, of P_2 and P_3 in ACN can be approximated by the sum of the spectra of dimethylaniline radical cation and pyrene radical anion. In less polar solvents, the spectra of P_3 are, however, different. In highly polar solvents, the stretched forms, $^+D^{\wedge\wedge}A^-$, prevail (cf. Scheme 3), with the electronic structure and spectra like those of the separated radical ion pair. In less polar media, the sandwich exciplex $^+D||A^-$, usually with nonzero orbital overlap, is more stable, exhibiting broad and less specific bands.[283]

In the case of polar exciplexes formed by tetracyanobenzene (TCNB) in toluene (the latter acting both as a donor and as the solvent),[284] the final product of the excited-state reaction has an absorption spectrum clearly composed of the maxima of $TCNB^-$ and of the dimeric donor, $(toluene)_2^+$.[285]

According to the biradicaloid theory,[5,286,287] the lower excited states of ethylenes should have an energy minimum in the perpendicular, twisted structure. The ground state of this twisted conformation should correspond to a nearly degenerate pair of biradical states: the singlet and triplet "covalent" states $^\bullet CR_2-^\bullet CR_2$. The first singlet excited state should correspond to a linear combination of two zwitterionic ^{1}CT states, $^+CR_2-CR_2^-$ and $^-CR_2-CR_2^+$. Tetraphenylethylene (TPE) relaxes in the excited singlet state within a few picoseconds, from the primary excited state (absorption band at 630 nm) to a strongly polar state absorbing at 425 nm. The absorption is similar to that of the radical cation Ph_2CH^+ and the radical anion Ph_2CH^-.[288]

The cation radicals and anion radicals of alternating hydrocarbons have very similar energies of electronic transitions ("pairing property" of their spectra).[289] The excited state of TPE seems to be a full CT state with an orthogonally twisted structure (Scheme 7). Nanosecond transient Raman spectra,[290] and the dipole moment, $\mu^* \approx 6$ D,[291] support the zwitterionic structure of the twisted excited state of TPE. Analogues of TPE, e.g., 9,9′-bifluorenylidene, show similar properties of their transient absorption spectra.[292]

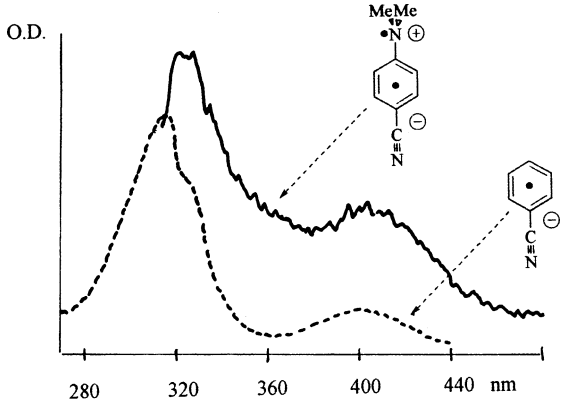

Figure 51. Transient absorption spectrum of excited DMABN in ACN (solid curve), delay time 100 ps (from ref 134). For comparison, the absorption spectrum of the radical anion of benzonitrile in aqueous solution is shown (dashed curve, from ref 296). Reproduced with permission from refs 134 and 296. Copyright 1999 and 1970 The Royal Society of Chemistry and Elsevier Science.

1. DMABN and Its Model Compounds

In the case of **1**, the electronic transient absorption spectra, studied mostly by Mataga and his team, clearly revealed the existence of two states; one spectrum appeared in nonpolar solvents or at $t \rightarrow 0$, and the other one appeared in highly polar solvents, at $t \gg 0$. In medium-polarity solvents, or during the temporal evolution of the spectrum, the transient absorption could be described by the sum of these two spectra in changing proportions. The transient absorption spectrum of **1** in ACN[134,293] is in a very good accord (taking into account different solvents) with that of benzonitrile radical anion[294,295] in aqueous solution[296] (Figure 51).

The absorption spectrum of the other radical ionic component (D^+) of the CT state, $-NMe_2^+$, is not observed in the accessible spectral region; the radical cation NMe_3^+ is reported to have a very weak and nonspecific absorption in the visible and near-UV, and to absorb more strongly only at $\lambda < 300$ nm.[297]

Transient absorption ($\Delta t = 100$ ps) of the model compound for the orthogonal structure, **22**,[134] reproduces the main features of the transient spectrum of DMABN. It is remarkable that the intense absorp-

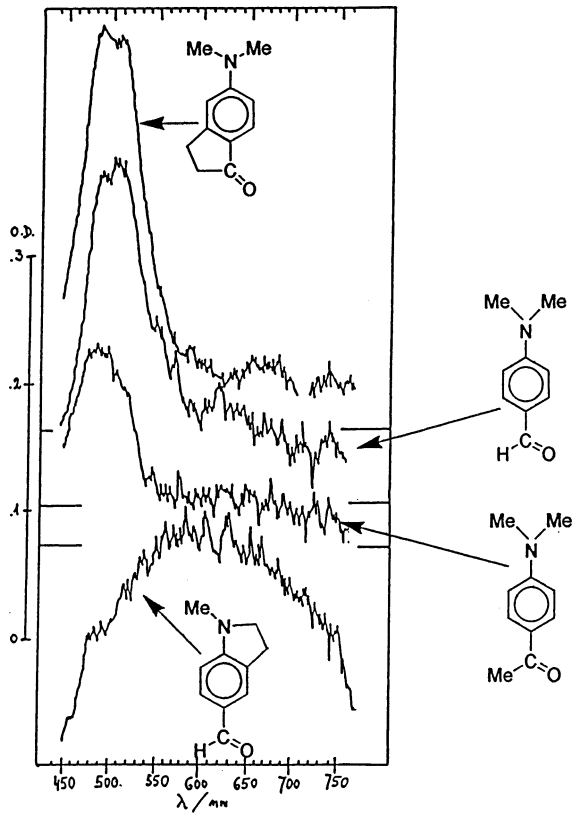

Figure 52. Transient absorption spectra at a delay time of 100 ps, $T = 290$ K. From top to bottom: 1.3×10^{-3} M **69** in ACN; 2.4×10^{-3} M **11** in ACN; 2.5×10^{-3} M **43** in *n*-PrOH; 9.5×10^{-4} M **70** in ACN. Adapted with permission from ref 246. Copyright 1987 Elsevier Sciences.

tion at 320 nm, characteristic of the benzonitrile radical anion, appears not only in ACN but also in hexane solution, indicating a similar character of the excited state of **22** in both media.

2. Carbonyl Derivatives

Another important piece of evidence is delivered by the *p*-carbonyl derivatives of *N*,*N*-dimethylaniline. A series of model compounds (**43**, **68**−**70**) were studied in parallel, by fluorescence (cf. section III.E.3) and by transient absorption spectroscopy. All molecules which reveal dual fluorescence in polar solvents (**43**, **68**, and **69**, i.e., the compounds with a rotatable $-NMe_2$ group) exhibit a characteristic absorption band around 500 nm, which is absent in the rigidly coplanar **70** (Figure 52). On the picosecond time scale, a rise of this absorption band was observed, at the cost of the primary transient absorption. The band at $\lambda \approx 500$ nm could be identified with the A^- radicals: $PhCHO^-$ and $PhC(O^-)CH_3$ (Figure 53).[142,198,246] The spectra of the radical anions were known (e.g., refs 298−300). The absorption of the D^+ radical ions (e.g., Me_3N^+) is expected in the UV range, inaccessible to the experiment.

Noticeable is the great similarity of the transient absorption bands for the series of compounds **68**, **43**, **69**, **44**,[198] and no effect of the nature of the polar solvent (ACN, propanol, pentanol) is noted. The shift of the absorption band at $\lambda \approx 500$ nm with solvent polarity could be expected to be negligible indeed, according to the assignment of this band to the $PhCHO^-$ radical anion and based on its theoretical description.[301]

3. Criterion of a Pure ET State?

Which criterion can we apply to assign — from experiment — a *pure ET state*, i.e., a state with a localization of full charges in the D^+ and A^- units in the case of a D−A compound? How can we discriminate it from a CT state, in which the respective orbitals extend beyond these structural units, to encompass in part the other one? There is obviously no clear-cut answer. Perhaps most useful would be the following three criteria. (i) The excited-state dipole moment should correspond to a full separation of charges. (ii) The transition dipole should be very small, corresponding to an overlap-forbidden transition in fluorescence. (iii) The absorption spectrum of

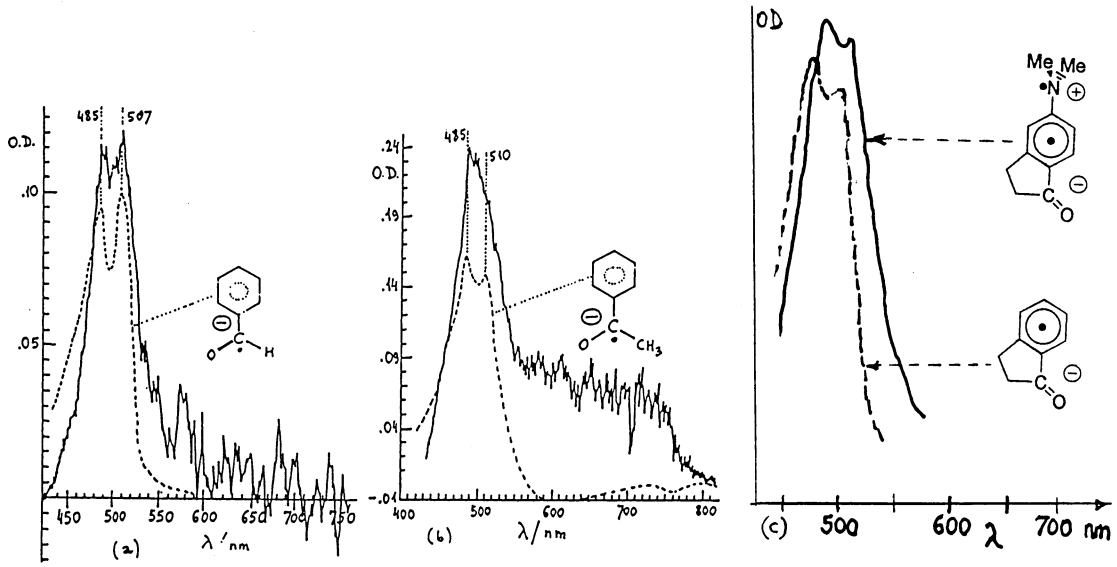

Figure 53. Transient absorption spectra of the CT states of some carbonyl compounds. (Left) **68**, 8×10^{-4} M in ACN, $T = 233$ K, delay time 60 ps. (Middle) **43**, 2.5×10^{-3} M in *n*-PrOH, $T = 290$ K, delay time 100 ps. (Adapted with permission from ref 246.) Each of the spectra is compared with the spectrum (dashed curve) of the respective ketyl anion radical in MTHF, $T = 77$ K. (Adapted with permission from ref 298.) (Right) **69** in ACN, $T = 290$ K, delay time 100 ps, and the spectrum of 1-indanone anion radical in PrCN, $T = 77$ K (courtesy of Dr. J. Dobkowski and Dr. M. Wolszczak, unpublished).

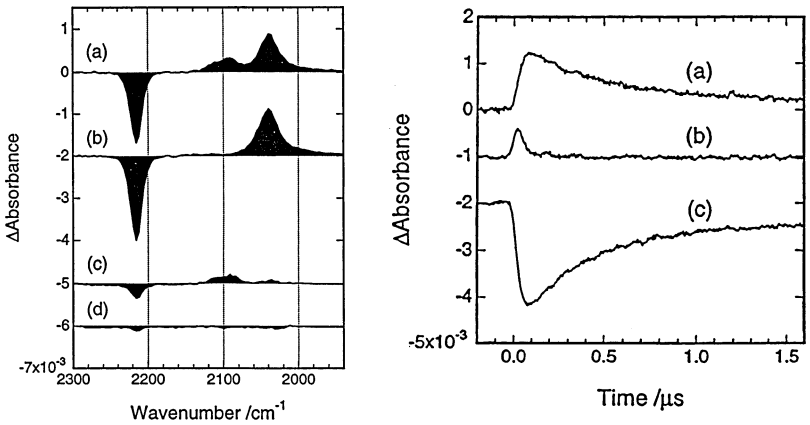

Figure 54. Time-resolved transient IR absorption of 5×10^{-3} M DMABN in *n*-BuOH at room temperature. (Left) Transient IR absorption spectra in a time gate after excitation: (a) 0−100 ns, (b) 100−200 ns, both deaerated; (c) and (d) the same, after saturation with O_2. (Right) Evolution of the IR transient absorption in time, all in deaerated solution: (a) 2040 cm^{-1} (triplet), (b) 2096 cm^{-1} (excited singlet), and (c) 2216 cm^{-1} (ground-state depletion). Reproduced with permission from ref 307. Copyright 1995 American Chemical Society.

the excited state should match the sum of the spectra of the cation radical D^+ and of the anion radical A^-.

The first two criteria are self-explanatory. Let us consider the last one. If the absorption bands characteristic of the D^+ and A^- radical ions appear at the proper wavelengths (e.g., in the case of **11**[246] or **1**[134]) and no other absorption features are present, then there is little doubt about the full charge separation. If, along with the bands of the radical ions D^+ and A^-, new maxima or other features appear, an alternative can be implied: either a coexistence, at the instant of measurement, of the ET state with some other state (which is often the precursor of the ET reaction; sometimes they are in equilibrium), or a considerable overlap of the D^+ and A^- orbitals and a coupling, which usually means a marked deviation from the orthogonal toward a quinoid planar conformation.

There are, however, some physical effects which may render the application of the transient absorption spectra inconclusive as a criterion of the purity of an ET state. First, the two radical ions of opposite charge, D^+ and A^-, are very close to each other, and even in the absence of any orbital interaction they mutually exert a strong (polarizing) electric field effect. The effect is strictly directional. The solvent molecules exert a further polarizing effect, spatially more distributed. In each case, the wave function of the radical ion will be perturbed, but the perturbation will mix only the different states *of the given radical ion*, e.g., in first order:

$$\Psi_i(\vec{F}) = \Psi_i^0 + \vec{F}\sum_{k\neq i} \frac{\vec{\mu}_{ki}}{E_i^0 - E_k^0}\Psi_k^0 \qquad (18)$$

where the wave functions Ψ and the transition moments μ_{ki} describe the given radical ion, and F is the electric field strength.[302,303]

Affected by the electric field of both the partner radical counterion and the polar solvent medium, the absorption spectrum of a radical ion can be shifted and broadened,[304,305] dependent on the nature of the states involved in the given transition. The solvent effect may sometimes be eliminated by comparing the spectra of the excited molecule and of the radical ion in the same solvent. Generally, the effect of the partner radical ion can be calculated. It can be large, as indicated, e.g., by the spectra of the ketyl radical anions associated (in a preferential position, close to the O atom) with the alkali metal ions; the absorption band shift strongly depends on the ionic radius.[306]

Such spectra, even somewhat shifted and/or broadened, still correspond to the definition of a *pure ET state* (eq 1), so far as the perturbation does not mix the wave functions of D^+ and A^-, or those of the whole ET state with the LE states of D or A. We can still ascribe a close-to-zero overlap structure to a nearly pure ET state observed.

B. Transient Vibrational Spectra

With the technical progress in nano- and picosecond time-resolved laser spectroscopy, vibrational spectra of excited molecules, the long expected target of investigations, became accessible. Hashimoto and Hamaguchi[307] first reported the transient IR absorption spectra of **1**, recorded at a low time resolution (100 ns time windows). After a pulsed excitation, in butanol solution at room temperature, the transient difference spectrum in the 1940−2300 cm^{-1} range exhibits a negative signal of the ground-state depletion at 2216 cm^{-1} and two positive maxima at 2096 and 2040 cm^{-1} (Figure 54). The 2096 cm^{-1} band appears only in the first 100-ns window. The 2040 cm^{-1} band lasts for hundreds of nanoseconds and is sensitive to O_2. The authors interpret their results in terms of the TICT model. They assign the 2096 cm^{-1} band to the C≡N stretch frequency (strongly downshifted, from 2216 cm^{-1} in the ground state to 2096 cm^{-1}) of the ^{1}TICT state. The band appears only in the polar solvent. It disappears with the lifetime of the F_A fluorescence, its frequency nearly matches that of the C≡N stretch vibration in the benzonitrile radical anion (2093 cm^{-1}), and its intensity corresponds to a very large dipole.

The assignment of the very broad 2040 cm^{-1} band to the hitherto not observed transient ^{3}TICT state seemed to be tentative and worth a closer examination, which came later (see section XII).

Scheme 8. (Left) CASSCF-Optimized Geometries for 1 (Bond Lengths in Picometers)[a] and (Right) Structure of the B* State, Best Fitting to the Vibrational Frequencies[320]

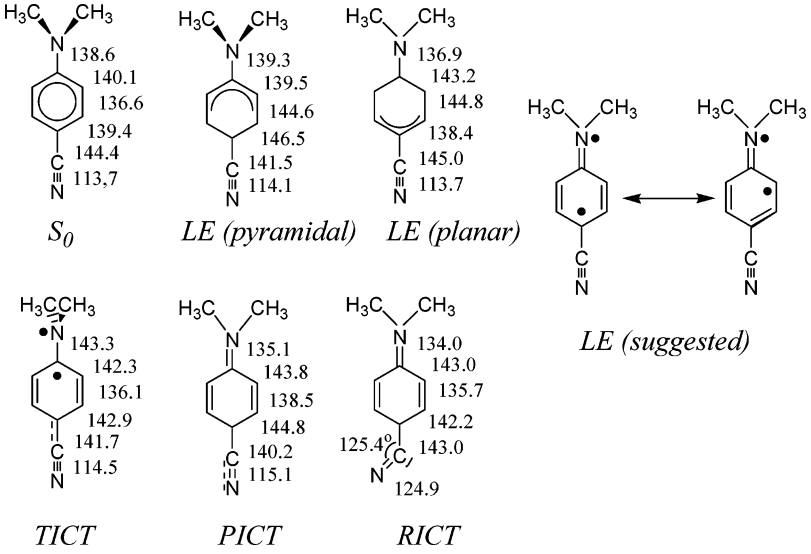

[a] Adapted from ref 310.

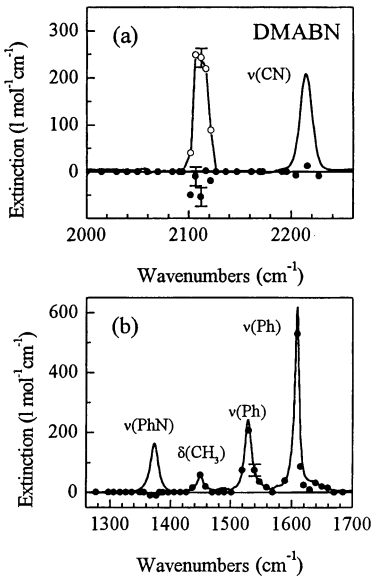

Figure 55. Mid-IR absorption spectra of 5×10^{-3} M **1** in (a) ACN and (b) CD_3CN. Solid curves, in the ground state. Excited molecules: full points, at 1 ps delay, assigned to the B* state; open points, the peak at 2112 cm^{-1}, measured at 15 ps delay, assigned to the CT state. Reproduced with permission from ref 308. Copyright 1999 Elsevier Science.

With the advent of femtosecond laser pulse excitation and probing, a discrimination of the fingerprints of the initially excited B* (LE) state and the A* (CT) state, arising with some delay, became possible. Most of these papers, coming from several very active research groups, confront the experimental findings with the results of quantum-chemical predictions for different models.

In the transient absorption spectra of **1** in the mid-IR (1270−1690 cm^{-1} in CD_3CN, and 2000−2230 cm^{-1} in ACN), reported by Chudoba et al.[308] (Figure 55), the stretching modes ν(phenyl−N) and ν(C≡N) initially vanish. Then, with a rise time of 4.0 ± 0.5 ps (in ACN both the decay time of F_B and the rise time of F_A fluorescence were found equal, $\tau = 6 \pm 1$ ps[133,309]), a new intense band appears at 2112 cm^{-1}, close to the previous finding (Figure 54). The authors assigned it to the C≡N stretch shifted down by 103 cm^{-1} and found no additional band above 1270 cm^{-1}.

CASSCF ab initio studies by Dreyer and Kummrow,[310] together with the work by Kummrow et al.,[311] extended their previous findings[308] on the femtosecond IR transient absorption of **1**. They used extensive CI in their excited-state optimizations (CASSCF with four electrons in four active orbitals and a 6-31G(d) basis set) to compare the theoretical structures (optimized for different models, Scheme 8, together with their expected vibrational frequencies and intensities) with the experimental IR results on the S_0, LE, and CT states of **1**. In the spectrum of DMABN in ACN at 1 ps delay, they obtained a satisfactory agreement for the planar LE state. They found important evidence in the C≡N stretching frequency, which is downshifted in the CT state, as already described,[307,308] by 104 cm^{-1}, from 2216 cm^{-1} in S_0 to 2112 cm^{-1} in the CT state. The theoretical downshift was 110 cm^{-1} for the TICT model, 36 cm^{-1} for PICT, and 800 cm^{-1} for RICT.[310] This allowed them to reject the RICT model, to express doubt regarding the PICT model, and to conclude that "the calculated TICT state reproduces the experimental features better".[311] The $C_{phenyl}-N_{amino}$ band at 1373 cm^{-1} disappeared in the excited ICT state, but no new band was found instead. The calculation indicated this stretching frequency at 1286 cm^{-1} for the TICT state, but such a band was not detected (possibly because of the limited spectral range of the measurement).

In the picosecond time-resolved IR spectra of **1** in the more extended range 900−1700 cm^{-1}, measured by Okamoto[312] with his method of signal detection,[313] several bands appear in this range for the excited state of **1** (but not in **114**). Most prominent among them, in ACN solution, appeared the band at 961 cm^{-1}, which was tentatively assigned to the phenyl−NMe_2 stretch, downshifted from the corresponding S_0 vibration at 1229 cm^{-1}. The band is polarized in the molecular axis and has a rise time of 10−15 ps (as compared a rise time of 4 ps in the previous

transient IR study,[308] or as compared to 6 ps reported for the F_A fluorescence rise time in the same solvent[309] or to the F_B decay times, e.g., 6 ps,[133,309] ≤10 ps,[314] 11 ps,[130,315] and 13 ps[316]). If the author's assignment were correct, this would correspond to a strong *lowering* of the phenyl−NMe_2 bond order in the CT state vs S_0 .

In a subsequent detailed study of the vibrational structure of **1** in the ground state, Okamoto et al.[317] measured and interpreted, using several theoretical approaches for comparison, the IR and the Raman spectra of the ground state of DMABN and of four of its isotopomers. Along with the natural DMABN, the isotopic forms were those with ^{15}N in the −C≡N group, with ^{15}N in the $-N(CH_3)_2$ group, with ^{13}C in the CH_3 groups, and the deuterated form with the $-N(CD_3)_2$ group. This analysis of the vibrational spectra compelled the authors to modify numerous reported assignments, including their own previous assignment:[312] the 1230 cm^{-1} IR band appeared not to be affected by isotopic substitutions, and thus not to correspond to the $C_{phenyl}-N_{amino}$ vibration. The $C_{phenyl}-N_{amino}$ vibration in the ground state is definitely identified with the 1372 cm^{-1} IR band, which is strong in IR but very weak in the Raman spectrum.

Okamoto et al. subsequently reported[318] the picosecond transient IR spectra of **1** and of four of its isotopomers (with vibrational modes assigned previously in the ground state[317]). At 277−289 nm excitation in ACN solution, with 16 ps delay time, the experiment covered the spectral range 920−1700 cm^{-1}. On the basis of the isotopic shifts, they identified the most searched $C_{phenyl}-N_{amino}$ stretch as the 1276 cm^{-1} band (strongly downshifted with respect to the ground-state band at 1372 cm^{-1}, and close to the previously calculated value[311] of 1286 cm^{-1}), corresponding to a single bond in the ICT state. Their own calculations, using CIS/6-31G(d) and allowing only for singly excited configurations, resulted, however, in similar frequencies for both the planar (1350 cm^{-1}) and the twisted forms (1379 cm^{-1}), close to the ground-state vibrational frequency. Among the ring frequencies, they tried to identify most of them as "benzenoid" and the other ones as "quinoid". The authors left their work inconclusive with respect to the molecular structure of the ICT state, describing it as an intermediate structure between the benzenoid and the quinoid one, contradicting neither the twisted nor the planar structure.[319]

Important studies, done in the laboratories of Phillips and Parker, of the transient resonance Raman spectra of **1** as compared to a series of reference compounds permitted many vibrational frequencies to be identified.[320,321] The probe pulses were at several different wavelengths, corresponding to the resonances with the transient absorption of either the B* or the A* state. The phenyl−N stretch frequency is found to be shifted from 1373 cm^{-1} in S_0 to 1423 cm^{-1} in the B* state (increasing bond order), which supported the treatment of the B* state as a planar quinoidal structure. This band was totally absent in the resonance Raman spectrum of the CT state (no 961 cm^{-1} band,[312] either). The prominent C≡N stretch frequency (2096 cm^{-1}), known from the IR absorption of the CT state,[307,308] does not appear in the resonance Raman at a probe wavelength of 415 nm[320] or 400 nm,[321] but it is the most prominent one at a probe wavelength of 330 nm.[321] It depends on the coupling of the given vibration with the excitation in the resonance (two different transitions in the transient absorption). The ring breathing (752 cm^{-1}), C=C stretch (1581 cm^{-1}), and C≡N stretch (2096 cm^{-1}) nearly match the respective frequencies of the benzonitrile radical anion, implying a decoupling of the $-NMe_2$ group in the A* state of **1**.[321]

Further insight into the vibrational spectra is obtained by the study of picosecond Kerr-gated time-resolved resonance Raman and transient resonance Raman spectroscopy of the isotopomers: DMABN, DMABN-d_6, and DMABN-^{15}N (in both cases, isotopic substitution was in the $-N(CH_3)_2$ group).[322] After a precise assignment of the ground-state frequencies (generally in accord with the independent measurements[317]), numerous bands were identified for **1** in methanol solution, at a delay of 50 ps, in the very broad spectral range 600−2200 cm^{-1}. In the CT state (excitation at $\lambda = 330$ nm), the transient resonance Raman signal at 1281 cm^{-1} is assigned, on the basis of the isotopic shifts, to the $C_{phenyl}-N_{amino}$ stretching vibration; 1286 cm^{-1} resulted earlier from the theory.[311,321]

A strong downshift of this most significant frequency (~96 cm^{-1} vs S_0) implies a substantial decrease in the coupling of the amino group with the ring, similar to that observed on protonation of the amino group (typical stretch frequencies are ~1200 cm^{-1} for the single C−N bond and ~1600 cm^{-1} for the double C=N bond). The finding contradicts the strong coupling (PICT model[110,111]) and seems to agree with the TICT structure (or very close to it, with a possibility of some pyramidality of the decoupled amino group) of the CT state. Most other frequencies were strikingly similar to those of the benzonitrile radical anion, indicating a decoupling of the dimethylamino radical cation and benzonitrile radical anion subunits.

Quite a new field of investigations is initiated by the picosecond X-ray diffraction study (using synchrotron radiation) of the transient structural changes in DMABN crystals after a femtosecond laser excitation.[323] The results are interpreted as a fast (80 ps delay time) planarization of the $-N(CH_3)_2$ group and a torsional motion of this group to about 9 or 10° out of coplanarity with the aromatic ring. Because in the crystal **1** does not emit the F_A fluorescence, the observed structural changes may be related to the primary excited state, B*. The new technique, however fascinating, uses crystals with their packing effects hindering the relaxations possible in solution, and a direct comparison to gas-phase or solution properties is difficult.[324]

C. Hydrogen Bonding, Isotope Effects, and Reactivity

1. Hydrogen Bonding

DMABN and most of its close analogues contain an electron donor in the form of an amino group, and

therefore, already in their ground states they are apt to form a hydrogen bond with protic solvents (**14**). In the excited ICT state, the H-bond to the positively charged dialkylamino group is expected to break, and new H-bonds are expected to form at the sites of high electron density — either at the acceptor substituent, e.g., at the cyano N atom (**97**), or in the ring, as a π- or σ-complex (**98** or **99**, respectively).

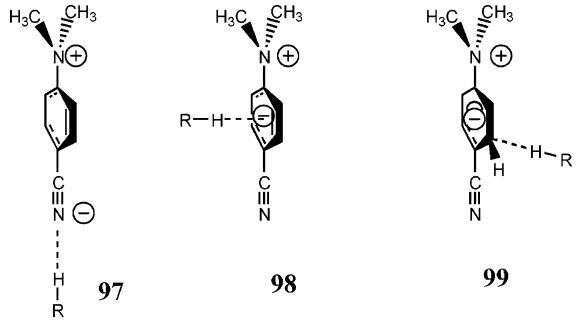

97 **98** **99**

The ground-state H-bonding was described by Cazeau-Dubroca et al. as the major (or even the only) cause of the TICT state formation: the tetragonal arrangement of bonds in the complex (**14**) should constitute, on breaking the H-bond in the excited state, a precondition for the twist.[83,86−89] Among the solutions of **1** in rigid polymer matrices, only in the protic poly(vinyl alcohol) was the F_A fluorescence observed.[82] The observations were extended to some other hydrogen-donating polymers, but due to its very long lifetime, $\tau \approx 1$ s, the emission was ascribed by Cazeau to a *delayed* intramolecular CT fluorescence.[325] The presence of the F_A fluorescence in *aprotic* solvents was assigned to the effect of traces of water.[83] The hydrogen-bonding effects complicate the ICT kinetics in **1**.[453]

Ample evidence is reported against ascribing the *promoting effect* in the formation of the CT, and in particular of the TICT state, to the *ground-state* hydrogen bonding of **1**. The fundamental role of humidity in aprotic solvents has been systematically reported from only one laboratory,[83,86−89] whereas this could not be reproduced in other ones. In particular, the addition of H_2O to ACN did not enhance but, to the contrary, strongly quenched the F_A fluorescence.[115] The ground-state H-bonding at the amino nitrogen, hardly detectable in **1**, seems not to play any promoting role (rather an inhibiting one[268,270]) in the formation of the ICT state. In numerous aza compounds (**79**−**83**), a marked promoting effect of ground-state H-bonding on the B* → A* reaction was observed indeed, but it was the H-bond to the *acceptor* moiety, not to the amino (*donor*) group of these molecules.[268, 270]

Strong effects of *H-bonding in the excited state* can be inferred from the slow component of the B* → A* kinetics in alcohols,[314,326,327] which is generally assigned to the breaking of the H-bonds existing in the ground state, e.g., **14**, and the slow formation of new H-bonds at the sites specific for the excited state,[327] e.g., **97**−**99**.

An excellent example of such a process is delivered by the pyrene derivative **101**.[328] In acidic solutions, its ground-state protonated form, **100**, dissociates in

Scheme 9

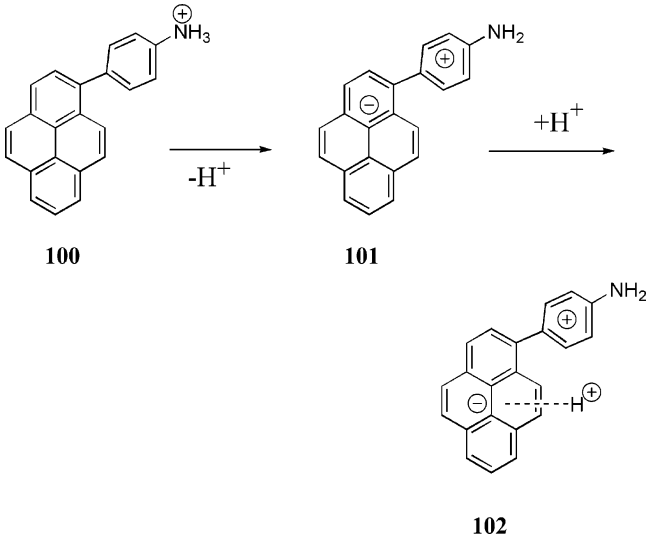

100 **101** **102**

the excited state to form the excited amine **101*** in its highly polar state, ascribed by the authors to a TICT structure (or close to that), with $\mu^* \approx 14.3$ D. The process is interpreted as the relatively slow relaxation (with a proton transfer to the solvent) of the primary excited cationic species **100** to the strongly dipolar CT state of the neutral amine **101**. The excited CT state of **101** is subsequently quenched by an H^+ ion[329] which attaches to one of the high-electron-density centers in the *radical anion* moiety of the excited molecule. This results in a π-complex **102** (analogous to **98**) or in a nonaromatic σ-complex (analogue of **99**) which is not fluorescent (Scheme 9).[328]

The quenching mechanism, via formation of non-fluorescent, nonaromatic σ-complexes with H^+ ions, is analogous to the previously observed quenching on acidification of, e.g., aminonaphthalenes and other analogous systems,[330,331] which was mysterious for some time but later was confirmed by photochemical H/D isotopic exchange.[332] This type of quenching effect, with alcohols, seems to be especially pronounced in the cases with full charge separation, as exemplified by the donor−acceptor−biphenyl series **103**−**105**. All three compounds emit from highly

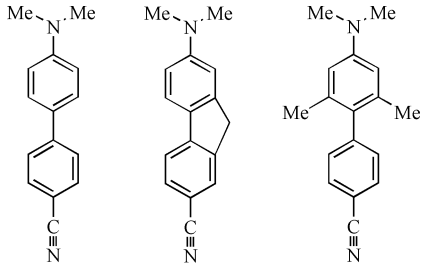

103 **104** **105**

dipolar CT excited states,[333,334] but only **105** shows transient absorption spectra corresponding to the sum of cation and anion radicals.[335] In conjunction with the reduction of the fluorescence transition moment for **105** in polar solvents, this indicated a small overlap, as in a TICT state.[333,334] Interestingly, only **105** underwent an alcohol-induced fluorescence

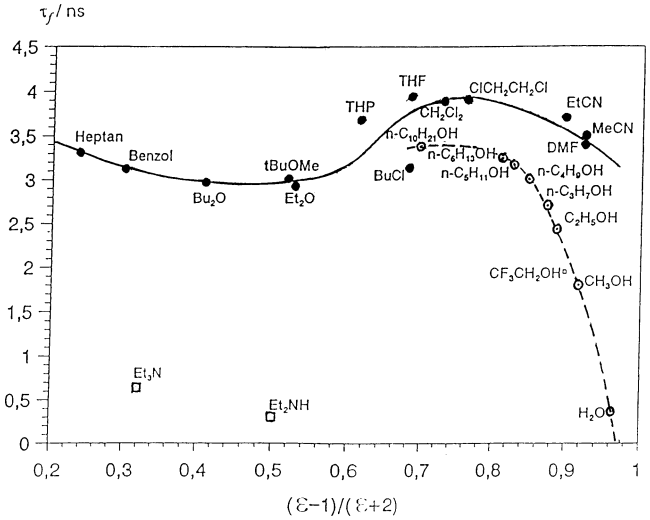

Figure 56. Solvent effect on the DMABN fluorescence lifetime, τ_f. In aprotic solvents of different polarities, the lifetimes are within the limits 3−4 ns. In protic solvents, with increasing proton-donating propensity, an evident quenching effect appears. Data from ref 344, with permission from the author. The aliphatic amines as solvents strongly deviate from any correlation, due to a quenching following a different mechanism,[95] vide infra.

quenching, but not **103** and **104** (their excited ICT states have a somewhat reduced excited-state dipole moment[333]).

All these cases are illustrative for a reactivity change consisting in the shift of the basicity site: the latter is localized on the donor (e.g., on the amino group) in the ground state and shifts to the negative pole (acceptor group) in the excited CT state.[303,336−341]

The existence of H-bonded solute−solvent exciplexes in alcohols was reported by many authors (see sections II.B.3 and III.A.1), similar to the well-studied case of NMe_3.[342,343] The effects related to the H-bonding of **1** to protic solvents (Figure 56) demonstrated the process to be a dynamic quenching in the excited state.

2. Solvent Isotope Effects

The isotope effect (deuterium vs hydrogen) of **1** and derivatives has been studied[345−347] in several solvents (Table 7) with unambiguous results: the fluorescence yields, ϕ_A, lifetimes, τ_A, and the intersystem crossing yield, ϕ_T, changed in the same way. The properties of the F_B fluorescence did not change. As the reaction B* → A* in these solvents was usually irreversible, the replacement of hydrogen by deuterium (in the −OH groups of the solvent) slows only the *internal conversion*, k_{IC}, from the ICT state A*, due to interaction with the protic solvent, most probably at the acceptor site (see above). Moreover, the isotope effect is (within the group of compounds **1**, **15**, **16**, and **17**) only solvent-dependent, but rather independent of the compound studied. The fact that deuteration of the aprotic solvent (CD_3CN vs CH_3CN) has no effect[346] indicates that it is not a general effect of reducing the frequencies of the accepting modes,[348,349] but it is rather due to a new radiationless deactivation channel involving the hydrogen bond linking the emitting species to the solvent.

Table 7. Hydrogen Isotope Effects on the CT Fluorescence Quantum Yields, $R_f = \phi_f(D)/\phi_f(H)$, on the Fluorescence Lifetimes, $R_\tau = \tau(D)/\tau(H)$, and on the Triplet Yields, $R_{ISC} = \phi_{ISC}(D)/\phi_{ISC}(H)$[a]

solvent	compd	R_f	R_τ	R_{ISC}
	1	(1.45)[c]		
D_2O/H_2O	**15**	1.62 ± 0.03	1.67 ± 0.02	1.6 ± 0.1
	17	1.7 ± 0.05		
	16	1.7 ± 0.05		
	15	1.27 ± 0.03		1.3 ± 0.1
		1.2[b]	1.2[b]	
	17	1.3 ± 0.03		
MeOD/MeOH	**16**	1.3 ± 0.03		
	21	1.06 ± 0.3[d]		
	22	1.0 ± 0.1[d]		
EtOD/EtOH	**15**	1.17 ± 0.02	1.17 ± 0.01	1.15 ± 0.05
CD_3CN/ CH_3CN	**15**	1.0 ± 0.05		
1,2-propane-diol-d_2/h_2	**1**	(1.6)[c]		

[a] Data from refs 346 and 347 unless otherwise stated. [b] Sample of MeOD of another origin. [c] Data not fully reproducible.[81] [d] Rotkiewicz, K., unpublished.

Strangely enough, in the case of two strongly *pretwisted* compounds, **21** and **22**, *the isotope effect was found to be very small or absent* (Table 7). This could be due to an increased contribution of intersystem crossing, ϕ_{ISC}, which diminished the role of the internal conversion channel in the deactivation kinetics of the excited state. In view of the similarity of the k_{ISC} and ϕ_T values of **16**, **17**, **21**, and **22** in EtOH (Table 29), however, this seems not to be the case. One can only tentatively state that the hydrogen bonds are probably similar in the excited state of all these compounds and occur at the negative acceptor moiety. But they may differ largely in the ground state, where the large twist angle of the amino group lowers the electron density on the acceptor unit and increases it at the donor site, as compared to the more planar structures.

In an early paper,[81] the D/H isotope effect in water as solvent on the intensity ratio F_A/F_B of **1** was reported to be large and dependent on the excitation wavelength. As implied by the reported data, the samples of **1** used were contaminated with some impurities, which were probably responsible for these excitation-dependent effects.

3. Excited-State Reactivity and Quenching

Excited-state reactivity can be additional (indirect) evidence for the structure of an excited molecule. Several significant observations were reported in the literature concerning **1** and related molecules. There appear to be three different mechanisms for what is often called "*quenching*": (i) *static quenching,* resulting from an interaction of the "quencher" with the ground state of the fluorescent solute, i.e., a ground-state complex formation; (ii) excited-state *dynamic* quenching, which affects both fluorescence bands in the regime of equilibrium B* → A*; and (iii) dynamic quenching of only one of the excited species, A* or B*, involved in the "*one-way*" B* → A* reaction (in the kinetic regime, cf. section VI.A.2).

Case (i) is trivial ("static quenching"[350]). If the ground-state complex is nonfluorescent, one is ob-

Table 8. Quenching of DMABN in Aqueous Solution by Simple Anions[351]

quencher	k_q[a] 1	k_q[a] 21	K_{SV}[b] Q1
F^-	1.4×10^8	no effect	no effect
Cl^-	7.3×10^7	no effect	0.11
Br^-	no effect	no effect	1.0
I^-	7.0×10^8	2×10^8	3.4
OH^-	2.4×10^8	*c*	*c*

[a] Rate constant, in M^{-1} s^{-1}. [b] Stern−Volmer constant, in M^{-1}. [c] Not studied.

serving a change of the fluorescence yield, ϕ_f, at an unchanged lifetime, τ_f. Case (ii) does not easily allow one to discriminate which of the excited species, B* or A*, reacts with the quencher (in a fast equilibrium, they both disappear at the same proportion in the overall quenching process, i.e., Φ_A/Φ_B does not change while both Φ values decrease; the respective expressions can be derived from eqs 19−21, section VI.A.2, by adding the quenching rate to the intramolecular deactivation rates, k_A *resp.* k_B). Only case (iii) allows the study of the reactivity specific for the CT state (A*). Thus, we refer here to these latter results preferentially, mentioning some other reports that are less clear regarding a structural interpretation.

At room temperature, excited **1** reacts "one-way" i.e., in the *kinetic regime*, in which the reverse reaction can be neglected (cf. section VI.A.2), only in the strongly polar solvents, e.g., in H_2O. The quenching itself can be used for testing the reversibility of the excited-state CT transformation: most probably, a quenching species such as O_2 reacts with both forms, B* and A*, often with a diffusion-determined rate. But in ACN, only the F_A emission of **15** is quenched under a high pressure of O_2;[315] i.e., the reaction is in the *kinetic regime*. In the less polar solvent CH_2Cl_2, both bands of this compound are quenched, indicating a reversibility of the process.[237]

The study of quenching of **1** in aqueous solutions by simple inorganic anions[351] gave astonishing result. Usually, in most of the other cases described, the sequence of the fluorescence quenching rates, k_q, of aromatic compounds is $I^- > Br^- > Cl^-$. The fluoride ion, F^-, generally does not quench. In the case of **1**, however, the sequence $I^- > OH^- > F^- > Cl^- \gg Br^-$ was found (Table 8).

The interpretation was that **1** is quenched by two different mechanisms. (i) I^- quenches as an external heavy atom or by electron transfer; the lack of quenching by Br^- ions indicates a change of the mechanism. (ii) OH^- and F^- (and to a lesser degree Cl^-) may act here as *hard bases*. According to the soft and hard acid−base theory,[352−354] less polarizable (*hard*) Lewis acids preferentially react with low-polarizability electron pair donors (*hard Lewis bases*). It was proposed that the $-NMe_2^+$ group, *if decoupled from the aromatic ring*, can be considered, with its localized positive charge, as a typical *hard acid*. In excited **106**, in which the positive charge is delocalized in the pyrrole ring, the quenching by F^- ions disappears, and the sequence is *normal* (Table 8). In excited **21**, in which the positively charged N atom is well screened (Figure 57), the hard base reactant

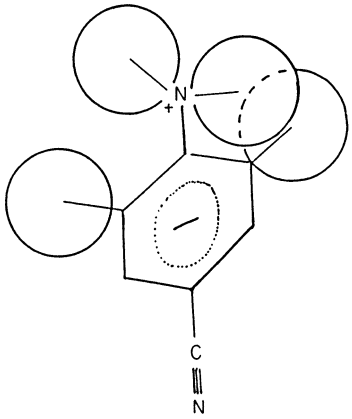

Figure 57. Methyl groups screen the amino nitrogen in **21** against a close approach of the voluminous I^- ion. Reproduced with permission from ref 351. Copyright 1982 Elsevier Science.

Table 9. Quenching of DMABN with Tertiary Amines:[95] Quenching Rate Constants k_q, in 10^8 M^{-1} s^{-1} Units

	quencher				
	ABCO[a]	$NEtMe_2$	NEt_3	NBu_3	$NEt(i\text{-}Pr)_2$
F_B (isooctane)	14.2	1.16	1.14	0.97	0.49
F_A (ACN)	63	*b*	12	*b*	*b*

[a] Azabicyclo[2.2.2]octane, quinuclidine. [b] Lack of data.

cannot approach to a bond length distance. The F^- quenching is absent, but the quenching by I^- persists (though with a lower rate than in **1**), but both suggested mechanisms (ET or heavy atom effect) act over distances far exceeding the bond length.

All these data are derived from the initial, linear range of Stern−Volmer plots (quencher concentration below 1 M). At high concentration of quenchers, the Stern−Volmer plots are strongly curved; e.g., in 4 M aqueous NaOH, the CT luminescence of **1** is again close to its intensity in the absence of the quencher.[355,356]

1 is efficiently quenched by aliphatic amines (see Figure 56).[95] It was found that the fluorescence in isooctane (i.e., from the B* state) is kinetically quenched by addition of amines, whereby the quenching of the F_B fluorescence was not accompanied by the appearance of the F_A band (in contrast to the general effect of addition of polar solvents). The rate constants (Table 9) did not correlate with the oxidation potential of the quencher (i.e., seeming not to be connected with an ET quenching) but rather with the steric accessibility of the amine N atom to the quenching molecule. Wang suggested the formation of a two-center,three-electron σ-bond between the two N atoms (cf. Figure 4, section I.C) to be the mechanism of quenching.[95] This immediately reminds us of the *hard base* hypothesis.[351] The $N\cdots OH^-$ or $N\cdots F^-$ three-electron σ-bonds would be weaker than the $N\cdots N$ bonds, and the corresponding rate constants for quenching of the F_A fluorescence are indeed found to differ by 1 order of magnitude (cf. Tables 8 and 9). Moreover, the rates of quenching of the B* state are much lower than the corresponding quenching rates for the CT (A*) state (Table 9). This can only be interpreted in terms of a structural change: there is

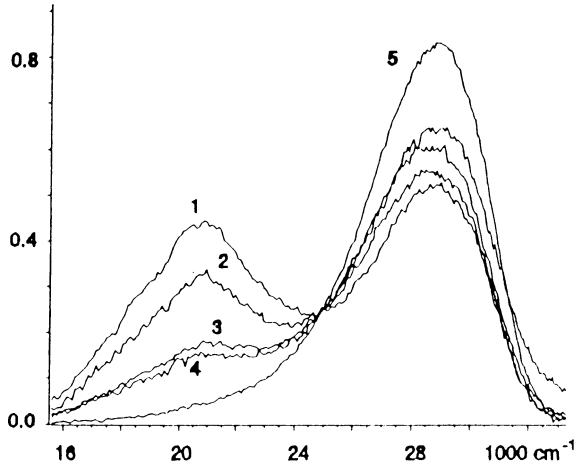

Figure 58. Unusual quenching by OH^- ions. Fluorescence spectra of the dually fluorescent secondary amine **52** in aqueous solution. [NaOH]: (1) 0, (2) 0.17, (3) 0.5, (4) 1.0, and (5) 4.1 M. Analogous addition of NaBr instead of NaOH has no quenching effect.

no singly occupied lone pair orbital on the N atom in the strongly conjugated π-electron system of the B* state of **1** (an l_a,π^* state in the terminology of Kasha[357]), so the formation of a three-electron bond would require additional energy. In the *decoupled* system (e.g., in a TICT state), the amino N atom has one electron localized in the p orbital perpendicular to the sp^2 plane, ready to form the three-electron bond.

In the case of the dual fluorescence of the secondary amine **52**, the F_A fluorescence is quenched by OH^- ions and disappears in strongly alkaline solutions; only the primary emission, F_B, is then observed. The regular *increase* of the F_B intensity accompanying the quenching of F_A (a well-defined isoemissive point appears at different NaOH concentrations; Figure 58) suggests an *inhibition* of the CT process B* → A* in this case.[355] The phenomenon is not yet explained and needs closer inspection.

Representing both a strong oxidant (D^+-) and a strong reducing agent ($-A^-$), the CT state can be quenched by electron transfer *to*, or *from*, the excited

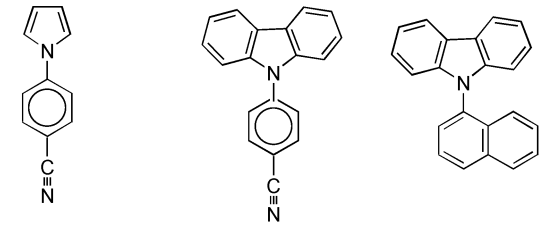

106 **107** **108**

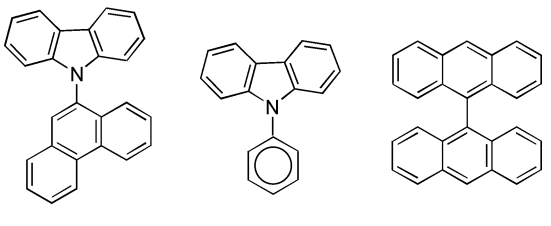

109 **110** **111**

Scheme 10

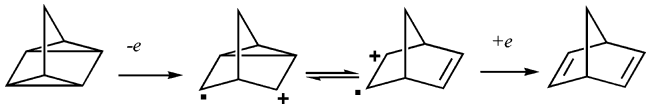

112 **113**

molecule. In the case of large aromatic donor and acceptor moieties, e.g., **107** or **108**, there is only one CT fluorescence band in polar solvents[358] (for these large molecules, the photophysics is often different from that of **1**, see section XI.A; in the present section, only the mechanisms of quenching of the CT states are discussed). Soumillon[359,360] investigated the kinetics of quenching of **108** by numerous oxidizing or reducing quenchers in ACN or DMF and found a good agreement with the Weller−Rehm equation[361] in both series of ET reactions. This was confirmed by further studies in this series, e.g., involving **107** and other carbazole and indole derivatives able to populate a TICT state.[362] The ET mechanism of quenching has been proved for **108** by photochemical reactions: quadricyclane **112** was isomerized to norbornadiene **113** (the reaction occurs in the radical cation, after the ET to **108***, see Scheme 10); pentachlorobenzene, an efficient electron acceptor, also quenches **108**, undergoing an anionic dechlorination (with a product distribution typical for the radical anion intermediate).[359,360]

107−**109** emit LE fluorescence in nonpolar solvents, closely similar to that of **110**.[358] The heavy-atom quenching of these compounds was studied in solvents of widely different polarity[363] relative to each other. Quenching by MeI or EtBr (the effect of the latter was about 40 times weaker) was more than 1 order of magnitude faster in nonpolar than in strongly polar solvents. The authors[363] interpreted the dependence of the CT state quenching rate on the solvent polarity as evidence for a narrowing of the angular distribution around the 90° conformation with growing polarity of the medium.

An unusual case of quenching with H^+ ions is reported[328] for the pyrene derivative **101** (cf. above, Scheme 9).

The quenching of the CT state of 9,9′-bianthryl **111** has been extensively studied. H^+ ions quench the CT fluorescence of **111*** in polar solvents ($k_q = 1.5 \times 10^9$ M^{-1} s^{-1} in MeOH, 2×10^8 M^{-1} s^{-1} in ACN; both are below the diffusion limit).[364] It is remarkable that the quenching rate of the nonpolar (triplet anthracene-like) triplet state ^{3}**111** is lower than that of the ^{1}CT state of **111** by 2−3 orders of magnitude.

The comparison of the quenching kinetics of **111*** and the excited anthracene molecule by a variety of anions and neutral quenchers in polar solvents[365,366] indicated a difference in the case of inorganic anions. The differences are explained by electrostatic interactions of the positive pole of **111*** and the anions (absent in the case of neutral anthracene). Remarkably, the quenching leads in the case of anthracene to the population of the triplet state, whereas in **111** quenching occurs to the ground state.[365,366]

4. Complexes of DMABN and of Its Analogues

a. Complexes with Metal Ions. Relatively little is known about the complexes of **1** with metal ions. The analogues with a crown ether system or with aza-macrocycles (**59**, **61**, **62**) are described in section III.E.1.d; coordination to the amino nitrogen results in lowering the F_A/F_B intensity ratio and in blue shifts. Coordination at the acceptor moiety of the molecule, as studied in the case of amide derivative macrocycles (**88**, section II.E.6) or pyrimidine acceptors (**79** and **80**, section III.E.5), strongly favors the ET and shifts the F_A band to the red.

In the case of ruthenium complexes of **1**, DMABN is coordinated to ruthenium by the —C≡N group. It is reported that both $[Ru^{II}(NH_3)_5(DMABN)]^{2+}$ and $[Ru^{III}(NH_3)_5(DMABN)]^{3+}$ emit two fluorescence bands in alcohols, but the intensity ratio F_A/F_B is much lower, especially for the complex of Ru^{III} than for **1** in the same solvent.[367] This behavior has not yet been interpreted.

In the complex with Os(II), $[(bipy)_2(CO)Os^{II}(DMABN)]^{2+}$ (where bipy = 2,2′-bipyridyl), **1** is also coordinated by the N≡C— group. In the excited state, **1** acts as an electron donor in a ligand-to-ligand ET process, transferring one electron to the bipyridyl ligand and thus quenching the fluorescence. **20** (planar) and **21** (strongly twisted) as ligands behave similarly to **1**, which hints at a reactivity of the molecule as a whole, not depending on a mobility of the amino group. The transient absorption spectra indicate a radical cation of **1** as the product of the ligand-to-ligand CT. [368]

b. Cyclodextrin Inclusion Complexes. The sensitivity of compounds such as **1** toward the polarity and viscosity of the microenvironment has been applied in various ways, e.g., for sensing polymers, surfaces,[369,370] micelles, or the interior of cyclodextrins (CDs). Here, we focus on the studies of cyclodextrin inclusion complexes, while the interested reader is referred to the literature on the polymer sensing by derivatives of **1**[12,259,371] and on the micellar inclusion complexes.[372]

In the first study of the dual fluorescence of **1** in cyclodextrins, reported by Turro et al.,[373] an enhanced short-wavelength LE emission was observed in aqueous β-CD solution,[374] as well as a comparable increase of the CT fluorescence, accompanied by a blue shift of the latter. A dramatic effect occurs in aqueous α-CD solution: a quantum yield enhancement by a factor ~10, accompanied by a 10-fold increase of τ_f. Also, the blue shift is the largest for these conditions.[375] No significant increase of intensity upon addition of γ-CD was noted. Generally, a blue shift of the CT (F_A) emission and an enhancement of the total fluorescence yield is observed for the CD inclusion complexes (being by far the strongest in the complexes with α-CD) of **1** and its derivatives, as compared to the aqueous solution. This is ascribed to a relatively low polarity of the interior of the CD cavities.

There are ample and, in part, controversial reports on the photophysical behavior of **1** and its analogues included in α-CD,[373,376−382] β-CD,[259,373,377,381,383−386] γ-CD,[377,387] and derivatized β-CD.[388]

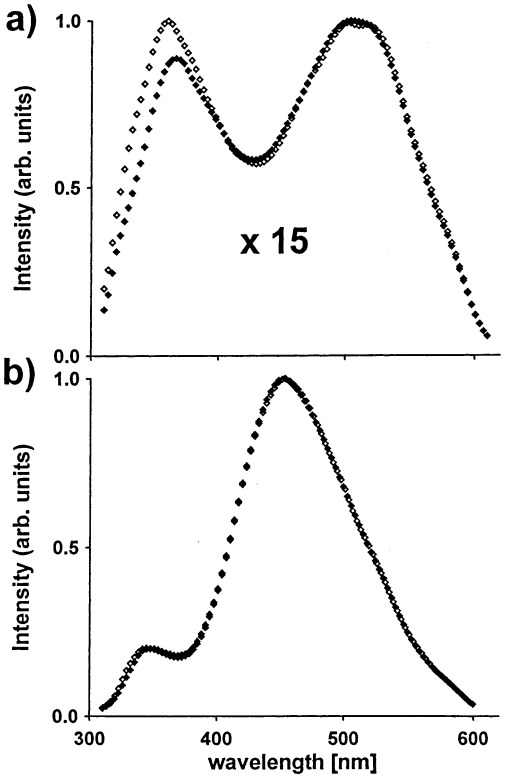

Figure 59. Fluorescence spectra of 5×10^{-5} M **1** (a) in H_2O and (b) in the presence of 2×10^{-2} M α-CD. Full diamonds correspond to freshly prepared solutions, open diamonds to the same solutions after 5 days. Some instability of **1** in aqueous solution is noted, but no change is observed in the complex with α-CD. The weak signals in the aqueous solution of **1** are amplified by the factor 15 to be comparable to those of the inclusion complex.

Even the stoichiometry of the complexes and the corresponding equilibrium constants of the complex formation, as well as the absolute and relative values of the quantum yields of both fluorescence bands, usually differ when reported by different sources. There were reports that the equilibration of **1** with α-CD in aqueous solutions needs days or even months to be established,[378,379] and the previous data were estimated to be unreliable. We could not reproduce these effects; the equilibration is fast (Figure 59).

There is no doubt that 1:1 DMABN:CD complexes exist. There are controversies, however, with respect to the proposed 1:2 and 2:2 "barrel-type" associates or "self-complexes" (Figure 60). The fluorescence spectra were interpreted[388] in terms of the formation of the 2:2 homo- or heterodimer complexes at relatively high concentrations of the reactants.[389] Molecular mechanics calculations support the association of complexes, indicating the inclusion complexes to be stabilized by van der Waals intermolecular interactions, while the further association occurs mostly by electrostatic interactions of the two outer rims of the β-CD hosts.[390]

Recently, the stoichiometry and structure of α- and β-CD:DMABN complexes were studied.[375] Absorption spectra, induced circular dichroism techniques, steady-state and time-resolved fluorescence, and triplet−triplet absorption were combined with computations (based on a DMC method including solvation effects and induced circular dichroism calculations). The

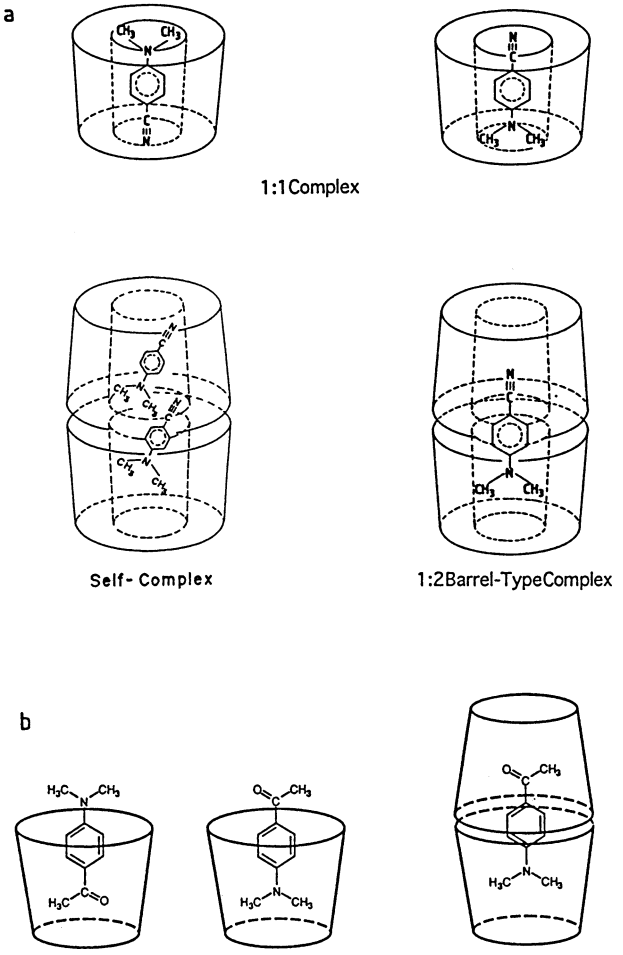

Figure 60. Suggested structures of the inclusion complexes of (a) **1** and (b) **43** with CDs (1:1 in two different orientations; barrel-type 1:2, associate 2:2). Adapted with permission from refs 378 and 382. Cf., however, other conclusions as to the structure of the 2:2 complexes.[375,390]

results present a consistent picture of the presence of 1:1 and 2:1 complexes in the case of the α-CD: DMABN system, and in the presence of 1:1 and 2:2 complexes in the case of *β*-CD:DMABN system in aqueous solutions.[375] The head-to-head orientation of the guest molecules, with the two NMe_2 groups facing each other in the 2:2 complex with *β*-CD, is found to be the most stable, in contrast to that with two CN groups facing each other, postulated on the basis of molecular mechanics calculations.[390]

The polarity experienced by the guest does not correlate with the value of the complex equilibrium constant, nor with the observed ϕ_A/ϕ_B ratio in the dual fluorescence. It seems obvious now that the increase of the F_A band in the inclusion complex, in comparison to the aqueous solution, is due to prevention of the otherwise efficient quenching by H_2O (cf. above, section IV.C.1). Access of H_2O to the guest molecule (more exactly, to its reactive site in the quenching process) is prohibited most strongly in the tight inclusion complex with α-CD, markedly less in the *β*-CD complex, and the least on inclusion into the voluminous *γ*-CD cavity.

Several authors noted differences in the excitation spectra for the F_A and F_B emissions in α-CD,[391] *β*-CD,[383] and *γ*-CD.[387] They are interpreted by several authors in terms of two possible orientations of the guest in a CD cavity, and in formation of the "barrel-type" 1:2 and 2:2 complexes (Figure 60). Most of these conclusions remain speculative. Molecular mechanics calculations indicated an increased stability for the orientation of **1** with the $-NMe_2$ group in the *β*-CD cavity and the $-C\equiv N$ group pointing out of the larger rim.[390] This is consistent with the observation of a much lower effect of inclusion in α-CD on the enhancement of F_A intensity in the case of **30** than in the case of **1**. It is suggested that **1** can enter the α-CD cavity either with the $-NMe_2$ or with the $-C\equiv N$ substituent, whereas **30** can enter it only with the $-C\equiv N$ group for steric reasons ($-NEt_2$ is more voluminous than $-NMe_2$).[373]

Contradicting conclusions were derived for the much discussed question: how far does the inclusion into a CD cavity affect the intramolecular rotation in **1**? Al-Hassan interpreted the different behaviors of **1** and **30** as an effect of immobilization of the $-NEt_2$ group in the α-CD cavity, which prevents the internal rotation.[379] It seems, however, that the polarity effects[373,377] and inhibition of quenching influence the observed photophysics of **1** much more than any restrictions to internal rotational motions. Aside from **1** and **30**, similar phenomena were described for the carbonyl derivatives **11**[380,392] and **43**.[382]

The new spectral and equilibrium data on the dual emission from **1** in CD derivatives[393] are self-contradictory. The excitation spectra hint at an impurity, and the fluorescence spectra of **1** at very low concentrations ($<10^{-6}$ M) in aqueous solution seem to indicate that the solute could be adsorbed on the walls of the optical cell.

It should be mentioned that, by covalent linking of a derivative of **1** with a CD (e.g., **89**, section III.E.6), one can build useful fluorescent probes capable of sensing nonionic analytes. [279]

V. Phenomena in the Gas Phase and in Molecular Jets

A. From Vapor Phase to Supercooled Molecular Jets

The question can be asked whether derivatives of DMABN exist which emit the typical long-wavelength CT band even in the absence of a polar solvent surrounding. The observations in nonpolar solvents have already been discussed above. Nevertheless, even alkanes, due to their electronic polarizability, exert some solvent stabilization. In the gas phase, when the solute molecule is isolated, even this stabilization is absent. Gas-phase studies can be done either in the thermalized vapor, by heating the sample to a sufficiently high temperature (vapor studies), or by expanding the vapor together with an inert carrier gas through a fine nozzle (molecular jet technique, leading to very strong cooling of the rotational, and usually also of the vibrational, modes).

The first molecule which was successfully studied showing a long-wavelength band even in the vapor phase was the *pretwisted* DMABN derivative, **21**.[135,394] The large dipole moment of the emitting state was

directly established by electrooptical emission measurements.[136] In sufficiently dense vapors, even **1** showed a red-shifted emission, which was assigned, however, to arise from the DMABN dimer or from higher clusters.[395] The emission of the DMABN monomer exhibited only a single short-wavelength band under hot vapor conditions. An interesting study joining the gas phase continuously to the condensed solution phase was reported for **1** in supercritical solvents such as CHF_3.[396,397] In this case, the number density of polar solvent molecules around the solute can be varied in a wide range, and strong effects on spectra and on the kinetics of CT formation were observed. The emission from **42** in the vapor is claimed to be an ICT fluorescence.[196] For the fluorescence of **74** in the vapor phase, a contribution of ICT emission is proposed.[248,249]

More refined and controlled conditions are possible when using the supersonic jet technique. Here, the hot vapor of the compound under study expands, together with a large excess of inert carrier gas, through a very small hole into a high vacuum backed by large pumps. Collisions in the early phase of the expansion lead to an adiabatic cooling through transfer of the vibrational and rotational energy of the molecule to the directed translational energy of the molecular beam. In this way, vibrational temperatures of less than 10 K can be achieved and lead to highly resolved spectra due to the population of only one or very few ground-state vibrational levels. This technique is usually employed in conjunction with narrow-band laser excitation at some distance from the nozzle, in a collisionless region of the molecular beam. This allows highly resolved fluorescence excitation spectra to be recorded by varying the excitation wavelength and observing the total emission (*laser-induced-fluorescence* (LIF) spectra). Alternatively, by using a high-quality emission monochromator, the dispersed fluorescence can also be studied as a function of excitation wavelength. The emission spectra are strongly dependent on the excitation wavelength, because in these collision-free conditions, the excess energy cannot be transferred to the heat-bath of the surrounding; therefore, Kasha's rule implying emission from the lowest excited state is generally not applicable, similar to any *resonance fluorescence* in gases. In favorable conditions, where one low-frequency twisting mode dominates the observed spectra, very accurate ground- and excited-state potentials can be extracted from the energy dependence of the dispersed fluorescence.[398,399]

Another advantage of jet spectroscopy is the observation of solute−solvent clusters, i.e. the fluorescence from *partially solvated* molecules. This technique allows one to answer questions such as, how many polar solvent molecules are necessary around **1** to generate the red-shifted CT fluorescence? A drawback of this technique, however, is the fact that, unavoidably, the mixture of solute and solvent generates a distribution of clusters of various sizes. Different cluster isomers of the same size are also possible. This complicates the investigations enormously, so that usually complementary techniques, like mass selection of the clusters (vide infra) or ion dip spectroscopy,[230] are necessary for a clear-cut assignment to be made.

A further interesting potential of jet spectroscopy comes from the possibility to rotationally resolve individual vibrational lines. Usually, this is done using spectrally narrowed dye lasers for excitation, and in this case rotational envelopes can be observed which allow one to discriminate between longitudinally and transversely oriented transition moments, and to conclude on the geometry of conformers and clusters. With still higher resolving equipment such as ring lasers, single rotational lines can be observed which allow one to obtain a wealth of structural data for both ground and excited states.

B. Early Jet Studies on Isolated DMABN and Derivatives

The first jet studies on the family of compounds related to DMABN were conducted by the group of Kajimoto.[138,400,401] These studies, including those on larger aromatics such as 9,9′-bianthryl **111** and anthrylanilines, are summarized in a review.[402] Most interesting is the completely different behaviors of **1** and **21**. Whereas the LIF excitation spectrum of **1** (Figure 61) is highly structured and allows one to determine even the rotational envelope and structural details, the LIF excitation spectrum of **21** (Figure 62) is completely unstructured, despite the vibrational temperature below 10 K. Instead of the highly structured normal fluorescence of **1** observed in the jet around 330 nm, **21** shows a red-shifted structureless emission peaking around 380−390 nm. In the case of **42**, the structure of the LIF spectrum disappears ∼600 cm^{-1} above the origin, which is interpreted as a coupling to an ICT state.[196]

The structureless excitation and emission features of **21** can be understood if a large structural rearrangement between the ground and excited states takes place, such that the potential minima differ strongly. This has been assigned to the twisting motion of the $-NMe_2$ group, which is twisted by ∼60° in the ground state,[137,166] and a relaxation toward perpendicularity seems likely in view of the very small emission transition moment observed in solution. However, it cannot be determined from these experiments whether the relaxed excited-state geometry really corresponds to 90°.

The fact that bare **1** does not show any broadened or red-shifted bands can then be taken as evidence that the transition to the CT state does not occur under isolated-molecule jet conditions. Possible reasons are the endoenergetic position of the CT state in the gas phase,[403,404] a reaction barrier, or a slow IVR toward population of the CT state. No red-shifted band appears on a large excess of excitation energy above the 0−0 transition (up to 3400 cm^{-1}).[395] In the case of **16**, at an excess of excitation energy up to 3500 cm^{-1}, the emission band gets broadened to the red, but no new band appears.[139]

In the case of the highly resolved spectra observed for **1** and other related compounds, a wealth of additional structural information can be drawn from this type of spectroscopy, especially when combined with complementary experiments. Kajimoto et al.[401]

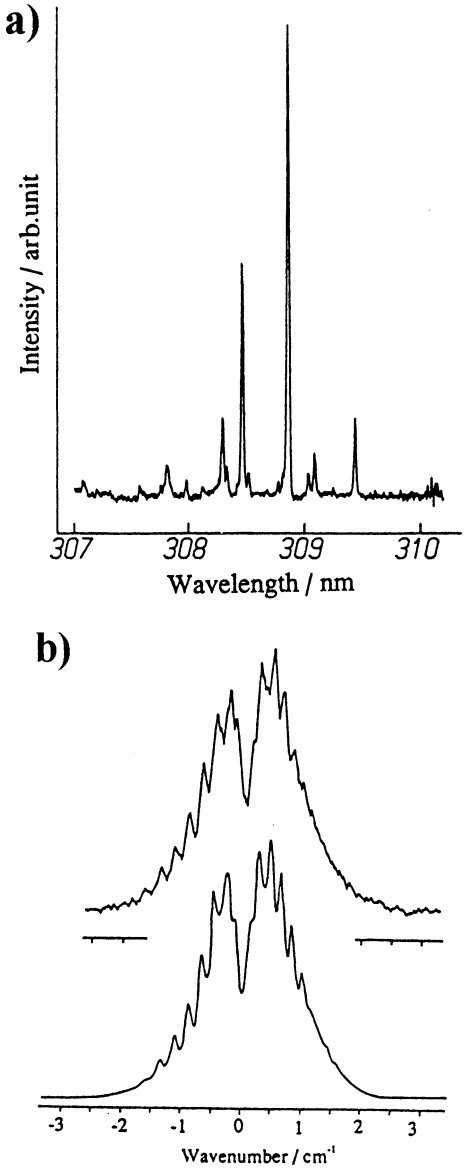

Figure 61. (a) LIF excitation spectrum of **1** in a free jet near the 0−0 origin. (b) Rotational envelope of one of the vibronic transitions of **1** in the 0−0 region, together with the best simulated spectrum (lower part). The depression in the center is indicative of a b-type spectrum with the transition moment parallel to the short molecular axis. Adapted with permission from ref 402. Copyright 1994 Elsevier Science.

used the microwave spectrum of **1** to draw conclusions about the geometry of the ground state, with the most important structural feature of the $-NMe_2$ group being its slight pyramidalization (15°) but nontwisted geometry. The crystal structure also points to a nontwisted geometry.[166] In the emissive locally excited state, the amino group loses its pyramidal character and becomes trigonal, but possibly somewhat twisted away from planarity. This was also the result of a further jet study using dispersed fluorescence.[405] Interestingly, ab initio excited-state optimization calculations[403] come to the same conclusion of a somewhat twisted equilibrium structure of the locally excited state. Whether this is really the case, in view of other theoretical results generally indicating a more planar geometry in the LE excited state as compared to the ground

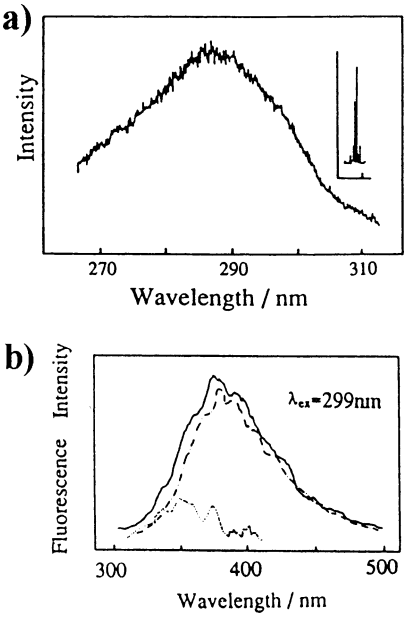

Figure 62. (a) LIF excitation spectrum of **21** in a free jet. The inset shows the corresponding 0−0 region of **1**, emphasizing the absence of sharp peaks in **21**. (b) Dispersed fluorescence spectrum of **21**, with excitation at 299 nm. The spectrum mainly consists of the strongly red-shifted band around 390 nm. Excitation at shorter wavelengths favors the importance of a second emission around 340 nm. Adapted with permission from ref 402. Copyright 1994 Elsevier Science.

state,[199,406,407] will perhaps be determined in the future by means of fully rotationally resolved spectra.

Following Kajimoto, many other research groups have investigated **1** and its derivatives or analogues with highly structured spectra in the jet.[122,229,230,270−272,395,405,408−413] No evidence was found for an additional red-shifted emission of the *bare* molecule. When such an emission was observed, it was either assigned to dimers or to higher self-clusters[230,395,414−417] which can be advantageously studied under mass-controlled conditions (see below).

Interestingly, the dimers of **1** and of the ester **73** show a strongly red-shifted emission, whereas the dimers of the corresponding aniline derivatives, **114** and **115**, show only weak red shifts.[230,417] This points to the possibility of a special mechanism for the $-NR_2$ derivatives, leading to the red-shifted dimer emission band of **1** (dimers of **1** are also well known in solutions[77,79,80,418]). At present, it is not yet clear whether this mechanism is connected with TICT formation.

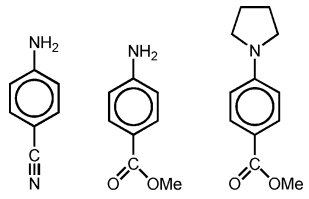

114 **115** **116**

Very recently, a femtosecond time-resolved study of **1** with mass selection of the fragments generated by photoionization was performed in the gas phase at elevated temperature and short-wavelength exci-

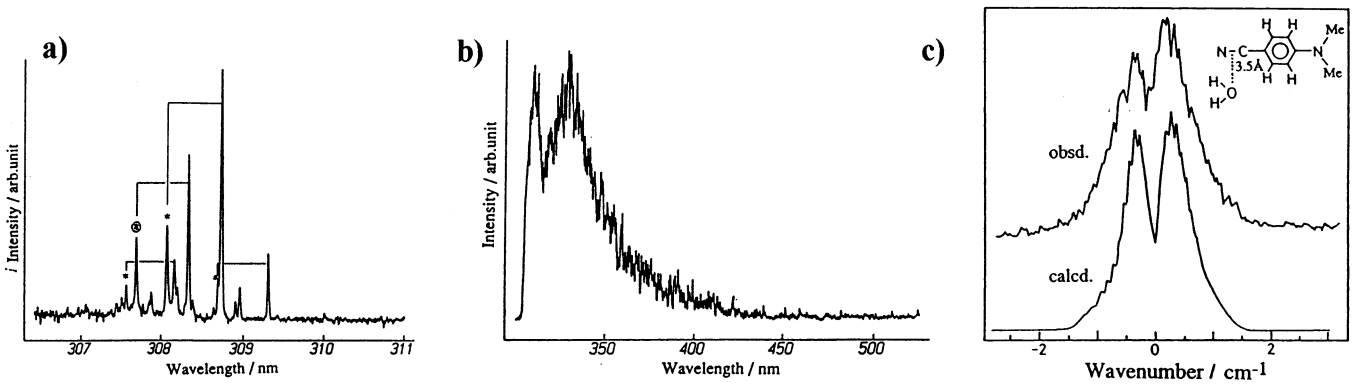

Figure 63. (a) LIF excitation spectrum of the DMABN−$(H_2O)_1$ cluster, marked by asterisks. The blue shift with respect to the corresponding peaks of uncomplexed **1** is also indicated. (b) Dispersed fluorescence spectrum of the DMABN−$(H_2O)_1$ cluster upon excitation of the 0−0 band. Only the blue fluorescence is observed. (c) Rotational contour of one of the bands of the LIF excitation spectrum of the DMABN−$(H_2O)_1$ cluster. The structure of the complex depicted resulted in reasonable agreement of the simulated spectra. Adapted with permission from ref 402. Copyright 1994 Elsevier Science.

tation (267 nm).[419] The results indicated that, under these conditions, both CT and B states are formed in parallel (within ~70 fs) and subsequently equilibrate with a time constant of around 1 ps. The ultrafast first step is interpreted as relaxation through a conical intersection.

C. Mixed Clusters of DMABN with Solvent Molecules

If **1** and a solvent are co-expanded in the jet experiment, then varying the partial pressure and temperature gives rise to different sizes of mixed solute−solvent clusters (van der Waals complexes). In general, a more or less broad cluster distribution will be present, and an efficient way of controlling this distribution is helpful. This can be done by ionizing the clusters and observing the resulting ions in a time-of-flight mass selection experiment. If the ionizing laser is tuned, excitation spectra for the various masses can be measured, which are often called *resonance enhanced multi-photon ionization* (REMPI) spectra. They can directly be compared to the LIF excitation spectra. One severe problem remains, however, even for this sophisticated detection system: the cluster ions may dissociate on their way to the detector. Therefore, the measured cluster distribution as seen by REMPI can differ from the cluster distribution actually present in the expansion chamber and emitting the fluorescence. A way to avoid this problem is to synthesize clusters not by co-expansion but by chemical means. An example is shown with the ester derivative **117** in the next section.

A further way of selecting clusters specifically is possible if the various clusters exhibit highly structured absorption (or excitation) spectra, which do not interfere with each other. This is not always the case.

Addition of a sufficient partial pressure of polar solvent in an expansion of **1** readily leads to the appearance of a red-shifted band. A great number of studies[229,230,401,402,405,409,414,415,420,421] have shown the complexity of the observed effects, which also depend strongly on the nozzle temperature. Clusters of various size contribute to the emission, and even solvated dimers and higher self-clusters are probably present.[414] We will therefore focus on a few studies where mass selection or high resolution was used and which allow one to draw clear-cut conclusions, e.g., regarding the question of how many solvent molecules are necessary to observe the CT band.

Figure 63 shows results for the DMABN−$(H_2O)_1$ cluster.[401,402,422] The LIF excitation spectrum (Figure 63a) is highly structured and slightly (18 cm^{-1}) blue-shifted with respect to bare **1**. No red-shifted fluorescence component is visible (Figure 63b). The blue shift can be understood on the basis of dipolar interaction due to complexation at the acceptor end, and some CT character upon excitation.[402] The rotational envelope supports this conclusion being consistent with an in-plane complexation at the nitrile group (Figure 63c). This most stable structure of the DMABN−water complex is consistent with the theoretical findings of Kato[407] and contradicts the structure assumed in the Dubroca-Cazeau mechanism for explanation of the solution-phase dual fluorescence (water complexation at the amino group).[82,83,87,88] Higher water clusters of **1** also have a structured absorption, as seen by MPI excitation spectra,[230] but seem to be very weakly emissive, or not emissive at all. Phillips et al.[409,410] suggested, as a possible reason, that in this case the CT state was populated but connected with fast, nonradiative processes. Such effects may also be related to different cluster isomers. In the case of DMABN−$(H_2O)_1$, it could be-shown by ion dip spectroscopy that two different cluster species, both with structured absorption, are present.[230] This could be achieved by using two tunable excitation lasers for the MPI excitation spectra. Whenever both lasers excite the same cluster isomer at different frequencies, a reduction of the ion intensity is observed. In this way, the individual spectra of different cluster isomers of the same mass can be determined.

DMABN−(acetonitrile)$_1$, on the other hand, has a much broader excitation spectrum[230] with both structured and unstructured components (Figure 64a), which are again assigned to two cluster isomers. It also shows some red-shifted emission (Figure 64b), ascribed to the cluster isomer with unstructured and homogeneously broadened red-shifted absorption. The structure of this cluster is thought to correspond

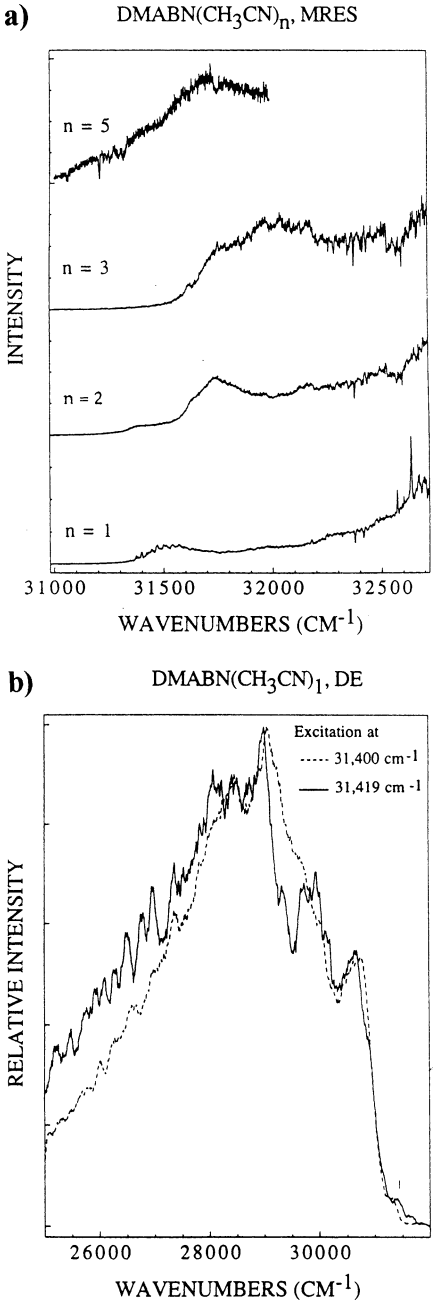

Figure 64. (a) Mass-resolved excitation spectra of different cluster sizes of the complex DMABN−$(CH_3CN)_n$. (b) Dispersed fluorescence spectrum of the DMABN−$(CH_3CN)_1$ cluster with excitation at 31 400 cm^{-1} (sharp peak) and in the background close to the sharp peak. Adapted with permission from ref 230. Copyright 1992 The American Institute of Physics.

to the acetonitrile molecule sitting on top of the aromatic ring, with its dipole moment oriented antiparallel to that of **1**, while the cluster with structured absorption corresponds to the complexation at the cyano group of **1**. The assumption is often made that broadened excitation spectra and the appearance of an excitation background are indicative of a reactive transition to a CT state. Both the homogeneously broadened absorption and the red-shifted fluorescence component with a lifetime different from the blue part of the fluorescence suggest that, in contrast to both DMABN−$(H_2O)_1$ isomers, in this DMABN−(acetonitrile)$_1$ cluster the CT state is populated.[230] However, a more recent thorough study was performed on the spectroscopy of **1** (compared to the model compounds, *p*-aminobenzonitrile and the rigidly planar **29**) in a supercooled molecular jet, with mass selection.[124] One of the results was that the dual fluorescence of the monomer of **1** is observed only when it is complexed with a minimum of five ACN molecules. No CT emission was observed for 1:1 complexes, and the different behavior of **1** and **29** hints at the importance of a twisting motion in the formation of the CT state.

A comprehensive review appeared[423] on the molecular jet spectroscopy of the TICT molecules and their van der Waals complexes with polar molecules. Special attention was paid to distinguishing the CT and the excimer emissions.

D. Aza and Ester Analogues of DMABN

Various pyrimidines were compared to the corresponding derivatives of **1** (**16**, **21**). The same effect of the substitution pattern was noted.[271] As opposed to **79** or **81**, the compounds pretwisted by steric hindrance, **80** and **82**, show a red-shifted fluorescence in methanol clusters in the jet.[42,271] Moreover, the sterically hindered pyrrole derivative **164c** emits a fluorescence which is red-shifted (as compared to the sterically not hindered analogues) even in the absence of other molecules in the gas phase.[5]

This result is most revealing in several respects. It clearly shows that the way to induce predictably anomalous (red-shifted, probably ICT) fluorescence behavior is in the pretwisting of the molecular ground-state conformation. This result holds for both solution and jet studies. If the pretwisting is enhanced, as in **21**, then even the uncomplexed molecule shows the red-shifted fluorescence. The fact that **1** and 4-(dialkylamino)pyrimidines (**79**−**82**) behave in a parallel way is strong evidence against the recently suggested alternative *cyano-bending* mechanism,[9,10,424] as the pyrimidines have no cyano group. For some compounds, it was also noted that short-wavelength excitation (with a certain excess excitation energy) increases the width of the observed dispersed fluorescence spectrum.[139,267]

A further family of analogues of **1** is that of the corresponding esters. Here, methyl esters are preferred to ethyl esters because they show a simpler excitation spectrum.[412] This can be traced back to the population of more than one rotational conformer in the ethyl ester case. In the first paper on this family of compounds,[408] the comparison was made to the jet behavior of the correspondingly substituted derivatives of **1**, and two features were noted which were absent for the nitriles while present for the esters: at a certain threshold energy above the 0−0 band, the excitation spectrum acquired continuous components. These were linked with the occurrence of a second, red-shifted fluorescence component, tentatively identified with the CT fluorescence of the bare molecule. However, a temperature-dependent study[250] showed that this red-shifted fluorescence was due to aggregation, i.e., self-clustering of the ester molecules. Subsequent studies by various groups[122,123,230,414,417,420,421,425−427] have established that

the esters are more reactive than the nitriles, not only in solution (see above) but also in the jet, to form dimers or higher self-clusters in the ground state, and to show red-shifted emission from small clusters with solvent molecules. Whereas the DMABN−$(H_2O)_1$ complex shows no red-shifted emission,[230] this can readily be observed for the corresponding cluster with the methyl ester **73**, DMABME-$(H_2O)_1$.[123] We can thus conclude that one water molecule is sufficient for **73** to induce the dual fluorescence, whereas for **1**, two or more water molecules are needed. The increased reaction tendency for the esters can be traced back to the symmetry of the excited states and their correlation. In solution, the "locally excited" S_1 state of the esters is of ^1L_a type, i.e., long-axis polarized, and correlates directly with the TICT state of the same symmetry,[185] whereas for **1**, these two states are of different symmetry. High-resolution studies in the jet, however, indicate the ^1L_b state to be of lowest energy in both cases,[122] with the difference between the two compounds that the energy gap to the higher lying ^1L_a-type state is much narrower in the ester. This can serve as a basis for understanding the different sensitivity of nitriles and esters toward microsolvation, because fewer solvent molecules are needed in the case of the ester to reverse the states to the favorable situation of equal symmetry for precursor and product states.

It can be misleading, however, to look only at the number of solvent molecules in the cluster. While in the case of water there is the described clear-cut difference between 1:1 complexes of nitriles and of esters, the corresponding 1:1 clusters with acetonitrile are both reactive.[230,421] This is probably due to a different localization of the solvent molecule that can be complexed to the acceptor substituent (as is the case for H_2O[402]) or attached to the π-electron cloud above the molecular plane (for CH_3CN[405]). Pico- and femtosecond pump probe and ionization experiments on acetonitrile complexes of **73** of various size ($n = 0-3$) evidence an equilibrium formation between the two observed species within 5 ps.[426] The formation rate of the CT species increases with cluster size, reaching a time constant of $(1.5\ \text{ps})^{-1}$ for $n = 3$. Interestingly, even for the bare molecule **73**, bimodal kinetics characteristic of an intramolecular (CT?) reaction are observed.

In principle, high-resolution studies can yield indications regarding the details of clustering. An alternative approach is possible by chemical synthesis of the model clusters: a linking flexible chain can be placed between the "solute" and the "solvent" molecules. Examples of this kind are compounds **117** and **118**, in which the intramolecular OH group can assume the role of an alcohol solvent in a 1:1 intermolecular complex. There is, however, an important difference, namely that of the linking chain, which restricts the number of possible conformers. Molecular modeling calculations for **117** and **118** indicate that intramolecular complexing can be either at the carbonyl oxygen or at the ether oxygen. No complex formation with the π-electron cloud above the molecular plane is possible. The excitation spectra for **117** and **118** are clearly red-shifted with respect to those of **32**,[427] reflecting the intramolecular complexation, which increases the acceptor strength. **117** and **118** form these intramolecular "1:1" complexes in polar and nonpolar solvents and can be used to study the importance of alternative hypotheses, such as the solute−solvent exciplex mechanism.[7] The novelty of this approach lies in the fact that the properties of these clusters in the jet and in solution can be compared.

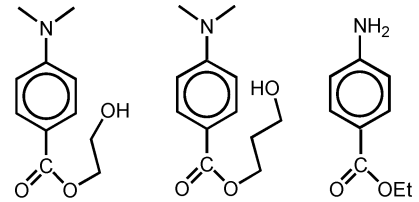

117 **118** **119**

E. High-Resolution Studies

Not only are molecular jet techniques appropriate to study the vibronic pattern of electronic transitions, but the high resolution achievable with this technique in principle even allows one to probe single rotational transitions which carry a wealth of information about molecular structure and conformations. There are numerous studies on derivatives of **1**[122,401,402,409−413,425,428−431] with partial resolution of the rotational pattern. This can be advantageously used to identify isomers, such as the gauche and trans isomers in ethyl esters,[411,425] and to assign the structure of solute−solvent clusters. Such studies allow one to conclude, for example, that the water or methanol clusters with DMABN or with esters such as **119** or **34** contain the solvent molecule in the acceptor site, close to the cyano group, *resp*. to the carbonyl oxygen.[401,402,411,413]

Moreover, the shape of the rotational envelope of such a vibronic band is also indicative of the orientation of the electronic transition moment with respect to the overall rotational axis, and is therefore in a sense equivalent to fluorescence polarization spectroscopy. This approach allows one, in principle, to compare the transition moments of corresponding nitriles and esters which differ in their fluorescence polarization in solution. **1**, excited in the maximum of the absorption band ($^1L_a \leftarrow S_0$), shows a negative (close to the 0−0 transition) to weakly positive fluorescence polarization of the B-band in solution. This led to the conclusion that the purely electronic transition moment in fluorescence is oriented perpendicular to the long molecular axis, and hence the emitting state corresponds to the ^1L_b-type state (cf. section III.D.1) The strongly positive fluorescence polarization of the corresponding ester established a ^1L_a-type emissive state of the B-band.[185] In the jet, esters such as **116** and **73** both behave like ^1L_b-type emitters from the lowest vibrational level, but the ^1L_a-type state is very close-lying, and the mixing of these two states for higher vibrational levels can be followed directly by the observation of the rotational contours.[122] For similar conditions, this mixing is absent in **1**. Such a comparison of solution and jet behaviors leads to the conclusion that nitriles have

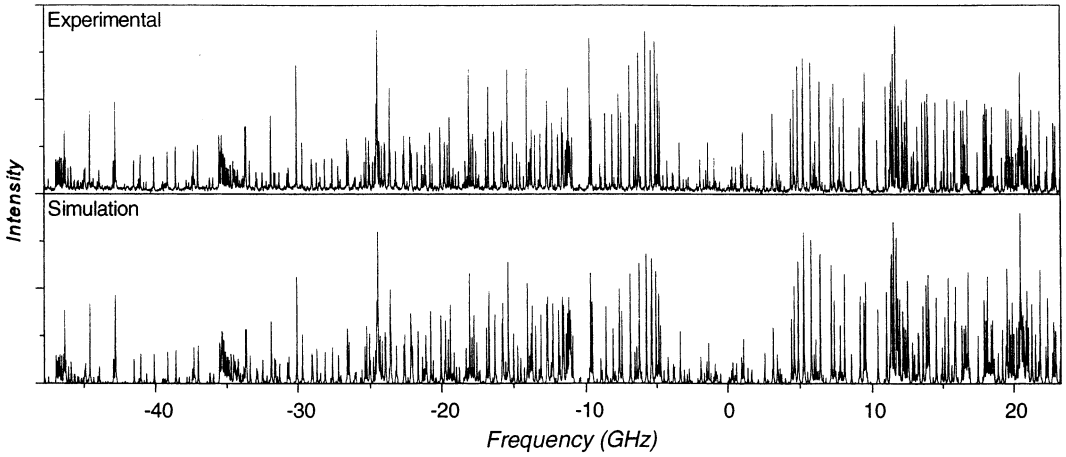

Figure 65. Part of the high-resolution fluorescence excitation spectrum of the origin vibronic band of **114**. The spectrum contains about 800 rotational lines; the observed line width is 26 MHz. Reproduced with permission from ref 431. Copyright 1997 Elsevier Science.

an emissive ^1L_b-type state in both jet and solution conditions, due to the relatively wide $^1L_a-{}^1L_b$ energy gap. In the esters, the gap is much narrower, ranging from weakly positive (^1L_a- above ^1L_b-type state in the jet) to negative values (^1L_a- below ^1L_b-type state in solution). These results are relevant in relation to the hypothesis on a PJT mechanism of CT in **1**, which considers this energy gap as the decisive factor for the photoreaction to occur.

Information that is even more detailed can be gained from spectra with ultrahigh resolution, where individual rotational lines can be distinguished. For the size of a molecule like **1**, the laser equipment must have a sufficient spectral resolution (of the order of 100 MHz or better), because one single vibrational band contains several thousand rotational lines, and the analysis is correspondingly difficult. This may be the reason why ultrahigh-resolution results have not yet been reported for **1**. There are, however, results on some simpler derivatives. In a study of benzonitrile,[432] the rotational constants derived from the spectral fits allow an evaluation of the interatomic distances in the ground and excited states. The small line widths indicate an absence of a fast process leading from an LE to a CT state with a bent cyano group, as postulated in the "cyano-bend" mechanism of **1** (cf. section II.B.5).[9,10]

Further studies involved aniline[433] and **114**;[431] the nitrogen, being pyramidal in the ground state, becomes planar upon excitation. For **114**, a pure *b*-type spectrum is observed, indicative of a transition moment perpendicular to the long molecular axis. From the rich rotational spectrum of the 0−0 vibrational band (Figure 65), the rotational constants for S_1 and S_0 states were determined, and structural conclusions could be drawn such as the pyramidalization angle (34°) in the ground state.

VI. Fluorescence and Reaction Kinetics

A. Formal Kinetics and Thermodynamics

1. Bimodal Kinetics

Stationary fluorescence spectra of DMABN demonstrate the complementarity of the two fluorescence bands: on changing the factors which influence the rate (or equilibrium), e.g., temperature, pressure, polarity, or viscosity of the medium, the decrease of intensity of the F_B band is accompanied by a corresponding increase of F_A, and vice versa. The time-resolved fluorescence measurements prove the parent−daughter relationship between the excited states of **1**, revealing the bimodal kinetics of the B* → A* reaction. The reversibility of the reaction, particularly in medium-polarity solvents, gives an insight into the back ET reaction and into the excited-state reaction thermodynamics.

2. Temperature Effects in Stationary Spectra

Lippert et al.[63] have already reported the effect of temperature on the stationary dual fluorescence intensities of DMABN. The diagrams of ln ϕ_A, ln ϕ_B, and ln(ϕ_A/ϕ_B) vs $1/T$ were investigated for several derivatives and analogues of DMABN in various solvents.[6,70,129,171] As a rule, they represent a functional relationship exemplified in Figure 66.

The simple kinetic scheme (Figure 67) in the steady-state approximation results in the quantum yields:

$$\Phi_B = \frac{k_{f_B}(k_A + \overleftarrow{k})}{k_A(k_B + \vec{k}) + k_B\overleftarrow{k}} \tag{19}$$

$$\Phi_A = \frac{k_{f_A}\vec{k}}{k_A(k_B + \vec{k}) + k_B\vec{k}} \tag{20}$$

$$\frac{\Phi_A}{\Phi_B} = \frac{k_{f_A}\vec{k}}{k_{f_B}(k_A + \overleftarrow{k})} \tag{21}$$

Assuming, for the sake of simplicity, only the forward and back ET reaction rates to be temperature-dependent, we can construct plots of log ϕ vs $1/T$ (analogous to those used for bimolecular excimer formation[151]), which can be represented in general form, for an exothermic reaction, as in Figure 68. The plot is characterized by the extrema or inflection

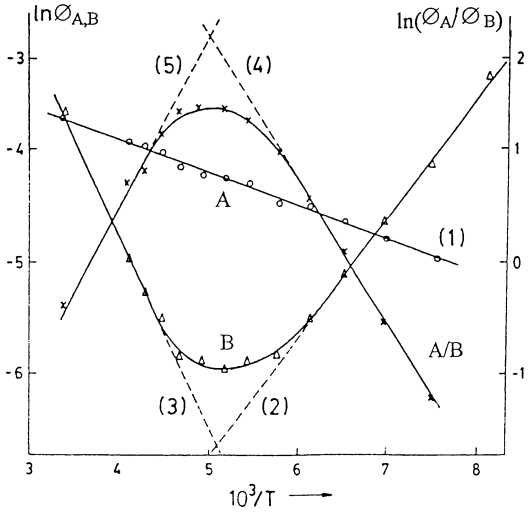

Figure 66. Fluorescence yields of both bands, ϕ_A and ϕ_B, of **17** in MTHF solution as a function of temperature:[4,70] ln ϕ_A, ln ϕ_B, and ln ϕ_A/ϕ_B vs $1/T$. Intersection of the dashed lines indicates the temperature T_1 (vide infra, eqs 22 and Figure 68). The slopes determine the energies, defined in this section and in section III.C.1−2. (1) $-\epsilon_1$, (2) E_a, (3) $\Delta H° - \epsilon_1$, (4) $-(E_a + \epsilon_1)$, and (5) $-(\Delta H° + \epsilon_1)$.

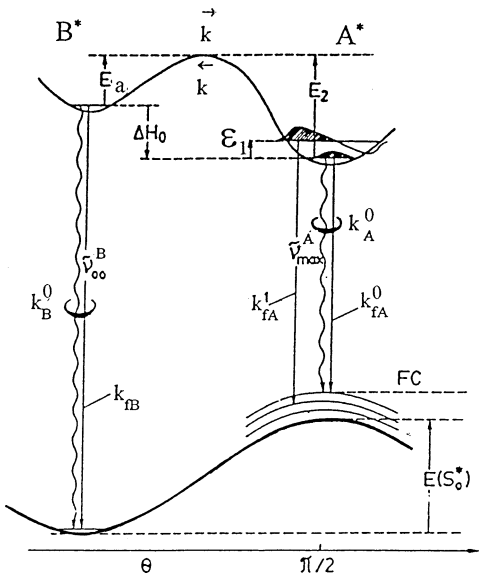

Figure 67. Schematic explanation of the processes and states involved in the photophysics of DMABN and its analogues, according to the TICT model.[4] Symbols are explained in the text. Emission from the zero vibrational level of the A* (TICT) state is forbidden; it is allowed from a vibronic excited state (ϵ_1). The Franck−Condon (FC) ground state is situated above the ground-state barrier to internal rotation of the $-NMe_2$ group ($E(S_0*)$) at the twist angle $\theta = \pi/2$ by an additional destabilizing energy resulting from the orientation of the solvent shell around the giant dipole of the A* state.

points corresponding to the temperatures T_1 and T_2, defined by the relations

$$T_1: \quad \overleftarrow{k} = k_A \qquad T_2: \quad \vec{k} = k_B \tag{22}$$

The maximum on the log(ϕ_A/ϕ_B) plot and the minimum on the log ϕ_B plot correspond to the transition from the *kinetic regime* (at lower temperatures), i.e., from a *one-way* ("irreversible") reaction, to the *equilibrium* (or *high-temperature*) *regime*, with the

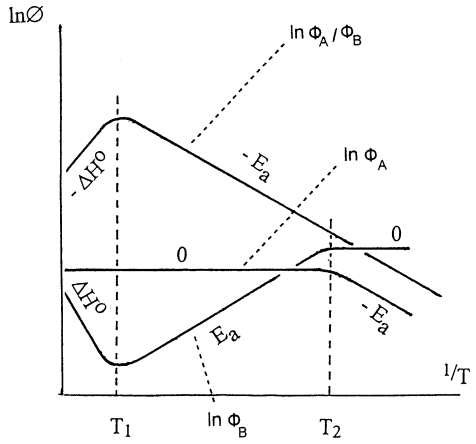

Figure 68. Logarithmic plots of eqs 19−21 vs $1/T$, for only two thermally activated processes: the forward and the back reaction rates. The meaning of the slopes is indicated. Temperatures T_1 and T_2 are defined by eqs 22.

reverse reaction prevailing over the photophysical deactivations. At temperatures $T > T_1$, the forward and back reaction rates are larger than all other ones:

$$\overleftarrow{k}, \vec{k} \gg k_A, k_B \tag{23}$$

T_2 is the limit of the *low-temperature regime*, with the forward reaction being slower than the remaining deactivation processes in B*.

The kinetic scheme of an actually observed reaction is often more complex, especially if there are more than two temperature-dependent rates,[434] such as k_{f_A} (cf. section III.C.2) or the nonradiative processes contributing to k_A and/or k_B (e.g., ref 236).

3. Reaction Thermodynamics

The equilibrium constants of the reaction B* ⇄ A* can be determined either from time-resolved measurements, $K = \vec{k}/\overleftarrow{k}$, or from the stationary spectra in both regimes, $T < T_1$ and $T > T_1$, complemented by lifetime measurements done in the *one-way* regime, $T < T_1$. $\Delta H°$ values were determined either from the temperature dependence of the ratio of the fluorescence yields,

$$\Delta H° = -R\frac{\mathrm{d}\ln(\Phi_A/\Phi_B)}{\mathrm{d}(1/T)} - \epsilon_1 \tag{24}$$

where ϵ_1 was defined in section III.C.2, or from the temperature dependencies of separately measured forward and back CT reactions.[133] The reported data are collected in Table 10.

The thermodynamic concepts can be applied to the excited-state equilibria if all other degrees of freedom, except the electronic one, are thermally equilibrated.[435] A doubt was expressed[237] if the values found from the direct kinetic measurements of the forward and back reaction rate constants, or from the plots like in Figures 66 and 68 (Table 10), represent a real equilibrium: the forward reactions are often as fast as the relaxation of the solvent, or even faster (see the next section). Hence, the still open question arises: How far does the incomplete solvent equilibration of B* (formed in the back reaction, B* ← A*)

Table 10. Equilibrium Constants,[a] K_{eq} = [A*]/[B*] at T = 298 K, and the ΔH^o Values for the B* → A* Reactions

compd	solvent	ΔH^o (kJ/mol)	K_{eq}
1	toluene	−5.9,[99] −11.6[111]	0.6 (2.6 at 183 K)[99]
	ether		1.1[99]
	1,4-dioxane		4.4[99]
	n-BuCl	−11.4,[b] −10.8[c]	3[153]
	CH_2Cl_2		14[153]
15	CH_2Cl_2	−6.2[g]	18[h]
17	CH_2Cl_2	∼−14.9[70]	
	MTHF	−15.3[70]	
43	ACN		128[237]
30	toluene	−12.3[111]	
	BuCl	−13.4[c]	
39	toluene	−15.0[111]	
23	BuCl	−12.4[c]	
32	BuCl	−11.4[d,e]	
	3-MP	−9.6[101]	
34	BuCl	−10.7[d,e]	
46	ACN	−15[133]	13.5[f]
23	ether	−13[133]	181[f]
	ACN	−16[133]	
24	BuCl	−9.8[c]	
	ether	−13[133]	
47	ether	−14[133]	
40	cyclohexane		0.9[99]
	benzene		8.7[99]
	toluene		8.9[99]
62	toluene	−14.8	18[225]

[a] So far as we can treat it as the equilibrium; see the text, section VI.A. [b] Evaluated from the data of ref 63. [c] Evaluated from ref 171. [d] For lack of data for ϵ_1, the value shown ($\Delta H^o + \epsilon_1$) is an upper limit for ΔH^o. [e] Evaluated from ref 457. [f] Evaluated from ref 133. [g] Evaluated from ref 70. [h] Data from ref 237, re-evaluated in ref 153.

distort the apparent thermodynamic functions? Some doubt may arise, because against the early estimates[101] no clear correlation between the thus-determined ΔH^o values and the spectral distance between the F_B and F_A band maxima has been found. The test would require a close inspection of the missing systematic studies of the temperature effects in the solvents of different polarities.

4. Measured Rates and Activation Energies

Beginning with the early works on the kinetics of the excited-state transformation in DMABN, it became obvious that the process belongs to the fastest reactions, and in liquid solutions it usually occurs within a few picoseconds.[314,315,436−438] The rates of these very fast excited-state CT reactions often appeared correlated with the solvent mobilities rather than with intramolecular vibrations. In numerous cases, the activation energies of the B* → A* reaction were close to, or slightly smaller than, the activation energies of the viscous flow in a given solvent,[6,70] while the rates were of the order of the Debye reorientational relaxation time.[315,437,439] Better correlations were discovered between the measured reaction rates and the *longitudinal* relaxation times, τ_L, or the average solvation times, τ_S,[440] of the solvents.[441−443] Later, it was found that the reaction is not always determined by the solvation dynamics: the reaction time can be shorter than τ_L[444] or τ_S,[467] and the processes can be nonexponential (see the next sections).

The dual fluorescence of **1** is a photoreaction which occurs entirely in the excited state and thus leads to the product being excited. Therefore, in principle, both the precursor and the product can be followed in time by fluorescence spectroscopy. Such a photoreaction has been termed an "*adiabatic* photoreaction".[445,446] Numerous electron-transfer processes in the excited state, and in particular those of the formation of TICT states, are beautiful examples of this class. The investigation of their kinetics can give important clues to our present understanding of how energetics (the shape of the reaction hypersurface) and dynamics (stochastic motion along various dimensions of the reaction coordinate) influence each other.

Specific efforts to identify or interpret the rate-determining steps in the CT-state formation or decay (e.g., linking the activation energies of a reaction with the viscous flow,[70] or the reaction time with the *longitudinal* relaxation time of the solvent, τ_L[441]) are referred to in connection with a particular compound or family of compounds. Experimentally, the kinetic observations are easier if the precursor and product fluorescence bands are spectrally well separated, and this is in general the case for **1**, for its simple derivatives, and for several families of mainly monocyclic analogues of **1** with different acceptor or donor groups. We will therefore confine our review on kinetics to this class of compounds.

B. Simple Precursor–Successor Model

In the study of the kinetics, if both the precursor and the product of an adiabatic photoreaction are fluorescent, the time dependence of the respective fluorescence signals should be directly proportional to the time-dependent population of these species — though the tacitly assumed proportionality can have exceptions.[447] The general solution of the system of differential equations corresponding to the dynamic equilibrium predicts two biexponential signals,[448,449] with an initial fast decay component $\tau_d(X)$ for the precursor X and a rise component $\tau_r(Y)$ of equal value for the product Y. The reciprocal of this short lifetime corresponds to the sum of the forward and backward reaction rates, $k_1 + k_{-1}$, in the case of an excited-state equilibration being much faster than the radiative and nonradiative decay processes (i.e., in the "*high-temperature regime*";[449] cf. section VI.A.2).

The second decay time, also identical for the precursor and the product, represents the decay to the ground state of the combined precursor−successor system after the dynamic equilibrium involving the forward and backward reaction has been established. The short time constants should be identical, $\tau_d(X) = \tau_r(Y)$, while the subsequent (longer) decay time $\tau_d(Y)$ reflects mainly the properties of the longer living product, and — if the product is absent at t = 0 and is formed only during the adiabatic photoreaction — the preexponential factors are linked: $A_d(X) = -A_r(Y) = A_d(Y)$.

The prediction $\tau_d(X) = \tau_r(Y)$[450,451] and also $A_d(Y) = -A_r(Y)$[98,231,270] has been tested in various solvents for **1** and its derivatives. It has been verified in a multitude of cases, mainly in aprotic solvents such

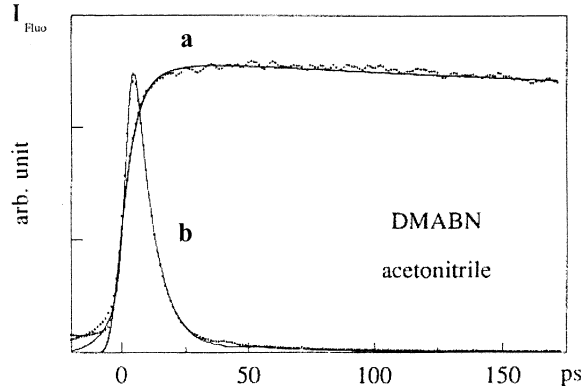

Figure 69. DMABN in acetonitrile. The decay of the short-wavelength fluorescence (b) can be described by a biexponential function, the short component of which (6 ± 1 ps) matches the rise time of the long-wavelength fluorescence (a). The relative weights of rise and decay of the latter are very close to −1. Reproduced with permission from ref 309. Copyright 1997 American Chemical Society.

as acetonitrile, butyronitrile, butyl chloride, diethyl ether, or toluene. An example from the recent literature is given in Figure 69. If the back reaction X ← Y can be neglected, then the precursor should decay according to a single-exponential law, which readily allows one to determine the forward reaction rate constant, k_1.

Comparison of the kinetics of closely related derivatives of **1** can allow one to approach the problem of identification of the reaction coordinate. This has been attempted with the pair of molecules, **37** and **38**[192] (section III.A.1.a). **38** has additional nonconjugated methyl groups which do not change the spectra or other photophysical properties (Figure 34) but which act like "paddles", slowing down the internal rotational motion.

If such a motion is involved in the reaction coordinate of CT state formation, then this dynamically hindered compound should exhibit reduced rates. This is, in fact, observed at low temperature (in the irreversible kinetic region, where the back reaction is unimportant), as testified by the reduced relative contribution of the CT band in the dual fluorescence spectra (Figure 34). The fact that at high temperatures, in the reversible kinetic region, the dual fluorescence spectra become identical, with identical relative weight of the CT band, is a consequence of the fast equilibrium leading to the same equilibrium constant. Hydrodynamical friction seems to slow the forward and the back reaction by the same factor (about 2) in the compound with the bulkier rotor.[171,192] This further supports the observation that the introduction of the methyl groups (not conjugated with the aromatic ring and not sterically overcrowding the molecule) does not affect the electronic and photophysical properties of the compound.

These rate constants, when plotted as ln k vs $1/T$ in an Arrhenius-type fashion, allow the determination of the Arrhenius activation energy, E_{Arrh}. The latter is also accessible from a corresponding plot of $\ln(\Phi_A/\Phi_B)$. It turns out that, in medium to highly polar solvents, where dual fluorescence occurs for **1**, E_{Arrh} is invariably similar to or slightly smaller than the corresponding activation energy for the viscous flow, E_η.[6]

Three factors have to be taken into account simultaneously. The polarity effect leads to an increase of the rate constant at higher polarities (i.e., at lower temperature). The viscosity effect lowers the rate constant at increasing viscosity (i.e., at lower temperature). The effect of an intrinsic reaction barrier, E_{intr}, along the reaction coordinate slows the rate constant at lower temperatures. One can therefore approximate the observed Arrhenius activation energy, E_{Arrh} (which summarizes the temperature-induced rate changes), by the sum of three contributions, eq 25:

$$E_{Arrh} \approx E_{intr} + \alpha E_\eta + E_{pol} \qquad (25)$$

where E_{intr} and E_η are positive, $\alpha \leq 1$, whereas $E_{pol} < 0$, because it increases the rate at low temperature. Various attempts have been made to separate these three factors. The group of Eisenthal[450,451] obtained an astonishing result. Working at room temperature in isoviscous solvent mixtures of different polarity, they determined the accelerating influence of E_{pol}. Then, they compared differently polar pure solvents at temperatures where their viscosity is equal (eliminating the effect of E_η) and corrected for E_{pol}. If the correction for E_{pol} is not done, "negative activation energies" are found; i.e., the observed rates increase as the temperature is lowered (compare a similar acceleration of the reaction if the pressure is increased at constant temperature for diethyl ether as solvent, as discussed below). From this treatment, they were able to determine E_{intr} (33.5 kJ/mol in alkanes as solvents), and this reaction barrier is lowered in butyronitrile to 13.4 kJ/mol by the polarity effect. Finally, the rates corrected for the effect of E_{intr} and E_{pol} are plotted versus viscosity. The unexpected result was that any viscosity dependence of these reduced rates is found to be completely absent ($\alpha = 0$).

This result is in conflict with the observation that a change of the value of E_η for many solvents is fully reflected in the measured values for E_{Arrh},[6,171,452,458] which suggests $\alpha \approx 1$. It is also in conflict with recent high-pressure measurements in the highly viscous medium-polarity solvent glycerol triacetate (GTA),[459] which possesses an extremely strong viscosity dependence ($E_\eta \gg |E_{pol}|$). In this case, the rate is slowed approximately proportional to the viscosity increase, consistent with $\alpha \approx 1$. On the other hand, in solvents with a less steep pressure dependence of viscosity, the polarity effect can be stronger than the viscosity effect, and then the observed rates can increase with increasing pressure, such as in diethyl ether,[107,460,640] but can still be consistent with $\alpha \approx 1$.

The conflict can be resolved if we consider more closely the underlying assumptions of the treatment by Eisenthal et al.[450,451] They propose that the polarity effect on the rate is reflected only in the exponential factor of the Arrhenius-type rate constant, i.e., via a reduction of the activation barrier. An alternative assumption can be made ascribing the polarity effect not to barrier changes but to an increase of the preexponential factor with polar-

ity.[455,456,464] If this is done, a number of further conflicting experiments can be explained (e.g., the variation of the rate constant for derivatives of **1** by up to 2 orders of magnitude although the observed Arrhenius slope is unchanged — for details see the following sections). Strong changes of the preexponential factor can be expected if the reaction profile is essentially barrierless, i.e., $E_{intr} \approx 0$. Such a view is also supported by the direct comparison of pressure- and temperature-induced rate changes[454,459] (for details, see below) and by the nonexponential precursor decays observed in high-viscosity solvents (see next section).

On the other hand, for low-viscosity solvents at room temperature, nonexponentialities have not been detected with the present time resolution (Figure 69), and the reported high-pressure experiments always contain both the viscosity and the polarity influences. We therefore want to leave open the question regarding the presence or absence of an activation barrier and suggest a possible crucial experiment. However, in the following sections, we prefer to use the barrierless or nearly barrierless model that is able to fit the puzzle of apparently conflicting experiments together.

A possible decisive experiment could rely on the derivatives of **1** which show dual fluorescence even in alkane solvents at room temperature (e.g., **74**, **75**, and **42**). In these nonpolar solvents, polarity effects should be absent for both lowering the temperature and increasing the pressure. Then the Hicks–Eisenthal treatment can be repeated (isoviscous alkanes at different temperatures without the necessity to correct the barrier for polarity effects; hence, the experimental Arrhenius slope would directly yield E_{intr})[450,451] and compared to the high-pressure/low-temperature treatment of data. Viscosity effects seen in the high-pressure data should be identical to those at low temperature if E_{intr} is essentially zero.[454,459]

C. Precursor–Successor Model Involving a "Time-Dependent" Rate Constant

In other experiments,[6,270,452−454,459,464] carried out in alcohols at low temperatures, and in other solvents of substantial viscosity, nonexponential precursor (B*) decays were observed (i.e., they could not be fitted by a sum of two or three exponentials), linked with product rise times apparently faster than the precursor decay time, $\tau_r(Y) < \tau_d(X)$. A kinetic analysis in terms of time-independent rate constants was unable to account for this observation[6,452] (see, however, ref 447). In some specific cases (4-(dialkylamino)pyrimidines in alcohols[268]), the nonexponentiality of the decay of X has been demonstrated to be due to different reactivities of several excited-state species hydrogen-bonded at different positions[270] (cf. section III.E.5). On the other hand, nonexponential precursor decays were also observed in highly viscous aprotic solvents such as glycerol triacetate (Figure 70).

The nonexponential precursor decay can be used directly to derive the explicit formal time dependence of the forward rate constant. An example can be found in Figure 71. The apparent contradiction of the product rise times being shorter than the precursor

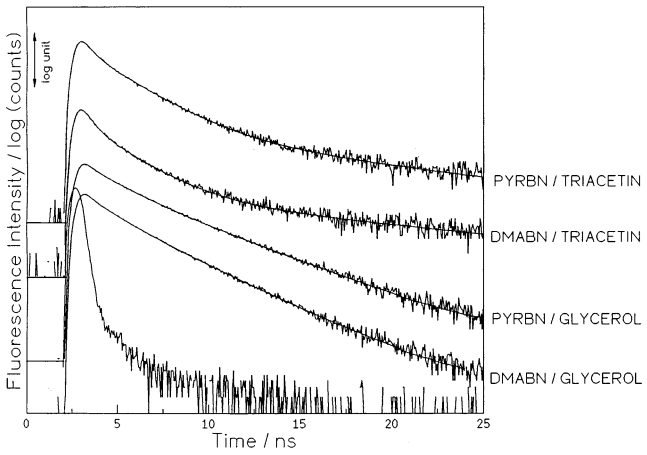

Figure 70. Fluorescence decay curves and triexponential fits of the short-wavelength band of **1** (DMABN) and **23** (PYRBN) in glycerol and glycerol triacetate (TRIACETIN) at 257 K. In this case, the derived individual decay parameters cannot be interpreted as species lifetimes, but they can be used to calculate an average lifetime which lengthens with increasing solvent viscosity. Reproduced with permission from ref 454. Copyright 1994 Elsevier Science.

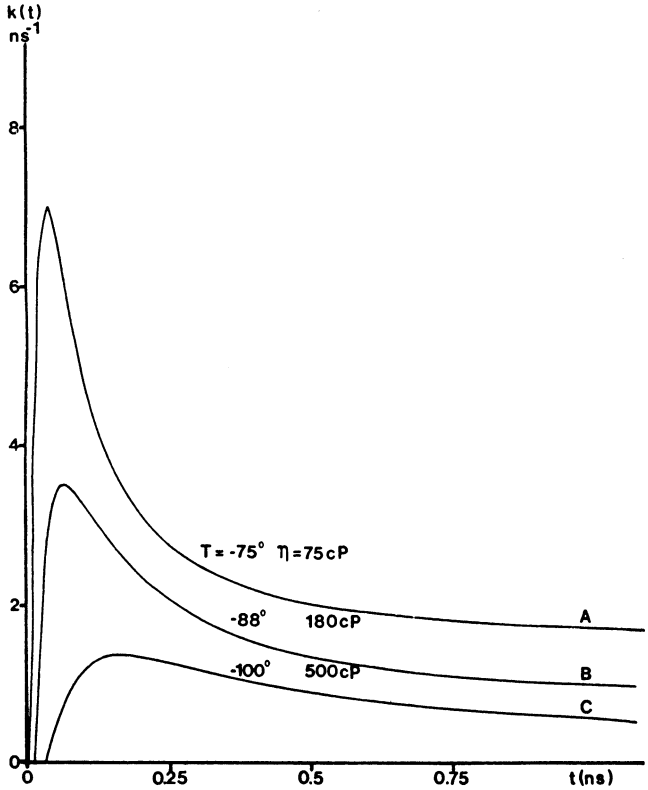

Figure 71. Temporal variation of the rate coefficient $k(t)$ for the CT reaction of **1** in propanol at low temperature, as calculated from the nonexponential fluorescence decay profile of the B emission. At long times, the observed rate coefficient converges to a constant value, k_{lt}. Reproduced with permission from ref 452. Copyright 1985 Elsevier Science.

decay times can be explained by taking a time-dependent $k(t)$ explicitly into account. Note that this observation of nonexponential precursor decays is not limited to protic solvents but has also been observed in highly viscous aprotic solvents, e.g., in glycerol triacetate — even stronger than in glycerol.[454,459]

Specific protic solvent effects can thus be excluded. Two-dimensional reaction theories indicate that the condition of the reaction rate being faster than the solvation time is especially prone to lead to nonexponential precursor decays and shortened product rise times.[404,480] In low-viscosity solvents with very fast solvation kinetics, such as acetonitrile, generally an exponential kinetic behavior is observed (Figure 69).[133,308,309] Due to the limited time resolution of the reported experiments, it is not possible to conclude on the absence or presence of nonexponential early-time contributions in acetonitrile. More systematic subpicosecond studies of DMABN kinetics in differently polar solvents with varying viscosity influence and dielectric relaxation time (or, more precisely, varying shapes of the dielectric relaxation function) are needed to clarify the source of the nonexponentiality: reaction on a barrierless potential or consequence of the two-dimensional reaction mechanism in the limit of slow solvents (see below; this is also valid for aprotic solvents) or multiple ground-state species (e.g., different specific solute−solvent complexes — this is mainly important for alcoholic solvents).

At first sight, such kinetic behavior, different compared to the simple kinetics described in the preceding section, seems difficult to account for within one model. Kinetic modeling of DMABN very often assumes the presence of activation barriers, which are lowered with increasing solvent polarity.[450,451,473,474,480] The resulting viscosity independence of the rate, as drawn from isoviscosity experiments,[450,451] is at variance with other experiments (see below), which demonstrate a strong influence of viscosity[454,459] and of rotational volume (see the comparison of **37** with **38** discussed above). These experiments show that variations in rate constants of more than 1 order of magnitude for related compounds can be accompanied by negligible changes in the activation energy.[209] A simple possibility to integrate and explain all these controversial facts is the alternative assumption that the polarity influence on the rate constant is reflected through the preexponential factor, rather than through the exponential one including the activation energy. This alternative view is a simple consequence of the fact that, for $E_{intr} = 0$, solvent polarity cannot lower the barrier more. Of course, there may be borderline cases, especially in weakly polar solvents, where E_{intr} can become nonzero, and both factors can then vary with solvent polarity.

With this alternative assumption, three important aspects of the photoreaction can be seen: (i) the nearly barrierless or completely barrierless shape of the reaction hypersurface; (ii) variation of its shape such that the preexponential factor can become polarity dependent; and (iii) the role of the relaxation of the polar solvent as a kinetically independent reaction coordinate. In the following, we wish to develop in more detail the view that the above observations are a simple consequence of these three factors and that kinetic models are at hand which can treat these cases.

D. The Barrierless Nature of the Reactive Hypersurface

Experimentally, for **1**, the reaction B* → A* rate constant increases with the solvent polarity for otherwise unchanged conditions (temperature, solvent viscosity).[450,451] As mentioned above, two alternative explanations can be given in terms of the Arrhenius equation for this increase of the reaction rate constant. The activation energy E_A decreases[450,451] or/and the preexponential factor A increases[455,456] with rising solvent polarity.

The importance of changes of the preexponential factor has previously been observed in the comparison of various derivatives of **1**. Variations in the rate constants of nearly 2 orders of magnitude are connected with negligible changes of E_A, as determined from the low-temperature slope of Arrhenius plots of the ratio of the dual fluorescence quantum yields, measured in the same solvent.[455−457] Moreover, the experimental E_A values are always very close to E_η and are too small to be consistent with any sizable intrinsic activation barrier larger than the thermal energy, kT.[6,458] Direct access to the *intrinsic* activation barrier E_{intr} (the potential barrier in the absence of viscous solvent hindrance) is possible by comparing the dependence of the kinetics on pressure- and temperature-induced viscosity changes.[454,459] If there is a viscosity effect, and if this is larger than the polarity effect, then the observed rates should slow with increasing pressure. If the same rate reduction factor is observed upon cooling the solvent, then intrinsic barriers, which would additionally slow the reaction by temperature changes of the population of the transition state region, must be absent. For the solvents studied (strongly polar glycerol and medium polarity glycerol triacetate), the complete temperature dependence of the rate constant for **1** and further derivatives could be shown to be due to viscosity changes alone; i.e., an *intrinsic* barrier was clearly absent. In this case, the kinetics are determined by the variation of an energetically flat part of the reaction hypersurface, which determines the preexponential factor. The observed nonexponential fluorescence kinetics are consistent with this finding (see the next section). Also at room temperature, in highly polar solvents such as acetonitrile, a nonexponential kinetic behavior would be expected on the basis of the barrierless model but has not been observed until now.[133,308,309] This is an important point for further research, e.g., with higher time resolution. The nonexponential transient kinetics part (see Figure 71) of the reaction in acetonitrile and other solvents with low viscosity could be in the subpicosecond region at room temperature. Then, the experimental observations available could correspond to the time-independent long-time rate constant k_{lt} (see below, eq 26, and Figure 71, at long times), resulting in an exponential time dependence.

From the above high-pressure experiments, the previously proposed model of a reaction, which is controlled uniquely by a solvent-polarity dependent barrier[450,451] and not by viscosity, could be shown to be at variance with the experiments. At high pressures, both solvent viscosity and polarity increase.

If there was no viscosity influence, the reaction rates should always increase with pressure due to reduced activation barriers at high pressure (hence increased polarity), but the opposite is observed,[454,459] at least in highly viscous solvents. For other solvents, with a less steep dependence of the viscosity on temperature, the rate constants can actually increase with pressure,[201,460,640] indicating a dominant polarity influence. Therefore, any model explaining the excited-state reaction kinetics of **1** has to take into account both polarity and viscosity effects. With the method of comparing high-pressure with low-temperature data,[459] both viscosity and polarity effects can be simultaneously eliminated to a large extent (they are both governed by the solvent density). This allows one to isolate the thermal influence alone, to establish the absence of an intrinsic barrier for **1** in medium and highly polar solvents at room and lower temperatures, and to quantify it in other cases in which the intrinsic barrier is nonzero.[459]

In the following two sections, we will review a barrierless kinetic model adapted to this problem and a hypersurface model that is able to explain the large polarity dependence of the preexponential factor in terms of the electronic states involved.

E. The Stochastic Staircase Model

The staircase model of Bagchi[461,462] was originally introduced to account for nonradiative decays of the excited state to the ground state (internal conversion). In this model, the access to the ground state is position-dependent, i.e., is possible only for certain geometries (values of a reaction coordinate x) which can be reached without an intrinsic activation barrier. This model can also be used to describe excited-state reactions, e.g., that of DMABN, because it focuses on the disappearance of the precursor state, monitored, e.g., by fluorescence. Whether this occurs by internal conversion to the ground state (no emission possible) or by transition to the CT (A*) state (emitting in a different wavelength region) does not influence the model. In this model, the initial flat part of a barrierless reaction profile is approximated by a horizontal potential step of length a, with a reflecting boundary at one end and an absorbing boundary at the other (Figure 72). After the absorption process, which brings the system to its initial position x_0, diffusion on the flat potential sets in and widens the initial distribution. If, as in the simplest case, the initial distribution is taken as a δ function, or if it is sufficiently narrow, the early diffusional motion will not lead to reaction until the downward step (i.e., the absorbing boundary corresponding to IC in the original model and to the photoreaction in DMABN) is reached. The reaction rate "constant" $k(t)$ is defined by the logarithm of the number of systems which cross this boundary per time increment divided by the total reactive population. It increases, reaches a maximum, and falls back to a constant value, k_{lt}, characterized by the long-time limit, when a dynamic equilibrium is reached between the diffusional processes to the left and to the right. This long-time rate constant k_{lt} (eq 26) is independent of the initial conditions x_0 but depends inversely on the square of

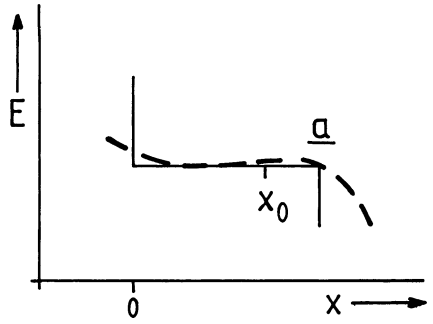

Figure 72. Staircase model (solid line) for calculating the survival probability on the flat part of a nearly barrierless potential (broken line), describing the precursor state B* of the CT reaction. The parameters are the step width a and the initial condition x_0, taken as the starting twist angle in the case of DMABN and derivatives. At the step ($x = a$), the system instantaneously reacts and B emission is stopped. Variation of the step width a and of x_0 can explain the broad range of observed rate constants in derivatives of **1** without the necessity of introducing different activation energies.[455]

the width a of the potential step (see Figure 72) and on solvent friction ξ;[455,462] it is larger when the step is narrow. Thus, $k(t)$ can be viewed as being composed

$$k_{lt} = \frac{1}{4}\frac{\pi^2 k_B T}{a^2 \xi} \tag{26}$$

of two phases: an initial phase, $k_{in}(t)$, reflecting the dynamic equilibration processes (transient phase), which is the source of the time dependence of $k(t)$ (see Figure 71) and which depends on the initial conditions, and a later phase, k_{lt}, which is independent of time and of initial conditions. Equivalent conclusions are derived from a related kinetic model, e.g., the so-called pinhole-sink model,[463] where the flat potential part and the reflecting boundary condition are replaced by a quadratic potential.

The simple staircase model contains all the elements necessary to understand a number of apparently contradictory observations:

(i) Nonexponential precursor decays are found in highly viscous solvents (the initial phase $k_{in}(t)$ governs the reaction dynamics), but exponential decays in low-viscosity solvents (the initial phase is of minor importance or unobservable for the experimental time resolution).[464]

(ii) Dual fluorescence spectra are independent of excitation wavelength for low-viscosity, medium-polarity solvents[63,465] but depend on it for high-viscosity conditions[464] (increasing importance of the initial phase which depends on the initial conditions).

(iii) The reaction rate constant increases with solvent polarity[450,451] although an intrinsic barrier is absent (the width a of the flat potential decreases).

(iv) The reaction rate constant increases for "*pretwisted* compounds", i.e., the compounds with a steric hindrance to planarity (the width a of the flat potential decreases).[209,455]

(v) Analogues of **1**, with the same dialkylamino group but differing acceptor substituent, can exhibit strongly different reaction rates[5,456] although an intrinsic barrier is absent in both cases or is very

small and equal. This is supported by the equality of all Arrhenius slopes, irrespective of the actual size of the rate constant.[457] The explanation is in a reduced width of the flat potential part *a*, due to the involvement of a conical intersection as part of the reaction coordinate in the case of **1** (see section VI.F below).

The alternative barrier-crossing model of Kim and Hynes (KH model, refs 473, 474, and 480 below) can explain points (i), (iii), and perhaps (iv) but is inconsistent with the observations reported in (ii) and (v). Points (iv) and (v) can be considered to be consequences of an entropic control of the excited-state reaction. The rate constant changes are determined not by the activation barrier but by the preexponential factor if different compounds are compared. Very simple consequences can even be seen in the steady-state fluorescence spectra: in parallel with the reaction rate, the relative contribution of the LE fluorescence markedly decreases for derivatives of **1** with increasing ground-state twist angle[171,209,457] because the flat potential portion determining the preexponential factor is strongly reduced. Such a strong variation is possible only if the flat potential portion is wide in the sterically unhindered compound **1**. The conical intersection model, as outlined in the next section, can rationalize this. The differences in rate and relative intensity of the CT band observed for the corresponding derivatives of the ester **32** are much smaller,[456] consistent with the reduced width of the flat potential portion, which leads to the overall strong increase of the reaction rate. A further consequence of the same factor is the much stronger solvent polarity dependence of the rate constant for the nitriles as compared to the esters.[456] At low solvent polarity, the esters react nearly 2 orders of magnitude faster than the nitriles, whereas in highly polar solvents this difference is much smaller. This dependence of the width *a* on solvent polarity and on the nature of the acceptor substituent is further elaborated in the next section.

F. Kinetics on Excited-State Hypersurfaces with Conical Intersections: A Model for Barrierless Reaction Profiles

Conical intersections between S_0 and S_1 are well-known topological features describing, e.g., so-called photochemical funnels, which lead to ultrafast fluorescence decay or to a photochemical reaction.[466] If the conical intersection does not involve the ground state but appears between two excited states, its presence does not necessarily lead to fluorescence quenching but can affect the dynamics of the respective adiabatic excited-state reaction. The following model of a conical intersection along the excited-state reaction pathway in **1** (Figure 73) can account for points (iii)−(v) of the above list. The model is based on the different symmetry of the two emissive states in **1**, as derived from polarization experiments of the two fluorescence bands observed.[185,186] A zero-order state crossing between the two lowest excited singlet states S_1 and S_2 along the twist coordinate transforms into a conical intersection if a further symmetry-reducing coordinate, q_n, is allowed to participate (Figure 73).[457]

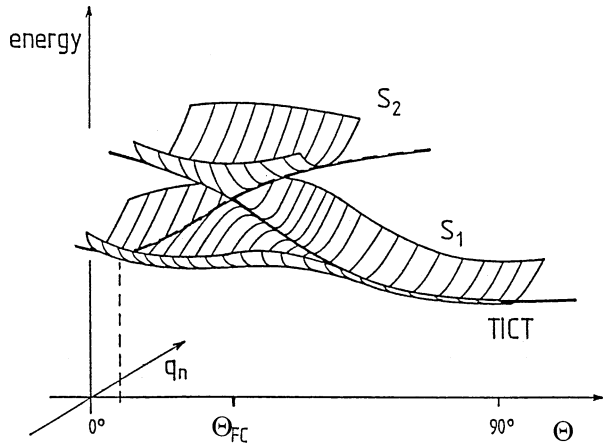

Figure 73. Schematic representation of the potential hypersurfaces along the reaction coordinate leading to the CT state in **1**. The crossing of the ^1L_a- and ^1L_b-type states causes a "conical intersection" of S_1 and S_2 at the critical twist angle θ_{cr}. These states vibronically couple involving a non-totally symmetric vibration q_n resulting in the cone on the lower surface. This cone has to be "surrounded" during the CT reaction, which therefore involves both twisting (coordinate θ) and movement along the coordinate q_n.[5]

If Kasha's rule holds, the reaction occurs on the lower of the two surfaces and can proceed through the "side valleys" surrounding the cone of the conical intersection and avoiding it, along a quasi-barrierless profile for the initial part of the reaction. The length of this initial portion (*a* in the staircase model above) is determined by the coordinate of the zero-order crossing. This, in terms of the twist angle θ, is placed at the critical angle θ_{cr}, and therefore the length *a* of the flat potential portion will strongly depend on the solvent polarity because the product state, with a larger dipole moment, is more strongly stabilized in polar solvents than the precursor state. Thus, increasing solvent polarity is predicted to decrease *a*.

This model delivers a simple explanation for (i) the observed strong polarity dependence of the rates in **1**[450,451] (the conical intersection) and the much weaker one in the corresponding ester[456] (no conical intersection) and (ii) the much faster reaction observed for the ester[231,456,457] (strongly reduced width *a*) as compared to **1**.

Thus, the overall effect of the conical intersection between S_1 and S_2 is to slow the reaction rate. In fact, for **1** in aprotic low-viscosity polar solvents such as acetonitrile, the reaction is much slower than the solvent relaxation.[133,308,309,316,467]

G. The Interplay of Internal and Solvent Relaxations: Need for Two-Dimensional Kinetic Models

We concluded above that the "transient period", $k_{in}(t)$, appears in some cases, leading to nonexponential fluorescence decays, whereas in other cases the decay is dominated by the kinetically equilibrated late-time rate constant, k_{lt}. What are the factors which govern this different behavior?

For this purpose, the intrinsic reaction dynamics and the solvent response have to be treated separately, as independent diffusive coordinates. This necessity derives from the fact that the internal motion may sense a completely different friction than the solvent relaxation.[404,477−479] The detailed reaction path of the system will then depend not only on the energetics but also on the response times (or diffusion coefficients) along the two coordinates; in this case, the reaction path can differ from that of the minimal energy, and even avoid the crossing from precursor to product at saddle points.[483]

Several different two-dimensional kinetic models have been introduced and in some instances applied to the case of **1**.[404,468−482] Predictions close to the experimental results have been reached with the models of the groups of Nordio[404,475−477] and of Hynes.[473,474,480,482] Their main difference regards the assumptions on the presence of activation energy and on friction being active along the solvent and internal coordinate, *x*, and the inclusion of the subtleties of solvation dynamics such as inertial effects. It turns out that the major parameter determining the behavior of a system is the time scale of the solvent motion as compared to the internal motion of the solute.[404,473,474,478−481] It can be measured as the ratio of the diffusion coefficient along the solvent (D_S) to that along the internal coordinate (D_R). A fast-solvent case ($D_S \gg D_R$) and a slow-solvent case ($D_S \ll D_R$) can be discerned.[404,478,479,481] For the latter case, nonexponential kinetics are predicted, which are reduced in the fast-solvent case. Additional complications arise from the fact that the solvation behavior of most solvents is nonexponential in itself, with an ultrafast inertial time scale. This nonexponential solvation dynamics has not yet been introduced into the Nordio model, and D_S can therefore be viewed as an averaged solvation parameter. For the case of "slow solvents" like glycerol, a "saddle point avoidance" is predicted, at least for not-too-large barriers; i.e., the molecule twists first, then solvates, and the main population flux does not cross the saddle point at the lowest possible energy.[483] This has been directly applied to the experimental data of **1**, e.g., in the aprotic highly viscous solvent glycerol triacetate (GTA) (Figure 74). It should be mentioned that the kinetic experimental results can be satisfactorily fitted with different kinds of 2D models, e.g., those necessitating an activation barrier (KH model)[473,474,480] and those not requiring it (Nordio model).[404,477,479] In contrast to the KH model, it is found with the Nordio model that, for "slow" solvents (such as GTA), the initial motion is along the inner (twist) coordinate, and solvation follows after the large-amplitude twisting motion, whereas in "fast solvents" (like acetonitrile), the initial motion is along the solvent coordinate, or the reaction path is completely simultaneous.[473,474,479,483]

In view of the importance of the two-dimensional kinetic representation, we will focus on the KH and Nordio models and point out their similarities and differences in more detail.

The KH model[473,474,480] involves a quantum-chemical treatment in a two-valence-bond description. The

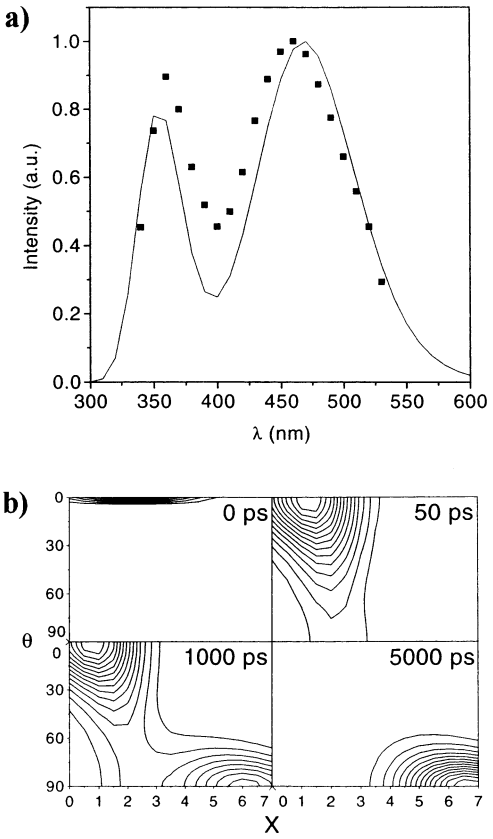

Figure 74. (a) Time-integrated fluorescence spectrum of **23** in GTA (■) and fit using the 2D stochastic model. (b) Contour plots of the calculated normalized population at different times on the 2D reaction surface along the twist coordinate θ and the solvation coordinate *X*. The population first moves along the torsional coordinate, with small variation of the solvent polarization, and reaches a metastable state, characterized by perpendicular conformation and nonequilibrium solvent distribution. Reproduced with permission from ref 479. Copyright 1996 Elsevier Science.

gas-phase potential along the twisting motion (coordinate θ) is taken from quantum-chemical calculations, and the influence of the second coordinate, the solvent coordinate, *X* in our nomenclature, is taken into account by using Onsager theory and the calculated dipole moment values. The stochastic solvent motion is introduced by a fluctuating Hamiltonian. The two diabatic states LE and CT are allowed to interact via an angle-dependent resonance energy β. Diagonalization yields the energies (and wave functions) of the two adiabatic excited states as functions of θ and *X*, and the lower state is responsible for the relaxation kinetics. The functional form of β is determined by requiring that the calculated free energy barrier for DMABN in acetonitrile yields a value approximately consistent with the experimental determinations of Eisenthal et al. From this, a reaction free energy surface is calculated, yielding the CT minimum ca. 15 kJ/mol below the LE minimum, and the transition state ca. 6−8 kJ/mol above it.

The Nordio model[404,475−479,481] involves a stochastic model for diffusion on a given two-dimensional potential based on the same quantum-chemical results as used in the KH model, but with a resulting considerably lower activation energy for acetonitrile (about 2 kJ/mol, comparable to the thermal energy

k_BT). A 2D Smoluchowski diffusion equation is used, and the time evolution of the population $P(\theta,X,t)$ is followed. "Slow solvent" and "fast solvent" cases are defined by comparing the viscosity-dependent correlation time for internal twisting with the average solvent relaxation time (or, alternatively, the corresponding diffusion coefficients D_R along θ and D_S along X for twisting and solvation, as used above). Matrix techniques are used for the numerical solution of the diffusion equation.

The models are similar in the fact that they both allow for nonequilibrium solvation along the reaction coordinate and both include the dissipative friction effects on both coordinates. They differ, however, essentially in the reaction paths predicted and in the details of how solvents are qualified. In the KH model, e.g., all reaction paths are required to pass through the transition state (the saddle point of the two-dimensional surface), even for the "slow solvent" case. The KH model involves frequency-dependent friction; i.e., only the fastest friction components of both solvation and twisting diffusion are effective, depending on the comparison with the inverse barrier frequency at the top of the transition state. The latter (determined as 1/18 ps) as well as the inverse of the calculated internal torsional frequency (1/14 ps) are therefore important parameters in the model. Consequently, the KH model places acetonitrile as a "slow solvent" and methanol, with its much faster inertial solvation component (1/30 vs 1/8 ps for acetonitrile), as a "fast solvent", although its late-time solvation component is much slower than that of acetonitrile (5 vs 1/4 ps for acetonitrile). In the KH model, movement across the saddle point for acetonitrile is mainly twisting; for MeOH, the motion is mainly along the solvent coordinate X. In the Nordio model, the average solvation time is taken as the decisive parameter, and acetonitrile can be considered as a "fast solvent", methanol would be somewhat slower, and GTA and glycerol are "slow solvents".

The importance of the frequency-dependent friction in the KH model leads to the prediction that long solvation times and high viscosities do not lead to slow reaction rates. This is a basis for reaction times being faster than the solvation times and for viscosity-independent reaction rate constants, as implied by the experiments of Eisenthal et al. In the Nordio model, reaction rates are always strongly dependent upon viscosity, as implied by the high-pressure experiments in GTA, but they can also be faster than solvation in the "slow solvent" limit. In contrast to the Nordio model, the KH model also takes into account the complexity of the solvent relaxation dynamics and of the dielectric response of the solute to the changing dipole moment along the reaction coordinate. This can lead to different kinetics even if viscosity effects would be identical.

A further important difference is the presence of an activation barrier, which is necessary for the KH model to be applicable, whereas the Nordio model can deal with both cases, with and without barrier. Also in the presence of a barrier, both models predict a different behavior. For the case of solvent control ("slow solvent"), the KH model predicts a passage through the transition state along the solvent coordinate. In the Nordio model, the transition state is avoided and the population moves on an isoenergetic pathway toward a metastable state which is characterized by a perpendicular conformation and a nonequilibrium solvent distribution; further relaxation to the CT minimum is governed by the slower solvent relaxation. The KH model predicts essentially exponential kinetics in all cases, whereas the Nordio model predicts exponential kinetics for the "fast solvent" case (with nonzero barrier) but nonexponential kinetics for all "slow solvent" cases with and without barrier.

Both models were sucessful in fitting experimental results. The KH model was applied mainly regarding room-temperature kinetics, whereas the Nordio model was applied also regarding dual fluorescence spectra as a function of temperature, both in the presence and in the absence of a barrier and for "slow solvent" and "fast solvent" cases. The ability to fit a given experiment is therefore not yet a proof that the details of the assumptions of the corresponding model are correct. Only the comparison of several complementary experiments and their simultaneous explanation can give an answer, e.g., regarding the question of whether an activation barrier is present or whether the relaxation is on a barrierless potential, as discussed above, or whether a given solvent can be regarded as "fast" or "slow".

VII. Theory

A. Quantum Chemical Calculations

Early calculations on the nature of the CT state formation in DMABN considered the twist angle θ as the only reaction coordinate and placed the free molecule in a vacuum.[4,235,484] The next step involved the explicit consideration of the solvent polarity effects on the energetics of the states, with the general result that the ET reaction of **1** is of endothermic nature in the absence of solvent and may become exothermic with increasing solvent polarity, due to a dipole moment increase with the twist. This has been done in three different approaches:

(a) Nonpolarizable solute in a solvent continuum.[167,199,247,406,485−487] Here, the changes with respect to the energies in a vacuum derive directly from the angle-dependent dipole moments, with application of the Onsager model.

(b) Polarizable solute in a solvent continuum. This approach uses the rather recent implementation of self-consistent-reaction-field (SCRF) calculations, i.e., explicit inclusion of the solvent stabilization energies into the Hamiltonian of the system. In this case, not only polar states are stabilized, but also their wave functions are altered such that the dipole moment increases with solvent polarity.[200,232,403,488,489] These polarizability effects do not change the main conclusions regarding endothermic potentials in the gas phase and in nonpolar solvents, and exothermic potentials in polar solvents. On the other hand, it is remarkable that the polarizability of the TICT state, despite the twisted structure and the experimental evidence shown above, has been calculated to be

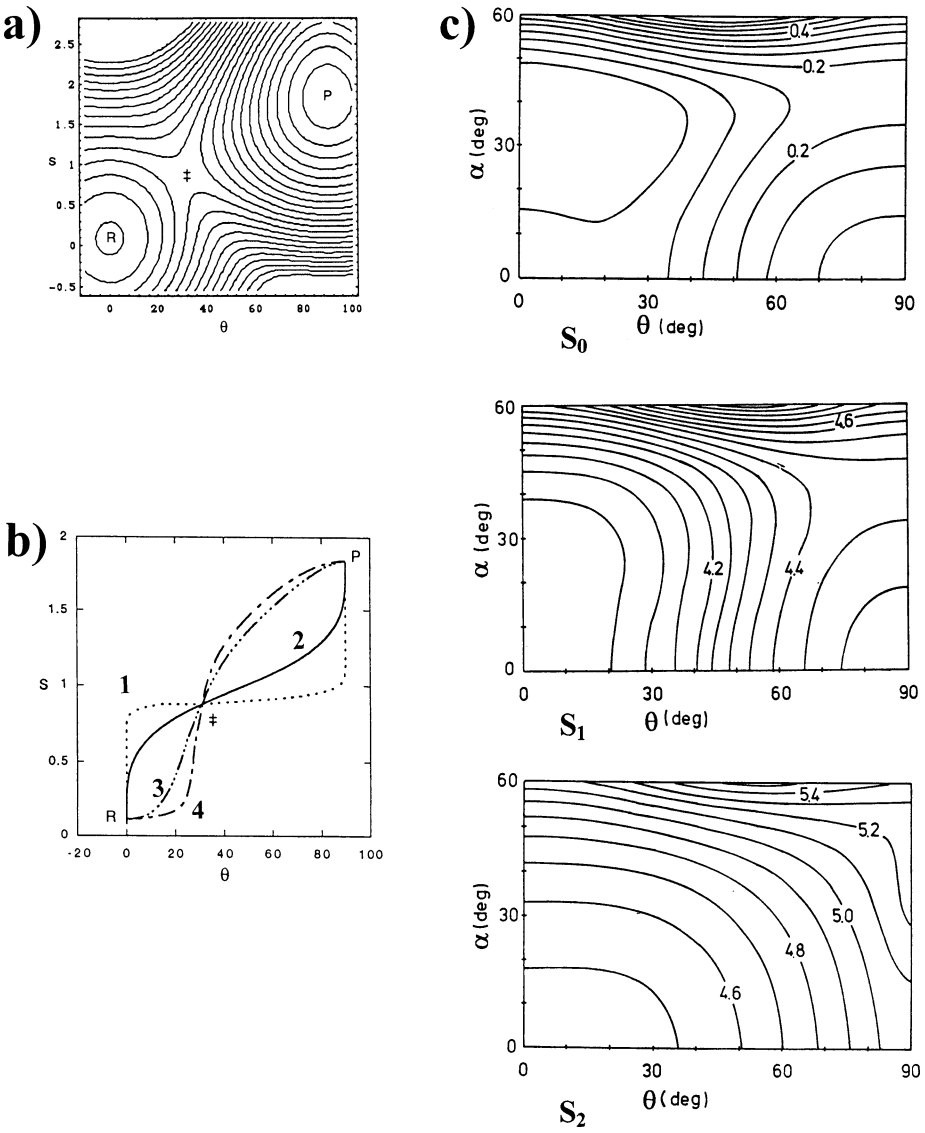

Figure 75. (a) Two-dimensional representation of the reaction free energy surface for DMABN as a function of an internal coordinate (twist angle θ, vertical axis) and the solvation coordinate, s. (Adapted with permission from ref 473.) R, P, and ‡ denote the reactant (θ and $s \approx 0$), product ($\theta \approx 90°$ and $s \approx 2$), and transition-state locations, respectively. (b) Different solution-phase reaction paths for DMABN in a polar solvent with different solvent models. Solvent frequencies employed are (1) 3, (2) 8.3, (3) 30, and (4) 75 ps^{-1}, as compared to the torsional frequency of DMABN in a vacuum (15 ps^{-1}). The reaction from the R to the P minimum always starts along the slowest coordinate in the KH model. For the fast solvent case (4), the inner movement (twist) is rate determining; for the slow solvent case (1), the initial movement is along s. (c) Two-dimensional representation of S_0, S_1 (^1L_b), and S_2 (^1L_a/CT) states as a function of the two internal coordinates: twist angle θ (horizontal axis) and pyramidalization or wagging angle α for **1** in the gas phase (ab initio large-scale CI calculation). (Adapted with permission from ref 407. Copyright 1990 American Institute of Physics.) Note that the TICT conformation is a transition state in the gas phase (barrier around 20 kcal/mol), and only by solvent interaction with the large TICT dipole moment does this energy maximum transform into an energy minimum (part a) of the figure. Contour spacing is 0.05 eV for S_0 and S_1, and 0.1 eV for S_2.

larger than that of the LE state.[403] These SCRF calculations are also able to explain why meta derivatives of **1** do not show dual fluorescence,[232] as they have similar calculated dipole moments in both their S_1 and S_2 states.[228,232]

(c) Solute in a discontinuous solvent. This approach explicitly takes into account the number of solvent molecules, the motions of which are averaged in a Monte Carlo or molecular dynamics treatment. It has been applied to **1** by Kato et al.[407,490] with similar conclusions (Figure 75a) and more recently by Sudholt et al.[491] These studies reveal the important aspect of incomplete solvation, which can generate potential barriers in the excited state and change the excited-state crossing between the lowest-lying energy surfaces. A related theoretical work in this direction has been published by Kim and Hynes.[480]

A further step of refinement is gained when the pyramidalization on the amino nitrogen is explicitly taken into account, in addition to the twisting of the amino group. Then, the two-dimensional hypersurfaces which can be constructed indicate an untwisted but somewhat pyramidal nitrogen in the ground state, consistent with experiment,[166,495] depending on the type of amino group[202] and a reduction or even loss of pyramidalization upon excitation, especially for the highly polar TICT state.[199,406,407] A similar observation is made upon ionization of anilines:

Table 11. Theoretical Calculations of the DMABN Molecule (Structure, Energy)[a]

author (year)	method	method of including solvent effects	pyramidalization angle in optimized S_0 state (barrier to planarity)	TICT formation			refs
				in gas phase	in alkane	in ACN	
many authors, since 1962	experiment	full	9−17°	endo	endo	exo	4,5,63,166, 404,495
Cowley (1977)	PPP	rigid dipole + Onsager	not consd				4,235
Rettig, Bonačić-Koutecký (1979)	ab initio + CNDO/S	not consd	not consd				484
Lipiński (1980)	INDO	rigid dipole + Onsager	not consd	endo	exo	exo	485
Kato (1990)	ab initio (STO-3G)	rigid dipole + Monte Carlo	38° (1.6 kcal/mol)	endo		exo (water)	407
Bhattacharyya (1991)	MNDO	rigid dipole + Onsager	twisted ground state found	endo	endo	exo	486
Marguet (1992)	CSINDO	rigid dipole + Onsager/solvaton model	not consd	endo	exo	exo	247
Broo, Zerner (1994)	ZINDO	polarizable dipole + Onsager	planar	endo	exo	exo	200,488
Gorse (1993)	AM1 (AMPAC)	rigid dipole + microstructural solvent model	18° (0.07 kcal/mol)	endo	exo	exo	199,406
Soujanya (1995)	AM1	rigid dipole + Onsager	not consd	exo	exo	exo	487
Serrano-Andrés, Roos (1995)	CASSCF+pert.	not consd	10−20°	exo			167
Sobolewski, Domcke (1996)	CASSCF+pert.	not consd	planar	endo			9,10
Gedeck (1997)	AM1 (VAMP)	polarizable dipole + microstructural solvent model	25° (1 kJ/mol)	endo	endo	exo	232,489
Scholes (1997)	ab initio (+CIS)	polarizable dipole + Onsager	slight	endo	endo	endo	403
Parusel, Grimme (1998)	DFT-CI[b]	not consd	planar	exo[d]			164,497
Lommatzsch, Brutschy (1998)	ab initio (different basis sets)		slight to medium	not consd			494
Sudholt, Sobolewski, Domcke (1999)	ab initio (+CIS) in optimization; CASPT2 in energy	not consd	not consd	endo			106
Parusel (1999)	STEO-CCSD[c]	not consd	not optimized	endo			497
Dreyer, Kummrow (2000)	ab initio CASSCF for optimization	not consd	41.6°	not given			310

[a] not consd, not considered; endo, endo-energic; exo, exo-energic. [b] Density functional theory with single excitation configuration interaction. [c] Similarity-transformed equation-of-motion coupled-cluster method with single and double excitations. [d] Minima at 0°, 60°, and 90°.

neutral dimethylaniline is pyramidal, whereas the radical cation is fully planar.[492] Inclusion of this second coordinate changes the energetics of the minimal energy reaction path. The calculated twist potential, e.g., in the ground state, is reduced as compared to that with rigidly planar (sp^2-type) nitrogen, because the twisted ground state is more strongly pyramidal than the planar one (Figure 75c). The ground state is calculated to be somewhat pyramidal but with only a very small barrier to planarity (1.6 kcal/mol[407] or much smaller, see Table 11) which slightly increases with solvent polarity.[489] For a 90° twist, the pyramidalization of the amino group increases, with a correspondingly larger barrier to planarity (>3 kcal/mol, from ab initio calculations[407]). The rotational barrier along the minimal energy path in S_0 involves both twisting and pyramidalization coordinates and is calculated as 5.9 kcal/mol. The comparison between dimethylaniline and **1**[406] nicely shows that the para-acceptor substituent strongly lowers the tendency for pyramidalization.

In S_1, the rotational barrier (12.1 kcal/mol) is more than doubled with respect to S_0, reflecting an increased mesomeric interaction between benzonitrile and the amino group in the excited state. This is also reflected in the more planar minimum geometry (no pyramidalization for the nontwisted geometries). In S_2, this tendency is further increased, generating a planar nonpyramidal minimum, as well as a nonpyramidal transition state at 90° twist. The latter can be understood on the basis of a strong increase of positive charge on the $-NMe_2$ group, generating the characteristic high dipole moment of the limiting TICT conformation.

In this context, the possibility of geometrical optimization becomes important because these two-dimensional hypersurfaces should ideally be a cut along the minimum energy of all the remaining coordinates through the hypersurface of full dimensionality.

This seems to be no problem today for the ground state if a method is taken which has been tested to

perform well for DMABN (e.g., DFT and AM1 calculations). However, both semiempirical and ab initio studies using other Hamiltonians or basis sets have been reported with geometrical results at variance with experiment such as X-ray structures.[166,495] Some of them were at variance with most other calculations, such as a 50° twisted ground state of **1** in a MNDO calculation[486] or planar amino groups in primary anilines and overestimated bond lengths between the amino group and the phenyl ring (for a comparison of various semiempirical and ab initio calculations with experiment, see ref 503). The methods which do not compare favorably with experiment should therefore be taken with care. There are, however, few examples with geometry optimization in the excited state.[9,10,199,308,310,403,406,422,493,494] All theoretical methods, whether semiempirical[199,406] or ab initio,[10,167,404,407] agree that the relevant coordinate which brings about the charge separation is the twisting motion and not the pyramidalization of the amino nitrogen. On the other hand, pyramidalization effects are important to understand the nature of the strongly red-shifted A-band: an additional red-shift arises[202] because the TICT state possesses a nonpyramidal positively charged amino group,[407] but the equilibrium conformation of the twisted amino group is strongly pyramidal in the ground state.[202,407] The theoretical results vary strongly in the prediction of the ground-state pyramidalization (see Table 11). For ab initio calculations, the basis set (e.g., inclusion of diffuse functions) plays an important role.[310,491,494]

A further coordinate that strongly changes along the reaction path is the bond length between the ring and the amino nitrogen. It is calculated by the AM1 method to be considerably shortened in the highly polar TICT state, due to the Coulomb attraction,[489] from 1.388 Å in the ground state (experimental, 1.367 Å[166] or 1.356 Å[495]) to 1.331 Å.

The $-C\equiv N$ group bending has also been proposed as a possible coordinate leading to a low-lying CT state in DMABN.[9,10,104,496] The nature of this CT state is strongly different from the TICT state discussed above, because it is low-lying also in the compounds having no amino group, e.g., benzonitrile. It has been argued that it may be connected with amino group twisting in **1** through an interplay of coupling and tuning modes which are relevant for a conical intersection.[10] Cyano group bending has also been included in a recent DFT-CI calculation (see below).[497] The role of the cyano group bond length changes, which indirectly influence the reaction toward the TICT state, has been considered by Calzaferri et al.,[498] and the role of geometry deviations from the limiting TICT theory (twist angle 90° with infinitely small angular distribution) has been stressed.[499]

A stringent test of the quality of the various theoretical models is their ability to reproduce the experimental absorption spectra and, more difficult, the relative energetics of photochemical reactions. Most advanced in the former respect are the ab initio complete active space self-consistent field (CASSCF) calculations with perturbation correction (CASPT2),[9,10,308,421,424,492,496] or coupled-cluster calculations with single and double excitations[500] and the recent development of density functional theory calculations with configuration interaction (DFT-CI) for excited states,[164,497] which allow much faster calculations and therefore the extension to significantly larger systems. Table 11 summarizes the most relevant results regarding the model of a twisting reaction coordinate: most calculations predict correctly the experimental fact that, in the gas phase, the formation of a TICT state is endothermic, and only through solvent interaction is this highly polar state stabilized below the S_1 excited state of planar geometry. The methods differ, however, in the prediction of which solvent is polar enough to induce an exothermic reaction. Several calculations predict an exothermic TICT reaction even in nonpolar hydrocarbon solvents, at variance with experiment.

Table 11 also allows one to draw some conclusions regarding the ground-state pyramidalization of the amino nitrogen in **1**. The optimum pyramidalization angle is calculated quite differently by various methods, but the barrier to planarity is extremely small, much lower than the thermal energy at room temperature, such that an effectively planar model for **1** seems to be a good approximation in the discussion of kinetics and energetics under thermal conditions.

Two important theoretical papers appeared on the excited CT state and solvation of **1**.[491,501] Sudholt et al.[491] combined advanced ab initio calculations of the molecular and electronic structure in the free molecule with a study of the microscopic mechanism of solvation by molecular dynamics. The results are decisively in favor of the TICT structure of the CT state (although the authors argue for further high-level ab initio calculations). The molecular dynamics results indicate that the ACN molecules (taken as nonpolarizable dipoles) relax within 0.2 ps, orienting themselves around the charged structural groups of the polar molecule (and not in the molecular dipole field as a whole).[502] The calculated observables generally agree with the experimental data, except for the Stokes' shift, which is highly underestimated, by 0.3 eV.

In the second paper,[501] a time-dependent density functional theory and the polarizable continuum model are applied. Among their results, the authors note that, in ACN solution, the ^1L_a state should be the lowest planar excited singlet state, not the ^1L_b. The calculated dipole moments in ACN solution are 13 D in the planar state (^1L_a) and 17 D in the TICT state, the oscillator strengths being $f = 1.04$ and 0.059, respectively.

Parusel,[609] with a DFT/MRCI study of the CT states of **1**, **163a**, and **164a**, compares the electronic and molecular structures in free molecules and in the solvent cage (in the Onsager approximation). For symmetry reasons (nodal plane of the HOMO at the pyrrole N atom), a largely decoupled CT state can be found at any twist angle θ. The most stable excited-state conformation depends on the relative stabilization, *resp*. destabilization, and on the subunit localization of the orbitals involved in the ET as a function of the twist angle θ. The twisted ICT state (TICT) should be the lowest excited state for **163a** only in polar solvents, whereas in nonpolar solvents

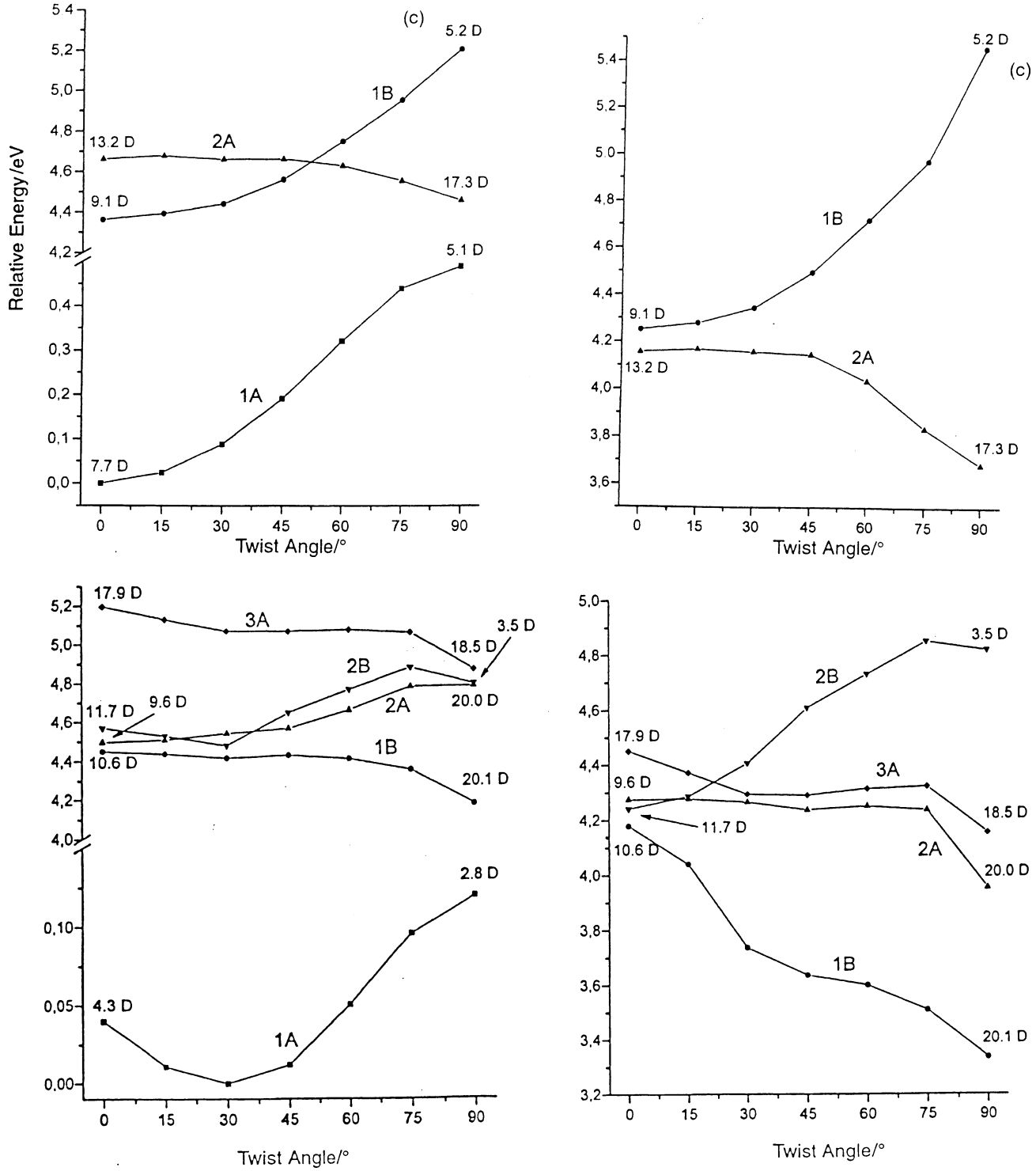

Figure 76. Calculated energies for DMABN (above) and for 4-(*N*-pyrrolo)benzonitrile **164a** (below). (Left) The ground state and the two lowest excited singlet states in vacuo. (Right) The two lowest excited singlet states in acetonitrile as solvent. The energy of the states is plotted as a function of the twist angle θ, in the notation of the C_2 point group symmetry. The calculated dipole moments are shown for the planar and the 90° twisted conformations. Adapted with permission from ref 609. Copyright 2000 The Royal Society of Chemistry.

the planar ICT state (PICT) is lowest, while for **164a** the TICT state is lowest, even for nonpolar solvents (against the older estimate[168]). In the case of **1** and **164a**, the solvent polarity effect strongly favors the $\theta = 90°$ TICT conformation (Figure 76); the results are more complex and ambiguous for **163a**. In the case of the pyrrole derivatives, several low-lying ICT states are calculated for every geometry, differing in their symmetry. In particular, the lowest TICT state of **164a** ($\theta = 90°$ in polar solvents) does not belong to the representation *A* (as usual for "classical" TICT states, e.g., in **1**) but to the representation *B* in the C_2 symmetry point group.

The author concludes that the DFT/MRCI method leads to results (perpendicular minimum) that are more consistent with experiment (especially the

forbidden emissive property) than the DFT/SCI method,[497] which located the energy minimum of the CT state in vacuo at a different twist angle ($\theta \approx 60°$).

A comprehensive comparison of ground- and excited-state geometry optimization with several high-level quantum-chemical methods has been recently completed,[503] and the results are confronted with the available experimental data (structure, excitation energies, emission spectra, dipole moments, reaction path energetics). The methodologies of the theoretical methods are critically discussed. It is noted that the optimized geometries of the TICT state obtained with the methods ab initio/CIS, ab initio/CASSCF, and the semiempirical AM1/CISD differ significantly in the prediction of the $C_{ar}-N_{amino}$ bond length and the alternation pattern in the benzene ring.

Further ab initio/CASSCF calculations have been done[504] on some pyrrole derivatives of **1**, namely **163a** and **164a**. The importance of the quinoid (Q) and antiquinoid (AQ) distortion in the lowest excited state of *A* symmetry is pointed out. The antiquinoid distortion is linked with a lengthening of the two central CC bonds in the benzene ring (**121**). As the AQ configuration involves significant doubly excited character, it could not be calculated with CIS optimization methods. For **163a** and **164a**, two minima were found for the ^{1}A state. The Q minimum has a shortened $C_{benzene}-N_{pyrrolo}$ bond and shortened central bonds in the benzene ring, as well as a coplanar pyrrole moiety (**120**). In the AQ minimum (**121**), two central bonds in the benzene ring are significantly elongated and the other bonds shortened, while the $C_{benzene}-N_{pyrrolo}$ bond is elongated. For the AQ structure, stabilized

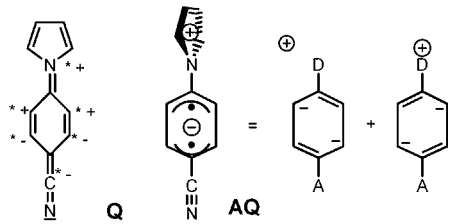

120 **121**

by two allylic electron configurations, there is a steep energy minimum for the pyrrole group to be perpendicularly twisted. The bond lengths in the pyrrole ring are also considerably modified. Both minima of the CT state of **164a** are discussed in terms of valence bond structures: the Q and AQ minima can be identified with the PICT and the TICT states, respectively. This study is the first one that consistently links these two states in one single model and emphasizes the ring coordinates as determining the structural relaxation process in the CT state, along with the hitherto mainly discussed torsional coordinate.[504]

B. The Biradicaloid Model: Interaction of Ground and Excited States

A simple model to understand the behavior of twisted single and double bonds can be constructed by considering the interaction of just two atomic p-orbitals (AOs). In the case of their non-interaction

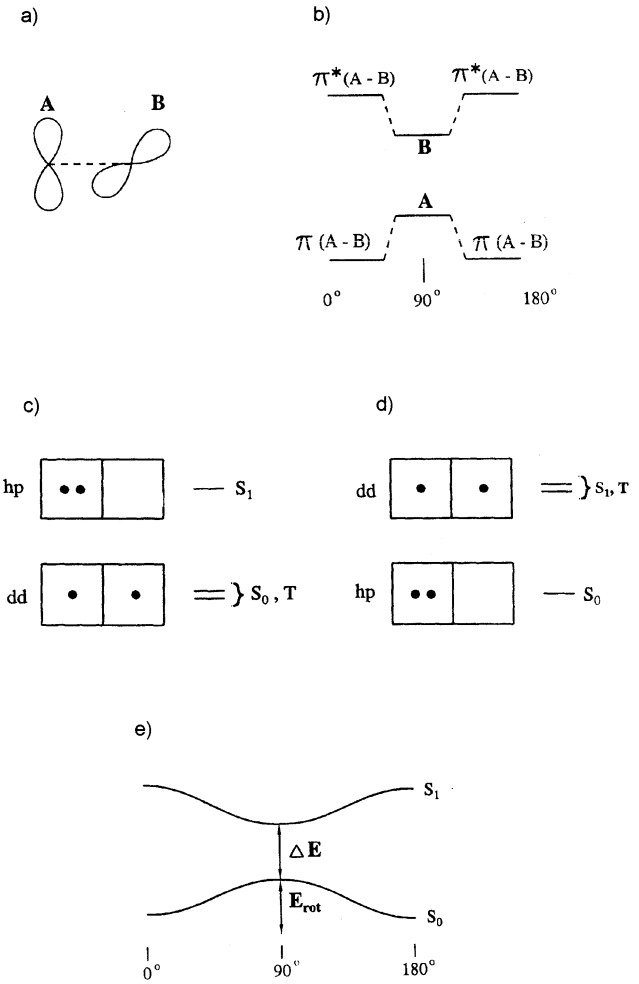

Figure 77. (a) Two orthogonal p-orbitals as a prototype biradicaloid system. (b) Twist-angle-dependent molecular orbital energy changes. (c) Possible electronic occupation patterns (hole−pair, *hp*, and dot−dot, *dd*) in the biradicaloid conformation and derived system states for small and (d) for large electronegativity difference of the centers. (e) Interaction between *hp* and *dd* states increases for deviations from 90° and creates an energy minimum in the excited state and a maximum in the ground state if interactions with $\pi\pi^*$ states are absent.

(large distance or mutual orthogonality; see Figure 77a), the molecular orbital (MO) energies are given by the energies of the AOs, and the MOs are localized on the centers A and B and correspond to the AOs. For smaller distances or twist angles $\theta \neq 90°$, the interaction of the p-orbitals leads to an energy decrease of the lower MO and an energy increase of the upper MO (Figure 77b), linked with a delocalization of the π-MOs over both centers.

The biradicaloid model[11,12,505] is connected with populating this MO system with two electrons. Two situations can arise for the limiting non-interaction case (MOs correspond to pure AOs):

(i) The "*hole−pair*" (*hp*) case, with two electrons in the lower MO and zero electrons in the upper MO (the reverse filling is not relevant here because it is always higher in energy).

(ii) The "*dot−dot*" (*dd*) case, with one electron in the lower MO and one in the upper MO. The *dd* case is always associated with the very close-lying corresponding triplet configuration (Figure 77c,d). In both

cases, the electronic charge is localized according to the MOs; i.e., the *hp* state in our example carries a large electron density at center A.

Which one of the two situations, *hp* or *dd*, is the lower energy one for the non-interaction situation depends on the interplay of two factors: (i) the sum of AO energies associated with each electronic occupation pattern and (ii) the interelectronic interaction energy. If it were only for factor (i), *hp* would always be the lower and *dd* the higher energy case. Factor (ii) works in the opposite way because two electrons localized on one center repel each other more strongly than if localized on different centers, and are thus associated with a higher energy. As a consequence, for equal centers with no energy difference between the AOs (as in the twisted ethylene), *hp* is always of higher energy than *dd* (Figure 77c), resulting in a singlet−triplet pair at the ground-state level. For strongly unequal centers (e.g., donor−acceptor-substituted ethylenes, or aminoborane), factor (i) overcompensates the factor (ii), and then a singlet−triplet pair in the excited state results (Figure 77d).

If the interaction between *hp* and *dd* states is switched on, e.g., by twisting away from 90°, these states start to repel each other energetically, leading to a downward curvature for the S_0 state and an upward curvature for the S_1 state in both cases (Figure 77e). This simple model predicts that the S_1 state for these purely biradicaloid systems has an energy minimum for the geometry with the least overlap (where the ground state exhibits its energy maximum, connected with a rotational barrier, E_{rot}, for the case of bond twisting; Figure 77e). The minimum energy gap, ΔE, between S_0 and S_1 is variable and depends sensitively on the interplay of factors (i) and (ii). If these two factors cancel each other, then ground and excited states touch, leading to so-called photochemical funnels.[12]

The polarity (dipole moment) of such minimum overlap structures depends on whether they belong to the *hp* or the *dd* type, and how the nuclear charges compensate the electronic distribution. Intuitively, the *hp* situation would be associated with a large dipole moment. But this is true only if the AO centers bear similar nuclear charges, like in ethylene. Therefore, the S_1 minimum in (slightly unsymmetric) ethylene is predicted to have a large dipole moment.

The typical limiting TICT situation is described by an S_1 minimum of *dd* type. This *dd* state can be weakly polar if the two centers correspond to similar atoms, as in the case of donor−acceptor-substituted ethylenes. But it is highly polar, e.g., in aminoborane, H_2N-BH_2, due to the different nuclear charges. Aminoborane has therefore been termed the prototype TICT system.[505]

C. Extension of the Biradicaloid Model to Larger Systems

If more than two electrons are necessary even for a crude description of the molecular system, other types of electronic states are additionally relevant at the minimum interaction geometry (e.g., orthogonally twisted π-systems): the locally excited (LE) states, i.e., the $\pi\pi^*$ excited states localized on the mutually perpendicular subsystems. These states are often strongly mixed with the *hp* states because the relevant occupied orbitals of both *hp* states and LE states are confined to one of the π-subsystems. The LE states often carry oscillator strength, but they cannot interact with the pure *dd*-type states due to orbital overlap or local symmetry. With deviation from the limiting geometry (90° twist), the excited *dd* state starts to interact with both S_0 (possessing a large weight of the *hp* state) and the LE states. The latter generally have a large energy maximum for 90° twist, because of the decoupling (loss of mesomeric interaction). Depending on the mixing coefficients and the relative energies of the states, an additional interaction with LE states can thus bring about both types of situations. An energy minimum appears in S_1 for 90° (predominant interaction with the ground state for twist angles deviating from 90°) or a flattened energy maximum (the ground state interaction is not strong enough to produce an energy minimum, but it reduces the curvature). The latter situation is encountered in most experimentally relevant TICT systems in the gas phase, including **1** (Figure 78a).

Although the gas-phase potential may show an energy maximum at 90°, dipolar interaction with the surroundings can still change the situation. Due to the twist angle dependence of the mixed wave function and the negligible interaction with LE states for the limiting geometry, an excited *dd* state of large dipole moment (aminoborane or **1** case) will always exhibit a maximum of the dipole moment and a minimum of the transition dipole moment or oscillator strength *f* for the limiting (minimum overlap) geometry (Figure 78b). For the strong mixing cases, the whole hypersurface can be regarded as the intramolecular CT state, with relatively large charge separation, also for the planar geometry. The regions of the hypersurface with largest dipole moment will preferentially be lowered in a polar solvent, proportional to the square of the dipole moment. This may easily amount to energies in the 2 eV range, such that higher-lying ICT states can be pulled down by the solvent below other LE states to become the photophysically relevant S_1 state. Consequently, the ICT state can develop a second energy minimum at the position of the maximal dipole moment (Figure 78c). The excited species corresponding to this minimum has the properties of the limiting *dd* state — enhanced dipole moment and reduced transition moment (forbidden emissive character) — but it must be borne in mind that an angular population distribution is present, weakening in reality these limiting *dd* state properties[12] in the observable properties of TICT states. A further way to reach *dd*-type excited-state minima is by "*pretwisting*" induced by substituents which disfavor the planar conformation (Figure 78d).

The *dd*-type minima can be viewed as linking S_0 and S_1 in a molecular photodiode way because they allow access to S_1 from ground-state minima with large transition moment (e.g., planar conformation) and lead, through the self-decoupling mechanisms

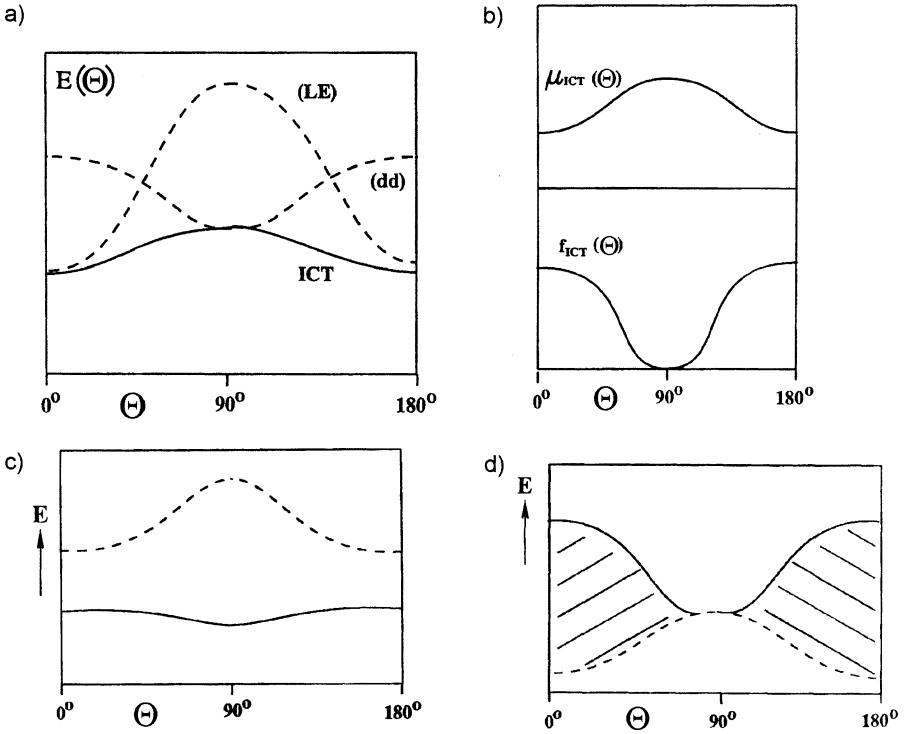

Figure 78. (a) Due to the angle-dependent interaction of *dd* and LE states (- - -) in larger bichromophoric systems, the typical angular dependence of the lowest ICT state in the gas phase (—) has an energy maximum for the non-interaction geometry (90° twist). (b) The dipole moment and oscillator strength of the ICT state show a maximum and minimum, respectively, for the non-interaction geometry. (c) Polar solvent stabilization of the angle-dependent dipole moment can transform the endothermic potential (- - -) into an exothermic one with a minimum for the non-interaction geometry. (d) Population of the non-interaction geometry can likewise be enforced by substituent-induced steric crowding (shaded area).

outlined above, to an excited-state minimum with a forbidden return to S_0.

To summarize, there are three ways of producing these self-decoupling excited-state minima with *dd* state properties:

(i) Systems without LE states or with weak LE−*dd* or LE-*hp* mixing and/or in which the LE states are much higher lying than the ICT states tend to have *dd*-type or *hp*-type minima for the decoupled geometry, even in the gas phase, i.e., without additional assistance from the surrounding. Examples (theoretical) are ethylene (*hp*-type) and aminoborane (*dd*-type).[1,505] Tetraphenylethylene may also belong to this class.

(ii) Polar solvent assistance to produce a 90° minimum from potentials with a 90° maximum. Examples are **1** (see below) and the donor−acceptor biphenyl **103**, which shows no sign of populating a *dd*-type minimum, but theoretical calculations indicate such a minimum, although separated by a sizable activation barrier.[506]

(iii) If the excited-state barrier is so large that it prevents the population of the *dd*-type minimum, it can be mastered with the additional help of *pretwisting*. This has been shown for a sterically hindered derivative of **103**, namely **105**:[507] in highly polar solvents, **105** acquires forbidden emissive character, consistent with the population of a highly twisted conformation, whereas in low-polarity solvents, increased emissive transition moments indicate an emissive minimum at more planar geometries than in S_0, a behavior similar to that of **103**.

These considerations have been investigated for the case of one twisting bond, neglecting other reaction coordinates. If more than one bond twists simultaneously, or if the π-subsystems are otherwise deformed, e.g., through out-of-plane deformations, the symmetry of the system may be destroyed, and then the coupling of LE and *dd* states can be much larger because the limiting (zero overlap) geometry is not reached. As a possible consequence, *dd*-type minima can emerge with relatively large transition moments to the ground state and hence sizable fluorescence quantum yields, as encountered recently for some molecules.[508,509]

Another interesting observation in this respect is the fact that the radiative rate for the ICT emission of **23** is about 10 times smaller than for **1** or the related six-membered ring system **24**.[171] This signifies a reduced *dd*−LE mixing for **23** and a more perfect approach to the minimum overlap geometry. Considering the geometric and orbital overlap control of the CT emissive rate constant of such systems,[172] this seems to indicate a smaller average deviation from the limiting geometry (perpendicular twist and sp^2-hybridization of N) in the somewhat strained and more rigid five-membered ring of **23**, as compared to the more flexible compounds **24** and **1**.

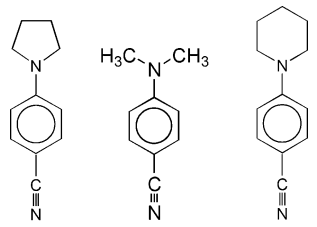

23 **1** **24**

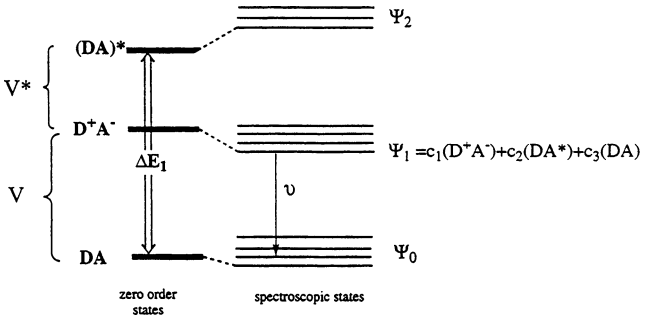

Figure 79. Three-state model for mixing of the CT state (D^+A^-) of *dd* character with the LE state (DA)* and the ground-state DA of a donor−acceptor molecule. The matrix element V* is responsible for the emissive properties of the CT state. The energy separation between the LE and CT states, and thus their mixing, is strongly affected by the polarity of the solvent. Adapted with permission from ref 512.

For weak coupling between LE and *dd* states, a three-state model has been developed (cf. below, section X),[510−513] with a more general version of the treatment given in ref 145 (Figure 79). This ascribes a large part of the radiative properties of the *dd* state to its coupling with the more allowed LE state, in addition to the contribution from the direct coupling of the CT state with the ground state. One can derive the numerical values of the coupling matrix elements by a parabolic fitting involving the radiative rates (in different solvents) and the emission energies.

In principle, this approach should also be applicable to the radiative rates of the TICT systems **23** and **1**, provided the coupling matrix elements, which in this case could be interpreted as a measure for the geometric deviation from the minimum overlap geometry, are sufficiently small for this theory to be applicable. In such a case, the different radiative rates cannot be due to the direct coupling of the CT with the ground state, because excited-state dipole moments and emission energies of the two compounds are similar. In the three-state model, the results are consistent with a closer approach of the average emissive conformation to the minimum overlap geometry for compound **23** as compared to **1**. The deviations from this limiting geometry may involve both the twisting and the pyramidalization coordinate at the amino nitrogen. Other coordinates, e.g., those localized in the benzonitrile group, are less likely to account for the different emissive rates observed for these two compounds which vary only in the amino substitution pattern and both show very little steric hindrance to planarity.

VIII. Crucial Evidence for the TICT State

Most of the collected data seem to support the TICT hypothesis on the structure of the large-dipole excited ICT state of DMABN, as compared to the other hypotheses. Nevertheless, two pieces of evidence seem to deliver a proof for the TICT (or very similar) structure.

A. Vibrational Spectra

The vibrational frequencies of the ICT excited state of **1** (Table 12), along with time-resolved IR absorption,[307,308,310,318] were most exactly studied with picosecond time-resolved resonance Raman spectroscopy.[320−322,514,515] The ring frequencies were close to those of the benzonitrile radical anion. The transient absorption was localized in the acceptor,[133,293] probably leaving out of resonance the phenyl−N stretching mode, which was most strongly looked for.

Table 12. Some Vibrational Frequencies of DMABN (in cm^{-1}; TR, Time-Resolved; RR, Resonance Raman)

	ICT			
S_0[a]	TR IR	TR RR[e]	benzonitrile anion radical[d]	assignment
2214	2096[b,c]	2095	2093	C≡N stretch
1609		1580	1592	ring-elongating str.
1372	1276[f]	1281		$C_{ring}-N_{amino}$ str.
1203	1220[f]			$C_{ring}-CN$
1182		1170		ring in-plane bend
788		756	760	ring breath

[a] Reference 317. [b] Reference 307. [c] Reference 308. [d] Juchnovski, I.; Tsvetanov, C.; Panayotov, I. *Monatsh. Chem.* **1969**, *100*, 1980. [e] Reference 515. [f] Reference 318.

After many unsuccessful attempts, the transient resonance Raman peak of the $C_{phenyl}-N_{amino}$ stretching vibration is identified by isotopic shifts at 1281 cm^{-1}.[515] A strong downshift of this crucial frequency (~96 cm^{-1} vs the ground state) implies a substantial decoupling of the amino group and the ring. This is quite opposite to the strong electronic coupling in the PICT model[110,111] but *seems to definitely support* the TICT structure (or very close to it, with a possibility of some pyramidalization of the decoupled amino group) of the CT state. A very similar frequency (1286 cm^{-1}) was predicted by earlier calculations.[310,311] Most other frequencies were strikingly similar to those of the benzonitrile radical anion,[321] supporting the hypothesis of decoupling of the dimethylamino radical cation and benzonitrile radical anion subunits in the TICT state. Nevertheless, in view of the $-CD_3$ isotopic effects on some other vibrations, the authors do not exclude some pyramidal character of the amino group. Detailed, critical analysis of the vibrational frequencies[515]—including the model compounds and ions—makes the assignment really convincing. Further support of the decoupling hypothesis has been added recently by the comparison of the picosecond IR spectra of **1** and **106**.[516] The transient bands corresponding to the CT state are very similar, although the donor group is different.

B. Stereochemical Proof

The pyridine derivative **122** was specially synthesized to perform a decisive test to verify or falsify the TICT hypothesis.[517] The compound emits dual fluorescence closely resembling that of **1**. The two (syn−anti) rotamers **122** and **123** (in the ground state) should differ in their NMR spectra. At room temperature, the rotamerization is fast, but at −90 °C the interchange is already sufficiently slow, such that the NMR ^1H signals at ~3 and ~1.2 ppm differ in their chemical shift and in their intensities. If — and only if — the excited CT state involves a 90° rotation of the dialkylamino group, its deactivation will lead to an equal population of **122** and **123**. The experiment showed that irradiation (accompanied by the CT

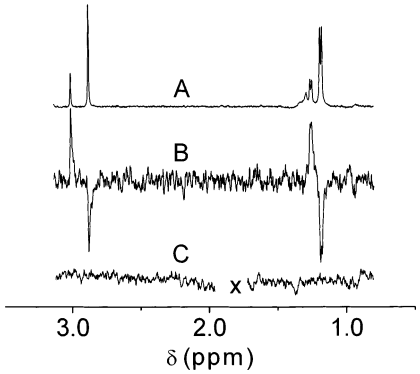

Figure 80. ^{1}H NMR spectra of **122** and **123** at 183 K: (A) in CH_3OH, prior to irradiation; (B) differential spectrum, light−dark, in CH_3OH; (C) differential spectrum, light−dark, in THF. Adapted with permission from ref 517. Copyright 2002 American Chemical Society.

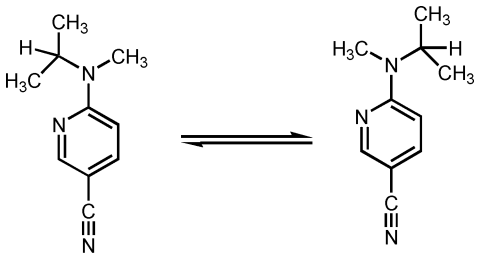

122 **123**

fluorescence, which is evidence of the population of the excited ICT state) results in depletion of the originally more intense NMR signal and in the simultaneous enhancement of the less intense signal (Figure 80). Moreover, the effect (NMR signals) increases in parallel with the intensity ratio, F_A/F_B, in the mixed solvents, MeOH + THF. The authors conclude that the TICT proposal has passed a critical test.[517]

IX. Comparison of Different Models for DMABN, and Conclusions

In view of a multitude of proposed models for the CT state of **1** and of its analogues, and a vast number of different experiments, this section attempts to summarize them in a tabular form (Table 13). Its aim is (i) to give an overview of the most important models, (ii) to point out the implications following from these models, (iii) to enumerate test experiments for or against a given model, and (iv) to show the outcome of these experiments which can be viewed as the important experimental milestones. In most cases, it is insufficient to consider only one type of experiment. The last column summarizes the conclusions.

It is worth noting, summarizing these tables, that the different mechanisms do not exclude each other in all respects. About half of the mechanisms have at least partial relevance for the reaction; i.e., they apply under certain conditions of solvent, concentration, compound, but are not general: they do not apply (i) for all conditions studied and (ii) without simultaneous assistance of another mechanism. The only exception is the twist mechanism, in which the experiments fulfill all the implications derived from the model. This twist mechanism cooperates with several other factors. One of them is the state crossing (for **1**, but not for all dually fluorescent amines). Another is the dipole−dipole solvation, which may be sometimes treated as a solute−solvent exciplex formation (especially in protic solvents, but certainly not in alkanes). Further factors are the amino group pyramidalization in some compounds, and the interaction of close-lying excited states (pseudo-Jahn−Teller coupling, which appears relevant not for the CT emission, but for the short-wavelength LE band). These additional factors do not constitute any general mechanism, but they have to be taken into account in a correct description of the reaction coordinate. Whether they apply for a particular system can be answered by scrutinizing the experiments that test the implications and the predictions, verifying or falsifying them.

Most evidence — and now even proofs — is in favor of the TICT model for the structure of the ICT state of **1** and of many other similar compounds discussed in the preceding sections. In these cases, the F_A emission exhibits a strong solvatochromic red shift, consistent with a very large dipole moment of the emissive CT state; the CT emission is *forbidden*; i.e., it has a very small radiative rate constant. In the highly viscous solvent glycerol triacetate, the rate constant of CT state formation is slowed under high pressure (which increases both the solvent viscosity and polarity). Planar model compounds, which cannot relax toward a twisted geometry, do not exhibit a CT band. All other model compounds, including that with a rigidly perpendicular geometry (**22**),[518] show an energy of the CT band maxima very similar to that of **1**. This indicates an approximately common relaxed conformation, and the only possibility is a nearly perpendicular arrangement.

The comparison of **57**,[8,92,133] with the amino nitrogen held in the seven-membered ring, and **55**, with a six-membered ring, is more difficult to interpret within the state interaction than within the TICT model. Interaction of the two lowest excited states, and a pyramidalization of the N atom, are possible in both compounds, as shown by the example of the compounds with a five-membered ring, **20**, while it would be difficult to explain within the state interaction model why a CT fluorescence appears in **57** but not in **55**. On the other hand, the increased ring flexibility of **57** creates a better access to conformations twisted more out of coplanarity than **55**, although a perpendicular TICT conformation cannot be reached in this case.

Some points which are evidently not yet solved will be resumed in the last section ("open questions").

X. Quantitative Treatment of Electronic and Structural Effects

A. State Interactions and the Coupling Matrix Elements

A general quantum mechanical treatment, revealing the analogies and permitting the prediction of properties of whole classes of compounds, is possible

Table 13. Different Models of the Dual Fluorescence in DMABN

implications	predictions	experimental tests	conclusions
A. Lippert's Solvent-Polarity-Induced Reversal of ^1L_a- and ^1L_b-Type States (1962)[63]			
two close-lying emitting states S_1 and S_2 with mutually perpendicular transition moments and different dipole moments, $\mu_1 < \mu_2$	band B polarized perpendicularly to the long molecular axis and to band A	satisfied for **1** in EtOH,[129] not in glycerol;[1] not satisfied for **32** in EtOH;[185] not applicable to **17**, where ^1L_a and ^1L_b are already mixed in absorption	bands A and B can be related to ^1L_a- and ^1L_b-type states; two fluorescence bands can, however, appear even in the absence of the state reversal
	solvent-induced reversal of S_1 and S_2 is possible only if $\mu_1 < \mu_2$	state reversal does not occur for dual fluorescent **32** because $\mu_1 > \mu_2$ already in weakly polar solvents,[100,185] but it occurs in the model compound **33**, which emits only band B[181]	band B can reveal a state reversal even in the absence of dual fluorescence
	band A should have larger k_f than band B because $k_f(^1L_a) > k_f(^1L_b)$	$k_f(A) \ll k_f(B)$;[4] for some compounds with no band A, a polarity-induced increase in k_f (state switching) has been observed within band B[181,184,568]	band A does not directly derive from ^1L_a state; state reversal for band B is independent of the dual fluorescence
B. Excimer (or Dimer) Mechanism (1972)[71−74]			
ground-state dimer preformation and/or excited-state dimer *(excimer)* formation	concentration dependence of dual fluorescence and possibly a ground-state dimer absorption band should be observable	concentration independence of dual fluorescence in the usual concentration range[1,75,76]	dual fluorescence is due to a *monomolecular* mechanism in the low-concentration range, but excimer/dimer can additionally appear at high concentrations or conditions favorable for dimerization
		emission wavelength of the real excimer of **11** is polarity-independent[77]	
		red-shifted excimer bands are observable for dimers and/or higher oligomers of **1** in supersonic[414,420] jets or in cooled alkane solvents[79,80]	
C. Solute−Solvent Exciplex Mechanism (1971, 1980)[7,90,91,94,251]			
excimer stabilization energy should depend on the electronic structure of the solvent partner (e.g., on its lone pair energy and availability)	no band A should appear in solvents having no lone pairs (unable to form a complex)	band A can also occur in the gas phase[135,136] and in solvents with no lone pairs (alkanes,[99] benzene, toluene[98−100,185])	band A can appear without solute−solvent complexation
		band A is more prominent in a solvent with a smaller number of lone pairs[114]	
	no linear correlation of band A emission energy with solvent polarity is expected	solvatochromic correlations exist indicating that most of the red shift is due to nonspecific polar interactions; correlation, however, is not perfect: there are additional (weak) specific interactions, especially with protic solvents[81]	main solvent red shift of band A is due not to exciplex formation but to nonspecific dipole solvation
	dipole moments should increase on complexation in a partner-specific way	gas- and solution-phase dipole moments correlate smoothly, with no indication for a specific dipole moment increase through complexation[116]	no evidence for exciplex formation
	quasi-instantaneous band A formation in pure polar solvents	in pure polar solvents, the rise time of band A can be considerably longer than the solvent relaxation time[467] and can differ by factors of 10[231] or even 80[455,456] for different derivatives of **1** in the same solvent	no kinetic evidence for an exciplex formation stage
	specific complexes (e.g., 1:1) expected	supersonic jet studies on small clusters **1** + (solvent)$_n$ indicate that $n = 1$ is usually not enough to induce the band A emission;[124,423] the needed n is smaller for **32** than for **1**[123]	a 1:1 complex is usually insufficient for a CT emission to appear in the gas phase; higher (unspecific) complexes are not proper exciplexes
	excimer transient absorption should be solvent-specific	transient absorption spectra (in polar solvents) are independent of the solvent[246,293]	an evidence against the exciplex as the origin of dual fluorescence

Table 13 (Continued)

implications	predictions	experimental tests	conclusions
		D. Twisting Mechanism (TICT) (1973−1979)[1,2,4]	
molecule must be capable of internal rotation or large-amplitude torsional motion of acceptor vs donor	planar model compounds should suppress while *pretwisted* ones should enhance band A	rigid model compounds show no band A; pretwisted compounds show enhanced (or only) band A, at various acceptors,[5,70,130,131,171,181,209,246,457] and are dynamically accelerated[209]	no exception is known for the twisting possibility (even if limited as in **57**) as condition for dual fluorescence
in the CT state, the amino substituent should be in the symmetry plane perpendicular to the ring	in the CT state, the memory of any asymmetry of the amino group vs the plane perpendicular to the ring should be lost	an equal population of syn and anti rotamers, **122** and **123**, on passing through the CT state is detected by NMR after the irradiation[517]	the 90° conformation of the amino group (perpendicular to the benzene ring) in the CT state is proved
molecular shape and viscosity of the medium should influence the rate of the process	strong viscosity influence expected for isopolar−isothermal conditions	pure viscosity control in viscous solvents;[454,459] solvent-polarity-dependent barriers are evident in fluid solvents,[450,451] but also the preexponential factor depends on polarity,[455,456] which can be misinterpreted as an apparent viscosity independence[451]	viscosity and polarity both control the rate of the excited-state ICT reaction
	larger rotors should slow TICT formation dynamics	of two derivatives of **1**, with the same donor−acceptor properties and identical dual fluorescences under equilibrium conditions, that with the larger-sized donor reacts slower (in the kinetic range, band A is reduced);[192] in numerous cases with unequal dual fluorescence at room temperature an opposite effect is pronounced[99,111]	band A formation is linked with a large-amplitude twisting motion, but there is a strong counter-evidence, still under discussion (e.g., ground-state twist angle effects)
practically full separation of charges	properties of the emitting state (dipole moment, transient absorption spectrum) should correspond to localization of charges within the donor and within the acceptor, respectively	dipole moments measured with different methods fulfill the condition (cf. Table 3)	virtually full separation of charges: + localized on the donor, − localized on the acceptor
		transient absorption and vibrational spectra of the CT states of **1**, **22**, **11**, etc. match the absorption spectra of the radical anion A^- (absorption of the radical cation D^+ lying in the not yet accessible UV range)[134,246,515]	
suitable dependence on donor−acceptor properties expected	compounds with a weaker donor and/or acceptor group should show no or a reduced band A	−NHMe or $-NH_2-$ analogues of **1** show no band A,[4,5,99] except for −NHMe when pretwisted[8,211]	correlation of spectral data with donor and acceptor properties is supported (provided the corrections for structural changes in the D−A emitting CT state vs the isolated D and A molecules are taken into account)
	correlation of ν_f of band A with the IP−EA or $E_{1/2}^{ox}(D) - E_{1/2}^{red}(A)$ with a slope ∼1	slope of 0.91 is found;[126] apparent independence of ν_f of the IP of aliphatic *tert*-amine donors[133,197] is explained by planarity of amino radical cations in the CT state[202]	
the phenyl−N bond should be a single bond in the CT state with decoupled amino donor and benzonitrile acceptor	bond order (in the ground state intermediate between 1 and 2) should become 1 in the CT state	vibrational frequency of the phenyl−N stretch down-shifted by 96 cm^{-1} to a typical single bond frequency of 1281 cm^{-1}	in the CT state, the donor and acceptor are decoupled, as in the TICT model
		E. Water Cluster Mechanism (1983)[82,325]	
only possible in the presence of traces of water; B and A fluorescence have a different origin (bare and H-bonded molecules)	no band A should be emitted from bare molecules in the gas phase in the absence of clusters	**21** shows band A in the gas phase in the absence of water clusters,[116,135,136,*a*] but water clusters and clusters with other solvents can help to induce band A[123,271,421]	water clusters are not the source of band A in aprotic polar solvents; they can, however, play an important role under jet conditions, similarly to the clusters with other polar molecules
	band A should rise with water content	addition of H_2O to dried ACN *quenches* the prominent band A[115]	
	decays of B and A fluorescence should be uncorrelated	B decay and A rise are perfectly linked by a precursor−successor relation in solutions (except for the ground-state complexes[98,231])	

Table 13 (Continued)

implications	predictions	experimental tests	conclusions
	F. Pyramidalization Mechanism (1992)[99] (also Named WICT)		
twisting not necessary; orbital decoupling and large excited-state dipole moment possible through pyramidalization around the amino N atom	bridged molecules with residual flexibility for pyramidalization could emit band A	molecules with medium-sized bridges (**20**, **29**, **55**) flexible enough to form ground-state confomers[131] yield only band B, similar to doubly bridged molecule **56**;[209] those with a seven-membered ring (**57**) or bridging the $-NR_2$ groups into rings of various sizes, with intramolecular rotational flexibility,[8,44,92,171,197,457,640] also emit band A	pyramidalization can be an important element of the reaction coordinate but cannot alone account for the band A emission
	.....	.....	
	for a small amplitude of wagging motion $sp^2 \leftrightarrow sp^3$, a very small viscosity effect is expected	band A formation in some viscous solvents is fully viscosity controlled[454,459]	
	.....	.....	
	band A should not preferentially occur for twisted molecules	importance of band A does not correlate with pyramidalization but usually with the S_0 twist angle[209,211]	
	.....	.....	
		quantum-chemical calculations indicate that the conformation of the state A* involves a more sp^2-type amino nitrogen than for the other states (with S_0 being the most strongly pyramidalized[407]), the pyramidalization decreasing with the number of alkyl substituents;[406] orbital decoupling through pyramidalization is possible for untwisted geometries but at the expense of several eV of excess energy[167,199]	
	G. Solvent-Induced Pseudo-Jahn−Teller (PJT) Mechanism (1993)[8]		
two close-lying states mix through solvent-induced vibronic coupling; properties of the mixed state (transition and dipole moment) are intermediate between the two extremes of the pure states; in the absence of solvation, the state with a higher dipole moment must be S_2	dipole moment of the A* state should not exceed that of the more polar of the two interacting states	dipole moment of the A* state exceeds that of the ^1L_a-type state of **1** and of related molecules[4,5,99,116]	the PJT mechanism cannot explain the observed properties of the A* state;[228] for some compounds, it is the F_B band which shows signs of a PJT mechanism
	.....	.....	
	the transition dipole moment of the A* state cannot be smaller than that of the less allowed of the two interacting states	the transition dipole moment of the A* state is considerably smaller than that of ^1L_b-type state of **1** or related molecules[4,172]	
	.....	.....	
	no correlation with twisting is expected; planar derivatives of **1** should also be able to show band A	correlation of band A with S_0 twist angle exists;[209] no band A is found for bridged (planar) compounds;[4,5] some compounds (**33**,[181] **115**[184]) indeed exhibit solvent-induced state mixing (describable by the PJT mechanism) which results, however, in (i) solvent-polarity dependence of fluorescence B anisotropy and radiative rate[184,b] and (ii) absence of CT fluorescence; in **63**,[233] the solvent-induced interaction of two states is seen in absorption, but no CT emission appears	
	.....	.....	
	no band A possible if S_1 is the more polar state, or if S_1 and S_2 are not close-lying	fluorescence A occurs also in molecules where the two lowest $^1\pi,\pi^*$ states are far apart, e.g., **22** (for pyrimidine derivatives, the lowest $^1\pi,\pi^*$ and $^1n,\pi^*$ states are close-lying, but the second $^1\pi,\pi^*$ is distant by >5000 cm^{-1} [268]), or where S_1 is the more polar state (**32**, **43**, **68**[100,185,202])	

a strong interaction of the diabatic LE and CT states appears in the adiabatic ET along the solvent coordinate model for the much larger molecules, **26** and **111**, beyond the scope of this table[550,556]

Table 13 (Continued)

implications	predictions	experimental tests	conclusions
	H. Cyano-Bending Mechanism (RICT) (1980[104] and 1996[9,10])		
as a well-defined mechanism, it is possible only for cyano- or related (suggested: acetylene) derivatives	band A needs a suitable acceptor substituent	band A is observed also for pyridine and pyrimidine derivatives[267,268] and in *N*-phenylpyrrole, where the phenyl ring is the acceptor[606]	the CN bending mechanism cannot explain band A alone, but it may be part of the reaction coordinate
	band A should also appear in planar rigid compounds	no band A for planar bridged compounds[4,5]	
	very little viscosity dependence is expected	viscosity dependence is large[459]	
	band A is expected for acetylene derivative[10]	acetylene derivative **19** does not exhibit band A[107]	
	I. Planarization Mechanism (PICT) (1997−2000)[110,201]		
in polar solvents, the S_2 (^1L_a, ICT) state becomes the lowest one in a dynamic state reversal with conformational changes (excited-state ICT reaction); the resulting ICT state has a planarized, quinoid structure	planar analogues of **1** should emit preferentially the A fluorescence	the rigidly planar analogues of **1** do not emit the A fluorescence at all [4,5]	planarization of **1** is incompatible with the experimental evidence
	the *pretwisted* D−A compounds, with a sterical hindrance to coplanarity of D and A, should not be able to emit F_A	the pretwisted compounds emit preferentially (or only) F_A;[130,c] the perpendicular rigid **22** emits the CT band spectrally very close to **1**	
	in the quinoid structure, the $C_{phenyl}-N_{amino}$ bond should be shortened and its stretch frequency upshifted	the $C_{phenyl}-N_{amino}$ stretch frequency is strongly downshifted, by 96 cm^{-1}, in the resonance Raman spectrum of the CT state of **1**[515]	
the emitting state A* is the ^1L_a, ICT state	if the S_1 state already is of ^1L_a ("ICT") nature, only F_A emission band should appear	in the ester derivatives of **1**, with S_1 being of ^1L_a nature, dual emission (B and A) is observed[100,185]	

[a] Kobayashi, T.; Futakami, M.; Kajimoto, O. *Chem. Phys. Lett.* **1987**, *141*, 450. [b] Heisel, F.; Miehé, J. A.; Eckert C.; Rettig, W. *Chem. Phys. Lett.* **1991**, *187*, 45. [c] Grabowski, Z. R. *Acta Phys. Polon.* **1987**, *A71*, 743.

Table 14. Overlap Matrix Elements between the Lowest ^{1}ET State ($A^-−D^+$) and the Ground or Locally Excited (with the Main HOMO → LUMO Configuration, ^1L_a) States[50]

	A−D	A−D*	A*−D
$A^-−D^+$	$2^{1/2}\langle$HOMO(D) LUMO(A)$\rangle$	$\langle$LUMO(D) LUMO(A)$\rangle$	$-\langle$HOMO(D) HOMO(A)$\rangle$

mainly in the framework of simple MO theory. Such a treatment proved to be very successful in the case of the D−A molecules.

The electronic structure of D···A complexes has been most carefully described by Beens and Weller.[50,519] On the basis of Mulliken's theory of intermolecular CT interactions,[520] and introducing the mixing between the ET state, the ground state, and the locally excited state,[521,522] they defined the interaction matrix elements in terms of the orbitals involved (in the simplest case, only the frontier orbitals of D and A) and their overlap integrals. In the nearly non-interacting systems of D and A, the interaction matrix elements decisively depend on the overlap integrals between D and A (Table 14).

The concepts of the *molecules in molecules* (MIM) model[523] have been applied to the D−A molecules.[171] The wave function of the spectroscopic CT state can be represented as

$$\Psi_{A^-D^+} \approx a_{ET}\Psi^o_{A^-D^+} + a_G\Psi^o_{A-D} + a_{A^*}\Psi^o_{A^*-D} + a_{D^*}\Psi^o_{A-D^*} \quad (27)$$

where $\Sigma a_i^2 = 1$. Other wave functions are also suitably modified by the interactions, e.g, that of the ground state:

$$\Psi_{A-D} \approx b_G\Psi^o_{A-D} + b_{ET}\Psi^o_{A^-D^+} + b_{A^*}\Psi^o_{A^*-D} + b_{D^*}\Psi^o_{A-D^*} \quad (28)$$

The coefficients *a*, *b*, etc. depend on the Hamiltonian matrix elements and on the respective energy differences between the states. The transition dipole moment between the ground and the CT state will be

$$\vec{M}_{G,CT} = \langle\Psi_{A-D}|\hat{\mu}|\Psi_{A^-D^+}\rangle = a_G b_G\vec{\mu}_G + a_{ET}b_{ET}\vec{\mu}_{ET} + a_{A^*}b_G\vec{M}_{A,A^*} + a_{D^*}b_G\vec{M}_{D,D^*} + \ldots \quad (29)$$

The transition moment can be found either from the emission (eq 17) or from the absorption:

$$|\vec{M}_a|^2 = \frac{3hc10^3\ln 10}{8\pi^3 N_A n}\int_{band}\frac{\epsilon(\tilde{\nu})}{\tilde{\nu}}\,d\tilde{\nu} \quad (30)$$

In several series of A−D molecules with dialkylaniline as D and large aromatic systems as A, the CT emission is by no means forbidden. In the case of such acceptor moieties as naphthalene, pyrene, and fluoranthene, the transitions were as allowed as, or even more than, the local transitions: $M_{CT,G} \geq M_{A,A^*}$, M_{D,D^*}.[145,267,507]

The ground-state dipole moment, μ_G, and the local transition moments, M_{A,A^*} or M_{D,D^*}, can reach values up to 4−5 D. However, the μ_{ET} value is usually very high, often 15−20 D or higher, and can decisively contribute to the intensity of a "CT" transition in absorption or in emission, which is often forbidden for the zero-order wave functions, Ψ°, and zero or negligible orbital overlap. In the large aromatic D−A systems mentioned above, the transition dipole moments in emission amount to several (3−5) Debye units.[524] This was a hint for the principal role of the second component on the right-hand side of eq 29, i.e., of the interaction of the CT and the ground states. Equation 29 in a simplified form delivers the coupling matrix elements if one of the components of eq 31 is dominant.

$$\vec{M}_{G,CT} = \frac{V_G^{CT}(\vec{\mu}_{ET} - \vec{\mu}_G)}{hc\tilde{\nu}_f} + \sum_j \frac{V_{CT}^j \vec{M}_{Gj}}{E_j - hc\tilde{\nu}_f} \quad (31)$$

Kapturkiewicz and Herbich[61,524,525] adapted the existing formalism[50,526] to the case of the singly bonded D−A molecules. As the overlap occurs here virtually only between the atomic orbitals localized on the two atoms forming the central bond, which links the D and A moieties, a satisfactory approximation can be reached by taking into account only these local interactions. These can be expressed in terms of the LCAO coefficients on these two atoms in the frontier orbitals. The electronic coupling matrix elements, under such simplifying assumptions, are

$$V_G^{CT} = c_{LUMO}^A c_{HOMO}^D \beta_{AD} \cos\theta_{A-D} + \text{const.}$$

$$V_{CT}^{A^*} = c_{HOMO}^A c_{HOMO}^D \beta_{AD} \cos\theta_{A-D} + \text{const.} \quad (32)$$

$$V_{CT}^{D^*} = c_{LUMO}^A c_{LUMO}^D \beta_{AD} \cos\theta_{A-D} + \text{const.}$$

Assuming that the remaining interactions between the atoms of D and A can be neglected (const. = 0), the coupling matrix elements can be estimated from the experimental data and can contribute to the elucidation of the molecular structure of the CT state in a direct way from the resulting value of the twist angle, θ. In some cases it could be demonstrated that the admixture of the nearby locally excited states in the CT state is pronounced (and detectable in the lowering of the corresponding local transitions in absorption), especially in nonpolar solvents.[172] With growing solvent polarity, the energy gap between the CT state and the locally excited states increases. The observed changes of the transition moment, M_f, with solvent polarity (or a solvent property depending on it) can therefore deliver important evidence as to the structural changes in the CT state. The molecules can become either more planar or more twisted by relaxing in the excited state. Both types of possible behavior are reported for different series of D−A molecules (see below, section XI). In the case of several series of D−A compounds composed of large aromatic donors and acceptors, the results indicated twist angles much smaller than 90°, sometimes less than for the conformation of the ground state (*planarization*, possibly toward a more quinoid structure[145]). Some of these structural implications are reported in the following sections for specific families of large aromatic D−A compounds.

B. Spectral Band Shape Analysis

The current theory of electron transfer in radiative and nonradiative transitions[144,511,527−529] has been consequently applied to the structure of the relaxed CT states of D−A molecules by Herbich and Kapturkiewicz.[61,145,172,510,524,525] They chose several series of D−A compounds, mostly with aromatic donors (dialkylanilines, carbazoles) and large aromatic acceptors (anthracene or other polycyclic arenes, acridine, cyano- and dicyano-substituted phenyl or pyridyl). These compounds usually exhibit, along with a CT fluorescence, a CT absorption band (as the lowest energy transition in absorption). This allowed the authors to determine the dipole moments from the solvent shifts (solvatochromism) both in emission and in absorption, using the solvent polarity function not neglecting the polarizability α of the solute, but assuming $\alpha_e \approx \alpha_g \approx (1/2)a_o^3$, as in eq 33:

$$hc\tilde{\nu}_a \approx hc\tilde{\nu}_a^o - \frac{2\vec{\mu}_g(\vec{\mu}_e - \vec{\mu}_g)}{a_o^3}\left[\frac{\epsilon - 1}{\epsilon + 2} - \frac{1}{2}\left(\frac{n^2 - 1}{n^2 + 2}\right)\right] \quad (33)$$

The analysis of the band shape of the CT spectra was done following the Marcus method,[144,524] in terms of the reorganization energy (Figure 81).

The CT fluorescence band profile (radiative ET) is described as

$$\frac{I(\tilde{\nu}_f)}{n^3\tilde{\nu}_f} = \frac{64\pi^4}{3h} M_f^2 \sum_{j=0}^{\infty} \frac{1}{j!}\left(\frac{\lambda_i}{hc\tilde{\nu}_i}\right)^j e^{-\lambda_i/hc\tilde{\nu}_i} \sqrt{\left(\frac{1}{4\pi\lambda_o}\right)} \times \exp\left[-\frac{(jhc\tilde{\nu}_i + \lambda_o hc\tilde{\nu}_f + \Delta G_{ET}^o)^2}{4\lambda_o RT}\right] \quad (34)$$

where the reorganization energy $\lambda = \lambda_i + \lambda_o$. λ_i is the *inner* reorganization energy of the solute (in this approximation, it is represented by an arbitrary averaged *single mode*, ν_I). λ_o is the *quasi-classical* part, corresponding to the solvent reorientation, λ_s, and to the classically treated low-frequency modes of the solute, $\delta\lambda_o$. M_f is the radiative ET transition moment in fluorescence,[532] and ΔG_{ET} is the standard free enthalpy of the ET. Figures 81 and 82 illustrate the concepts.

If the CT absorption band is separable from the other absorption bands, one can apply to its profile an expression closely analogous to that valid for fluorescence:

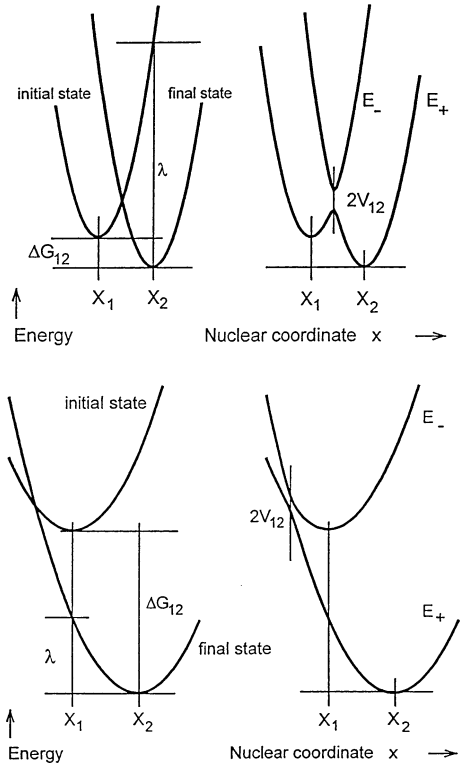

Figure 81. Marcus plots of potential energies of the reactant and product of an ET reaction as a function of a generalized coordinate *x* including both the inner (solute) and the outer (solvent) coordinates; λ, reorganization energy. (Top) In the "normal" Marcus region; (bottom) in the "inverted" Marcus region (highly exothermic reaction). (Left) Diabatic (zero-order) approximation; (right) adiabatic (first-order) approximation. Adapted from ref 530 with permission from the author. The initial state in the inverted Marcus region is ex definitione an electronically excited state of the system.[143,531]

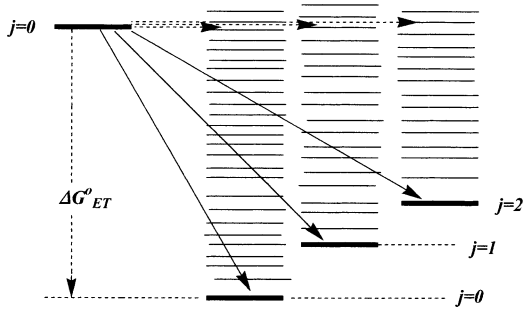

Figure 82. Nonradiative electron transfer occurs primarily isoenergetically (horizontal transitions) to a quasi-continuum of low-frequency (mainly solvent) modes built on various higher frequency vibrational levels of the final state (hence the "energy-gap law"). The radiative ET represents a sum of component transitions to various vibrational levels of the final state (solid oblique arrows). Adapted from ref 530 with permission from the author.

$$\frac{\epsilon(\tilde{\nu}_a)}{n\tilde{\nu}_a} = \frac{8\pi^3}{3c\ln 10} M_a{}^2 \sum_{j=0}^{\infty} \frac{1}{j!}\left(\frac{\lambda_i}{hc\tilde{\nu}_i}\right)^j e^{-\lambda_i/hc\tilde{\nu}_i} \sqrt{\left(\frac{1}{4\pi\lambda_o}\right)} \times \exp\left[-\frac{(jhc\tilde{\nu}_i + \lambda_o hc\tilde{\nu}_{a'} + \Delta G^o_{ET})^2}{4\lambda_o RT}\right] \quad (35)$$

A first estimate of the unknown parameters, λ_o, λ_i, and ν_i, is found by a multiparameter fit to the experimental spectral band profiles by eqs 34 and 35.[529] The value of ΔG^o_{ET} is usually known from the electrochemical data of the D^+/D and A/A^- systems. It can also be estimated as being close to the 0−0 transition of the (possibly pure) CT transition, $-\Delta G^o_{ET} \approx {}^1/_2(h\nu_a{}^{max} + h\nu_f{}^{max})$. Another approximate estimate of the relevant values is given by the Stokes' shift of these bands: ${}^1/_2(h\nu_a{}^{max} - h\nu_f{}^{max}) \approx \lambda_i + \lambda_o$.

If $h\nu_i \gg kT$, the expression for the fwhm ($h\Delta\nu_{1/2}$) of a CT band[144,529] can be simplified to a practical form:

$$(hc\Delta\tilde{\nu}_{1/2})^2 \approx 8(\ln 2)(2kT\lambda_o + \lambda_i hc\tilde{\nu}_i) \quad (36)$$

One obtains λ_o from, e.g., a plot of $(h\Delta\nu_{1/2})^2$ vs T. Plotting λ_o vs a solvent polarity function, one arrives at the components of λ_o: the *solvent reorganization energy*, λ_s, from the slope, and the quasi-classical part (small quanta) of the *inner reorganization*, $\delta\lambda_o$.

The values of λ_i and $\delta\lambda_o$, and their dependencies on structural or environmental parameters, can be interpreted in terms of structural changes between the ground state and the excited CT state. This was successfully done in numerous cases of large aromatic D−A molecules (see section XI) but is not easily applicable to **1** and the compounds similar to it, as discussed in the preceding sections, mainly because of the absence of a direct $^1CT \leftarrow S_0$ absorption band. A Marcus-type scheme of the processes involved in the photophysics of **1** or its analogues is schematically shown in Figure 83.

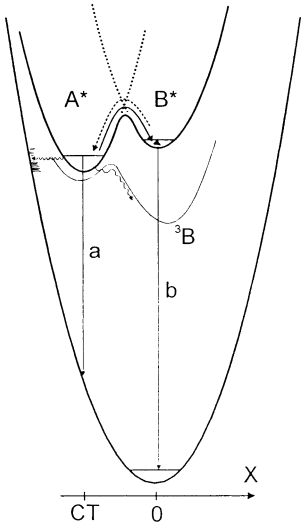

Figure 83. Marcus-type diagram (in the adiabatic approximation) of a dually fluorescent D−A system, e.g. **1**, in a polar solvent. Along with the B* → A* ET reaction, an ISC process to the $^3B^*$ state (directly or via the $^3A^*$ state), and an internal conversion of $^1A^*$ to S_0, are the back-ET processes in the "normal" region and in the "inverted" Marcus region, respectively.

XI. Overview of Different D–A Systems

A. Systems with Aromatic Donor or/and Polycyclic Acceptor

The existing evidence on the structure of the CT states is usually more ambiguous in large π-electronic

D−A systems than in the case of **1** or its close analogues, with a single aromatic ring (usually in the acceptor unit). In the majority of cases, the polycyclic molecules studied consist of donor and acceptor units mutually twisted already in the ground state − sometimes even by 90° − due to steric interactions of the aromatic ring systems. Often only one fluorescence band appears, and special means have to be applied (e.g., low temperature to slow the CT reaction, or time-resolved spectra to reveal the short-living primary species) to demonstrate a dual luminescence. Moreover, in contrast to **1**, in many families of D−A compounds a CT absorption band appears as the lowest transition, the CT state being thus directly reached in the very act of excitation. The CT transition is not always forbidden; in some structural groups it is even more allowed in emission than in absorption, and a close inspection of the photophysical data indicates that, in some markedly twisted ground-state structures, the excited-state relaxation *reduces* the twist angle θ.

Much of the topic related to this broad class of compounds is discussed in another overview,[203] and so we shall treat in this section only some exemplary families of compounds, reviewing them less comprehensively than the previously described simpler compounds, which are more closely related to **1** in their behavior.

1. Anthracene Acceptor, Dialkylaniline Donors

Anthracene differs from benzene in its sequence of states: the ^1L_a is the lowest excited singlet state, ^1L_b lying above it. As compared to benzonitrile ($E^{red}_{1/2} = -2.35$ V vs SCE), anthracene is a better electron acceptor ($E^{red}_{1/2} = -1.96$ V vs SCE). 1-, 2-, and 9-aminoanthracenes all possess a broad and structureless first absorption band, indicating a CT-type transition. They all emit fluorescence from states markedly more polar than their ground states, but the μ^* values (6−9 D)[533,534] are lower than those expected for a full ET (13−28 D, depending on the substitution site). A preliminary study of 9-Me_2N-anthracene[535] seems inconclusive, as there are two emissions with two different excitation spectra.[536] A comparative investigation of the amino-substituted 10-cyanoanthracenes (9-NH_2-, 9-NH(CH_3)-, and **124**),[537] with cyanoanthracene being a much stronger acceptor than the parent hydrocarbon, resulted in finding two emission bands for each of these compounds. One band was anthracene-like, the other one being broad and structureless, but, in contrast to the expectation for a CT emission, at the same wavelength for all three compounds. Here again, the excitation spectra of the

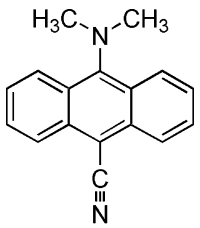

124

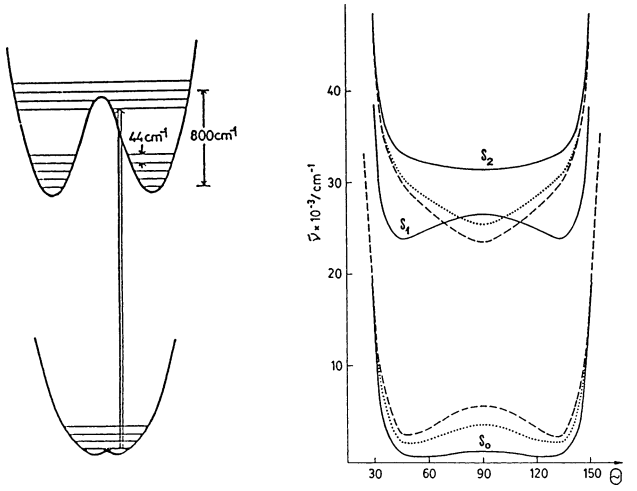

Figure 84. Conformational behavior of **26**. (Left) Schematic representation of the torsional potentials for the S_0 and S_1 states of **26** in the gas phase, as inferred from the LIF excitation spectra (Adapted with permission from ref 542.) (Right) Calculated potential energies of **26** in S_0, S_1, and S_2 states. Solid curves, for the free molecule; dotted curves, in ethyl ether; dashed curves, in ACN as solvent. Adapted with permission from ref 236.

two bands differed radically. Photophysical data, based on the clearly seen dual fluorescence of **124**, indicate a high yield of internal conversion (∼0.95) and, by analogy to the naphthalene derivatives,[565] are interpreted as a high-amplitude *anti-twist*, i.e., planarization in the CT state of a pretwisted molecule. The anomalies in the excitation spectra are found to be due to an impurity efficiently emitting a structured fluorescence.[538] Thus, the previous findings[537] are dubious.

In the case of *p*-(9-anthryl)aniline, the LIF excitation spectrum in the supercooled molecular jet reveals the existence of two weakly coupled electronic states, which are interpreted as closely lying LE (anthracene-like) and intramolecular CT states.[539]

The dimethylaniline derivative of anthracene, **26** (ADMA), is one of the first studied D−A molecules emitting a CT fluorescence.[2,91,540,541] Due to the steric interaction between the anthracene and the benzene ring, the ground-state conformation of **26** is strongly twisted, being estimated on the basis of the LIF excitation spectra[542] to be about 65° , or to be close to but deviating from 90°, or to be 84° ± 5° on the basis of molecular mechanics calculations.[145] The excited-state conformation in the gas phase is estimated from the molecular jet spectra as corresponding to a twist angle $\theta \approx 60°$ (Figure 84a). A semiempirical quantum-chemical calculation (INDO/S and PCILO)[236] indicated that the S_2 state is of intramolecular CT character, with the dipole moment rising with the twist angle θ up to 20.3 D at $\theta = 90°$. Including the solvation effect in the form of the Onsager reaction field in a very simplified form (which neglects the polarizability of the solute),

$$E_{solv} \approx (\mu^2/a_o^3)[(\epsilon - 1)/(2\epsilon + 1)] \qquad (37)$$

the calculations predict a lowering of the CT state with growing polarity of the solvent, below the LE state at high values of θ (Figure 84b).

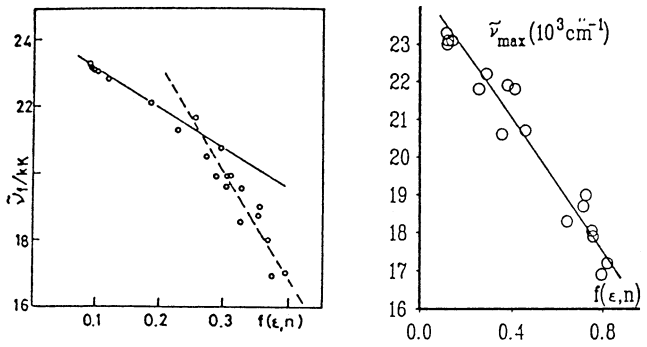

Figure 85. Solvent effect on the fluorescence band maximum of ADMA (**26**). (Left) Plotted versus the solvent polarity function $f(\epsilon,n)$ as in eq 14. (Adapted with permission from ref 543; points from ref 540.) (Right) Plotted versus the polarity function $f(\epsilon,n)$ as in eq 38. Reproduced with permission from ref 510. Copyright 1991 Elsevier Science.

In solution, **26** emits a single fluorescence band, somewhat structured in nonpolar solvents, which becomes broad, structureless, and strongly red-shifted with increasing polarity of the solvent. The solvatochromic shift is nonlinear (Figure 85a) in the plots vs the polarity function $f(\epsilon,n)$, such as in eq 14. This indicates that, in strongly polar solvents, the emitting CT state has a dipole moment $\mu^* \approx 18$ D[539] or 20.5 D.[543] Quantum chemical calculations[236] show that, in the 90° twisted (TICT) state, the positive charge is distributed over the whole dimethylanilino radical cation,[544] which particularly contrasts to **1** (and to other TICT states with aliphatic amino groups as donors), with the positive charge being localized on the amino nitrogen atom.

Electrooptical emission measurements (in weakly polar solvents) resulted in $\mu^* = 15.2$ D for **26**.[4,545] Baumann et al.[545] stated, however, that the electrooptical properties of **26** and its derivatives did not necessitate the existence of two electronic states, LE and CT. An alternative explanation is possible, with only one dipolar excited state having a very high electronic polarizability. Later, on the basis of the solvent independence of the measured excited-state dipole moments of the compounds studied, they withdrew[546] from this high polarizability hypothesis. The interpretation of the solvatochromic shifts (Figure 85a) in terms of two states resulted in dipole moment values of 12.5 and 20.5 D.[543]

Herbich and Kapturkiewicz[510] found that the solvatochromic plots of **26** and of many similar compounds become linear (Figure 85b) if plotted against the modified polarity function:

$$f'' = \frac{\epsilon - 1}{\epsilon + 2} - \frac{1}{2}\left(\frac{n^2 - 1}{n^2 + 2}\right) \qquad (38)$$

This corresponds to a highly polarizable dipole with $\alpha_g \approx \alpha_e \approx (1/2)a_o^3$, i.e., to a single excited-state model, with the electronic structure continuously changing with the polarity of the medium.[547] The excited-state permanent dipole moment in the vacuum evaluated for **26** in this way is only 13.7 D (17.3 D for **27**).[510] Later, the same authors admitted that the dipole moments calculated with such a polarizability assumption are underestimated.[524]

In the controversy on the nature of the emitting state of ADMA (**26**), important evidence was delivered by the behavior of the model compounds, by the time-resolved absorption and fluorescence spectra, and by the fluorescence kinetics. The first specially synthesized model compounds were **27** and **125**.[2] **125**,

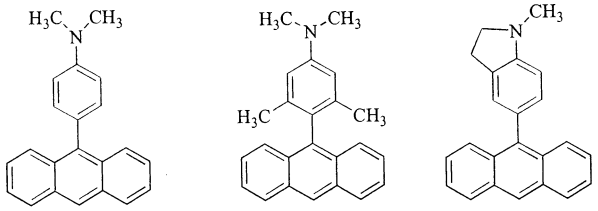

26 **27** **125**

with the amino nitrogen immobilized in the planar position, behaved very similar to **26**. The strongly sterically hindered molecule **27** also exhibited a similar behavior, but its absorption spectrum was better structured (Figure 86), much more resembling

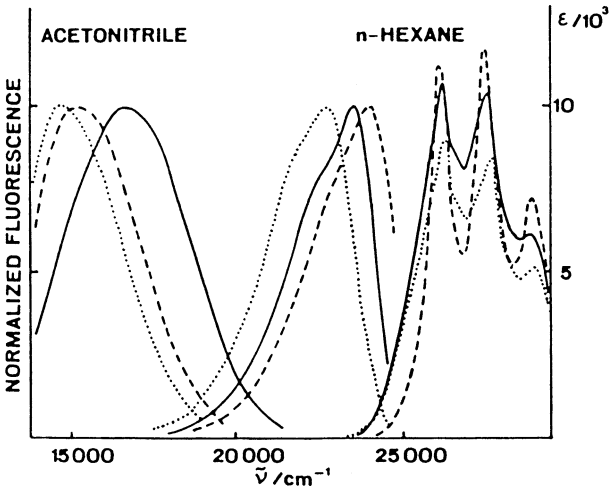

Figure 86. Absorption spectra in *n*-hexane, and fluorescence spectra in *n*-hexane and in acetonitrile, at room temperature: solid curves, **26**; dashed curves, **27**; dotted curves, **125**. Reproduced with permission from ref 2. Copyright 1977 Elsevier Science.

anthracene than the other two. This was evidence for a nearly full decoupling of the two aromatic systems in the ground state of **27**. The rate of formation of the CT state was also higher for **27** than for the other two molecules.[2,236,548] It seemed evident that the twist around the anthryl−phenyl C−C bond is important in this case, not the rotation of the amino group.

The kinetic studies showed that the excited-state reaction in alcohols is slower than the longitudinal relaxation time, τ_L,[549] and that the reaction proceeds in stages, only some of which are solvent mobility controlled.[548] Highly time-resolved reaction kinetics of the ET process in **26** revealed a very fast stage, much shorter than the solvation time, and another stage, also very fast, but approaching the solvation kinetics.[550]

Subsequently, a whole series of further derivatives[510,551] gave better insight into the formation and structure of the CT state. Transient absorption

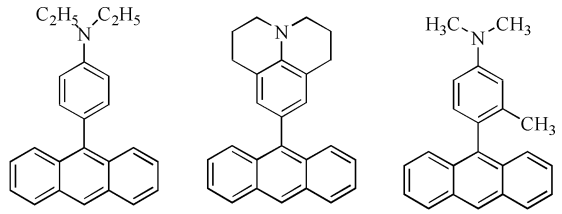

126 **127** **128**

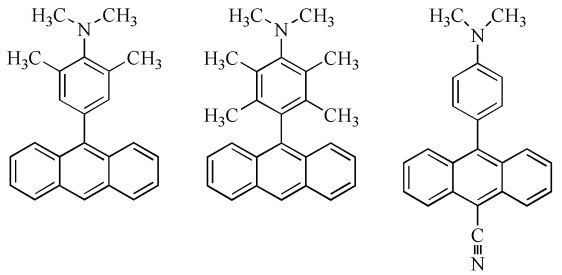

129 **130** **131**

spectra of **26** are radically different in alkanes and in highly polar solvents. In the latter case, they resemble the sum of the absorption spectra of the radical anion of anthracene and the radical cation ϕ-$N(CH_3)_2^+$.[543] A similar change is observed in the course of the CT reaction, on comparing the time-resolved spectra at the shortest delay time and after a relaxation time, e.g., at $\tau \approx 100$ ps. The evidence for two widely different electronic structures was unquestionable. The electronic structure of the equilibrated CT state in strongly polar solvents was similar to, but still somewhat different from, the decoupled D^+-A^- system.[552] The transient absorption of **131** in polar solvents was similar to that of the relaxed exciplex 9-CN-anthracene$^-$ + dimethylaniline$^+$.[553] The electrooptical methods in emission in different solvents indicated the existence of two species, with dipole moments of 14 and 24 D.[553] The temporal evolution of the time-resolved absorption spectra in polar solvents indicated, however, that there were also some intermediate structures, associated probably with stepwise solvation and different twist angles, both in excited **26** and **131**.[554]

Much controversy arose around the transient absorption spectra in the solvents of medium polarity. In the cases of **27**, **130**, and **131**, the transient absorption spectra correspond to the sum of respective contributions of the two limiting spectra.[546,552,553] In the cases of **26**, **125**, and **129**, the observed time-resolved spectrum deviated from such additivity, revealing some additional features which were interpreted in terms of some further (intermediate) states along with the limiting two states, LE and CT.[543,546,552]

In contrast to the stationary spectra of **26** and its derivatives, in which usually only one fluorescence band is observed at room temperature (except for **131**), the time-resolved spectra in cooled liquid solutions reveal two emission bands.[2] It is demonstrated

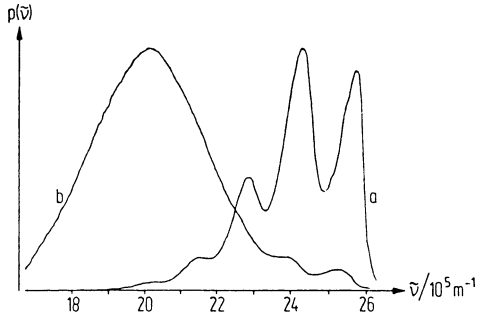

Figure 87. Fluorescence spectra of **130** at $T = 298$ K: (a) in cyclohexane and (b) in medium-polarity benzotrifluoride, ϕ-CF_3. Reproduced with permission from ref 546. Copyright 1988 American Chemical Society.

that, for excitation within the long-wavelength CT absorption shoulder, the CT fluorescence is emitted with higher yield than when excited in the main (anthracene-like) absorption band.[236] Such red-edge effects were assigned to the presence of different conformers.[545] The fluorescence spectra in different solvents, at different pressures,[549,555] or electrooptical measurements[546,551] usually show that there are two distinct limiting states.

On the basis of ultrafast kinetic and spectroscopic measurements, Tominaga et al.[550,556] created a consistent model of photophysics of **26**, with the diabatic LE and CT states forming an ET system in the Marcus inverted region. Strongly interacting, these states produce the adiabatic S_1 state, and the relaxation along the solvent coordinate represents the further stages of the ET reaction. The simulations of the transient spectra reproduce well the experimental data. In the initial stages, the emitting S_1 state has *mainly* the spectroscopic characteristics of the LE state, then it becomes an adiabatic mixture and finally reaches the energy minimum with *mainly* CT character. It is not quite clear how the solvent coordinate model, neglecting the intramolecular coordinates, explains, e.g., the sterical effects (e.g., the differences between **26** and **27** in the absorption spectra, and especially the differences in fluorescence spectra, **26** vs **130**; see Figure 87).

At intermediate polarities (or delay times), one observes either a changing population[557] (*resp*. an equilibrium[543]) of two limiting states, or some additional states[552,558] or conformers.[236,548] The hexamethyl derivative, **130**, clearly exhibits two emission bands in the stationary spectra (Figure 87).[546] The excited-state dipole moments (determined by electrooptical emission methods)[546] of the model compounds with a strong steric hindrance at the amino group, **129** and **130** (Table 15), are evidently smaller than expected for an ET from the amino group to the anthracene ring; nevertheless, the time-resolved absorption spectra indicate the features characteristic for the anthracene radical anion.[546]

In a series of papers, Herbich and Kapturkiewicz compared a large number of D−A molecules including the anthracene derivatives.[145,172,510,524] They performed a thorough analysis of the stationary absorption and fluorescence spectra, evaluating the transition moments and the coupling matrix elements of the CT state with the LE states or the ground state, and

Table 15. Photophysical Characteristics of 26 and Its Derivatives[a]

compd	solvent	M_a^{CT}/ D	ν_f/ 10^3 cm^{-1}	k_f/ 10^7 s^{-1}	M_f/ D	μ^*/ D
26	*n*-hexane		23.6[e]			(19.6)[b]
	ethyl ether		21.5[c]			(13.7)[c]
	C_6H_5F		20.7[g]			
	n-butanol		19.0[f]	4.1[e]		
	butyronitrile		18.05	2.1	2.1	
	acetonitrile		16.7[e]			
27	cyclohexane		23.5[g]			(30.1)[b]
	C_6H_5F		19.1[g]			(17.3)[c]
	n-butanol		17.0[f]	0.5[e]		
	butyronitrile		16.45	0.29	0.88	
125	*n*-heptane		22.6[g]			(18)[d]
	C_6H_5F		17.9[g]			
	n-butanol		16.3[g]	1.6		
126	cyclohexane		23.1[g]			(20.7)[b]
	C_6H_5F		20.5[g]			
	butyronitrile		18.20	1.7	1.8	
127	MCH	2.6	21.68	11.0	3.5	
	butyl ether	2.5	19.15	4.8	2.8	(28.8)[b]
	THF	2.5	15.95	1.9	2.3	(18.5)[c]
	butyronitrile	2.6	14.20	0.85	1.9	
128	ethyl ether		20.70	4.1	2.4	(13.2)[c]
	MTHF		19.15	2.3	1.9	
	butyronitrile		17.20	0.65	1.2	
	acetonitrile		16.20	0.43	1.15	
129	propyl ether		23.0[g]			(18.2)[b]
	C_6H_5F		21.1[g]			(13.5)[d]
130	cyclohexane		24.2[g]			(31.7)[b]
	C_6H_5F		19.8[g]			(18)[d]
131	cyclohexane		21.3[g]			(20.8)[b]
	propyl ether		20.1[g]			
	C_6H_5F		17.7[g]			(24)[d,h]

[a] Data according to Herbich and Kapturkiewicz (refs 145, 510, and the following: Herbich, J.; Kapturkiewicz, A. *Chem. Phys. Lett.* **1997**, *273*, 8) unless otherwise stated. M_a, M_f, transition moments in absorption and in emission, respectively; MCH, methylcyclohexane; (M)THF, (2-methyl)tetrahydrofuran. [b] From the "classical" solvatochromic plot.[510,540,551] [c] From the modified solvatochromic shift *vs* f'' as defined in eq 38; these values are too low, underestimated by the method used.[524] [d] From electrooptical method in emission.[546] [e] From ref 236. [f] From ref 2. [g] From ref 551. [h] From ref 553.

trying to determine the twist angles θ in the solvent-equilibrated emitting CT states. The transition moments in fluorescence were large (often larger than those in absorption) and indicated an important contribution from the dipole coupling of the CT and S_0 states. The longest-wavelength shoulder in the absorption spectrum (see Figure 86), shifting somewhat to the red in polar solvents and was assigned as a CT absorption band,[540] in some compounds clearly seen as a separate band (Figure 88), which made it possible to carry out a full band shape analysis (cf. section X.B). Some exemplary data are collected in Table 15, and the method of resolving of the spectra is shown in Figure 88.

In that way, a self-consistent model is built of *one* polarizable CT state. It involves a CT excitation and varying contributions from the upper LE states and from the ground state. These contributions depend on the changing energy gap between the interacting states, e.g., on the polarity of the medium. The evaluated coupling matrix elements are interpreted in terms of the torsional angle θ, according to eq 32. The main result from the point of view of the molecular structure is that the excited-state relaxation occurs toward *smaller values of* θ.[145,510] There is also some evidence that **26** emits from a less twisted conformation (deviating more from orthogonality) than the sterically hindered **27** or **130**. In the original TICT model, their equilibrium twist angle, $\theta = 90°$, should be the same; the average twist angle depends, however, on the population distribution within the more or less steep potential well.

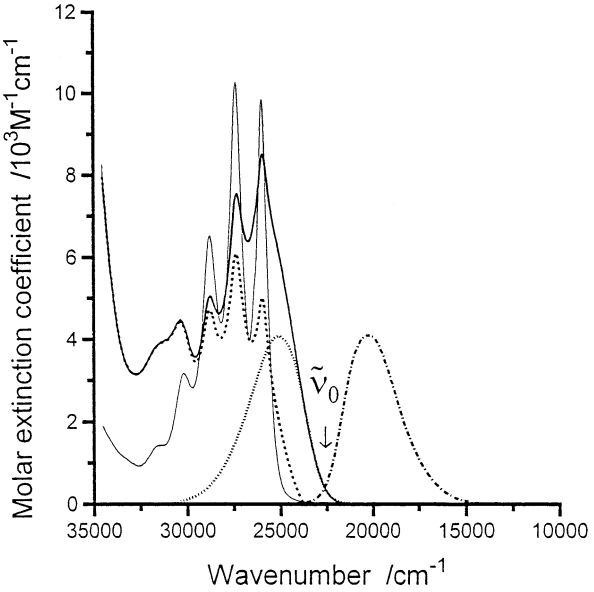

Figure 88. Room-temperature absorption and fluorescence spectra of **127** in dibutyl ether. Thick solid line, absorption; dash−dot line, fluorescence; dotted line, the lowest CT absorption band, separated under the assumption of a mirror relationship between the reduced CT absorption and fluorescence spectra[559] with respect to the crossing point ν_0; dashed line, the anthracene-like $^1\pi,\pi^* \leftarrow S_0$ transition, resulting from a subtraction of the CT band (dotted). The lowest absorption band of anthracene (thin line) is shown for comparison. Reproduced with permission from ref 172. Copyright 1991 Elsevier Science.

With growing polarity of the solvents, the emission rates k_f and the transition moments regularly decrease (Table 15, Figure 89). As a good measure (an internal standard) of the polarity of the media, the authors often use the wavenumber of the CT emission maximum. The fact that the emission becomes more strongly forbidden with growing polarity of the solvent is connected with the growing CT character of the transition. On the basis of their evaluation, the authors find that the coupling matrix element to the ground state diminishes in strongly polar solvent, being lowest in the sterically hindered molecules.[524] This indicates that the average twist angle θ of the emissive CT state increases with solvent polarity and with sterical hindrance. They estimate that the conformation of the excited molecules studied, in particular of **127**, in strongly polar solvents approaches that of the ground state,[524] i.e., close to perpendicularity.[145,542] This is different from the situation in nonpolar media or in the gas phase, where clearly a relaxation to smaller twist angles appears, away from the Franck−Condon conformation.

In a recent subpicosecond transient absorption study of **26** in solvents of different polarity,[560] the rate

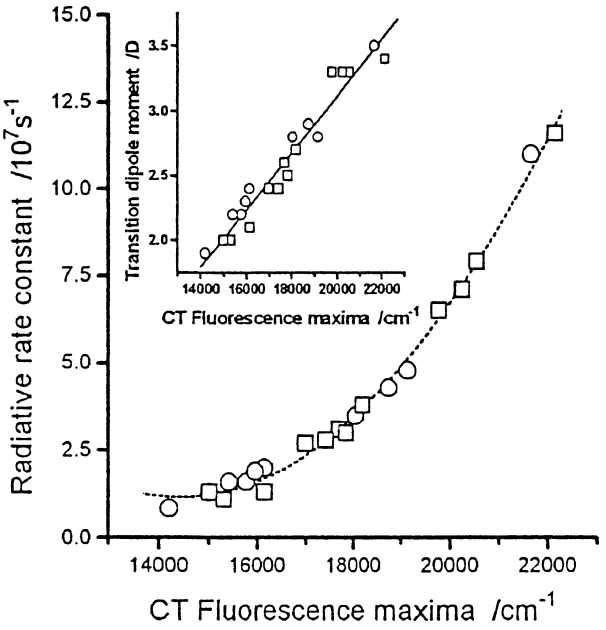

Figure 89. Emission rate constant of the CT fluorescence as a function of the solvent polarity, in a broad range of solvents. Radiative rate constants, k_f, and (inset) the transition moments, M_f, as functions of the spectral position of the CT fluorescence maxima of **127** (squares) and its acridine analogue, **136**. Reproduced with permission from ref 524. Copyright 1998 American Chemical Society.

of transition from LE to CT was shown to strongly depend on the solvent properties. It was generally slower than, or similar to, solvation dynamics. The results were explained by a two-dimensional model involving the ultrafast inertial torsion and the solvation coordinate. The relative contributions depend on solvent polarity and relaxation times (see section VI.G).

2. Acridine as Acceptor

Acridine derivatives, with respect to their excited CT states, behave much like those of anthracene (cf. the preceding section), except that acridine is a much stronger electron acceptor ($E_{1/2}^{red} = -1.54$ V vs SCE in ACN) than anthracene ($E_{1/2}^{red} = -1.95$ V). Most information on the fluorescence and on the excited-state properties, as well as the quantitative interpretation along the lines referred to in section X, comes from a series of recent papers.[145,172,510,524,561] In particular, the longest-wavelength CT band in absorption is more prominent and better separated from the structured bands of the parent ring system in all acridine derivatives than it is in the case of anthracenes.

Among the acridines linked with aliphatic amine donors (**132**−**134**), the most information is known about the morpholino derivative **134**.[561] **132** had to be very carefully treated, as it easily oxidizes to the corresponding *N*-oxide. For steric reasons, all acridine derivatives presented in this section are noticeably pretwisted around the D−A bond. The solvatochromic plots of the fluorescence of these compounds were nonlinear, showing excited-state dipole moments about 14−15 D in strongly polar solvents, and the radiative rate constants in butyronitrile at room temperature were rather low, $k_f = 5 \times 10^6$ s^{-1} (**133**)

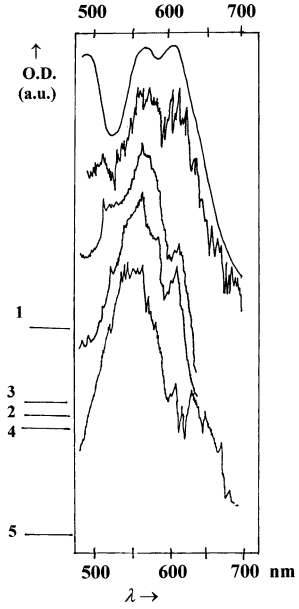

Figure 90. Absorption spectra, from top to bottom: (1) acridine anion radical[562] in DMF, room temperature. Transient absorption spectra of the excited states, excitation with 355 nm laser pulses, fwhm 25 ps: (2) **135** in *n*-propanol, room temperature, delay time $\tau = 60$ ps; (3) **134** in butyronitrile, $T = 193$ K, $\tau = 480$ ps; (4) **133** in butyronitrile, $T = 193$ K, $\tau = 200$ ps; (5) acridine in *n*-propanol, room temperature, $\tau = 100$ ps. At the left side, zero lines are indicated for each spectrum.

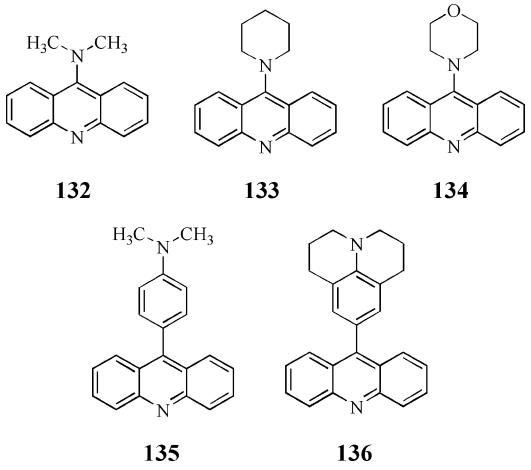

or 1.1×10^7 s^{-1} (**134**).[561] These high values of μ^* and the forbidden fluorescence transition are similar to the TICT states in the aminobenzonitriles. The transient absorption spectra (Figure 90) are compared with the absorption spectrum of acridine anion radical.

These absorption spectra of the excited ^{1}CT state seem to disfavor the perpendicular TICT structures (decoupled donor and acceptor π-electronic subsystems) in the case of N-donors, as in **133** or **134**. Only the transient absorption of **135** (Figure 90), with an anilino donor, is very similar to that of the acridine radical anion.

The interactions contaminating the pure ET character in the real CT states were quantitatively studied for the derivatives with aromatic donors, **135** and its derivatives.[524] The absorption spectra of the

acridine 9-derivatives with an aromatic donor (**135**−**141**). clearly indicate that the lowest transition in

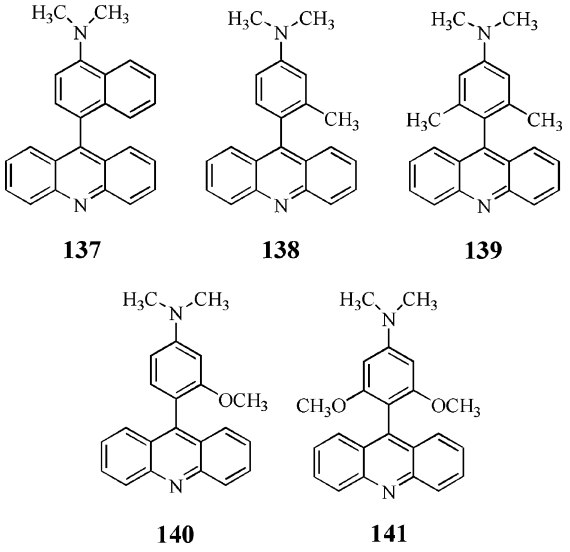

137 **138** **139**

140 **141**

absorption is of CT character: a broad, structureless band, shifting to the red with growing polarity of the medium, diminishing and shifting to the blue with growing steric hindrance (increasing twist angle θ in the ground state) (Figure 91a). The fluorescence band for each of these compounds has a Stokes' shift strongly growing, and an increasing bandwidth, with increasing solvent polarity (Figure 91b). These are also typical signs of a radiative ET in emission.[144] The excited-state dipole moments were found in the range 26−30 D[524] from the solvatochromy of the Stokes' shift, according to eq 13.

From the transition moments in emission, which often somewhat exceed those from the CT absorption, it is evident that the emitting CT state (i) deviates from the $\theta = 90°$ conformation more strongly than the corresponding ground state and (ii) borrows intensity from the upper LE states (which was seen, as in the anthracene derivatives in Figure 86, in the lowering of the absorption of the latter). These two factors were still insufficient: to explain the values of M_f, a coupling of the CT state with the ground state had to contribute, too, with a suitable fraction (see eq 31) of the huge μ^*_{CT} value. The corresponding coupling matrix elements are collected in Table 16. Both matrix elements, V_0(A) and V_1(A), diminish with the growing steric effect of the substituents, i.e., with the approach of the ground-state twist angle θ to 90°. The emission rate constants and, correspondingly, the transition moments dramatically decrease with the polarity of the solvent (cf. the data for **136** in Figure 89). The effect of the polarity of the medium cannot be due solely to the growing energy gap $E_{LE} - E_{CT}$, and it is not counterbalanced by the diminishing energetic distance to the ground state, $E_{CT} - E_G$. It is due to a change of the excited-state equilibrium conformations approaching orthogonality in strongly polar solvents. According to the authors cited,[524] the excited-state conformations are close to those of the respective ground states in strongly polar solutions. Gedeck,[213] however, interprets the solvent

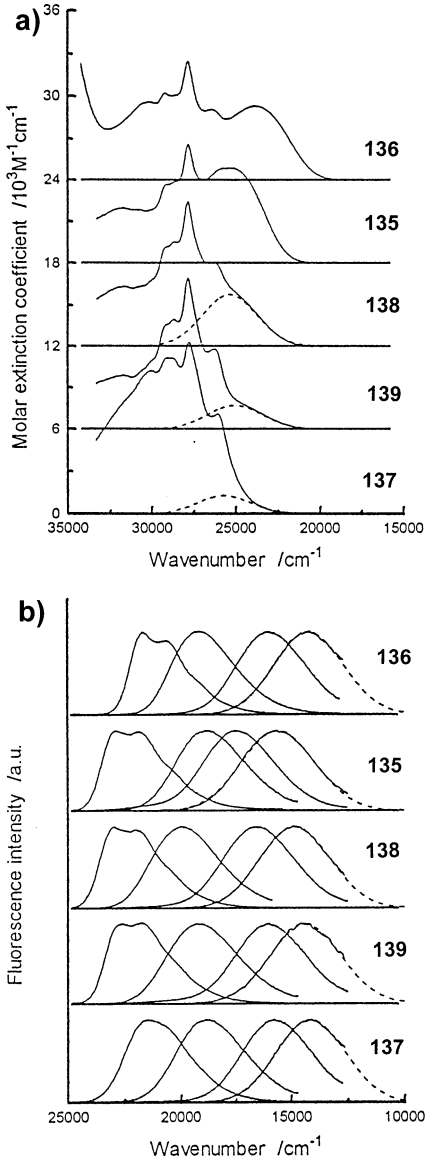

Figure 91. Absorption and fluorescence spectra of 9-(aromatic donor)-acridines **135**−**139**, at room temperature. (a) Absorption spectra in THF, shifted along the *y* axis by steps of 6×10^3. Dashed lines, CT absorption bands, obtained in a similar procedure as shown in Figure 88. (b) Corrected and normalized fluorescence spectra in MCH, butyl ether, THF, and butyronitrile, from left to right, respectively. Dashed lines, extrapolation by numerical fit to the band shape expression (eq 34). Adapted with permission from ref 524. Copyright 1998 American Chemical Society.

polarity and the temperature effect as a changing distribution of the conformers around the torsional angle $\theta = 90°$.

The phenomena observed in these acridine derivatives are fairly general for the whole field of D−A molecules. Stabilization of the CT state with increasing polarity of the medium occurs in parallel with a change of the contributions of the upper states (stabilizing the CT state) and of the ground state (destabilizing the CT state but strongly increasing its transition moment M_f). This state mixing increases with a flattening of the molecular structure, i.e., with the twist angle θ diverging from 90°.

A very interesting case concerns the D−A systems with quinoxaline as acceptor: **142** and **144**, and their

Table 16. Derivatives of Acridine, 135−141: Coupling Matrix Elements between the CT State and the Ground State, V_0, or the Upper LE Singlet State ^1L_a, V_1, Evaluated from the Absorption (A) or Fluorescence (F)[a]

compd	V_0(A)[a]/ eV	V_1(A)[a]/ eV	θ_{A-D}(G)[b]/ deg	C^D_{HOMO} [c]	V_0(F)[d]/ eV
136	0.18	0.21	64	0.42	0.15
135	0.20	0.12	68	0.44	0.22
140	∼0.15	∼0.09	80	0.48	0.16
138	∼0.12	∼0.06	80	0.45	0.14
141	∼0.15	∼0.06	82	0.52	0.14
139	∼0.06	∼0.06	82	0.46	0.10
137	∼0.08	∼0.02	84	0.31	0.12

[a] All data from ref 524. [b] From the transition moment M_a of the room-temperature CT absorption band in THF solution and the effect of *borrowing* from the acridine-like LE state. [c] Twist angle in the equilibrated ground-state conformation, computed with the AM1 method. [d] $2p_z$ LCAO coefficients for the HOMO of the donor molecule, at the atoms forming the D−A bond. For acridine, position 9, $C^A_{HOMO} = 0.38$, $C^A_{LUMO} = 0.48$. All values computed with the AM1 method. [e] From the transition moment of fluorescence in benzonitrile as solvent, according to an approximated form of eq 31.

models **143** and **145**, planarized by an S-atom bridge.[563] The spectra of both groups of molecules are

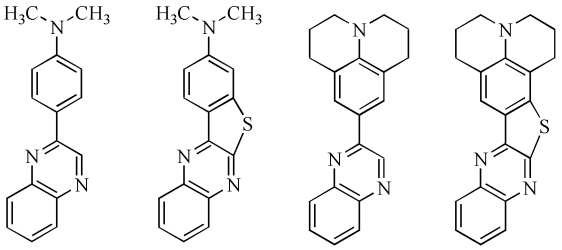

142 **143** **144** **145**

very similar, with the solvent shifts indicating a CT character both in absorption and in fluorescence. In fluorescence, they all reveal a single emission band, structured in MCH and broad and unstructured in THF, strongly red-shifted with increasing polarity of the solvent. The great similarity in the behavior of **142** and **144** proves that the rotation of the $-NMe_2$ group is not involved in the CT. The HOMO and LUMO orbitals of **143** indicate some delocalization of charge, but with a pronounced localization on the donor group in the HOMO and on the quinoxaline acceptor in the LUMO; the sulfur bridge is not involved. The dipole moments of the CT states are found to 18−19 D for **143** and **145**, but somewhat larger (21−22 D) for the nonrigid compounds **142** and **144**. The transition moments in fluorescence are very high, $M_f \approx 4-4.5$ D, similar to those in absorption, and independent of the solvent polarity. Here again, there is a small difference: the M_f values are within 3.8−4.2 D for the flexible compounds, and 4.1−4.5 D for the rigid ones. These compounds behave totally opposite to the TICT model. They clearly demonstrate that large aromatic systems can form planar, nearly full CT states (PICT). In these cases, the torsional motions, with deviations from the full CT structure, diminish somewhat the μ^*_{CT} and the M_f values.

3. Naphthalene as Acceptor

(Dimethylamino)naphthalenes exhibit only a single fluorescence, which is considerably red-shifted with increasing solvent polarity.[564] They exhibit a strong nonradiative relaxation channel in alkane solvents which disappears in polar solvents and was ascribed to internal conversion linked with the difference of the amino group twist angle between the ground and the excited states, the conformation in the S_1 state implied to be planar.[565] Theoretical calculations did not exclude the relaxation of excited **146** to a TICT state in highly polar solvents, due to the relatively small energy gap between the S_1 (LE) and the TICT states, 0.3 eV, with a $\mu^* = 10$ D (calculated with INDO/S[566]). DFT/SCI calculations indicate that the TICT state of **147** ($\mu^* = 16$ D) is situated 0.7 eV higher than the planar S_1 LE state, but the solvation is estimated to stabilize it as the lowest excited state.[567]

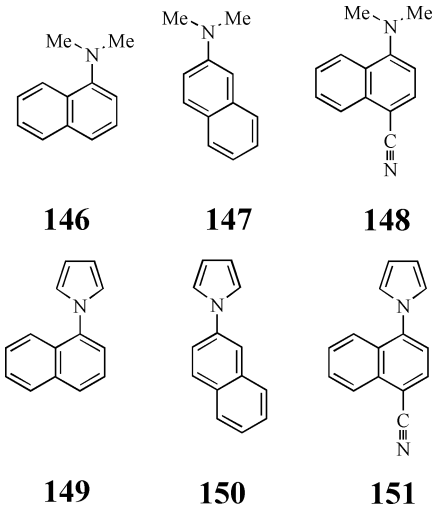

146 **147** **148**

149 **150** **151**

Introduction of an acceptor substituent into the naphthalene ring brings the CT state into close proximity to or below the LE state. In the following, we briefly report on the fluorescence behavior of the derivatives with a −C≡N, >C═O, or $>SO_2$ substituent. **148** emits a dual fluorescence, which was interpreted in terms of the TICT model.[568−570] The calculated energy gap between the LE and the TICT state is only 0.13 eV; thus, the TICT state formation may be easy in polar solvents.[566] The short-wavelength emission, moreover, is composed of two mutually perpendicularly polarized transitions.

The N-pyrrolo donor group, as compared to the $-NMe_2$, causes an increase of the dipole moment in the ground state of substituted naphthalenes, but a decrease in the LE state. Due to the orbital symmetry of the pyrrolonaphthalenes, a CT state may appear already in the planar conformation of the molecule, similarly to the case of the pyrrolobenzene derivatives discussed below (section XI.A.5). However, due to the nonperfect local symmetry of the naphthalene moiety at the donor position (only approximately symmetric or antisymmetric with respect to the plane perpendicular to the aromatic ring and containing the D−A bond), an orbital localization can be full only in particular, favorable cases. Calculated planar CT states are energetically higher than the TICT state.[566]

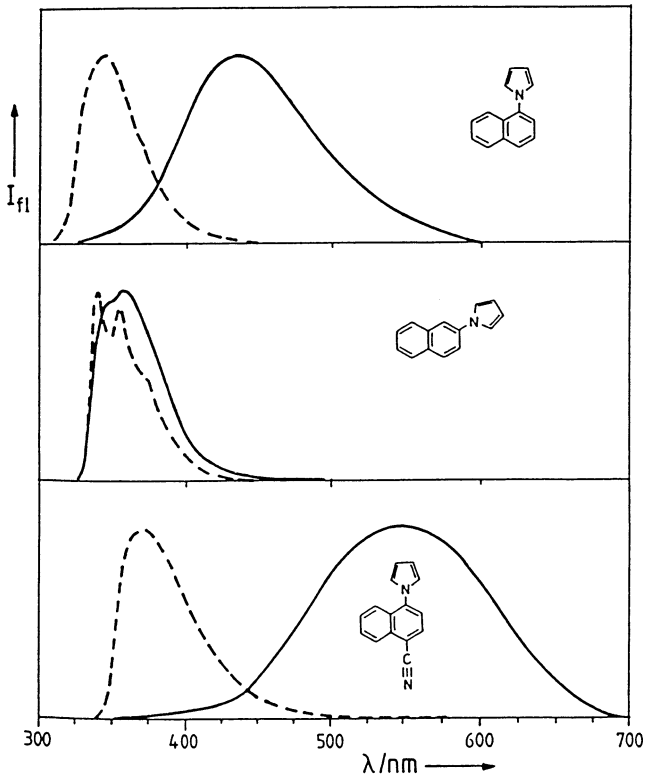

Figure 92. Corrected fluorescence spectra of pyrrolonaphthalenes in *n*-hexane (dashed curves) and in ACN (solid curves). Reproduced with permission from ref 566. Copyright 1993 Elsevier Science.

In contrast to **150**, **149** shows a very strong solvatochromic red shift with increasing polarity of the solvent (Figure 92).

The cyano derivative **151** emits a typical CT fluorescence (Figure 92) which was interpreted in terms of the TICT model,[113] analogous to the case of **148**. The calculation supports this description; in the free molecule, the TICT state lies only 0.46 eV higher than the planar S_1 (LE) state, so that in solution the TICT state formation should be easy. The planar CT state is higher lying and cannot become the emitting state, even in strongly polar solvents.[566]

In the rigidly linked naphthalene derivatives **3** and **4** (section I.A),[18] the donor and acceptor units are separated by saturated rigid spacers and are not very flexible. These compounds model structurally nonrelaxed *distant* exciplexes, with very high μ^* values. Both compounds emit only a single fluorescence band in every solvent under study, strongly red-shifting with increasing solvent polarity.[18]

PRODAN (**152**) has been the subject of many studies during the past two decades, due to its high sensitivity to the environment, which makes it useful as a fluorescent probe in biochemistry,[571] similarly to **153** (DANCA)[572,573] and some other derivatives with long alkyl chains used in the studies of membranes.[574,575] **152** emits an intense, single, broad fluorescence, strongly red-shifted with increasing solvent polarity. According to theoretical calculations,[576] **152** is probably planar in the ground state, while its twisted excited conformer emits a CT fluorescence in alcohols. In nonpolar solvents, the fluorescence occurs from the LE state, as inferred

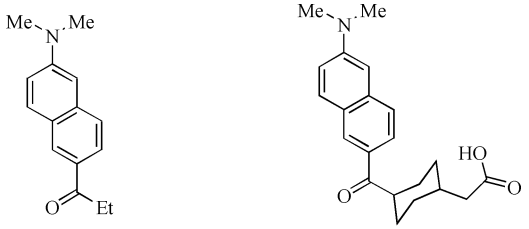

152 **153**

from the high-pressure effects on fluorescence.[555] It was also reported that the fluorescence in *n*-butanol or glycerol has two contributions, with that from the LE state increasing with pressure. From phase modulation fluorescence spectroscopy, it was deduced that the spectral relaxation is a multistep process in *n*-butanol at 218 K.[577] Steady-state (Figure 93) and time-resolved fluorescence studies of **152** in *n*-butanol led to the conclusion that the initially excited state undergoes relaxation to an energetically lower CT state, with both bands considerably overlapping.[578]

Though numerous papers report applications of PRODAN and similar compounds as fluorescent probes,[574,575] its photophysics seems to be far from clarity, because of a lack of sufficient experimental evidence, mainly convincing model compounds or

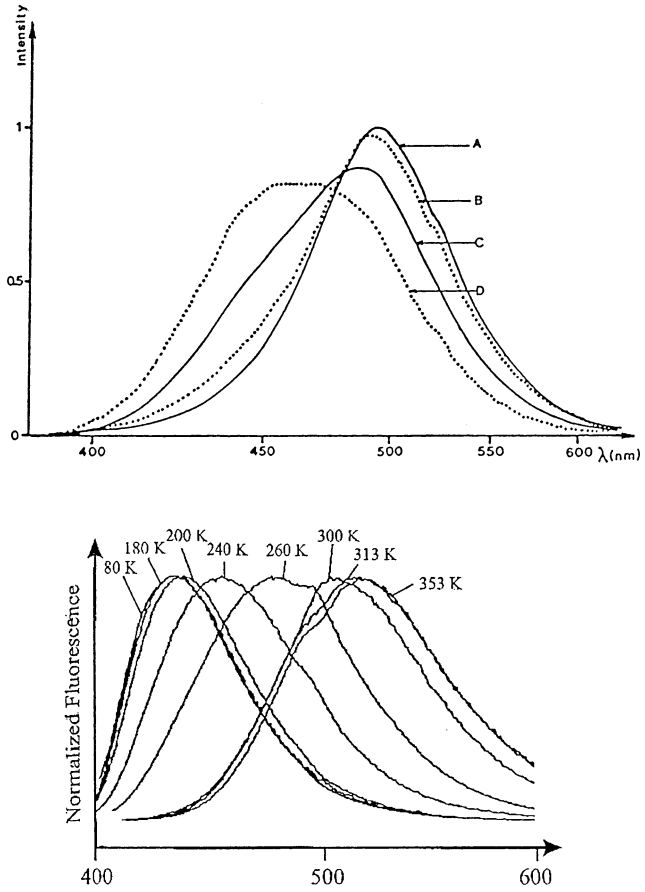

Figure 93. Fluorescence spectra of **152** as a function of temperature. (Top) In *n*-butanol at (A) 249, (B) 232, (C) 211, and (D) 198 K. Adapted with permission from ref 578. Copyright 1978 Elsevier Science. (Bottom) In glycerol. Adapted with permission from ref 583 by permission of Dr. A. B. J. Parusel.

transient absorption data. Semiempirical[567] as well as ab initio calculations[567,579] arrive at an explanation of the fluorescence properties of PRODAN (**152**) in terms of the TICT model. The low-lying excited state in the planar (ground-state) geometry has, according to DFT/SCI calculations, significant CT character, but the formation of an intramolecular CT state by twisting of either the $-NMe_2$ (N-TICT) or the $-(C{=}O)Et$ group (O-TICT) leads to a large increase of the dipole moment. Similarly to the case of carbonyl analogues of **1** (cf. section III.E.3, Scheme 5), the N-TICT appears at somewhat lower energy than the O-TICT state. Experimental values of μ^* for the emitting CT state are within 10 and 12.5 D.[580−582] According to theoretical calculations, the planar S_1 π,π^* state of **152** is of CT character ($\mu^* = 12.6$ D[576] and 8.5−16 D,[567] dependent on the approximation used). For the TICT state, the theoretical estimates[567] are much higher, $\mu^* \approx 18-23$ D for the N-TICT and 22−31 D for the O-TICT, the N-TICT state in a free molecule lying about 0.5 eV above the planar S_1 (CT) state.

The excited-state dipole moment of PRODAN (**152**) was determined by the transient dielectric loss method as $\mu^* \approx 10$ D in benzene and dioxane.[584] The authors interpret this value as evidence against the pure CT character of the emitting state (the μ^* value is too low for an N-TICT or O-TICT), concluding that its structure is not very different from that in the ground state, while the large solvent shifts are rather caused by specific solvation, at least in the weakly polar solvents investigated. Some members of the family of (arylamino)naphthalenesulfonates (ANS) are highly emissive in nonpolar solvents but strongly quenched in very polar solvents, especially in water, and are applied as biological sensors (e.g., for the estimation of the protein binding site polarity).[585−587] Kosower et al. studied the nature of the excited states and the solvents effects of this group of compounds, **154**,[585] **155**,[586,588,589] and **156**[590] and their derivatives.

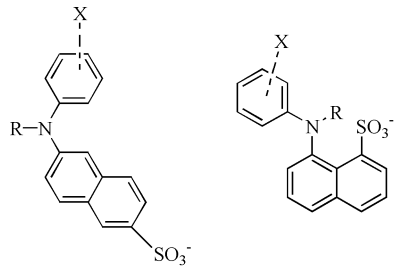

154

155

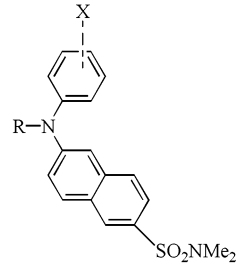

156

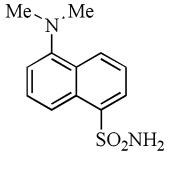

157

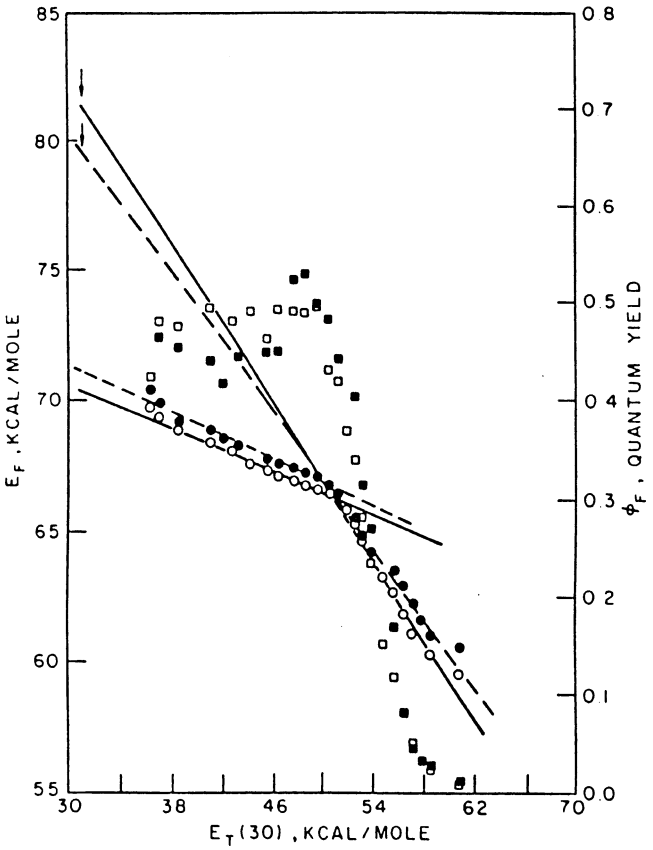

Figure 94. Plot of emission energies, E_F (in kcal/mol), and fluorescence quantum yields, φ_F, of **154** (solid symbols, R = H; open symbols, R = CH_3) vs the solvent polarity parameter, $E_T(30)$, in dioxane−water mixtures. Points, E_F; squares, φ_F. Adapted with permission from ref 585. Copyright 1978 American Chemical Society.

A single fluorescence band was usually observed, but the time-resolved measurements clearly reveal two different emission bands, with a mother−daughter relationship, $^1LE \rightarrow {}^1CT$.[591] Plots of the emission energy or of the quantum yield vs $E_T(30)$ show a dramatic change of their slopes at $E_T(30) \approx 50$ in all cases under study (Figure 94).[437,585,586,588−590,592−594]

On the basis of the analysis of the emission energies and quantum yields as functions of the Hammett substituent constants σ, the authors suggested in their early papers[585,586] the existence of two ^1CT states, in addition to the primary excited ^1LE state. The two states should have differed in the extent of conjugation, depending on the substituent on the nitrogen atom in **154**−**156** (R = H or R = CH_3). This difference between the two groups of compounds seems to be tacitly dropped in subsequent papers.[84,85] The nature of the previously proposed two forms of the ^1CT state (Figure 95)[595] is then related rather to a specific relaxation of the secondary amine H-bonded to the solvent.[84]

Bimodal kinetics of the CT process (in the picosecond time range) was found for **156**.[437] The decay times of the ^1LE state of **156** correlate with the longest relaxation times, τ_L, of the linear alcohols, the points for **156** lying on the same correlation as those for **1**.[441] The similarity of both systems is related not

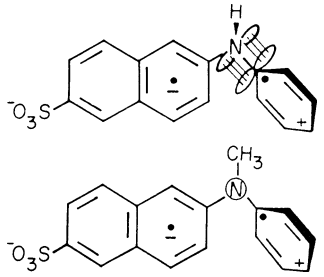

Figure 95. Two structurally different forms, postulated for the ^{1}CT state of **154**. In the upper structure (R = H) the n_N orbital is conjugated with the phenyl ring; in the lower structure (R = CH_3) the n_N orbital is decoupled from the phenyl ring but conjugated to the naphthyl π-electronic system. Adapted with permission from ref 585. Copyright 1978 American Chemical Society.

only to the alcohol solvent dynamics controlling the rate of the CT processes; it extends also to the structural changes involved. In both systems, **1** and **156**, the relaxed CT state has the donor nitrogen atom (amino, *resp.* anilino nitrogen) decoupled from the acceptor π-electronic system (most probably, orthogonal to it).

The radiative rate constants decrease with increasing solvent polarity by approximately an order of magnitude, below 10^7 s^{-1}, whereas the rate constants of nonradiative deactivation grow in the same range by ca. 2 orders of magnitude, to about 10^9 s^{-1}. It is most remarkable how sensitive the quantum yields of the CT states are to the polarity of the medium (Figure 94, squares). CT fluorescence intensity is used also, e.g., in the application of **153** as a probe for polymers.[596]

4. Purine as Acceptor

Among the purines, several alkylamino derivatives of adenine, one of the nucleic acid bases, show dual fluorescence,[597−599] even in nonpolar solvents (Figure 96). Adenine itself exists in the ground state mainly as the 9H tautomer. It was shown,[600] however, that its fluorescence is mainly emitted by the 7H tautomer (Scheme 11). The phototautomerization in the excited

Scheme 11

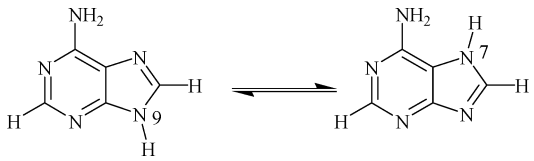

state can be protic solvent- or dimerization-assisted.[601]

Therefore, the authors[597,598] use in their study the derivatives of the 9H tautomer stabilized against tautomerization by a substitution at the N9 position, like in adenosine, **158**. The authors ascribe the lower energy band, A, to a CT or TICT state, and the high-energy band, B, to a local excitation, mostly within the purine rings. The dual fluorescence is similar to that of **1** in some respects, whereas in others it differs. Among the similarities one can count, e.g., the small radiative rates, k_{f_A} being of the order of 10^6 s^{-1}, and the low transition energy for band A. The latter is markedly lower for tertiary amines than for the secondary ones, along with the change in the oxidation potential (**159** or **161** vs **160** or **162**, Figure 97, similarly to **52** vs **16**). There seems to be a

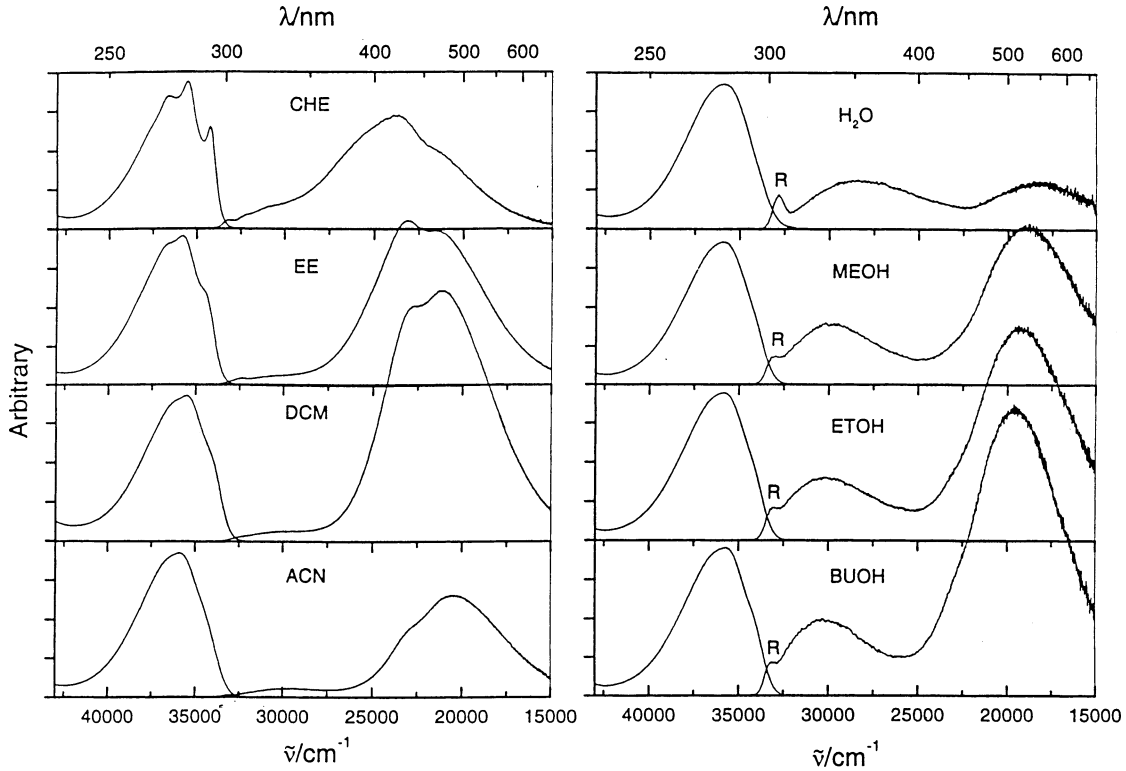

Figure 96. Absorption and fluorescence spectra of **162** in aprotic solvents (left panel; CHE, cyclohexane; EE, diethyl ether; DCM, CH_2Cl_2) and in protic solvents (right panel; MEOH, MeOH; ETOH, EtOH; BUOH, BuOH). Intensities in each panel can be directly compared. R = Raman scattering from the solvents. Adapted with permission from ref 598. Copyright 1999 American Chemical Society.

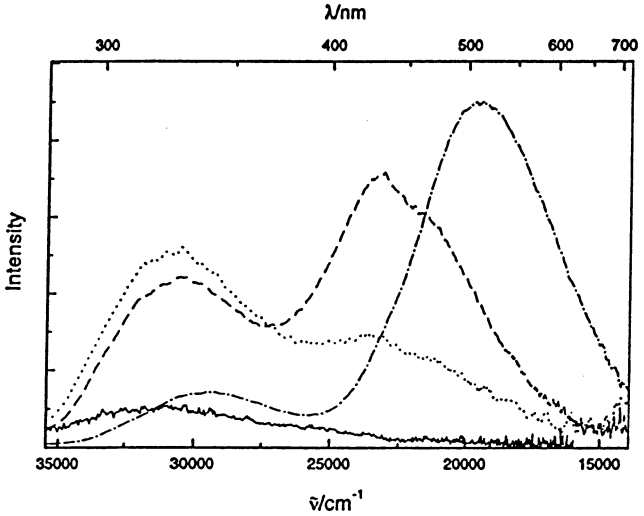

Figure 97. Room-temperature fluorescence spectra of **160** (dash−dot curve), **159** (dotted curve), and **161** (dashed curve) in ACN and of **158** in H_2O (solid curve). The intensities of the emissions are arbitrarily scaled. Reproduced with permission from ref 598. Copyright 1999 American Chemical Society.

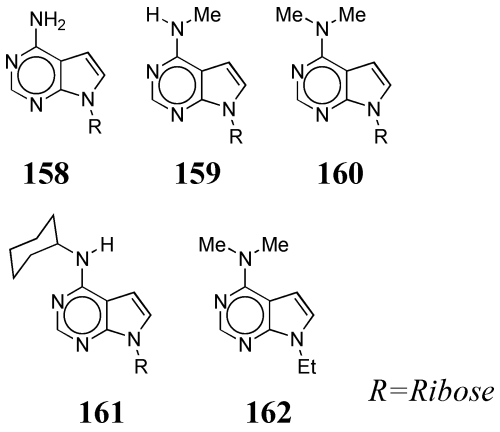

sensitivity to the twist angle of the donor around the C−N bond (compare **159** with **161** in Figure 97). Band A undergoes quenching in protic solvents (cf. section IV.C.1). It is practically independent of temperature, whereas band B is strongly thermally quenched in the range 77−300 K (apparently recalling the kinetic regime in the TICT model, cf. Figure 68).

Unlike in the case of **1**, the dipole moments in the ground and CT states are mutually nearly perpendicular, and the solvatochromic shift, proportional to $-2\mu_A(\mu_A - \mu_G)/a_o^3$, in aprotic solvents corresponds to a value of $\mu_A \approx 9.5$ D, which is too small for a pure ET state. In protic solvents (alcohols), however, the emission energies correlate on a different plot, with about 3 times larger solvatochromic slope. The resulting dipole moment is about 16−17 D for the hydrogen-bonded excited state — such as can be expected in a full CT state.

The efficient thermal quenching of the locally excited state is found, however, not to be ascribed to the B* → A* process (or not only to it), as such thermal quenching seems to be characteristic of the local excitation of the adenine chromophore,[602] also in the absence of the long-wavelength emission band, e.g., in **158** (Figure 97). A very important experimental evidence, casting doubt on the analogies with **1**, seems to be the lack of any clear dependence of the intensity ratios, φ_A/φ_B, on the polarity of the aprotic solvents. Moreover, the long-wavelength band reveals some structure in aprotic solvents (cf. **162** and **161**, Figures 96 and 97, respectively). The authors conclude that the two emitting states are populated from a common Franck−Condon precursor state, and then independently decay to the ground state.[598]

It is reported,[599] however, that on lowering the temperature, $d \log \varphi_B/d(1/T) \approx -d \log \varphi_A/d(1/T)$ (within the limits of error), though the rise of φ_B appears at much lower temperatures than the decrease of φ_A. The branching model proposed by Albinsson et al.[598] for **149** would correspond to a different temperature dependence. Parusel et al.[599] instead suggest the precursor−successor mechanism, e.g., LE → TICT. The shift in the temperature ranges of the φ_A and φ_B behavior can be explained by a fast radiationless deactivation of the LE state, competing with the ICT state formation. Such a deactivation process is characteristic of nucleic acid bases.

We think that the hydrogen bonding on one of the purine ring N atoms in protic solvents increases the acceptor strength and results in a photophysical behavior typical for the CT states.[603]

Dimethyladenine (**160**, R = H) can tautomerize like adenine in Scheme 11. It emits two fluorescence bands, the "normal" one at about 330 nm, and a CT band, Stokes-shifted by 7000−9000 cm^{-1}. The apparent $\mu^*_{CT} = 11$ D (from solvatochromic shifts) and the fluorescences are very similar to those of **160**; hence, the emission probably originates from the 9H tautomer, in contrast to adenine.[601]

5. Pyrroles as Donors

Several D−A molecules, derivatives of *N*-phenylpyrrole (**163a**), have been studied. In contrast to the

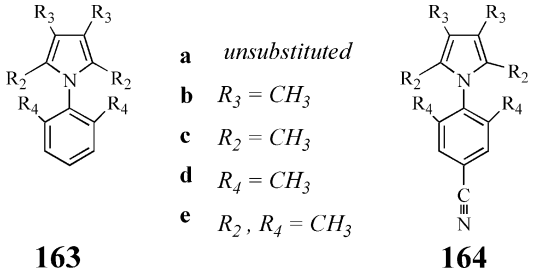

dialkylamino donors, with the pyrrole donor a CT fluorescence band appears, even for unsubstituted benzene as the acceptor. Already **163a**, with the donor ionization potential higher than that in the methyl-substituted derivatives (**163b**,**c**,**e**) and the electron affinity of the acceptor lower than that in the cyanophenyl derivatives (**164a**−**e**), shows a long-wavelength tail in the fluorescence spectrum of its solution in acetonitrile (Figure 98). This is due to the relatively low ionization potential of pyrrole, 8.23 eV (a_2 orbital) and to the fact that pyrrole as the donor retains its already planar structure (sp^2 nitrogen) on ionization.

Table 17. Photophysical Properties of Some D−A Compounds with Pyrrole as the Donor: Excited-State Dipole Moments, μ^*_{CT}, from Solvatochromic Shifts, and Ground-State Twist Angle, θ_G, Estimated from Photoelectron Spectroscopy and from the Ground-State Dipole Moments

compd	μ^*_{CT}/D	solvent	$\nu_f^{max}/10^3$ cm^{-1}	ϕ_f	τ_f/ns	$k_f/10^6$ s^{-1}	θ_G[c,d]/deg
163a[e]	(14.1)[a]	HEPT	37.3	0.27			32
		ACN[e]	29.4[f]				
163c[c]		ACN	23.7				62
163d[c]		ACN	27.4				81
163e[c]		ACN	24.1				∼90
164a[b]	22	HEX	28.7	0.028	2.42	11.6	∼30
		ACN	20.7	0.036	8.20	4.3	
164b[d]		HEX	28.0		2.5		27
		ACN	19.8		5.1		
164c[b]		HEX	23.8	0.006	2.9	1.9	50, 70, 48[b,j]
		ACN	18.9	0.014	10.7	1.3	
167[g]	($\Delta\mu$ = 12.3)	HEX	29.4	0.22			
		ACN	20.8	0.02			
168[b]	22[b]	HEX	30.1	0.033	1.36	24.1	
		ACN	20.4	0.029	5.90	4.9	
169[h]	17.2	HEX	23.4	0.015	7.4	2.0	
		ACN	19.6	0.018	16	1.15	
170[h]	16.3	HEX	18.6	0.012	13.6	0.9	
		ether[i]	17.2	0.004	5.5	0.8	

[a] Reference 113. [b] Reference 605. [c] Reference 606. [d] Reference 168. [e] Reference 610. [f] At ν_{exc} = 33 300 cm^{-1}; with ν_{exc} = 37 300 cm^{-1}, an intense (ϕ = 0.33) fluorescence appears, ν_{max} = 32 200 cm^{-1}. [g] Reference 273; data obtained with ACN as solvent refer to the long-wavelength band. [h] Reference 612. [i] Unobservable in ACN. [j] From the absorption coefficients: $\epsilon/\epsilon_{ref} = \cos^2\langle\theta\rangle$.

The absorption spectra of the derivatives of **163** and **164** show no significant changes in solvents of increasing polarity. The solvatochromic effect in fluorescence, however, is rather large, indicating a high charge-transfer character of the emitting state (Figure 98). In the case of **163a**, the CT emission is seen in the form of the long-wavelength tail and has to be separated from the LE fluorescence.

Some photophysical characteristics of the pyrrole derivatives are collected in Table 17. The excited-state dipole moments (Table 17) correspond to a full ET from the pyrrolic nitrogen to the center of the phenyl ring (**163a**), or still farther toward the acceptor substituent (**164a**, **168**). The radiative rate constants are very low, of the order of 10^6 s^{-1}, similar to those of the typical TICT states. However, except for **168** and **164a**,[604] such low values of k_f are found also for the solutions in nonpolar hexane. The k_f values are nearly constant in a broad temperature range (**164a**) or rise slightly with increasing temperature (**168**).

Similarly to the TICT states (cf. section III.H.1, Figure 56), alcohols markedly quench the fluorescence, increasingly with their proton-donating ability. **168** is much more strongly quenched than **164a**.[605] One can infer that the reaction site for the proton-donating quencher is located at the acceptor substituent (−C≡N, −COOR), which bears much of the negative charge in the CT state.

The absorption seems to lead primarily to the less polar ("LE") state. Only in the pretwisted compound **164c**, a long-wavelength shoulder appears in the absorption spectrum in hexane and is tentatively assigned to a radiative absorption transition leading directly to the CT state.[605]

Discussion of the conformation of the CT state in this group of molecules differs from that in the case of **1** because of the special orbital symmetries. The pyrrole donor orbital, HOMO, is antisymmetric with respect to the plane perpendicular to the ring, i.e., it has a nodal plane on the pyrrolic nitrogen atom, whereas the benzonitrile acceptor orbital, LUMO, is

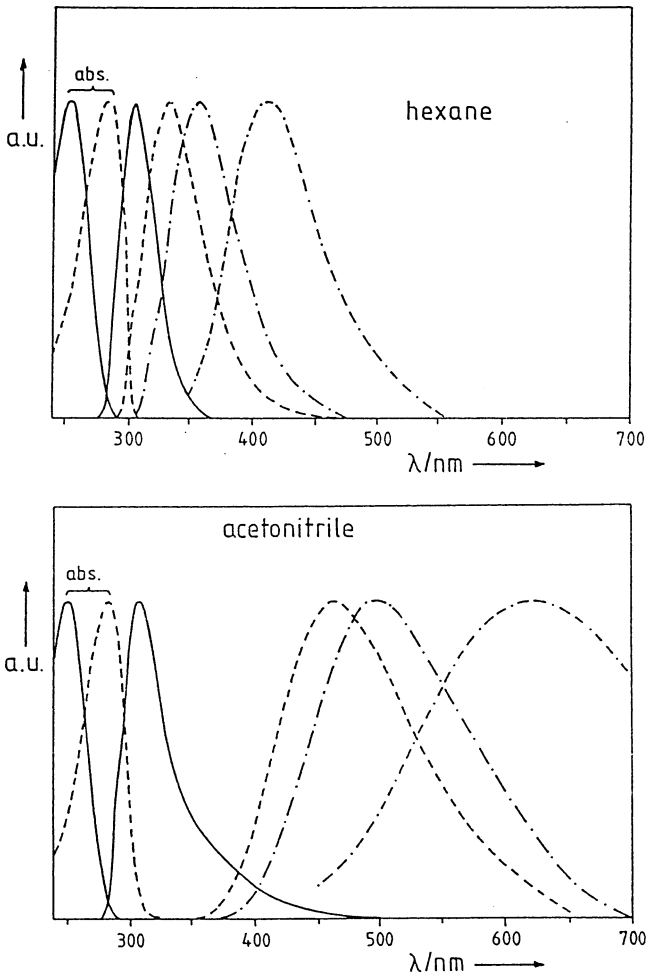

Figure 98. Absorption and fluorescence spectra of **163a** (solid curve), **164a** (dashed curve); **164b** (dash−dot curve), and **164c** (dash−dash−dot curve), (a) in *n*-hexane and (b) in acetonitrile.[168]

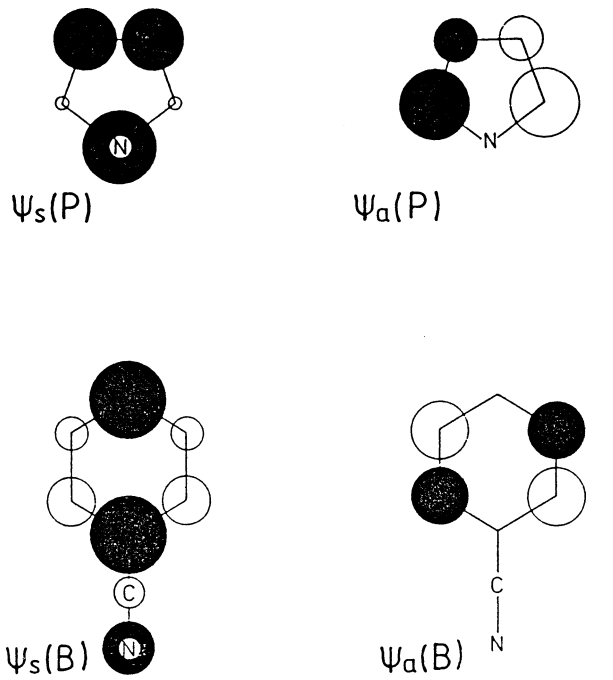

Figure 99. The two highest occupied orbitals of pyrrole (P) and the two lowest unoccupied orbitals of benzonitrile (B). Coefficients calculated with the CNDO/S approximation.[168]

symmetric (Figure 99). Between twist angles of 0° and 90°, the C_{2v} symmetry of the molecules is reduced to C_2, but the orbitals retain their different symmetries, belonging to the *a* and *b* representation, respectively. Therefore, a small overlap condition can be met *at every twist angle*, including the coplanar conformation.[11,113,606] Strong charge separation can thus occur, even without twisting. According to calculations, the CT state is the lowest one for both planar and perpendicular conformations, with a slight preference for the planar arrangement in the early calculations[168] but a clear preference for the twisted structure in more recent ones.[609] Also, an ab initio study resulted in a low-lying twisted charge-transfer structure.[504] Recent ps-IR results indicate that the two subgroups are decoupled in the CT state.[516]

The fluorescence rate constant, k_f, is larger for the derivative **164a**, initially close to planar, than that for the more pretwisted **164c** (in the ground state, Table 17), although in both cases a pure CT state should be the emitter in polar solvents.[605] It is possible that this difference in k_f is linked to the fact that the conformations of the CT states of these two molecules differ, although the theoretical calculations predict a similar TICT conformation (vide infra).

At room temperature, only one unstructured emission band is observed in polar solvents. The emission spectra of **164a** and **168** in hexane differ from those in polar solvents; there appears a trace of a vibronic structure, and the k_f values are relatively high (Table 17). Upon cooling, the structured part in the spectrum diminishes, and at low temperature only the unstructured long-wavelength emission remains.[605] This can be interpreted as evidence for dual emission from a CT state and a slightly higher-lying LE state, even in the case of nonpolar solvents for **164a** and **168**. In polar solvents (specially in rigid media), a well-separated dual fluorescence appears, with a second, spectrally separate short-wavelength band emerging.[605] The relative intensity of both emissions depends on the temperature and on the excitation wavelength. In rigid media, the LE emission (more allowed transition) is thermally activated, the CT state evidently lying somewhat *lower* than the LE state, similarly as in liquid solvents. Above the melting point of the polar solvents, only the red-shifted, forbidden CT emission is seen. Probably the conformational change lowers the energy of the CT state, and the reorganization of the solvent additionally increases the energetic distance between the two states. The origin of the "LE" state can be sought in the orbitals of the same symmetry, e.g., Ψ_s(B) and Ψ_s(P) (Figure 99), which would rather prefer the coplanar conformation, for its high orbital overlap,[168] than the twisted conformation with a much lower d-type overlap.[113] With respect to the excited-state structures, one can say that the pyrrole ring remains probably planar, with no pyramidalization at the N atom, and that the behavior of **164a** with respect to anionic quenchers hints at a distribution of the positive charge over the entire pyrrole ring, instead of being located on the N atom, as in **1**.[351] Recent jet results indicate[607] that **163a** is somewhat twisted in the ground state (∼40°) and becomes more planar in the LE state (∼20°); the barrier height for internal rotation at 90° is much higher in the S_1 state of the free molecule than in the S_0 state. Ab initio calculations on the CASPT2 level[608] confirm the presence of low-lying excited CT states with an energetic preference for the perpendicular conformation, probably populated in polar solvents. Another theoretical calculation, using the DFT/MRCI approach,[609] indicates the presence of a CT state at a nearly planar conformation of **163a** and **164a**, along with the TICT minimum. The latter appears in **163a** only in polar solvents, the minima being separated by a considerable barrier. In **164a**, the calculated TICT conformation is energetically the most stable one already in the free molecule.

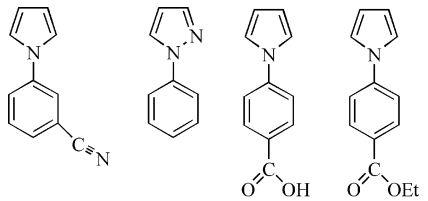

165 **166** **167** **168**

Sarkar and Chakravorti investigated **163a** and **166**.[610] They found also dual fluorescence of **163a** in polar solvents, leaving doubts, however, in their description of the decay kinetics and excitation spectra. In the mixed solvent ethanol−water, the long-wavelength fluorescence was assigned as emission from aggregates appearing at water concentration ∼40%. This emission has an excitation spectrum matching that of the LE emission. Addition of β-cyclodextrin to aqueous solution results in the appearance of the LE emission only, which is ascribed to the splitting of **163a** aggregates and to the nonpolar

character of the CD cavity.

166 emits from a definitely non-CT state, which is ascribed to the higher ionization potential of pyrazole than that of pyrrole.[610] Dual fluorescence is found for **167** in polar solvents,[273] but the conclusions leave some doubt, as the authors do not take into account the possibility of protolytic dissociation of the acid.

165 displays, similarly to **164a**, a broad and strongly red-shifted fluorescence in polar solvents.[611] In a supersonic jet, the van der Waals complex **165** + CH_3CN (1:1) was identified; it emits only the normal fluorescence. With increasing acetonitrile vapor pressure, in the 1:*n* complexes, a red-shifted emission appears, assigned to a TICT state.[611]

Recently, spectroscopic and theoretical studies on dimesitylpyrroloboranes with different ground-state twist angles were reported.[612] These compounds are closely related to H_2N-BH_2, which has been studied theoretically as a model structure for the TICT state.[505] For pyrroloboranes, **171** was used as the model in the ab initio large-scale CI computations.[612]

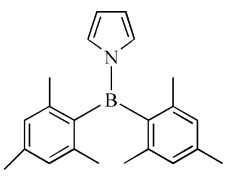

169

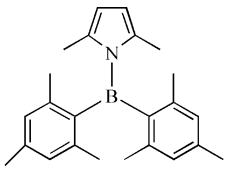

170

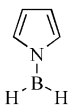

171

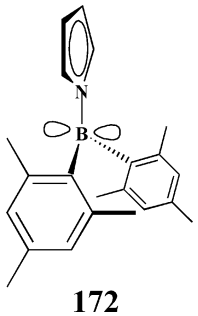

172

Literature data indicate the structure of the ground state of **169** to be analogous to that resulting from theoretical calculations of **171**. It has an almost planar pyrroloborane unit; the bulky mesityl groups are, however, twisted by 50−90° with respect to that plane (cf. **172**).

The absorption and fluorescence spectra (Figure 100) reveal enormous Stokes' shifts and a much more red-shifted emission of **170** than that of **169**. Two methyl groups in the pyrrole ring undoubtedly form a steric hindrance. The mesityl rings of **170** are twisted more than those in **169**, and the pyrroloborane unit becomes nonplanar. In particular, the ionization potential of the pyrrole donor, lower by 0.7−0.8 eV,[168,606] shifts the CT emission of **170** in hexane to the red by 0.6 eV with respect to that of **169**.[612] Similarly, in the absorption spectrum **170** displays a weak shoulder on the red edge, observed also in the excitation spectra, being obviously the direct CT ← S_0 absorption, which is hidden in **169** under a much stronger main absorption band.

The fluorescence radiative rates, k_f, of **169** are very low (still lower, by a factor of ∼2, are those of **170**;

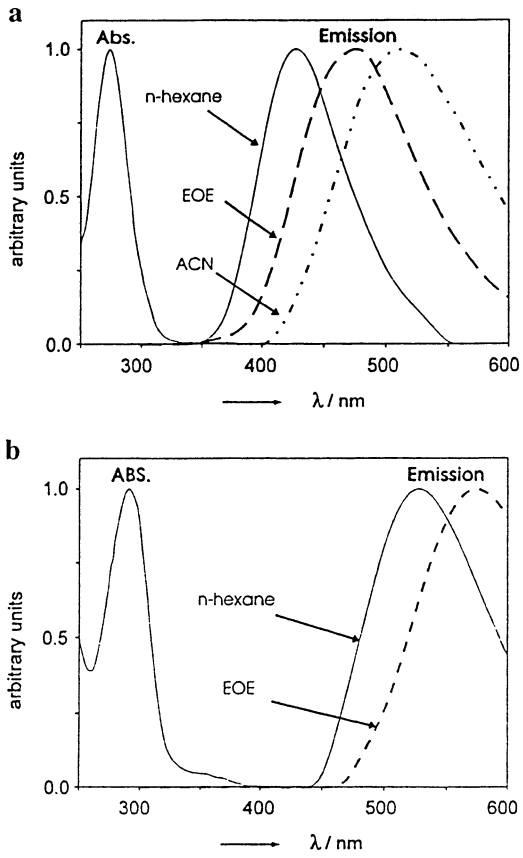

Figure 100. Absorption and fluorescence spectra of (a) **169** and (b) **170** in several solvents at room temperature. EOE = diethyl ether. Adapted with permission from ref 612. Copyright 1999 American Chemical Society.

cf. Table 17), nearly independent of temperature and of the solvent polarity.

The structure of the excited CT state is not yet clear. The dipole moment of the model compound **171** was calculated as $\mu^* \approx 7-8$ D for the S_1 state (theoretical charge separation at the N−B distance, increasing in S_1 to 1.6 Å), nearly the same value in the 90° twisted conformation and in the planar conformation (zero orbital overlap at every twist angle). The experimentally found μ^* values for **169** and **170** are, however, much higher, 16−17 D (Table 17). This indicates a contribution of the mesityl rings in increasing the dipole moment. The fluorescence maxima of both compounds are strongly red-shifted already in the nonpolar solvent, whereas they shift to the blue by ∼2000 cm^{-1} with a change to a rigid glass at low temperatures. This indicates a considerable conformational change (apart from the change of the dipole moments), which is inhibited by the rigidity of the medium.

The structure of pyrroloboranes in their excited CT state, whether twisted or planar, awaits clarification.

6. Indoles as Donors

Indole itself displays fairly complex photophysics, being sensitive to the polarity of the solvents (inversion of states). *N*-Methylindole possesses an oxidation potential in MeOH +1.09 V vs SCE, and in ACN +1.28 V vs $Ag/AgNO_3$ electrode,[613] close to that of NMe_3. Indoles, and particularly derivatives of **175**,

have a rich photochemistry,[613−615] but some of them emit a CT fluorescence.

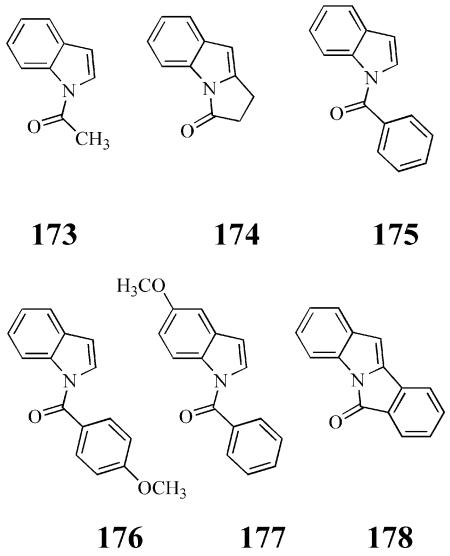

173 **174** **175**

176 **177** **178**

Among the *N*-carbonyl-substituted indoles, neither **173** nor its rigidly coplanar model compound **174** fluoresces. The aromatic derivatives, **175**, **176**, and **177**, emit a strongly polarity-dependent weak fluorescence, very far Stokes' shifted from the solvent-independent absorption band (Stokes' shift exceeding 10 000 cm^{-1}, even in hexane as solvent).[616] Only one emission band is observed, broad and structureless, in contrast to the structured phosphorescence. The fluorescence is strongly red-shifted with increasing polarity of the solvents, and the values $\Delta\mu^* \approx 15$ D for **175** and $\Delta\mu^* \approx 20$ D for **176** and **177** were evaluated from Lippert plots, indicating an additional separation of charges at a mean distance of 3−4 Å.

The fluorescence yields, low even in nonpolar solvents ($\sim 10^{-2}$), decrease in strongly polar solvents by several orders of magnitude, the emission falling down below the detection limit.[615,616]

The behavior of indole derivatives is closely similar to that of **1**, except there is the one emission band only, F_A. Comparison of the flexible molecules, **175**−**177**, with the rigidly coplanar model compound, **178**, leaves no doubt that the torsional motions are needed to attain the emitting ^{1}CT state. Elucidation of the relaxed structure of this CT state needs further experiments and theoretical calculations.

7. Carbazole or Phenanthridinone Donor

Carbazole has the same symmetry as pyrrole and an oxidation potential (in ACN, $E_{1/2} = 1.1$ V vs SCE) close to that of pyrrole. Zander noticed early that certain aromatic hydrocarbon N-derivatives of carbazole (**108**, **109**,[617] **179**[618]), which possess absorption spectra very similar to the sum of the individual components (carbazole + the aromatic hydrocarbon), emit only a single fluorescence band, strongly red-shifted with growing solvent polarity and evidently indicative of CT character (in contrast to **110**, which emits an essentially solvent-independent fluorescence). The dipole moments, found from the solvent shifts as in eq 5, were $\mu^* = 13$ D for **108** and 16 D for **179** (rather underestimated, because of the high value of a_o used).[502,619] All these compounds are not coplanar for sterical reasons, the calculated ground-state twist angle being $\theta = 55°$ for **108** and **109**, and 38° for **179**.[358]

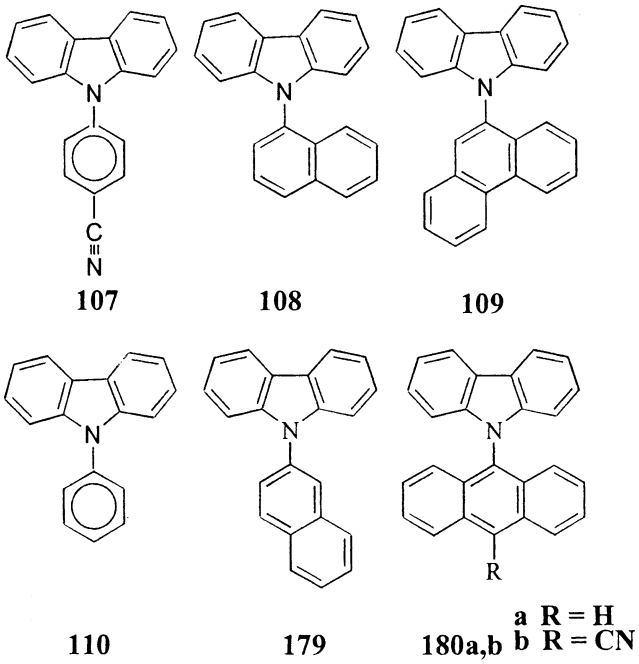

107 **108** **109**

110 **179** **180a,b**

a R = H
b R = CN

Some of the authors found similarities between the excited states of these molecules and the TICT states, supported also by quantum-chemical calculations (CT-state minima at the 90° twisted conformation). In the free molecule **108**, the TICT state was, however, calculated to be higher lying than the S_1 (LE) state by 1.09 eV, and thus experimentally inaccessible. The radiative rate constants were found to be high, e.g., $k_f = 5 \times 10^7$ s^{-1} for **107** in BuCl as the solvent. In the absorption spectra, a CT band could be separated by subtraction, and the solvent dependence of the fluorescence emission rate was explained by an intensity borrowing from the nearby LE state of the carbazole unit.[358]

Taking the TICT character of the excited state of **108** for granted, Jivan and Soumillon applied it as an electron-transfer sensitizer. Depending on the reaction partner, the assumed TICT state of **108** reacted either as a naphthalene radical anion (strong electron donor) or as a carbazole radical cation (strong electron acceptor), according to their expectation (cf. section IV.C.3).[359]

The excitation and fluorescence spectra of the anthracene derivative **180a**, thoroughly studied under isolated conditions in the supersonic jet, revealed that the molecule in the ground state has a minute energy barrier (20 cm^{-1}) at 90° between the shallow minima (θ = 77°, 103°). A considerable barrier appears in the lowest excited singlet LE state, and the energy minima at $\theta = 64°$ and 116° are shifted farther away from 90° (Figure 101).[203,399,416,620]

The dispersed fluorescence spectra and the fluorescence lifetimes exhibit a considerable anomaly at 470 cm^{-1} above the 0−0 transition. The anomaly is interpreted as a diabatic surface crossing with another weakly coupled state bearing no significant

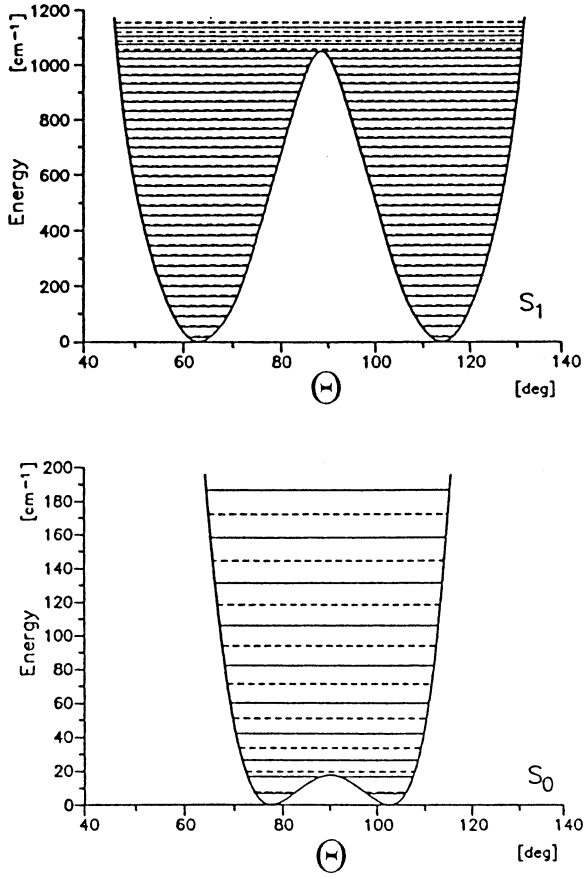

Figure 101. S_0 and S_1 torsional potential of **180a**, as deduced from excitation and dispersed fluorescence spectra in a molecular jet. The flat bottom potential in the ground state and the strong change of the potential by excitation lead to extremely long progressions within the excitation spectrum. Note the change of the energy scale for S_0 and S_1. Adapted with permission from ref 399. Copyright 1993 The American Institutes of Physics.

oscillator strength. It is suggested to correspond to a CT state with a potential energy minimum at $\theta = 90°$.[399]

In solutions, **180a**, as well as its 10-cyano derivative **180b**, show, after an initial relaxation, the transient absorption spectra with the pattern of the corresponding anion radical of the anthracene, *resp.* cyanoanthracene, unit.[621,622] The relaxation processes probably involve both solvation and torsional movements. Although there is evidence for decoupling, the conformational structure of the CT state is still not yet proved.

In a systematic study of a large series of derivatives with different acceptors,[61] instead of carbazole, 3,6-di-*tert*-butylcarbazole has been used, the radical cation of which is less reactive than that of carbazole. As acceptors, benzonitrile, nicotinonitrile, and dicyanobenzenes were used (with the acceptor properties increasing in that order), in various positions of substitution: **181**, **182**, and **183**. The (somewhat nonlinear) solvatochromic plots yield dipole moments $\mu^* \approx 19-21$ D for the molecules with a $-C\equiv N$ group in the position ortho to carbazole, and $\mu^* \approx 22-24$ D for the other ones. The usually separable CT absorption bands permitted the band shape analysis to be applied (as described in section X). The transition moments in emission were low, similar to those of **1**

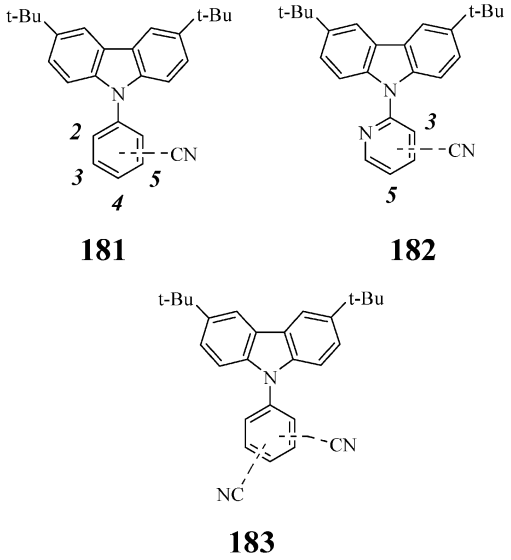

181 **182**

183

or less ($M_f \approx 0.7-1.2$ D, k_f in ACN between 2×10^6 and 1×10^7 s^{-1}), except for all those isomers which have a cyano substituent in the position para to carbazole: **182** (5-CN), **181** (4-CN), and **183** (2,4-$(CN)_2$ and 3,4-$(CN)_2$). The radiative rate constants, k_f, in all cases systematically decrease with increasing solvent polarity, but the transition moments, M_f, do not change much (with increasing polarity of the medium, the CT emission band shifts to lower wavenumbers; for the mutual relation of k_f and M_f, see eq 17). Qualitatively, the isomeric dependencies are justified by the C_{LUMO} coefficients of the acceptors at the position of the substitution of the donor (the CT and ground-state coupling, with the coupling matrix element V_G^{CT} as in eq 32). The estimates of the twist angle are within 65° and 75°. The conclusion was that the torsional angles, θ, do not noticeably change upon excitation. This is based on a rather arbitrary division of the reorganization energies into the parts related to *large*, *medium*, and *small* vibrational frequency modes.

In a more recent paper,[623] Kapturkiewicz et al. described the properties of carbazole with several aromatic ketones as acceptor units, all substitutional isomers of **184** and **185**. Remarkably, also in these

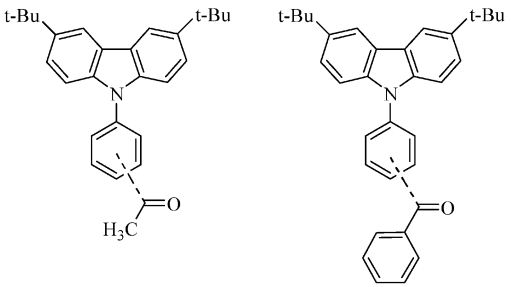

184 (o-, m-, p-) **185 (o-, m-, p-)**

two series, the para isomers have by far the most pronounced red-shifted CT band in the absorption spectrum. The molecules do not fluoresce in nonpolar media (fast ISC, as in many other carbonyl derivatives[78]). Here again, only the para isomers have somewhat higher emission rates, on the order of

Scheme 12

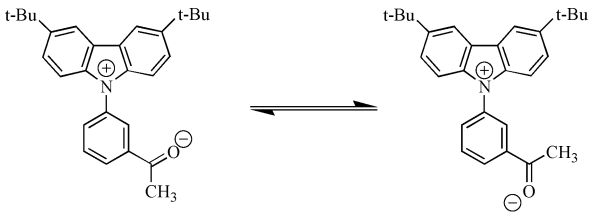

m-**184**

10^7 s^{-1} in the strongly polar solvent DMF, corresponding to transition moments $M_f \approx 2$ D. All other isomers have k_f in the range of $(2-5) \times 10^6$ s^{-1} and a smaller M_f of 0.7−0.9 D. These low values correspond to forbidden transitions, like those (or still lower than) in the case of **1** (cf. Table 5 for the corresponding values for **1**, **21**, and **22**).

The excited-state dipole moments in this group of compounds are in the range $\mu^* \approx 15-20$ D for *o*-**184** and *o*-**185**, while for all other isomers $\mu^* \approx 20-25$ D. Remarkably, the oxidation and reduction potentials of these D−A molecules are very close to the oxidation potential of the donor, and to the reduction potential of the acceptor; i.e., the coupling of these subunits in the ground state is very weak.

Inconsistencies in the reorganization energies, λ_o, as a function of the solvent polarity led the authors to conclude that there are two possible conformers of *m*-**184** and *m*-**185**. One exists in low-polarity media, $\epsilon < 5$ and the other one − with a larger distance of separation of charges and thus with a higher dipole moment − in high polarity solvents (Scheme 12) (compare the conformations of intramolecular exciplexes, Scheme 3 in section I.D).

Also in this series of compounds, the fluorescence intensities are related to the coupling of the CT with the ground state. The values of reorganization energies, evaluated from the band shape analysis, eq 34, and from the Stokes' shift (cf. section X), are divided into the *inner* (λ_i) reorganization energy, related to the higher vibrational quanta, $h\nu_i$, and the classical part, λ_o, including the solvent reorganization and the low-frequency inner vibrations, in which the authors include the A−D torsional modes. The inner reorganization energy λ_i, assigned to vibrations around 1600 cm^{-1}, remains fairly constant in different solvents. The λ_o values correspond mostly to the solvent reorganization.[624] The authors conclude that the (not explicitly estimated) twist angles θ do not markedly change in the CT state. The very high values of the Stokes' shift, ~10 000 cm^{-1} (between the transitions with apparently the same CT character in absorption and fluorescence) seem, however, to indicate a marked structural (or orbital) change between the Franck−Condon state and the emitting state.

Among numerous other polycyclic systems emitting dual or CT fluorescence, interesting from the point of view of the structural change, is a recent paper on A−D molecules with the phenanthridinone acceptor, **186**, **187**, and **188**. In the crystal structure of **186**, the phenyl ring is twisted by 80.6°. Dual fluorescence, with a typical CT emission band, is observed in **186**, with a much higher CT band in **187**, while none at all is observed in the case of the very strongly sterically hindered **188**. This is interpreted as clear evidence in favor of an *anti twist* (to a PICT state) in the relaxation of the ICT state.[625]

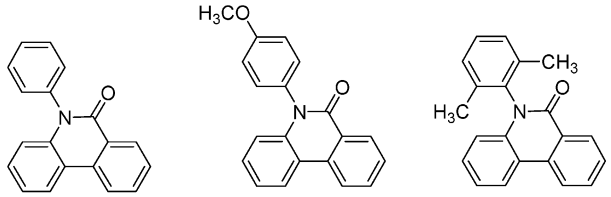

186 **187** **188**

8. Bispyrazolopyridine and Pyrazoloquinoline Acceptors

In the past few years, the derivatives of bispyrazolopyridine and pyrazoloquinoline, **189**[626] and **190a**−**c**,[627] have attracted attention due to their high emittivity, their biological activity, and their photophysical properties which are promising for nonlinear optics (large π-electronic D−A systems with large $\Delta\mu^*$ values). In the case of the derivative of **189** with the -ϕ-NMe_2 group in position 4, **t**he fluorescence is characterized by a high quantum yield and a relatively small solvatochromic shift in low-polarity solvents ($\epsilon < 10$). With increasing solvent polarity, the quantum yield decreases while the dipole moment of the emitting state dramatically increases.[626] Other photophysical parameters, like the transition moment in emission, change significantly in the same polarity range. Such behavior corresponds to an inversion of states. The emission occurs from the vertically excited π,π^* state in weakly polar solvents, whereas in strongly polar solvents the highly polar CT state is stabilized and becomes the emissive state.

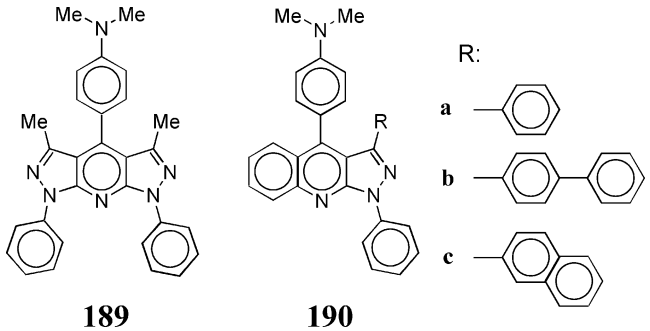

189 **190**

Theoretical calculations (INDO/s-CI[626] and CISD based on the AM1 Hamiltonian[628]) confirm a polarity-induced change in the energetic ordering of two emissive states of largely different charge-transfer character. The transition dipole moments in fluorescence,[626] as well as semiempirical results, hint at a planarization of **189** in the primary excited state, from about 80° in the ground state to 60°.[627] According to gas-phase calculations, S_3 is the lowest highly polar CT state at the equilibrium ground-state geometry, i.e., at a twist angle of $\theta = 81°$ between the planes of -ϕ-NMe_2 (donor) and bis-pyrazolopyridine (acceptor) moieties. This state achieves its maximal dipole moment, $\mu^*_{CT} = 26.5$ D, in the perpendicular (TICT) geometry, $\theta = 90°$. This value is close to the experimental value, $\mu^*_{CT} = 29$ D,[626] obtained from the solvatochromic shifts in polar solutions. An SCRF

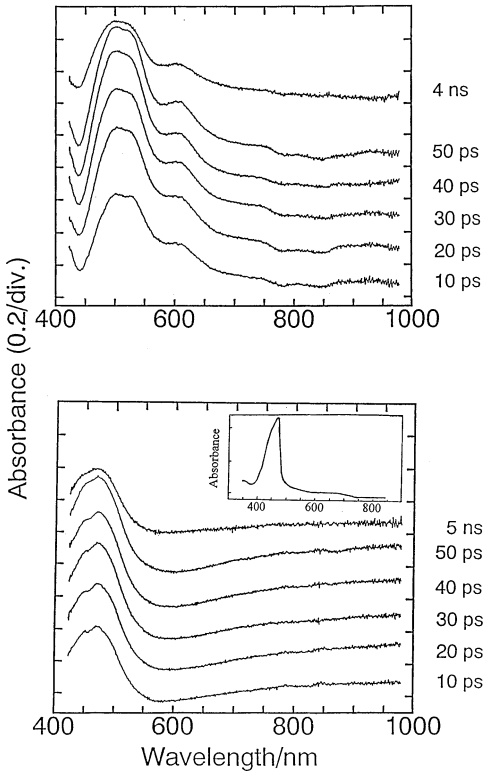

Figure 102. Transient absorption spectrum $S_n \leftarrow S_1$ of **189** (a, upper part) in hexane and (b, lower part) in ACN. (Inset) Absorption of ϕ-$N(CH_3)_2^{+?}$ in a Freon matrix, 77 K (from ref 298). Adapted with permission from ref 629. Copyright 1999 Elsevier Science.

computation with extension to excited states based on the AM1 Hamiltonian[627,628] reproduced very well the fluorescence solvent shift (e.g., the fluorescence transition in ACN is calculated at 17 500 cm^{-1} and observed at 18 100 cm^{-1}) and other excited-state properties.

The CT character of the fluorescent state of **189** in polar solvents was recently confirmed by picosecond laser photolysis studies:[629] the transient absorption spectra show a peak at 470 nm, characteristic of the cation radical of *N*,*N*-dimethylaniline (Figure 102). The charge separation process occurs within a few picoseconds in strongly polar solvents, such as ACN and MeOH. In methanol, the very fast CT process is followed by a markedly slower dynamic solvent shift. In medium-polarity ethyl acetate, the CT process is slower than that in strongly polar solvents; the evolution is observed within 17 ps.

The fluorescence behaviors of **189** and of the three donor−acceptor derivatives of pyrazoloquinoline, **190a**−**c**, are closely similar.[627,630] Dual fluorescence of **189** is observed only in polar *protic* solvents, whereas in the case of **190** and its derivatives it is detectable also in aprotic highly polar solvents.[631] In the former case, the effect was ascribed to the coexistence of two molecular forms in the ground state: H-bonded molecules, which after excitation emit the short-wavelength band, and the nonbonded ones, fast relaxing to the CT state and emitting the long-wavelength fluorescence. The H-bonding most probably occurs on the $-NMe_2$ group of the dimethylanilino donor. The dual fluorescence of **190** and its derivatives in aprotic polar solvents is ascribed to adiabatic reaction with a barrier related to the reorientation of the solvent dipoles; the molecular dipole moment in the ground state (oriented parallel to that in the CT state) has a different direction in the LE state.

Semiempirical calculations,[630] similarly to the case of **189**, hint at the S_3 state as the lowest one with a pronounced CT character ($\mu^* \approx 11$ D). This state achieves the maximal dipole moment, $\mu^* = 24.5$ D, for the fully decoupled donor and acceptor subunits (i.e., at the twist angle $\theta = 90°$). Calculation of the solvation effects with the SCRF method yields a dipole moment increase from 24.5 to 30 D and locates the CT state only slightly above the S_1 state in hexane. In ACN, this CT state becomes the lowest one.

B. 9,9′-Bianthryl and Other Biaryls

9,9′-Bianthryl **111** (BA) is the most thoroughly investigated member of the family of symmetrical, nonpolar biaryls which undergo a *symmetry breaking* with formation of a highly polar intramolecular CT state in the excited state and especially in polar solvents. We owe the discovery of the previously unexpected CT fluorescence of the nonpolar **111** to Schneider and Lippert.[632−634] **111** has an absorption spectrum and (in rigid media) a fluorescence spectrum closely similar to those of anthracene. Both experimental data and quantum-chemical calculations indicate that the ground-state conformation corresponds to a twist angle $\theta \approx 90°$. The red shift of about 1000 cm^{-1} with respect to the spectrum of anthracene corresponds to the excitonic splitting.[635] The peculiar behavior of bianthryl, quite different from that of anthracene, appears in the fluorescence: in polar fluid solvents the emission clearly occurs from a highly polar CT state. The symmetry-breaking and stability conditions in media of different polarities were generally defined by Beens and Weller for an intramolecular CT state of any species composed of two identical moieties.[636]

1. Thermodynamic Expectations

The preconditions for the stability of the CT states of various symmetrical biaryls in polar solvents were discussed first by Zachariasse[197,637−640] and then, in different form, by Zander and Rettig.[641] In the approximation of a full separation of charges, the CT state of a biaryl (A−A) can appear if

$$E_{ET}(AA) \approx E_{1/2}^{ox}(A) - E_{1/2}^{red}(A) - \frac{e^2}{r\epsilon} + T\Delta S_o \leq E_{00}(AA^*) \quad (39)$$

where $E_{1/2}(A)$ is the reversible (oxidation or reduction) half-wave potential of the aryl A (i.e., the *free enthalpy*), e is the electron charge, ϵ is the dielectric constant of the medium, r is the distance between the centers of the separated charges, and ΔS_o is the standard entropy change in the reaction $A-A \rightarrow A^+-A^-$. $E_{ET}(AA)$ and $E_{00}(AA^*)$ are the *energies* of the CT state and of the primary excited (nonpolar, excitonic) state, respectively.

Table 18. Reduction and Oxidation Potentials of Aromatic Hydrocarbons A, and Coulombic Stabilization of Charges Separated by Distance *r* (Center-to-Center) in ACN ($\epsilon = 37.5$): Standard Free Enthalpy, ΔG_o, of the Reaction $(A-A)^* \rightarrow (A^+-A^-)$, and Energy of the Lowest Nonpolar Excited (Excitonic) State of the Biaryl AA, $E_{00}(AA^*)$[a]

aryl	$E_{1/2}^{ox}$	$E_{1/2}^{red}$	e^2/r	$E_{ET}(AA)$	$E_{00}(AA^*)$	ΔG_o	A^+-A^-
benzene	2.32[e]		0.09	5.81[l]	4.59[l]	+1.22[l]	−[i]
naphthalene-1	1.58[e]	−2.58	0.09	3.97	3.80[p]	+0.17	−[i]
anthracene-9	1.14[f]	−2.00[f]	0.09	2.95	3.19[b]	−0.14	+[i]
	1.16[d]	−1.93[d]		2.90		−0.19	
	1.09[m]	−1.95[m]		2.85		−0.24	
phenanthrene-9	1.38[e]	−2.35[f]	0.09	3.54	3.54[p]	0	−[i]
	1.58[d]	−2.20[d]		3.59		+0.05	
pyrene-1	1.16[g]	−2.07[g]	0.05	3.08	3.33[l]	−0.25	+[i]
perylene-3	0.80[e]	−1.68[n]	0.04	2.36	2.61[c]	−0.25	+[i]
	0.70[m]			2.26		−0.35	
	0.51[o]			2.00		−0.61	
pentacene-6	0.54[e]		0.09	(2.12)[q,r]		(−0.3)[r]	...[j]
benz[*a*]pyrene-5	0.88[e]		0.05	(2.85)[q,r]		(−0.3)[r]	+[i]
	0.94[m]						

[a] All values in eV. Last column, experimental evidence for the CT state of the biaryl. [b] From the spectra in rigid ethanol solution, 77 K.[632] [c] Average of 0−0 bands in absorption and emission, *n*-hexane.[509] [d] Kavarnos, G. J.; Turro, N. J. *Chem. Rev.* **1986**, *86*, 401. [e] Estimated from the ionization potential: $E^{ox} \approx 0.679(IP) - 3.952$ (Pysh, E. S.; Yang, N. C. *J. Am. Chem. Soc.* **1963**, *85*, 2124). [f] According to Meites L.; Zuman, P. *Electrochemical Data*; Wiley: New York, 1974. [g] According to Hayashi, T.; Mataga, N.; Umemoto, T.; Sakata, Y.; Misumi, S. *J. Phys. Chem.* **1977**, *81*, 424. [h] 0−0 transition in the parent arene, **A**. [i] See sections 2−4 below. [j] No data available. [k] *CRC Handbook of Chemistry and Physics*; West, R. C.; Lide, D. R., eds.; 70[th] ed., CRC Press, Boca Raton, FL, 1989; p.D-159. [l] according to.[639] [m] *CRC Handbook Series in Organic Electrochemistry*; CRC Press: Boca Raton, FL, 1976; Vols. I and VI. [n] *Reactions of Molecules at Electrodes*; Hush, N. S., Ed.; Wiley-Interscience: London, 1971. [o] According to ref 670. [p] Murov, S. L.; Carmichael, J.; Hug, G. L. *Handbook of Photochemistry*; Marcel Dekker: New York, 1993. [q] Pentacene monomer. [r] Estimated in ref 641.

Let us assume ϵ to be that of the solvent and r to be the distance between the centers of the aryls. For a bulky ion pair, A^+-A^-, one can estimate $T\Delta S_o \approx -0.1$ eV.[642] Thus, the standard free enthalpy, ΔG_o, of the excited-state reaction would be roughly

$$\Delta G_o \approx E_{ET}(AA) - E_{00}(AA^*) - T\Delta S_o \approx E_{1/2}^{ox}(A) - E_{1/2}^{red}(A) - \frac{e^2}{r\epsilon} - E_{00}(AA^*) \quad (40)$$

For most biaryls, at room temperature in ACN solution ($\epsilon = 37.5$), the Coulombic interaction of the separated charges $e^2/\epsilon r \approx 0.09$ eV. Using the reported electrochemical data, one can predict the stability of the polar excited states for several biaryls (Table 18). The thermodynamic estimates of ΔG_o as reported in Table 18 are not decisive: the different isomeric biaryls may behave differently, which is due to chemical effects (symmetry, differences in dipole moments and electron density distributions, thus different Coulomb integrals, which are especially sensitive to the MO coefficients at the carbon atoms linking the two aryls). Analogous tables were compiled, either on a similar principle, with somewhat different values,[197,639] or starting from the gas-phase IP and EA values, calculated Coulomb integrals, and estimated solvation energies.[641] Nevertheless, all these estimates agree in indicating a special stability of the CT states of **111**, **198**, or **200** and a thermodynamic instability of the CT states of several other biaryls vs their nonpolar excitonic states.

2. Fluorescence Spectra and Kinetics

For the flexible biaryls in nonpolar fluid solvents, the fluorescence spectrum ceases to be a mirror image of the highly structured absorption band; the vibronic bands become broad and somewhat red-shifted. In the first papers by Schneider and Lippert, the experiment was supported by calculations, indicating a double minimum in the excited state, estimated to be at $\theta = 78°$ (and 102°).[634] This was later confirmed by numerous, more sophisticated calculations and by experimental investigations of the spectra in supercooled molecular jets: $\theta \approx 67-78°$, the barrier height to perpendicularity being estimated in the range between 38 and 117 cm^{-1}.[398,643−647] Also in nonpolar solvents, a double minimum potential can be fitted (Figure 103). The excited-state minima are found to deviate more from 90° than in the gas phase (deviation ~30°), and the barrier between them is roughly twice as high as in the gas phase.[646−648]

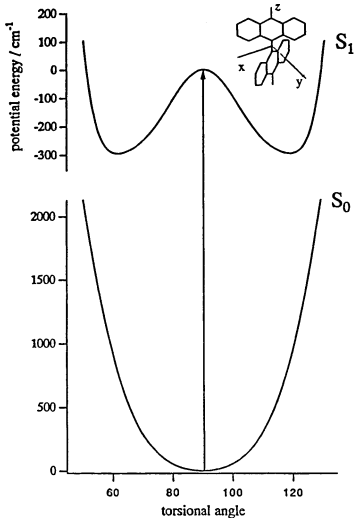

Figure 103. Torsional potentials of **111** in the S_0 and S_1 states in methylcyclohexane solution, calculated with the parameters best fitting to the experimental fluorescence spectra. Adapted with permission from ref 648. Copyright 1999 American Chemical Society.

Investigations of the kinetics in nonpolar solvents also prove the role of the hydrodynamic friction, which is characteristic of the torsional motions of large amplitude.[648] Bianthryl is exceptional in the respect that, although the spectra of its bare molecules in cool molecular jets do not show any evidence of a CT state, up to 6000 cm^{-1} excess energy,[644,645] such a state appears in van der Waals complexes of **111** with *only one* molecule of acetone[649] or H_2O.[650] With an increasing number of polar molecules in the cluster, the emission shifts to the red. It is remarkable, however, that there exist two isomeric 1:2 clusters with acetone: one of them emits a CT fluorescence, and the other one possesses a spectrum very similar to that of the bare molecule. Two polar molecules can be attached asymmetrically at one of the anthryl units (symmetry-breaking), or in a symmetrical way, each solvating one aryl and not leading to the CT state. With acetonitrile as solvent also, one solvent molecule is enough to lead to the red-shifted emission and to a strong lengthening of the lifetime.[651]

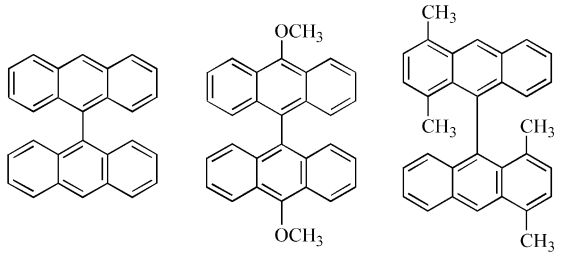

111 **191** **192**

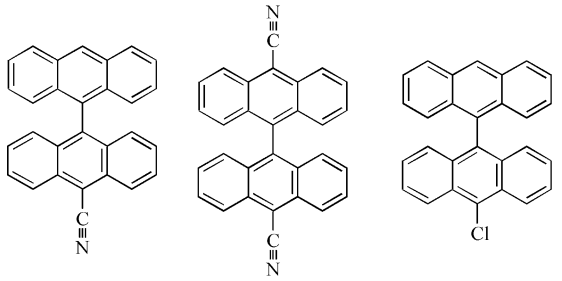

194 **195** **193**

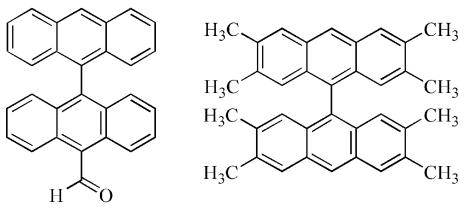

196 **197**

Similarly in fluid polar solvents, the symmetrically substituted bianthryls (**191**,[59] **192**,[632] **197**,[633] **195**[197]) behave very much like **111**, while the asymmetrically substituted ones (e.g., **193**, **194**, or **196**) form the CT state at a markedly faster rate than bianthryl.[197,622,643,652]

Typical fluorescence spectra are shown in Figure 104. The values of E_{ET}(AA), calculated and plotted according to eq 38, are related to the unobservable

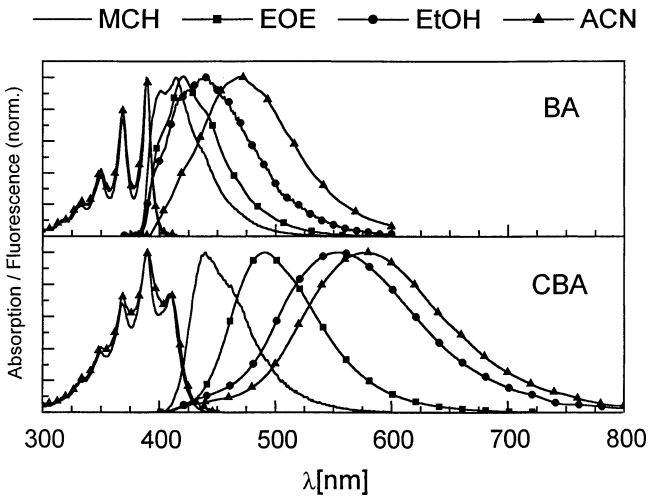

Figure 104. Absorption and fluorescence spectra of **111** (BA) and its 10-cyano derivative **194** (CBA) in the indicated solvents of different polarity. Adapted with permission from ref 622. Copyright 2000 Elsevier Science.

0−0 transition of the ET state. The experimental observable is the fluorescence maximum, red-shifted from the 0−0 position by at least a half-width of the emission band at half of its maximum height, typically by ∼1/4 eV. For **111**, the fluorescence maximum in ACN is at 2.62 eV,[59] while the calculated E_{ET}(**111**) = 2.85−2.95 eV (Table 18); in the case of **191**, the respective values are 2.33 and 2.74 eV.[59]

The dipole moment of the CT state (in polar solvents) is estimated from the solvatochromic shift as $\mu^*_{CT} \approx 20.6$ D[634] or 23.4 D.[653] The CT emission rate constants, k_f, fall below 10^{-7} s^{-1} in strongly polar solvent.[654]

From a wealth of evidence concerning the kinetics of the ET process in bianthryl, it seems that there is a mother−daughter relationship between the excitonic and the CT states. The kinetics of reaction rates seem to be determined by the solvent dynamics, but neither by the longitudinal relaxation time, τ_L, of the solvent[622,655] nor by a one-step process.[621,656,657] Spectroscopic and kinetic data are excellently reproduced by the adiabatic ET model,[556] whereby the transient spectra are very similar to those required by the parent−daughter two-state system. The model of movement of the system on the adiabatic S_1 state along the solvent coordinate only neglects the intramolecular coordinates. A test for the two models will be in a close inspection of the (symmetric) steric effects.

Additional complexities appear in protic solvents, especially the quenching by protons,[364] connected with the isotopically detected hydrogen exchange at the 10-position.[658] Also, the quenching by inorganic anions is conform to expectations for a charge-separated species.[366]

3. Transient Absorption Spectra

Initially, the transient absorption spectra of 9,9′-bianthryl in highly polar solvents were reported to be similar to the superposition of the spectra of anthracene radical cation (An^+) and anion (An^-), although somewhat broader and blue-shifted (Figure 100).[659] Similar effects (blue shift and broadening of

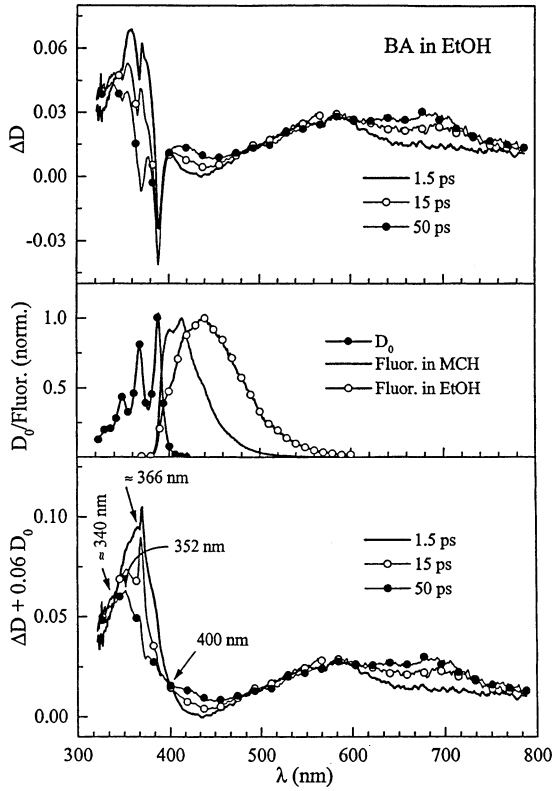

Figure 105. (Top) Time-resolved differential absorption spectra of **111** in EtOH with subpicosecond excitation at 370 nm, at several delay times. (Middle) Ground-state absorption (D_0) and stationary fluorescence spectra in two solvents. (Bottom) Transient absorption spectra corrected for bleaching and gain effects. Adapted with permission from ref 621. Copyright 2000 Elsevier Science.

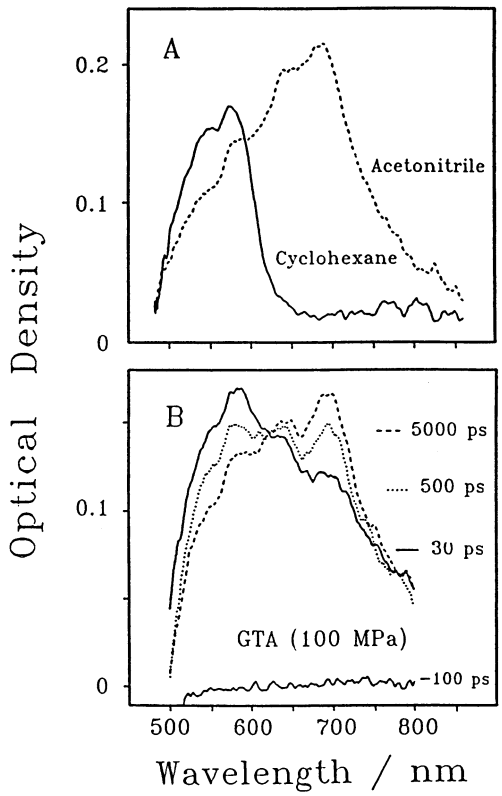

Figure 106. (A) Transient absorption spectra of **111** in cyclohexane (the excitonic, nonpolar state) and acetonitrile (a superposition of excitonic and CT state). (B) Transient absorption spectra of **111** in glycerol triacetate (GTA) as solvent, under the pressure of 100 MPa, at several delay times. Adapted with permission from ref 662. Copyright 1991 Elsevier Science.

the bands as compared to An^+ or An^-) were observed in the spectrum of radical ions of 9,10-diphenylanthracene[660] and that of bianthryl radical anion.[152] Later, thorough investigations of the transient absorption spectra as a function of solvent polarity, time, and pressure resulted in the finding that the evidence is more complex. The transient absorption spectrum of **111** in ACN could not be reproduced simply as a superposition of the absorption bands of An^+ and An^-; in medium-polarity solvents it was, however, a suitably weighed sum of two spectra: that appearing in cyclohexane and that recorded in ACN. In addition, the kinetics corresponded to a mutual transformation of these two species only. The authors concluded the CT state of **111** to be an *imperfect* CT state, contaminated with an admixture of the nonpolar LE states (and thus probably deviating from a 90° twist).[652] In a thorough study of the transient absorption of **111**,[661,662] the existence of only two excited states involved in the kinetics was strengthened by finding an isosbestic point at different delay times (Figure 106). These spectra were decomposed into two components, ascribed to the LE and the TICT state, both spectra being nearly independent of the solvent, pressure, and delay time. The TICT absorption closely resembled a superposition of the spectra of the radical ions, An^- and An^+, both blue-shifted by $\sim$750 cm^{-1}.

Mataga et al.[663] recovered time components much longer than the solvent relaxation time in the transient absorption kinetics, interpreting this as evidence for the slow step of a torsional motion *from a perpendicular to a tilted* conformation.

In a more recent experimental and theoretical study,[654] the transient UV spectrum of excited **111** in ACN ($\lambda \approx 315$ nm; the band is absent in nonpolar solvents) is found to match the absorption bands of the anthracene radical cation ($\lambda \approx 315$ nm) and anion ($\lambda \approx 320$ nm), the absorption coefficient of the superposition band being correspondingly higher. The decay time of the 315 nm transient in absorption matches the lifetime of the CT fluorescence in the same polar solvent.

This work[654] and the studies with femtosecond pulses[621,622] leave little doubt about the following points: (i) In nonpolar solvents, the originally mutually orthogonal anthryl units relax by torsional motion to a twist angle about 70°, and the emitting state does not involve appreciable CT character. (ii) At a dielectric constant $\epsilon \approx 5$, the nonpolar and the CT states are nearly degenerate. (iii) Even in strongly polar solvents, the CT formation process involves an initial torsional motion out of perpendicularity (which is favorable for the ET reaction). The ET is followed by the evolution of solvation and torsional motion. Different authors differ in their estimates of the equilibrium conformation of the CT state, which would still need an analysis like that described in section X. The emitting CT state has, however, a large dipole moment and a low fluorescence emission

rate, and especially the transient absorption spectra are close to an orthogonal radical ion pair, as in a TICT state.

The first report on the time-resolved resonance Raman spectra of **111** in solutions indicated some previously unnoticed distortions of the anthracene rings in the S_1 state.[493] A major breakthrough in the understanding of symmetry breaking and excited-state behavior in 9,9′-bianthryl **111** and its derivatives has been achieved with the recent transient dielectric loss study by Warman et al.[664] It reports intermediate dipole moments for bianthryl and for the symmetric dicyano derivative **195** in alkane solvents, which are much smaller than in the symmetry-broken derivatives such as **194**. These dipole moments increase to a limiting value with rising solvent polarity. This indicates a change of the easiness of symmetry breaking and of the emissive conformation, which depends on the solvent polarity and on the substituent pattern. The study confirms that symmetry breaking is possible in **111**, even in alkane solvents, although the emission is not forbidden and thus corresponds to a nonperpendicular conformation undergoing a charge resonance (*flip-flop* CT) with a nonpolar intermediate. This mechanism reminds us of a similar conclusion on the symmetric "DMABN dimer", **58**.[212,213] Adsorption of **111** to a porous glass surface also leads to symmetry breaking and CT formation, in this case even at 77 K.[665]

The symmetric 9,9′-bianthryl **111** has also been rendered unsymmetric by generating solute−solvent 1:1 clusters with He, Ar, Ne, and H_2O[666,667] in a supersonic jet. Using advanced techniques such as rotational coherence and hole-burning spectroscopy, the excited-state potentials were evaluated and shown to increase in asymmetry in the above order. The solvent molecule being located in an off-axis position causes the asymmetry.

A new understanding has also been gained with the carbazolyl derivatives of bianthryl, **180a** and **180b**. The resonance-type photochemical dark reaction, quenching the fluorescence of **180a** only at a specific excess energy but much less above and below it, has been known from the jet studies.[399] It has been interpreted as a crossing/conical intersection between two states, which is supported by femtosecond wave packet calculations (for a review, see ref 203). The state interaction has now also been verified in absorption by cavity ring-down studies, and the nature of the dark state has been identified as CT, thus supporting the TICT model for the reaction.[620] For the corresponding cyano derivative, **180b**, the CT state is expected to be preferentially lowered in energy, and the crossing should therefore occur at a smaller excess energy. Recent measurements[668] support it. **180b** in solution even shows a longest-wavelength CT absorption band, indicating that the CT state is the lowest excited state.[669]

A CT emission from an aza analogue of bianthryl, 9,9′-biacridyl, has also been noticed.[633]

4. Other Biaryls

Biphenyl, 1,1′- and 2,2′-binaphthyls, 9,9′-biphenanthryl, and 3,3′-bifluoranthyl all do not reveal any CT character in their fluorescence spectra, consistent with the thermodynamic expectations (Table 18). The polarity of the solvent has a negligible effect on the spectral position and shape of their emission spectra.[639,641]

Biperylenyl should form the most stable CT state among the symmetric biaryls. Previous investigations of the photochemistry of perylene, Pe, revealed indeed that (instead of an excimer formation, Pe* + Pe → Pe_2*) the reaction Pe* + Pe → Pe^- + Pe^+ occurs in polar aprotic acetonitrile.[670,671] 3,3′-Biperylenyl (**198**) was synthesized, along with its derivative, **199**, which appeared to be more stable and easier to purify than **198**.[509,672] The fluorescence of **198** appeared to be strongly polarity dependent, indicating a CT emitting state; most experiments were, in fact, done with **199**.

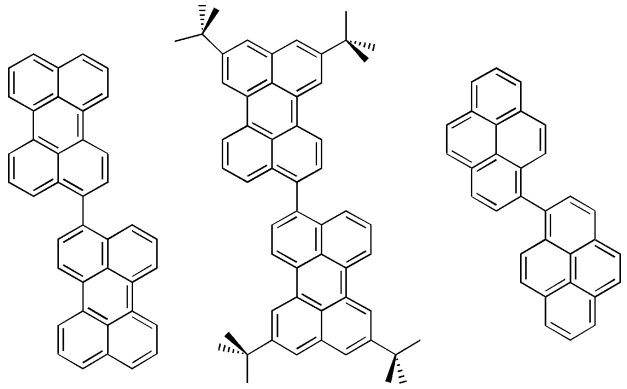

198 **199** **200**

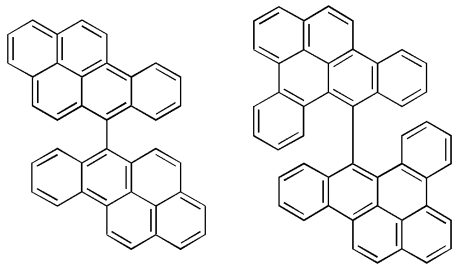

201 **202**

There was only one fluorescence band, structured in nonpolar solvents, which lost the vibronic structure and was markedly red-shifted with increasing solvent polarity. The excited-state dipole moment was found from the solvatochromic shift in polar solvents as $\mu^* \approx 17-20$ D, much less than the value of ∼42 D expected for the pure ET (TICT) state. Additionally, the transition dipole moment was high — higher than that of perylene — which indicates a considerable deviation from the electronic structure of a pure ET state.

The excitonic state, Ψ_+, should possess a higher transition moment than that of perylene.[673] Considering its admixture to the ET state in its most simplified form, $\Psi_{CT} \approx a\psi_{ET} + b\psi_+$, and neglecting the mutual contamination of the ET and ground states (which might otherwise contribute with a fraction of the huge μ_{ET} to the transition moment[50]), one obtains $0.43 \leq a^2 \leq 0.65$ from the transition

moments. Hence, the dipole moment $\mu^* \approx a^2\mu_{ET} \approx$ 18−27 D, is in accord with the experimental result. Alternatively, the data could be interpreted in terms of a coupling of the ET with the ground state. The coupling mechanism operating here is not yet conclusively proved.

In view of the parallel orientation of the transition moments, the excitonic interaction of two perylene moieties would be rather independent of their mutual twist angle. Therefore, it would be difficult to make a judgement on the conformation of the CT state only on the basis of the incomplete separation of charges and the transition moment in emission.

A comparison of **198** and the Pe* + Pe reaction may be misleading: the latter occurs at a distance of several angstroms (typical encounter distance for ET being about 7 Å[674]), and neither the excitonic nor other delocalized states of the biaryl can operate in its products — the kinetically free, solvated radical ions. In **198** or **199**, however, the coupling between a nonpolar (e.g., excitonic) state and the ET state seems to be strong.

The difference in the behavior of the CT states of **198** (allowed emission) and **111** (forbidden transition), their excitonic states being of similar nature, seems to be in the symmetry restrictions in the state mixing that is operative for **111**. In view of the nonplanarity of numerous polycyclic arenes, among them perylene,[675−679] in **198** (C_1) there seems to be no symmetry restrictions at all. With respect to the ground-state conformation, **111**, with its very strong steric interaction of the two aryl systems, has an orthogonal conformation in S_0; **198** has a much weaker steric hindrance, like that of 1,1′-binaphthyl.

1,1′-Bipyrenyl (**200**) was investigated long ago by Zachariasse, who found a CT emission, but with a solvatochromic shift much lower than that of **111**, i.e., corresponding to an incomplete separation of charges (which may be due to a state mixing or spectral overlap of two transitions).[197,637,639] A dipole moment in the excited singlet state was detected also with the microwave conductivity method.[639] **201** is strongly sterically hindered, like **111**, and probably has a mutually perpendicular conformation of the two aryls in the ground state.[641] The excited-state dipole moment, estimated from the solvatochromy as $\mu^*_{CT} \approx$ 26 D, is close to that predicted for a full separation of charges. Accompanying the *nonpolar* emission (F_B), the F_A CT emission is found to dominate, even in *n*-hexane as solvent. This CT fluorescence has a vibronic structure, against the general belief. The authors explain it by a similar equilibrium conformation of both the ground and excited (CT) states (90° twist) and no need for reorientation of the nonpolar solvent environment.[641]

Still much more sterically overcrowded than the preceding biaryls is **202**.[680] Its ground-state conformation cannot differ much from perpendicularity. The fluorescence of **202** has a CT character and exhibits a vibronic structure even in polar solvents. Against expectation, the dipole moment of the CT state, as estimated from solvatochromic shifts, is considerably smaller than that of **111**. The authors suggest that the side benzene rings protrude over the plane of the other aryl moiety,[680] thus causing more overlap between the π-electron system of the two aryls than is present in the other biaryls discussed. Such an increased overlap counteracts a full separation of charges.

Several *asymmetric* biaryls (**203**−**205**) were studied,[681] inter alia, for comparison with the *symmetric* ones (**111**, **199**, and **200**). The absorption and fluorescence spectra in solvents of different polarity (solvatochromic effects) indicate a weak CT character of the excited state of **203**, a scarcely detectable amount of CT in **204**, and no trace of such behavior in **205**. The transition dipole moments in emission are high in all these biaryls ($M_f \approx 4-6$ D), with some decrease of the M_f and k_f values with the polarity of the solvent in the case of **203** and **204**, and a solvent-independent high value of $M_f = 6.1$ D in the case of **205**.

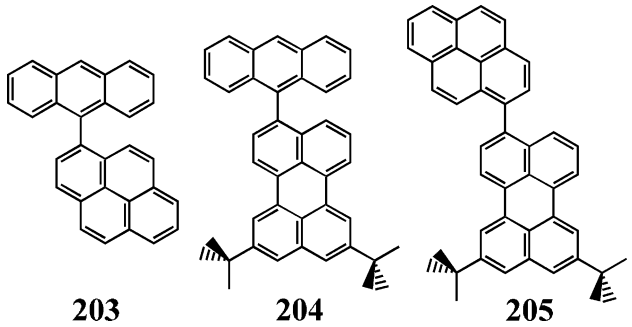

5. Oligoanthracenes and the Mnemonic Systems

Separation of charges in the TICT behavior of the singly bonded D−A molecules inspired the idea to use the phenomenon in molecular electronic devices, in particular for molecular memory units. Stolarczyk and Piela[682] suggested a long polymeric $(-D-A-)_N$ chain, with a theoretically predictable optimal $E_{ox}(D) - E_{red}(A)$ value, at which the system could act as a molecular bistable memory unit ("*mnemon*"). The photoinitiated separation of charges, calculated as a sequence of *n* bipolar units in the *N*-mer chain, $(D^+-A^-)_n-(D-A)_{N-n}$, at a certain *n* (at a sufficiently long charge separation distance) would provide similar stability of both the nonpolar and the CT forms (bistable system), separated by a barrier. At a suitable orientation, a sufficiently strong external electric field should remove not only the degeneracy of the two states but also the barrier between them, thus erasing the previously stored information.[682]

Such a system was conceived to be realizable, e.g., in the form of a polymeric chain of 9,10-anthrylenes, embedded (and thus oriented) in a liquid crystal.[683] Several oligoanthrylenes were synthesized (**206**−**211**), and their behavior was compared to that of bianthryl **111**.[684−686]

The alkyl (*tert*-butyl or *n*-hexyl) substitution at the outer positions of some rings increases the solubility of the compounds but also exerts some influence on the CT states; e.g., the photophysical behaviors of **208** and **209** are different.[684] In particular, the *tert*-butyl derivatives **206** and **208** form the CT state only in strongly polar solvents, in contrast to **111**, **207**, and **209**, which undergo an intramolecular ET much more

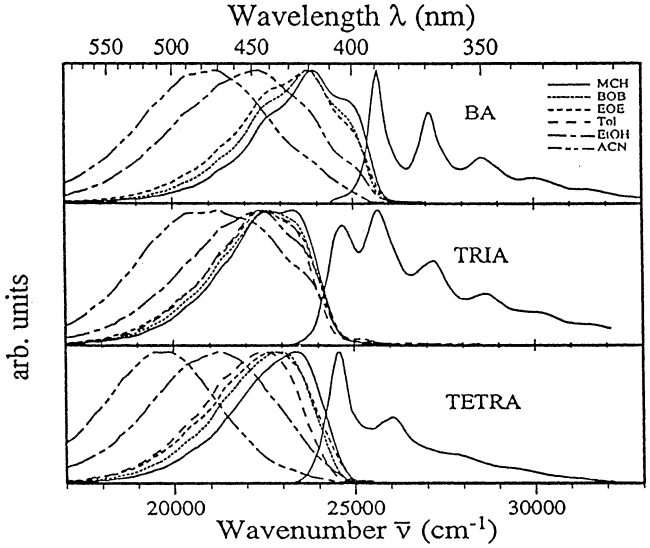

Figure 107. Absorption and fluorescence spectra of **111** (BA), **209** (TRIA), and **211** (TETRA) at room temperature in several solvents of different polarity: methylcyclohexane (MCH), di-*n*-butyl ether (BOB), diethyl ether (EOE), toluene (Tol), ethanol (EtOH), and acetonitrile (ACN). Adapted with permission from ref 685.

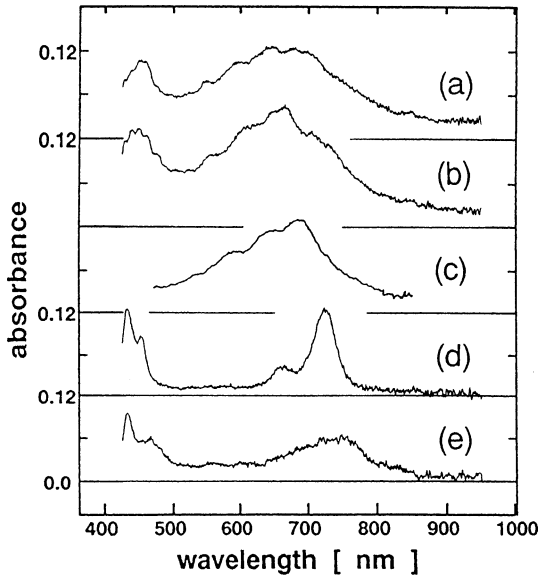

Figure 108. Transient absorption spectra, at 100 ps delay time, of the excited state of (a) **209** in ACN, (b) **211** in DMF, and (c) **111** in ACN. For comparison, the absorption spectra of 2,3-dihexylanthracene radical ions in ACN are shown: (d) radical cation, obtained by the reaction with *p*-dicyanobenzene; (e) radical anion, obtained by the reaction with *N*,*N*-dimethylaniline. The absorption bands in the 400−500 nm region in (d) and (e) are due in part to the triplet state, to the mentioned reactants, and to their radicals. Reproduced with permission from ref 685. Copyright 1997 American Chemical Society.

easily. This is explained as a strong screening of the former molecules by the bulky *tert*-butyl substituents, markedly weakening the energy of solvation (increasing the Onsager cavity). In the very strongly polar solvent *N*-methylformamide ($\epsilon = 182$), there is a similar separation of charges in analogous compounds of both groups.[686]

All these compounds (except the asymmetric polar **210**) have two nearby excited states in nonpolar solvents: the primarily excited (nonpolar) excitonic state and the CT state. In polar solvents, after a relaxation, the CT state becomes the lowest excited state. There appear two fluorescence bands (Figure 107): one structured (primary, excitonic) and the other broad and unstructured, strongly shifting to the red with increasing polarity of the solvent.[685] Compared to the best known compound of this group, **111**, **211** forms the CT state even in a rigid solvent at 77 K,[685] while **208** and **209** show a reduced tendency toward charge separation.[684]

The transient absorption spectra in alkanes are primarily similar to those of the related simple (monomeric) anthracenes, i.e., corresponding to the mutually perpendicular conformation of the neighboring anthracene units in the ground state. They become broad and blue-shifted, with relaxation times between 10 and 15 ps.[685,686] There is obviously a geometrical relaxation in the excited state, leading probably to an equilibrated conformation of the excitonic state, with a lower torsional angle, similar to the case with **111**.

In polar solvents, the equilibrated transient absorption spectra are very similar to the spectrum of **111**, and are similar to the sum of the spectra of the radical cation and anion of the respective monomeric anthracene (however, they are somewhat broadened and spectrally shifted by several hundred cm^{-1} to the blue; Figure 108). Femtosecond pulse spectroscopy

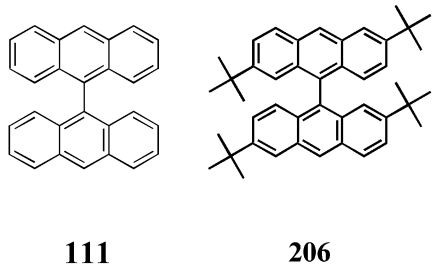

111 **206**

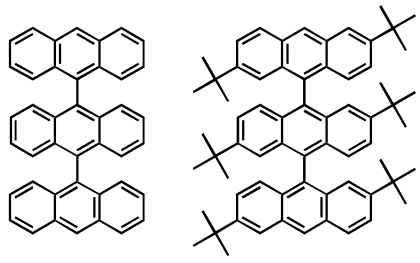

207 **208**

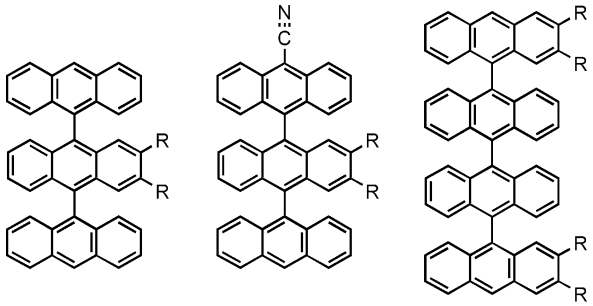

209 **210** **211**

$R = C_6H_{13}$

Table 19. Excited-State Dipole Moments, μ^* (in Debye Units), of the Oligo-anthrylenes, from the Solvatochromic Shifts in Polar Solvents[685,686] and from the IEOEM Method[686]

compd	μ^* (a_o)[a]	μ^* (a_o)[b]	μ^* [c]	μ^* [d]
111	20 (6)		21	7.4[e]
206	12 (6)	15 (7.0)	21	7.2
207	31 (9)	21 (6.8)	42	9.8
208	16 (9)	12 (7.5)	42	6.5
209	35 (9)	27 (7.5)	42	9.0
210	32 (9)	25 (7.7)	>42	24.5
211	70 (12)	42 (8.6)	63	

[a] Cavity radius which covers the molecule without the substituents. [b] Estimated from the cube root of the ratio of molecular weights vs that of **111**. [c] Calculated for a full separation of charges located at the centers of the outermost rings. [d] From the IEOEM method, in trifluorotoluene as solvent; see the remark with ref 116. [e] In dioxane.

revealed the evolution of the transient absorption spectra from the excitonic to the CT state in a DMF solution, within the time range 1.1−1.5 ps for **209** and **211**,[685] similar to the 1.8 ps found previously for **111** in ACN.[652]

The excited-state dipole moments were difficult to estimate, as the solvatochromic shifts of the fluorescence exhibit two regions: a nearly constant spectral position in less polar solvents (the excitonic state) and a strong shift in the more polar solvents (the CT state). The solvatochromic shifts in the high-polarity region result (depending on the choice of the Onsager radius) in μ^* values lower than or similar to a full separation of charges across the entire aromatic system.[685,686] The values resulting from the integrated electrooptical emission (IEOEM) method are much lower; the difference may be due to the simplified assumption in the IEOEM model, taking into account the purely electronic polarization of the molecules only, but neglecting the structural and conformational changes (cf. Table 19).[116,686] Therefore, these latter values seem rather dubious to the authors.[686]

In a recent transient microwave conductivity study,[687] the dipole moments of the excitonic states of **111**, **209**, and **211** were compared and found to range within 7−9 D. Furthermore, the dipole reversal times were also very similar (8 ps). It was concluded that the excitonic state, although possessing a net dipole moment, involves the interaction of two neighboring anthracene units only and is different from the CT state.

To conclude, the hitherto investigated oligoanthrylenes seem able, with a favorable structure and medium, to separate charges at the full length of their ring systems. The radiative rates, k_f, are low but still of the order of 10^7 s^{-1}. The transient absorption spectra do not fully correspond to the sum of those of the anthracene radical cation and anion. Hence, the component anthracene units are most likely not in a zero-overlap conformation but are coupled with the excitonic state, probably less so than in the case of biperylene.[509]

Moreover, the separation of charges is still short-lived: the fluorescence decay times are of the order of 10 ns. Therefore, the oligoanthrylenes, however most interesting as an object of study, did not give until now any real introduction to the *mnemons*.

C. Ionic Compounds

This section is devoted to *ionic* dyes, which have been discussed in the literature as belonging to the same family of compounds in which twisting relaxations and charge-transfer interactions simultaneously play a role. Nevertheless, as the compounds are ionic, charge transfer leads not to charge separation but to a charge shift. We therefore want to keep these compounds clearly separate because the photochemical products may show properties rather different from those of the previously discussed CT states.

1. Ionic DMABN Derivatives

The smallest dye systems in which a TICT-related charge shift (CS) was postulated are the protonated or *N*-methylated (dimethylamino)pyridines and -pyrimidines, such as **212** and **213**. A salient feature was the absence of emission from the CS state, as opposed to the emission of the corresponding TICT state of the neutral pyridines and pyrimidines (cf. section III.E.5).[267,268] This led to the suggestion that these CS states are very weakly emissive or nonemissive.

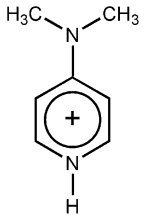

212

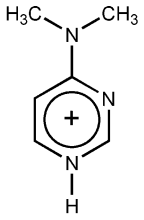

213

2. Ionic Biphenyl Derivatives

The photophysics of (dimethylanilino)pyridinium **214** and some unbridged and bridged derivatives, e.g, **215**−**217**, have been mainly described by Fromherz et al.[204,688−692] The results show that the photophysi-

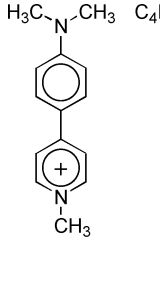

214

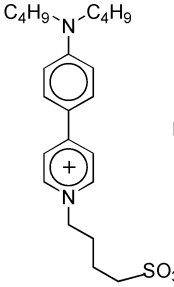

215

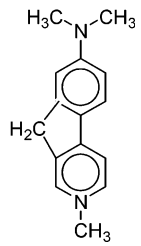

216

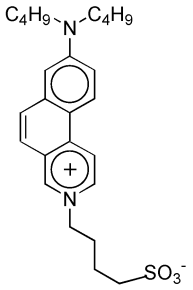

217

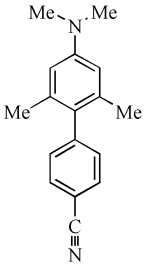

105

Scheme 13

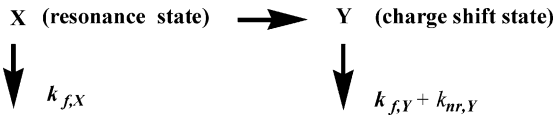

cal behavior strongly differs depending on the torsional flexibility of the compounds. Moreover, although only a single emission band is observed for the flexible dye **214**, it is considerably broader than that of the bridged model compounds **216** and **217** and suggests that the emission of **214** and **215** actually consists of two different components, only slightly shifted with respect to each other. The bridged compounds **216** and **217** are strongly fluorescent, $\phi_f \approx 0.5$, whereas the quantum yields for **214** are below 0.01 in low-viscosity solvents, rising to a few percent in **215**. A model (Scheme 13) to account for this behavior involves dual fluorescence for **214** and **215** from a precursor species **X** (resonance-type state with high mesomeric interaction and nearly planar geometry) and a successor species **Y** (twisted geometry, charge shift state). Indeed, the time-resolved experiments on **215**[692] showed the expected precursor−successor relationship with subsequent equilibration of the two states **X** and **Y**. The emissive rate constant k_f was determined to be high for species **X**, identical to that of the bridged model compound **217**, but also significant for species **Y** (40% of the value for **X**). This points to emissive geometries of **Y** which are not completely twisted to 90° but retain some residual orbital overlap. The question remains open whether the energetic minimum for **Y** is slightly different from 90° or a broad angular distribution around a perpendicular minimum is responsible for this effect.

When the temperature is sufficiently lowered[204] or the medium viscosity is increased,[692] viscosity effects slow the kinetics leading from **X** to **Y**, and the fluorescence quantum yield strongly increases. The strong viscosity dependence is direct evidence that the reaction **X** → **Y** is connected with a large-amplitude motion, but the fact that equilibration occurs indicates that the energy difference between **X** and **Y** is not large.

The very low fluorescence quantum yields (at room temperature), in conjunction with sizable k_f values for the species **Y**, indicate that the nonradiative decay rate constants from **Y** are very large and determine the overall fluorescence properties of these species. Interestingly, not only the **X** → **Y** kinetics are slowed by viscosity effects, but also the nonradiative decay of **Y**.[692] This points to a possible involvement of twisting also in the nonradiative process. Comparable nonionic biphenyl derivatives such as **105**, which also show a twist-related second (CT) emission band, have considerably smaller nonradiative rate constants,[334,335] whereas the radiative one is not much different ($k_f \approx (3-7) \times 10^7$ for both **215** and **105**). One of the features distinguishing TICT states in nonionic and CS states in ionic dyes therefore seems to be the different size of the nonradiative decay rate constant, i.e., the back electron transfer (BET) to the ground state. In terms of Marcus theory, this process is situated in the inverted region. It has been suggested by Mataga and Kakitani that BET in the Marcus inverted region is faster for ionic compounds than for nonionic ones, due to dielectric saturation effects of the surrounding solvent.[693] Although this mechanism has been questioned,[694] it would offer an explanation for the observed effects.

3. Ionic Stilbene Derivatives

Recently, some pyridinium derivatives of stilbene have been shown to emit from several excited species (multiple fluorescence). These systems, called DASPMI (and derivatives, see **218**−**223**),[688,691,695−698] possess two single bonds and one double bond, which can, in principle, twist in the excited state, and in addition the bond linking the dimethyl- (or dialkyl-)amino group. As in the case of **214**, bridged model compounds such as **217**[692] positively identify the twisting possibility as the reactive coordinate responsible for the large nonradiative decay. Selectively bridged derivatives such as **223** vs **222**[697,698] allow one to conclude that the main nonradiative channel is connected with single bond twisting and that double bond twisting is only a minor nonradiative pathway in these compounds. Time-resolved studies established a large contribution of solvation dynamics to the Stokes' shift[697,699,700] but also indicated some temperature dependence of the fluorescence rate constant, consistent with the involvement of several emitting species.[695,696]

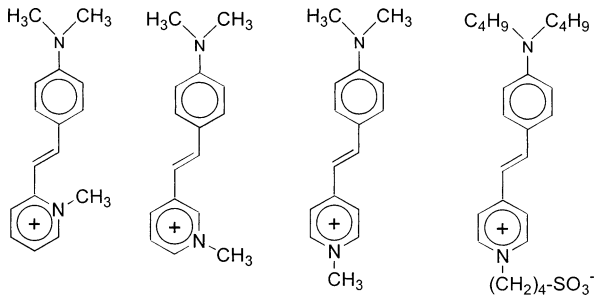

218 **219** **220** **221**

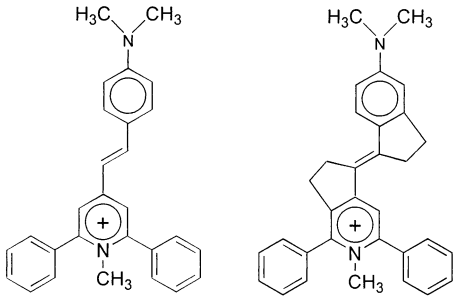

222 **223**

Interestingly, bridging a certain bond in a polymethinic or polyenic molecule does not always lead to enhancement of the fluorescence quantum yield, as would be expected from the loose bolt theory.[350,701,702] Anti-loose-bolt behavior, i.e., a reduced fluorescence quantum yield for the bridged derivative, has been observed in some cyanines (e.g., in **224**[703]) as well as in donor−acceptor stilbene **225**, in conjunction with multiple fluorescence in the polyene series **225**−**227**.[334,508,704−710]

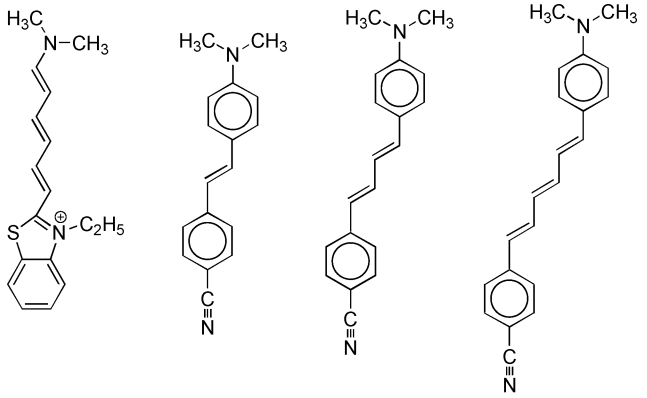

224 **225** **226** **227**

It is well known that the isomerization of ethylene, polyenes, and probably also cyanines proceeds through a conical intersection (COI) or a "photochemical funnel".[711] Recent high-level quantum-chemical calculations could even identify the structure of such a conical intersection.[466,712] They pointed to the importance of more than one bond being involved in the twisting process and highlighted the close relationship between COIs and twisted (TICT) structures.[713] Thus, the butadiene COI involves three perpendicularly twisted bonds and four unpaired electrons.[466] In view of the vast evidence that a single bond twisting can lead to dual fluorescence, the possibility arises to combine the seemingly separate observations of multiple fluorescence, anti-loose-bolt behavior, and photochemical isomerization through photochemical funnels into a common mechanistic model involving fluorescent and nonfluorescent twisted product species in the excited state.

An early mechanistic scheme was introduced nearly a decade ago with the three-state model (Scheme 14)

Scheme 14. Three-State Kinetic Model Used To Explain the Fluorescence Behavior of Donor−Acceptor Polyenes[714,715] and Ionic Derivatives[703] [a]

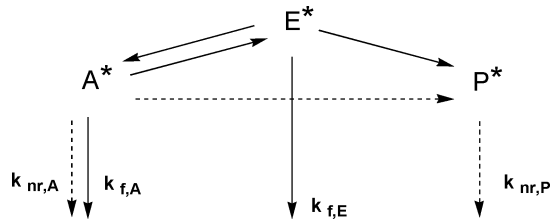

[a] E* is the highly emissive planar conformation, A* corresponds to one (or more) of the possible flexible single-bond conformations, and P* corresponds to the photochemical funnel involving twisting of the double bond and leading nonradiatively to the ground state. The presence or absence of a strong nonradiative channel from A* determines whether the compound shows a normal or an inverse loose-bolt behavior.

to explain the fluorescence behavior of **225**.[714] This model is able to explain the photophysics of compounds both with a normal and with an inverse loose-bolt effect. In the flexible dyes related to **220**, the nonradiative channel from the single-bond-twisted species A* is dominating. Fixing the conformation around the single bonds (**223**) closes the access to A*, which leads to a fluorescence enhancement (normal loose-bolt effect) and opens the photochemical trans−cis isomerization. If, however, $k_{nr,A}$ is unimportant, as in **225**, excluding the population of A* by bridging leads to an enhanced contribution of nonradiative decays via the P* channel (inverse loose-bolt effect).

DASPMI derivatives (**218**−**223**) can be regarded as unsymmetric cyanine dyes, in which aromatic rings bridge several of the bonds. These bridged cyanine dyes can be correlated with the corresponding unbridged cyanines if the interplay of the limiting structures (aromatic, polymethinic, polyenic) is properly taken into account according to the "triad theory" of organic dyes.[716−718] It is therefore not astonishing that unbridged cyanines, without aromatic bridging groups, can also exhibit such an anomalous behavior. This has been detected, e.g., for cyanine **224** and the bridged derivatives **228** and **229**.[703] In other related cyanines, a normal and an inverse loose bolt behavior can both be present, depending on which of the bonds is bridged selectively.[205]

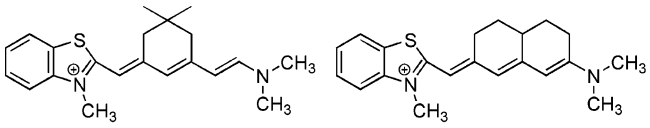

228 **229**

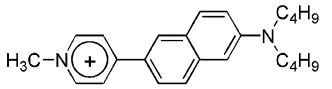

230

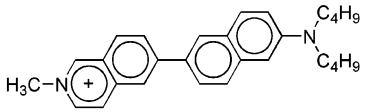

231

DASPMI and related compounds (especially **221**) can be used as fluorescence probes to sense the time profile of nerve pulses in living cells.[719,720] There are two possible explanations for this sensitivity: it can be due to an electrochromic effect on the dye embedded in the nerve membrane,[721,722] or it can be due to the environment sensitivity of the radiationless processes within the dye.[688,719] The model of three excited states (Scheme 14) can describe the latter mechanism. If the ratio of the photochemical rate constants depends on solvent polarity or, equivalently, on the electric field across a nerve membrane, then environment-sensitive fluorescence quenching is expected and observed.

A collection of such structures, which have been empirically optimized by Loew, Waggoner, and Grinvald,[721,723,724] is given by **221** and **230**−**231**. The most often used compound for nerve probes has been di4ANEPPS (the inner salt derivative of **230**).[719,720] It can be recognized that these structures possess a different number of annelated rings, but the central framework resembles that of DASPMI. According to the triad rules, the excited state therefore has a different proportion of polymethinic, polyenic, and aromatic character. It is conceivable that this influences the relative energetic position of the spectro-

scopic (E*) and the photochemical minima or funnels/conical intersections (A*, P*).

4. Triphenylmethane Dyes

a. Singlet Manifold. Since the pioneering work of Förster and Hoffmann[725] on the viscosity dependence of the fluorescence quantum yield of triphenylmethane (TPM) dyes, many further studies concluded a barrierless nature of the reaction coordinate involved (e.g., refs 461−463). This reaction coordinate was tacitly assumed to be connected with the twisting motion of the phenyl groups. Relatively few studies have been conducted which tried to investigate this point experimentally. Some early studies from Förster's laboratory investigated selectively bridged TPM model compounds,[726−728] and some of these compounds have been reinvestigated using time-resolved fluorescence techniques.[729] It was found that both an ability to twist and the donor−acceptor properties are important.[231,683,729,730] The most relevant structures are those of crystal violet and malachite green dyes and their bridged derivatives, **232**−**235**.

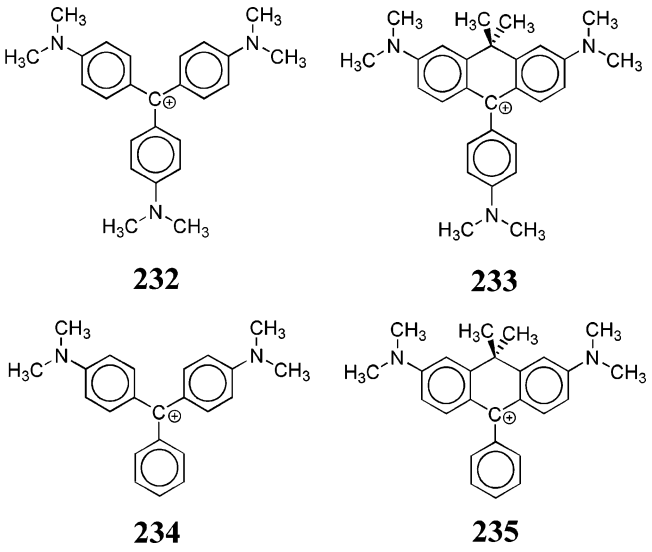

Figure 109 summarizes the temperature-dependent behavior of the fluorescence quantum yields of various TPM dyes in glycerol. Due to the high viscosity of this solvent, a limiting value of the quantum yield is approached already around 230 K, signifying that the large-amplitude intramolecular motions, which lead to fluorescence quenching, are frozen out. On the other hand, the effect of the excited-state reaction is shown by the reduction of fluorescence quantum yields toward rising temperatures. Interestingly, some of these dyes show a larger and some a smaller reduction of ϕ_f. This can be traced back to two factors: (i) the donor (and acceptor) properties of the moieties on either side of the twistable bond and (ii) the bridging pattern. The pairs of compounds **234/235** and **232/233** may serve as examples. Strong intramolecular fluorescence quenching is observed for **234** which is virtually absent in the bridged derivative **235** (a very minor quenching rate is still present, 2 orders of magnitude slower and connected with the still unbridged $-NMe_2$ groups). If **235** is accepted as a model compound for

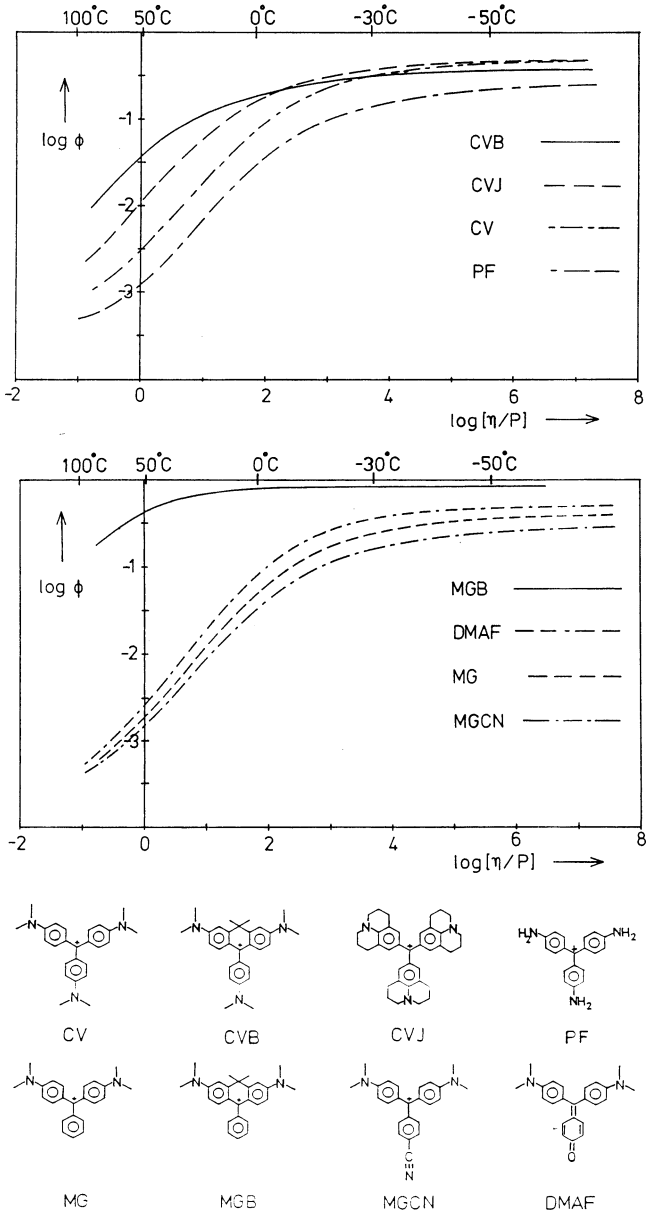

Figure 109. Fluorescence quantum yields of TPM dyes and their bridged model compounds (formulas and abbreviations in the lower part of the figure) as a function of temperature/viscosity in glycerol.[729]

234 (their excited-state energies are virtually identical), then the conclusion can be drawn that the fluorescence quenching is connected with the flexibility of the phenyl rings bearing the donor substituent. The flexibility of the third, unsubstituted ring is not relevant. This is corroborated by the fact that the quenching in **233** is sizable, only about 10 times smaller than that in **232**, because **233** possesses a donor-substituted flexible phenyl ring.[729]

These rules can be applied to other ionic (and nonionic) compounds, and further examples are the rhodamine laser dye **236** (see below: flexible phenyl group bearing an acceptor, large fluorescence quantum yield) and the donor-substituted derivative **241** (flexible phenyl group bearing a donor: ϕ_f reduced by several orders of magnitude[731]). This compound has applicational aspects because it can be used as a fluorescent on−off pH sensor (see below), e.g., for the interior of cells or for other microscopic purposes.

Many other fluorescent pH sensors are known,[732,733] but this compound is a beautiful example of one in which the photochemical quenching can be related to a detailed mechanism and therefore is amenable to optimization.

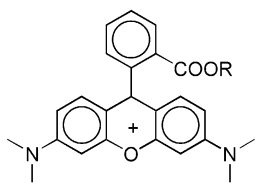

236

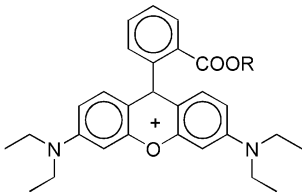

237

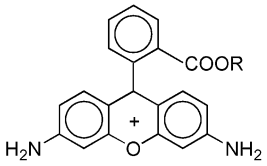

238

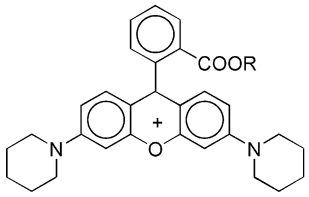

239

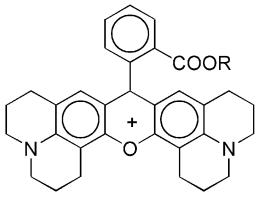

240

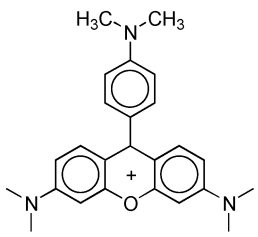

241

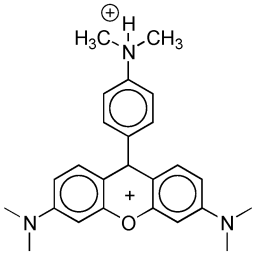

242

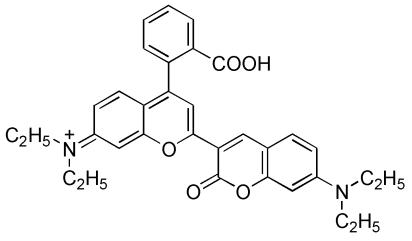

243

In the earlier investigations, the fluorescence decays of TPM dyes were most often described as biexponential.[734−736] Barrierless models emphasized that this biexponential decay is only apparent and that the decays are in fact of nonexponential nature.[463] Recent transient absorption and gain spectroscopic investigations could, however, positively identify two different excited species.[737−744] A more recent study, where transient absorption and time-resolved fluorescence were compared and globally analyzed, could even establish that both species are emissive.[745] Hence, the photochemically reached state of TPM dyes, often called S_x, is not a hot ground state[746,747] but an excited state.[739,740,742] One or both of these states decay according to a barrierless mechanism, leading to nonexponential fluorescence decay profiles. It is a challenge to understand how different species (precursor−successor) can be spectroscopically distinguished on a barrierless potential. Further experiments are needed to more precisely describe and explain the decay behavior of these states: S_x lives only a few picoseconds, and its lifetime seems to depend on viscosity and on the energy gap to the ground state.[741,742] If the nonradiative decay of S_x were only the internal conversion, its viscosity dependence would not be understandable. A possible extension of the kinetic scheme involving S_1 and S_x, used previously for TPM dyes, could therefore involve a further outstanding point on the S_1 surface, namely a conical intersection. If we introduce this idea, we can use the three-state kinetic scheme (Scheme 14) also for TPM dyes, identifying E* with S_1, A* with S_x, and P* with the conical intersection. Such a conical intersection can be expected due to the CT properties of the S_x state: CT involves charge localization on the donor, i.e., a donor radical cation linked to an acceptor neutral radical. This neutral radical, if flexible, is likely to have access to regions in phase space where S_1 and S_0 touch.[505,711,748]

Table 20. Triplet Lifetimes (τ_T) and Time Delays (τ_{delay}) of the Maximal Triplet Absorption after the Excitation Pulse for Crystal Violet (232) as a Function of Temperature[728]

	T/K				
	276	251	246	241	236
$\tau_T/\mu s$	10	220	500	1100	2700
$\tau_{delay}/\mu s$	6	38	70	120	300

Since the early studies by Förster and Hoffmann,[725] Oster and Nishiyima[749] and later Bagchi et al.,[463] the excited-state relaxation of TPM dyes has been assumed to occur on a barrierless potential. The barrierless nature of this potential has recently been confirmed experimentally[653,750] by comparing temperature- and pressure-induced rate changes, similarly as for **1**.[459]

b. Triplet Manifold. Due to the much longer lifetime of triplet states, photochemical reactions requiring large-amplitude motions are possible at much higher viscosities than for the singlet state. In fact, efficient triplet population occurs for TPM dyes only at low temperatures, where the matrix is sufficiently rigid that singlet photochemistry (to S_x and P*) is stopped. This is the case at ca. 260 K in glycerol.[728] Below this temperature, the transient absorption spectra of TPM dyes can readily be investigated. Three interesting features have been observed:[728] (i) the shape of the spectra strongly depends on temperature or matrix viscosity, (ii) the triplet lifetime is strongly viscosity dependent (Table 20), and (iii) the time trace of the absorption shows a rise behavior leading to delayed intensity maxima. This rise behavior is also slowed with increasing

viscosity such that the intensity maxima occur at longer times for lower temperatures (Table 20). Such a behavior could not be interpreted at the time of the observation some 30 years ago. It is, however, interpretable within the three-state model if it is assumed that this can also be active in the triplet state. Clearly, further studies in this respect are needed.

5. Rhodamine Dyes

Rhodamine dyes can be viewed as TPM dyes in which two dialkylaniline groups are rigidly bridged by an oxygen linkage, similar to compounds **233** and **235**. As the residual flexible phenyl ring is substituted with an acceptor group, fluorescence quenching from a low-lying charge-shift state does not occur, analogous to **235**. In many cases, there are, however, other flexible groups which may have strong donor character, e.g., in Rhodamine B (**237**) with two flexible dialkylamino substituents, or in **236**. This can lead to an alternative charge-shift quenching channel connected with rotation of this group. It has indeed been found very early by "trial and error" that bridged derivatives such as Rhodamine 101 (**240**) show a much better fluorescence behavior. The latter compound has a temperature-independent fluorescence quantum yield of unity,[751,752] whereas its flexible counterpart Rhodamine B (**237**) shows some fluorescence quenching at higher temperatures.[752] It can be shown by comparing other compounds with flexible amino substituents but of weaker donor character that the quenching channel is connected not only with twist but also with charge transfer. In these compounds, quenching is absent, e.g., in **238**.[753] By controlling the pretwist angle of the dimethylamino groups, the quenching rate can be enhanced or reduced, e.g., in **239**.[753] Also, acceptor variations change the quenching rate in a predictable manner.[754,755]

The above quenching due to the rotation of the dialkylamino groups is not very sizable in solvents such as ethanol at room temperature.[752−754] Opening the second channel due to rotation of a whole anilino group leads to much higher quenching rates. Such a comparison can be made for the amino-substituted rhodamine derivative **241**, which decays on the time scale of a few picoseconds in ethanol. In acidic ethanol, the dimethylamino group is protonated, and the compound **242** decays in the nanosecond regime.[731] Thus, it is understandable why protonation leads to a fluorescence enhancement of more than 2 orders of magnitude,[731] allowing very sensitive pH detection.[12] We can conclude that **242** has one (slow) quenching channel due to rotation of the $-NMe_2$ groups, while **241** possesses two quenching channels, the same slow one and a further one, faster by more than 2 orders of magnitude. In the TPM and rhodamine dyes, the inner flexible bonds are thus considerably more active than the outer ones in terms of photochemical reactivity leading to a quenching state.

In this context, it is interesting to note the connection to ordinary cyanine or polymethine dyes. TPM dyes can be viewed as bridged cyanine dyes in which bridging occurs through aromatic phenyl groups. This introduces some aromatic character into the polymethine properties and complicates the behavior which is dictated by the triad rules of color theory.[717] Comparative investigations for cyanine dyes bridged with nonaromatic bridges indicated a behavior contrary to that of the TPM dyes: the central bonds were found to be less active in photochemical quenching through rotation than the outer ones.[756] Moreover, the reactivity pattern depends sensitively on the number of π-atoms in the cyanine chain, as judged by comparison with quantum-chemical calculations on other systems.[757] The knowledge of the photochemical activity of flexible bonds is of high importance in molecular engineering of highly fluorescent dye systems. Not all bonds, but only the photochemically active ones leading to fluorescence quenching need to be chemically bridged. Thus, the molecule **243**, which still has three flexible bonds along the cyanine chain, is an efficient laser dye and shows sizable fluorescence quantum yields, even in polar solvents.[756]

6. Ionic Dye Systems Not Involving Amino Groups

Recently, several cases of pyridinium, pyrylium, and benzopyrylium systems bearing no amino nitrogen have been investigated which show either polar solvent-enhanced fluorescence quenching[758] or large Stokes' shifts,[759] or even dual fluorescence.[760−762] In the case of the benzopyrylium salts, bridged model compounds have clearly established the involvement of a rotation mechanism. While the fluorescence quantum yield of the flexible compound **244** is only 0.007 in butyronitrile, is rises to 1.0 for the bridged compound **245**.[758] If the donor system is biphenyl or

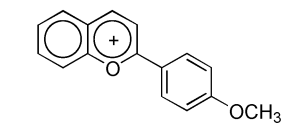

244

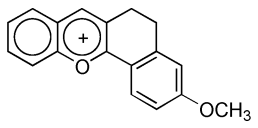

245

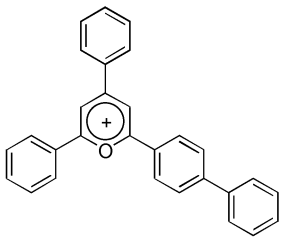

246

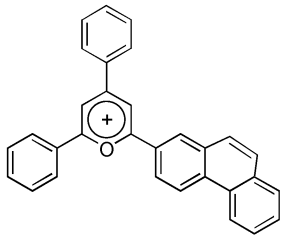

247

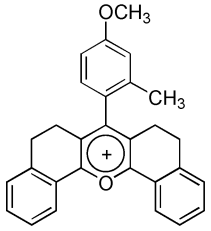

248

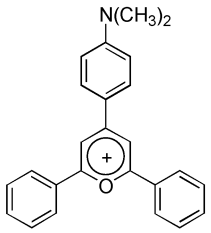

249

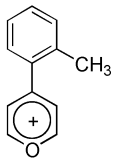

250

phenanthrene, as in **246** and **247**, the large Stokes' shifts observed at room temperature, which are

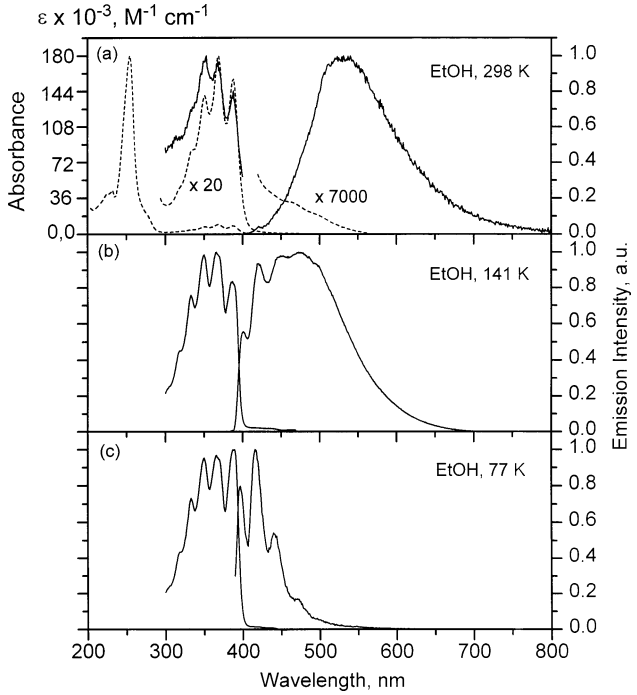

Figure 110. Absorption and fluorescence spectra of **251** in ethanol at different temperatures. At intermediate temperature, dual fluorescence is observed.[762]

absent at 77 K,[759] point to the possibility of strongly emitting charge-shift states. Some pyrylium dyes, such as **248**, show dual fluorescence[761] and substantiate the possibility of emission from a photochemical product state also in ionic compounds. Other related pyrylium dyes (**249**) decay mainly nonradiatively via an intermediate state which has been assigned TICT character[763,764] on the basis of both its viscosity-dependent formation rate and quantum-chemical calculations. Interestingly, its decay to the ground state is also viscosity dependent (an analogous observation has been made for TPM dyes, see above[742]). Sterically hindered simple pyrylium salts, such as **250**, exhibit a large Stokes' shift and a solvent polarity dependence, which corresponds to a large dipole moment change for the emitting state, $\Delta\mu^* \approx$ 15−17 D.[765]

An interesting behavior can be observed in dye systems which possess already a perpendicular conformation in the ground state, such as **251**.[762,766] In the absorption spectrum, a very weak, long-wavelength transition to a charge-shift state can be observed with an intensity corresponding to a radiative lifetime $\tau_r > 4000$ ns.[762] The fluorescence at room and low temperatures is strongly Stokes' shifted and dual (Figure 110), suggesting a reaction linking the two emissive states, one of LE anthracene type and the other of a charge-shift type. Interestingly, the radiative lifetime measured for the charge-shift emission is much shorter (79 ns) than that calculated from absorption. This seems to indicate a relaxation to an excited-state structure with more orbital overlap than for the relaxed ground-state conformation. Indeed, quantum-chemical calculations including excited-state optimization indicate a structure for the equilibrated charge-shift state which is perpendicular but bent at the pyridinium nitrogen and which is connected with a nonzero transition moment.[762] This behavior is clearly in contrast to the minimum overlap rule (section II.B.4), which postulates self-decoupling upon charge separation. A likely reason is the rehybridization behavior of nitrogen: if the nitrogen is in the donor moiety, as in **1** or **212**−**231**, the charge-shift or charge-transfer state involves a lowering of the electron density on the N atom. In the limiting case of complete ionization, the nitrogen acquires a trigonal, sp^2 hybridization; i.e., it is flat, as in NH_3^+. If the N atom is in the acceptor part of the molecule, charge shift or charge transfer leads to an increased electron density, favoring the pyramidal, sp^3-type hybridization, as in NH_3.[767,768]

An interesting case among the ionic CT excited states is a series of derivatives of the acridinium cation, which possess a donor substituent of intermediate strength, e.g., **252**. This compound exhibits not only a huge Stokes' shift (∼10 000 cm^{-1}) but also transient absorption spectra of the neutral acridinium radical and of the naphthalene radical cation.[769]

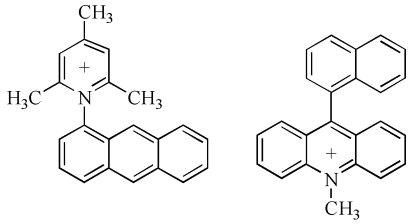

251 **252**

D. Coumarins and Spiro Systems

1. Coumarins

Some aminocoumarins (**253**, R = alkyl, R′ = CH_3 or CF_3), including numerous important laser dyes, emit a strong fluorescence with pronounced CT character. Because of strong solvent polarity and hydrogen-bonding effects, the coumarins were discussed in terms of a possible TICT state, **257**, which could be responsible for the emission.[786] Apparently,

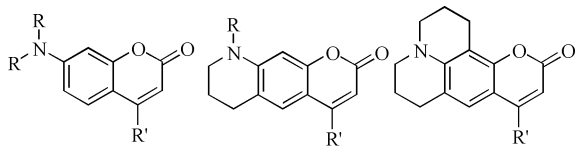

253 **254** **255**

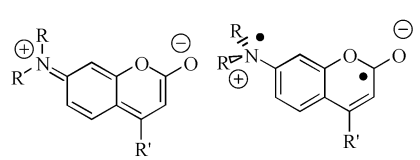

256 **257**

some evidence for a dual fluorescence was found in the two bands of the gain spectra (amplified spontaneous emission, ASE) in several of the coumarin dyes **253**,[770−772] in particular in the compound with R = C_2H_5, R′ = CH_3. The interpretation was in terms of a TICT emission in the long-wavelength band. Close

examination explained the unexpected effect in the gain spectra (as in the stationary fluorescence spectra only one band was observed) by the effect of damping the ASE by the transient absorption band of the excited dye, which is observed just between the two ASE bands.[773] A similar effect was recently reported for the "dual fluorescence" of **225** observed under high-intensity laser excitation.[710] Another explanation was discovered in the effect of traces of hydroxylic solvents in not sufficiently purified solvents, resulting in the emission from two forms of the dye—the uncomplexed and the hydrogen-bonded forms.[774,775]

The decisive evidence for the conformation of the fluorescent state can be drawn from the spectra and photophysical properties of the rigidly planar molecules (**254**, **255**). The emission spectra are closely similar to those of the compounds with a flexible $-NR_2$ group (**253**),[776,777] which disproved any suggestions concerning an emissive TICT state.[722,771,772] The emissive states of coumarins can be represented by the planar structures **256**.

The excited-state dipole moments of the coumarin dyes were measured by different methods. The values found with electrooptical methods, $\mu^* \approx 12-16$ D,[778] were the same for the flexible (**253**) and for the rigidly planar compounds (**255**), and did not change from the Franck−Condon to the equilibrated excited states. The solvatochromic data for the same molecule **253** ($R = C_2H_5$, $R' = CH_3$) resulted in $\mu^* = 9.2$ D.[779] For several compounds from all three groups, **253**, **254**, and **255**, the Lippert plots corresponded to $\mu^* \approx 12.5-14.3$ D, while the Suppan[780] plots resulted in reduced values, $\mu^* \approx 9.7-13$ D.[781] The time-resolved microwave dielectric absorption measurements in a similar group of coumarins resulted in the values $\mu^* \approx 8-12$ D.[782] On the basis of all these data, one can infer that (i) the CT property appears already in absorption and (ii) evidently, the emitters are the planar ICT states (**256**).[778]

There are, however, prominent differences between the flexible and the rigid coumarins, most importantly in their nonradiative deactivation. In the flexible molecules **253**, especially in those with $R' = CF_3$, the nonradiative rate increases with the polarity of the solvent (Figure 111), whereas in the rigidly planar ones, **254** and **255**, the effect is nearly absent.[776,777] The rate of the nonradiative process is also reduced by a partial immobilization of the flexible dye molecule by including it in a cyclodextrin cavity[783] or by binding it to the bovine serum albumin.[784] On the other hand, the nonradiative rates are enhanced for coumarins which bear a stronger acceptor substituent (COOR) in the lactone ring.[785] Now, most authors agree (supporting this by quantum-chemical calculations) that, in strongly polar solvents, and for coumarin dyes with a good acceptor substituent in the lactone ring, the TICT state becomes lower lying than the coplanar ICT state. The twisted ICT conformers **257** appear not as emitting states but as the source of a new deactivation channel, structurally corresponding to a TICT state, called a *nonfluorescent TICT state*.[781,785−788] There are also, however, other views contradicting this conclusion.[782,789]

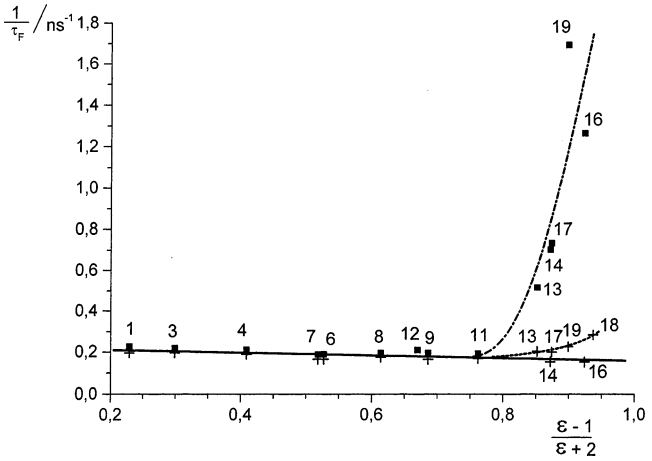

Figure 111. Inverse decay time, $1/\tau_f$, as a function of the solvent polarity function, $(\epsilon - 1)/(\epsilon + 2)$. Full points for the flexible **253** ($R = C_2H_5$, $R' = CF_3$), crosses for the rigid **255** ($R' = CF_3$). Numeration of the solvents as in ref 781. The upper branch of the crossed curve corresponds to the protic solvents. Used courtesy of Dr. K. Rechthaler.

New evidence for the nonemissive TICT states has recently been gathered for coumarin derivatives.[785] This class of compounds is important for biological and medical fluorescence labeling studies, and it is therefore vital to control the nonradiative channels that quench the fluorescence. Structures **258**−**261** show the maleimide used for specific labeling of thiol groups in proteins and several model compounds with a similar acceptor group in the 3-position of the coumarin ring. There is sizable fluorescence quench-

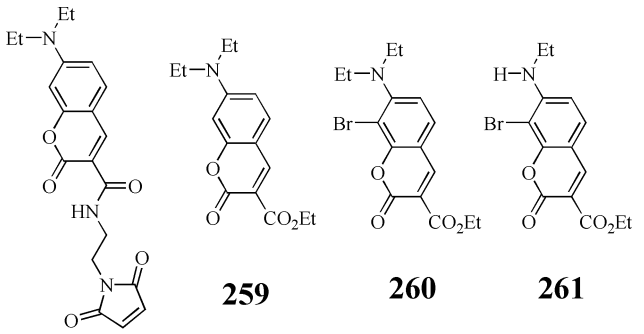

258 **259** **260** **261**

ing in **259** ($k_{nr} = 4.5$ ns^{-1}) which is strongly enhanced by ortho bromination in **260** ($k_{nr} > 20$ ns^{-1}). Heavy-atom-induced enhanced ISC can be excluded by the model compound **261**, which exhibits a 100-fold larger fluorescence quantum yield than **260**. The quenching in **260** can therefore be understood on the basis of enhancement of the formation of a nonemissive TICT state (already formed in **259**) due to the *steric* effect of the Br substituent.

2. Spiro Systems

The spiro compounds with separated donor and acceptor subunits represent a nearly ideal example of an intramolecular zero overlap, where an ICT process is still probable. The two very weakly interacting subunits are rigidly orthogonal and separated by two σ-bonds at a distance larger than in the hitherto discussed A−D molecules. The best studied

examples are the lactones of Rhodamine B (**262**)[155,790−793] and of Rhodamine 101 (**263**)[155,794] Both

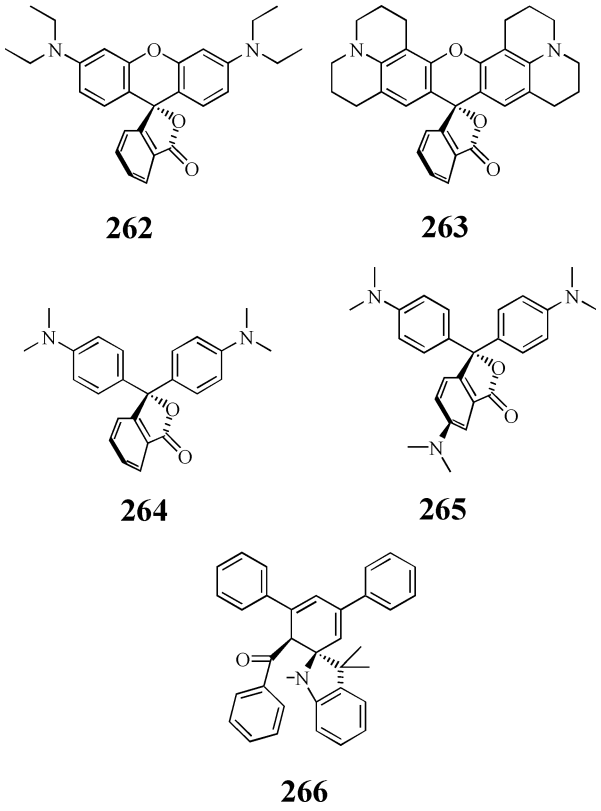

lactones emit a CT fluorescence[795] in all (aprotic) solvents, characterized by its very large Stokes' shift (~7000 cm^{-1} in nonpolar solvents, 12500 cm^{-1} in ACN).[790] The emission has forbidden character (k_f of the order of (3−6) × 10^6 s^{-1}) and a high dipole moment ($\mu^* \approx 25-26$ D).[155,790] It is remarkable that the radiative rate k_f, as well as the transition moment in emission, $M_{CT,G}$, remains nearly independent of the solvent polarity, within a factor of 2. This is similar to the prototypes of the TICT-state model compounds, **1**, **21**, and **22** (Table 5), but different from the CT states of numerous derivatives of anthracene, acridine, etc. (Tables 15 and 17). The high solvent-sensitivity of the emission rates of the latter compounds seems to be connected with the changes of their twist angle θ with the stabilization of the CT state. In contrast, in the lactones and in the molecules **1**, **21**, and **22**, the conformation of the CT state is close to $\theta = 90°$, independent of the polarity of the medium, due to the rigidity of the molecular skeleton or to the electronic structure inherent for the given molecule.

Similar CT emissions are observed from numerous other lactones or other spiro forms of numerous dyes, including the TPM dye lactones such as those of malachite green or of crystal violet, **264** and **265**.[796,797]

Other important photochromic spiro systems are, e.g., spiropyrans and spiroindolines.[798] In the case of the spiroindoline derivative **266**, the primary form emits a CT fluorescence. The solvatochromic effect indicates a considerable increase of the dipole moment upon excitation, $\Delta\mu^* = 14$ D.[799]

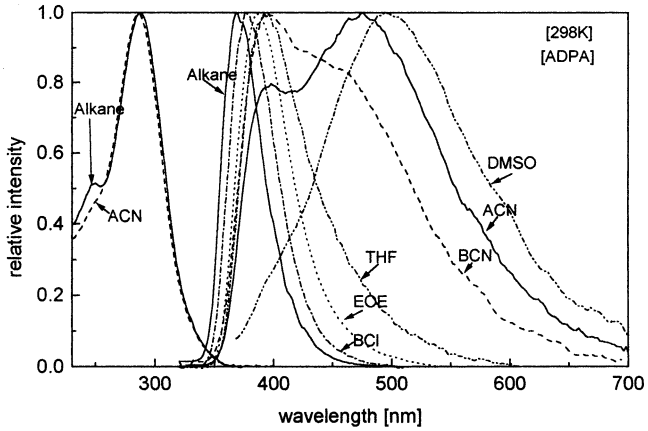

Figure 112. Absorption and dual fluorescence spectra of **267** at 298 K in solvents of different polarity (EOE, diethyl ether; THF, tetrahydrofuran; BCN, *n*-butyronitrile; ACN, acetonitrile; DMSO, dimethyl sulfoxide).

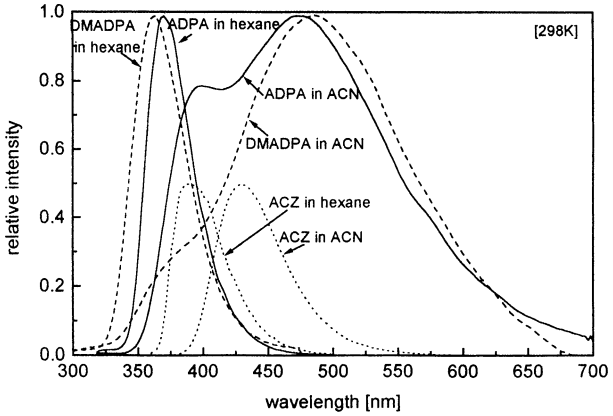

Figure 113. Fluorescence spectra of **267** (ADPA), **268** (DMADPA), and **269** (ACZ) in *n*-hexane and acetonitrile at 298 K.

E. Polyarylamines

1 can be viewed as an amine with one aromatic and two aliphatic substituents. The question can be asked what will happen to the dual fluorescence if one or more of the alkyl substituents are exchanged for aromatic groups. Several of these compounds have been investigated in the series of *N*-phenylnaphthylamines by Kosower et al.,[84,586,588,590,800] but well-separated dual fluorescence as in the case of **1** did not occur, and model compounds to test mechanistic hypothesis were not considered.

Recently, new evidence became available by the investigation of a series of diphenylamines with different donor−acceptor pattern and including sterically restricted model compounds[801−804] and aniline trimers. The most important evidence is represented in the Figures 112 and 113: the dual fluorescence of **267** (Figure 112) behaves very similarly to that of **1**, although no acceptor substituent in the usual sense is present in the molecule. Significant solvatochromic red shifts are observed for both bands and indicate CT character, with that of the long-wavelength (CT) band being stronger.

It is known from the studies on **1** and its derivatives that an amino group, as present in **267**, is not a sufficiently good donor to yield a low-lying TICT state. If the torsional relaxation of the excited state

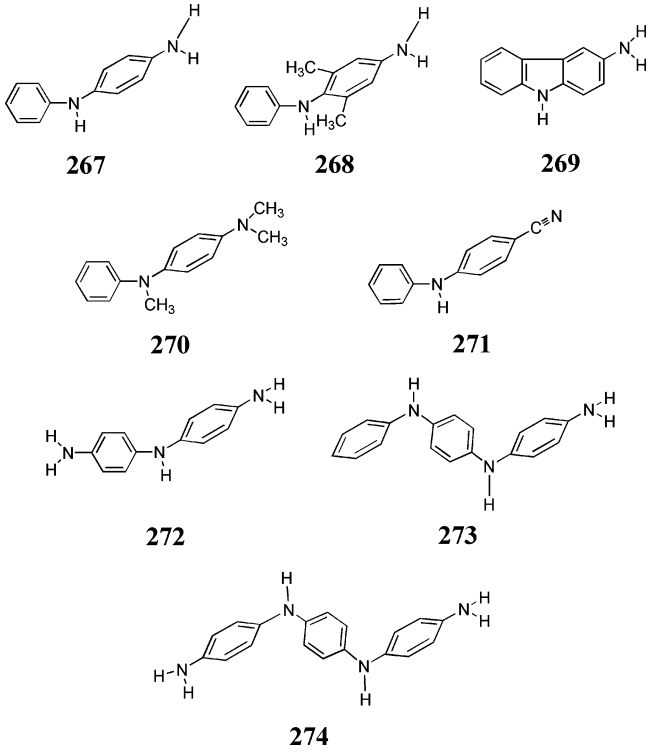

is the correct mechanistic description, then we can expect that the whole anilino group is involved in twisting, and we can check the hypothesis by using suitably tailored model compounds such as **268** and **269**. The resulting spectra are compared in Figure 113. In the nonpolar solvent *n*-hexane, all compounds exhibit only one fluorescence band, but that of **269** is somewhat red-shifted due to the ring closure by the direct bond between the donor and the acceptor, which introduces additional mesomeric interactions. In polar acetonitrile, these bands shift to the red for all three compounds, most strongly for **269**, indicative of its largest dipole moment (in *this* excited state), due to the flat molecular structure. Nevertheless, only the flexible compounds **267** and **268** develop a second fluorescence band in this solvent. Its absence in **269**, and its more pronounced presence in **268** than in **267**, give an indication that the important reaction coordinate favoring the second fluorescence band is connected with the twisting around the inner bond joining together the two aniline moieties in **267**.

267 is one of the few examples in which the compounds with amino instead of dimethylamino substituents show dual fluorescence, very similar to that of **1**. Another example is the anti-Lepra drug DAPSONE (4,4′-diaminodiphenyl sulfone).[805] From the bridging studies on Michler's ketone,[6] the corresponding ketone derivative (4,4′-diaminodiphenyl ketone) can be expected to behave similarly. Also, by analogy, *p*-(9-anthryl)aniline should show this type of dual fluorescence because the twist axis should be not the bond linking the amino but that linking the whole anilino group. This compound has recently been synthesized, and it reveals a ^{1}CT state which is close in energy to the lowest ^{1}LE state in the gas phase.[539] In solutions, it emits a CT fluorescence, very similar to that of the dimethylamino derivative, **26** (section XI.A.1).[539]

The compounds **267**−**274** can be used to draw a number of conclusions [802] regarding the fluorescence behavior of polyarylamines:

1. Molecular modeling studies indicate that the two phenyl rings in **267** in the most stable arrangement are unequally twisted with respect to the plane defined by N and the attached C atoms of the phenyl groups, the anilino moiety being more strongly twisted (66°), while the unsubstituted phenyl ring shows a weak twist (11−20°). This conformation corresponds to two relatively unperturbed aniline moieties joined by a bond, around which a strong twist occurs. The methyl groups in **268** induce a further pretwist of the anilino group (84°).

2. The fluorescence spectra evidence that the intensity ratio of the long-wavelength to the short-wavelength band (CT/LE) is always higher for **268** than for **267** (see Figure 113), establishing this bond as being important for the reaction coordinate because twisting of this bond leads to acceleration of the reaction.

3. A counter-example is **269**, in which stronger mesomeric interaction and higher dipole moments than in the LE state of **267** are present, but nevertheless, the CT fluorescence band is suppressed due to molecular rigidization of the bond, the twisting of which is necessary for the reaction.

4. The fully methylated compound **270** has a dual fluorescence very similar to that of **267**. This yields additional evidence that, unlike in **1**, the reactive bond is that to the anilino group and not to the $-NMe_2$ group.

5. Regarding the question of which of the two moieties in **267** is the acceptor and the donor, compounds **271** and **272** can be compared. For the donor-substituted **272**, the CT band is strongly reduced in its intensity, such that no evident dual fluorescence is present,[801] while **271** emits only the CT fluorescence, and the LE band is lacking.

6. The trimeric molecule **273** also shows dual fluorescence, however with a reduced CT component as compared to **267**, as could be expected from the study of **272**. **273** can be regarded as a model compound for polyaniline. Its LE band is somewhat red-shifted and indicates a larger conjugation length as compared to **267**.

7. Similar to **272**, the donor-substituted trimer **274** does not show dual fluorescence.

8. The photophysics of **267** indicate a more forbidden character for the CT emission (k_f(CT) $< 1 \times 10^7$ s^{-1}) than for the LE emission (k_f(LE) $\approx (3-4) \times 10^7$ s^{-1}), similar to DMABN, although the difference between the k_f values is not as large as for **1**.

9. Regarding a mechanistic description, the more forbidden character of the CT emission as compared to the LE emission cannot be explained with a state-coupling model such as the PJT mechanism.[8,133] That would require the coupled (CT) state to be more emissive than the LE state and, moreover, a pair of two closely spaced excited states, with S_1 being of lower polarity than S_2. From the strong solvatochromic red shift of the LE fluorescence, we can conclude a highly polar, hence ^1L_a-type, emissive S_1 state.

Regarding the cyano-bending mechanism also proposed for DMABN,[9,10] it would be difficult to apply it to the case of **267**, and the predictions regarding the behavior of **268** and **269** by both models are unclear, whereas they are straightforward within the TICT model and correspond to the experimental observation. A study of further derivatives of **270** indicated that the twisting around both bonds at the central nitrogen can lead to CT fluorescence.[806]

The charge-transfer phenomena evidenced by the dual fluorescence of aniline dimers and trimers are highly interesting due to the structural similarity of these compounds to polyaniline. This polymer possesses applicational aspects especially due to its electrical conductivity, which is connected with partial oxidation of the polyaniline backbone.[807] It is to be expected that there are parallels between an optically excited CT state of a neutral species and the ground state of the electrically conducting partially oxidized form of polyaniline, because in both cases electron transfer is involved, moving the electron one step farther along the chain. It could therefore be highly promising to study the connection of electrical conductivity of polyaniline with the twist angle between successive aniline units.

F. Triaryl Phosphinoxides

Triphenylphosphines are formally related to the di- and triarylamines discussed above. Their derivatives, **275**, **276**, and **277**, with a varying number of $-NMe_2$ groups, were reported to exhibit dual fluorescence with a precursor−successor behavior (Figures 114 and 115). Their characteristics are similar to those

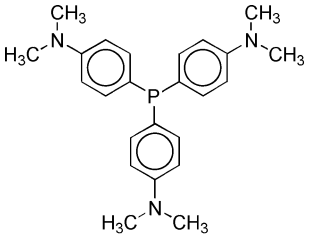

275

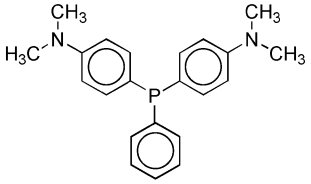

276

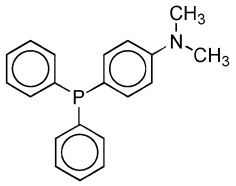

277

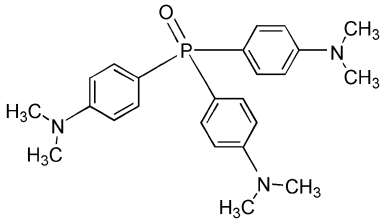

278

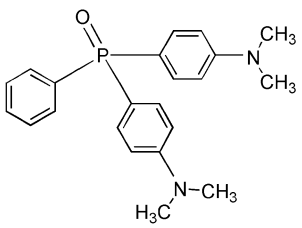

279

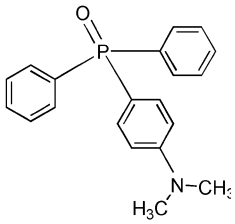

280

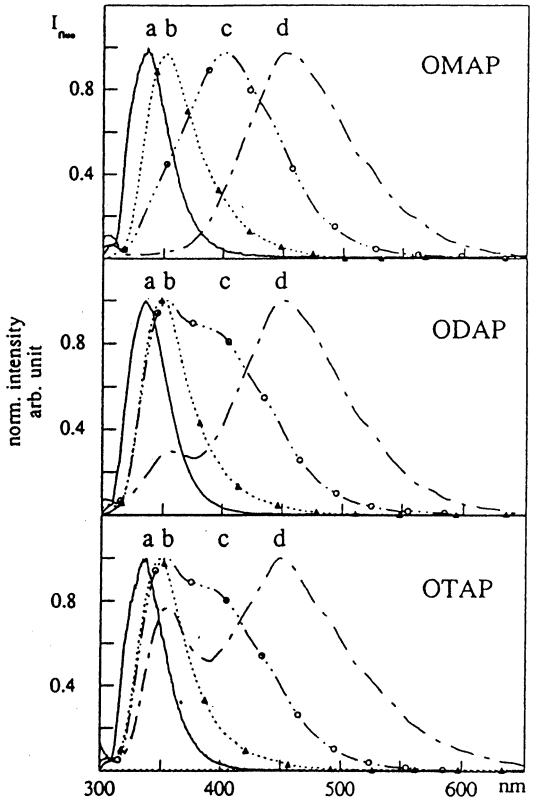

Figure 114. Fluorescence spectra of the dimethylamino-substituted triphenylphosphine oxides **278** (bottom, OTAP), **279** (middle, ODAP), and **280** (top, OMAP) in solvents of increasing polarity: (a) CHX, (b) dioxane, (c) THF, and (d) ACN. Adapted with permission from ref 811. Copyright 1997 Elsevier Science.

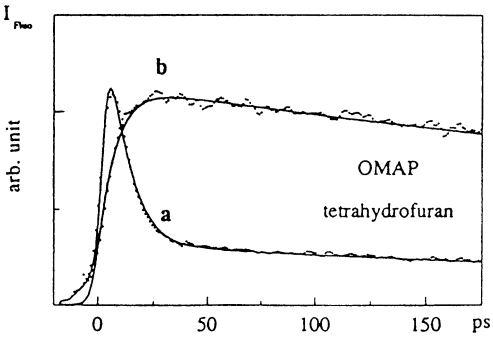

Figure 115. Precursor−successor behavior of **280** (OMAP) in THF, (a) monitored below 400 nm and (b) above 450 nm. Adapted with permission from ref 811. Copyright 1997 Elsevier Science.

of DMABN, i.e., a well-separated long-wavelength band of CT origin, the importance of which increases with increasing solvent polarity and with a reduction of the number of $-NMe_2$ substituents.[808−810] In more recent measurements, it became clear, however, that the emitting molecules in all these cases were in fact the oxidized compounds, **278**, **279**, and **280**, which form very rapidly during the solvation process if aerated solvents and small solute concentrations are used.[467,811] Nevertheless, previous experimental findings and conclusions remain valid if this initial oxidation is taken into account.

The compound series **278**, **279**, and **280** is interesting from the point of view that the compound with the smallest number of $-NMe_2$ groups, **280**, exhibits

the strongest charge-transfer band. This leads to the conclusion that not all $-NMe_2$ groups in **279** and **278** are engaged as donors in the electron-transfer process; their role is more that of a donor group situated on the acceptor side and modulating its acceptor strength. Thus, for **278**, the smallest acceptor strength results and, correspondingly, the slowest charge-transfer rate constant.[809] Only one of the dimethylanilino groups seems to act as the electron donor in the ET process. The nature of this donor group could be proved by transient absorption spectroscopy.[809,810]

If a twisting motion of this donor is involved along the reaction coordinate, a viscosity dependence different from that of **1** should be expected, because in the latter compound the size of the donor group is much smaller. To separate polarity and viscosity influence, the two nearly equipolar solvents, tetrahydrofuran and glycerol triacetate (triacetin), were compared. A strong difference between the viscosity dependence of **280** and **1** was found. Whereas for DMABN the reaction rate was slowed very little from tetrahydrofuran to triacetin, the viscosity effect was very strong for **280**.[467] This was interpreted as evidence for a different reaction coordinate for the two compounds, in accordance with the expectation from the TICT model with the differently sized twisting moieties in the two cases.

XII. Charge-Transfer Triplet State

In contrast to the CT processes and properties in the singlet manifold, those related to the triplet CT states were much less studied. No evidence for an absorption or emission from the ^{3}TICT state of singly bonded D−A compounds was found prior to the recent reports.[307,812]

All quantum-mechanical calculations indicate that the lowest triplet state of DMABN is the $^3A_1$ (^1L_a) state. With varying substitution, the phosphorescence maximum shifts in parallel with the $^1L_a \leftarrow S_0$ absorption,[347] which hints at a common orbital character of the triplet and singlet excited states of L_a character. Phosphorescence spectra were usually recorded in rigid low-temperature glasses, in which relaxation to the ^{1}CT state does not occur, and the phosphorescence derives from a triplet state of geometry similar to that of the ground state. In the case of the twisted derivatives, **16** and **21**, the phosphorescence was observed also in cool liquid ethanol or *n*-propanol, its spectral position being only negligibly red-shifted as compared to that of the alcohol glass at 77 K, in contrast to the strong red shift of the ^{1}ICT fluorescence. The phosphorescence in cold liquid solvents does not shift with the polarity of the medium. Hence, the dipole moment of the emitting triplet state should be similar to that of the ground state.[135,813] In the case of **1**, the weak phosphorescence in cold viscous solvents is overlapped by the tail of the much more intense F_B fluorescence. The interpretation of the emission in polymers is usually still more difficult.

The lowest triplet state of DMABN is not a ^{3}CT, but a "*locally excited*" $^3A_1$ state of planar conformation, irrespective of solvent polarity.[347] The $T_n \leftarrow T_1$ absorption spectrum of a ^{3}TICT state should be nearly identical to the $S_n \leftarrow S_1$ absorption of the ^{1}TICT state, i.e., to the sum of the component D^+ and A^- radical ions. The $T_n \leftarrow T_1$ absorption spectra of **1** and of its derivatives, **16**, **17**, and **21** (in fluid solvents), are closely similar to the absorption spectrum of the planar compound **20**,[335] but are clearly different from the absorption spectrum of the benzonitrile radical anion or that of the ^{1}TICT state of DMABN.[133,814,815] Also, the triplet-state zero-field splitting parameter *D* is very similar for the compounds **1**, **15**, **16**, **17**, and **21**, 0.090−0.098 cm^{-1},[347] the values being typical for $^3(\pi,\pi^*)$ systems of such benzene derivatives.

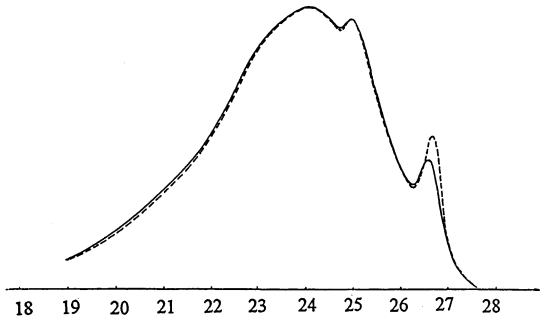

Figure 116. Phosphorescence spectra of **22** (solid curve) and of benzonitrile (dashed curve) in ethanol glass at 77 K. Adapted with permission from ref 347.

There is ample evidence that the lowest triplet state of **1** and of many of its analogues is not a CT state, but rather it is the (π,π^*) ^3L_a state, with a dipole moment intermediate between those of the ground state and the B* (^1L_a or ^1L_b) state, markedly less than that of the corresponding ^{1}ICT state. The evidence is based on results of TRMC[96,99,218] and of optoacoustic measurements.[816,817] The dipole moments of the lowest triplet state of both **1** and the coplanar **55** were estimated as ∼11 D (i.e., the ^3L_a state of **1** being planar[307]). The dipole moment of the $^3(\pi,\pi^*)$ state of the nonplanar **21** is found to be ca. 8 D.[96]

Similarly, other pretwisted derivatives of **1**, or the pyrimidine derivative **79**, which emit practically exclusively the F_A fluorescence, show the phosphorescence from the non-CT $^3(\pi,\pi^*)$ state.[265,347,525] The case of the rigidly perpendicular derivative **22** is very spectacular: its phosphorescence spectrum (and the phosphorescence lifetime) is practically identical to that of benzonitrile[132,347] (Figure 116). The main band (∼21 000 cm^{-1}) in the triplet−triplet absorption spectra of both compounds is also practically indistinguishable (Figure 117), and the triplet-state zero-field-splitting parameters D^* ($\Delta M = 2$) are in excellent agreement, 0.1379 and 0.1386 cm^{-1} for **22** and benzonitrile, respectively.[347]

From other data scattered in the literature, one can infer that a majority of the TICT-state-forming D−A molecules have their lowest triplet states of similar *non-CT* nature. Rather unexpectedly, the rate constant of ISC in the case of **1** is almost independent of the nature of the lowest singlet state (Table 21).[347]

Some triplet yields, ϕ_T, determined earlier by photosensitized isomerization[7,94] or by the photoacoustic method,[818] show an increase as the molecule can deviate from planarity, i.e., in the order ϕ_T(**20**) < ϕ_T(**1**) < ϕ_T(**21**).[94,347] An increase of ϕ_T is also

Table 21. Triplet-State Yields, ϕ_T, and Intersystem Crossing Rates, k_{ISC} (in 10^8 s^{-1} Units)

	in hydrocarbons			in aprotic polar solvents			in ethanol	
compd	solvent	ϕ_T	k_{ISC}	solvent	ϕ_T	k_{ISC}	ϕ_T	k_{ISC}
20[a]	HEX	0.75	1.4				0.16	2.0
1	HEX	0.80[a]	2.4[a]	THF[c]	0.69	1.57	0.55[a]	2.0[a]
		0.18[b]	0.62[b]	DIOX	0.37[b]	1.05[b]		
		0.76[g]			0.39[d]	0.97[d]		
	n-heptane[c]	0.73	2.15		0.63[c]	1.62[c]		
	CHX[d]	0.18	0.62	ACN	0.40[b]	1.00[b]		
					0.37[d]	1.05[d]		
					0.60[c]	1.36[c]		
16[a]	HEX	0.62	7.4				0.70	2.1
17[a]	HEX	0.32	7.1				0.57	2.0
21	HEX	0.95[a]	8.4[a]	DIOX[b,d]	0.74	4.6	0.74[a]	2.5[a]
		0.67[b]	6.7[b]	ACN[b,d]	0.59	1.8		
	CHX[d]	0.67	6.7					
42[g]	HEX	0.94	10.					
22[a]	HEX	0.95	9.5				0.75	3.4
BN[a,e]	HEX	0.51	0.33				0.28	0.35
11[c]	*n*-heptane	~1.0		THF	0.50			
				ACN	0.24			
107[f]	HEX		1.42	CH_3COOEt		0.88		
				CH_2Cl_2		0.54		
				ACN		0.49		
108[f]	HEX		1.15	CH_3COOEt		1.08		
				CH_2Cl_2		1.06		
				ACN		0.76		
292[h]	cyclopentane		0.05	BCN		0.03		

[a] Data from ref 347. [b] Data from ref 94. [c] Data from ref 816. [d] Data from Visser, R. J.; Weisenborn, P. C. M.; Varma, C. A. G. O.; de Haas, M. P.; Warman, J. M. *Chem. Phys. Lett.* **1984**, *104*, 38. [e] Benzonitrile, for comparison. [f] Data from ref 363. [g] Data from ref 170. [h] Data from ref 538.

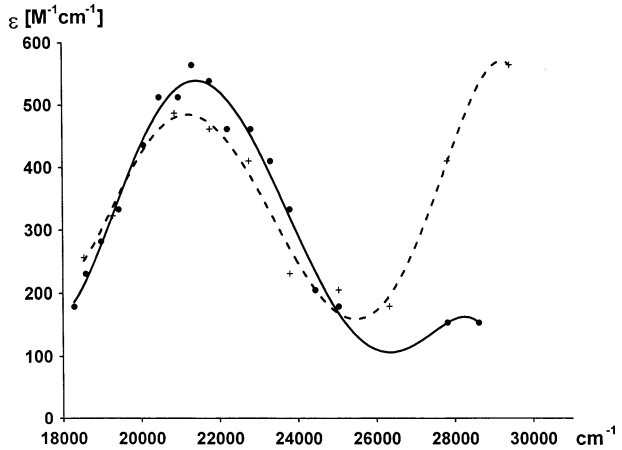

Figure 117. Triplet−triplet absorption spectra of **22** (crosses) and of benzonitrile (dots) in *n*-hexane, T = 293 K, 0.1−0.5 μs after the excitation laser pulse. Adapted with permission from ref 347. Copyright 1993 Elsevier Science.

noted with increasing alkyl length in the $-NR_2$ group.[99] With increasing solvent polarity, the k_{ISC} values of the pretwisted compound **21** are decreasing. (Table 21). Similar solvent polarity effects were noted for the external heavy-atom quenching of the fluorescence of **107** and **108** by CH_3I.[363]

With increasing polarity of the solvent, the energy difference between the highly polar ^{1}CT and the less polar lowest triplet state decreases, but the corresponding k_{ISC} values decrease in parallel,[819] apparently violating the energy gap law.[348,349,820] For a small energy gap, the kinetics belong to the initial (*classical*) range of the energy gap rule; the ISC may be considered as a thermal charge recombination in the *normal* Marcus' region. ISC slows with decreasing singlet−triplet energy gap (decreasing driving force) as the solvent polarity increases. Another suggestion was related to the angular distribution function around the ^{1}TICT equilibrium twist angle, getting narrower with growing solvent polarity,[13] but such an explanation would be inapplicable for the rigid compound **22**.

Despite the early suggestions[3,4] connected with the near degeneracy of these states, no direct evidence for a ^{3}TICT was found in the deactivation pattern of ^{1}TICT of **1** or its derivatives, until Hashimoto and Hamaguchi[307] found, in the time-resolved IR spectrum of **1** in butanol, a broad band around 2040 cm^{-1}, with a lifetime in the hundreds of nanoseconds range. The band disappeared in the presence of O_2 (Figure 54) and was therefore ascribed to a triplet state. In the nonpolar solvent hexane, instead of this band, another unusually broad band appeared around 2000 cm^{-1}. This band decayed at the same time as the (negative) depletion band of the ground state at 2216 cm^{-1} and disappeared in the presence of O_2. It was ascribed to a different triplet state, which relaxes directly to the ground state, being distinct from that characterized by the 2040 cm^{-1} band in butanol solution. The 2040 cm^{-1} band was tentatively ascribed by the authors to the transient ^{3}TICT state of **1**. Indirect evidence for the ^{3}CT is ambiguous.[821] The ease of detection of the intermediate ^{3}CT state would depend on the question of which of the consecutive processes is faster: k_{ISC} (from the ^{1}CT to the nearly degenerate ^{3}CT state) or k_{BET} (relaxation of the ^{3}CT to the $^3(\pi,\pi^*)$ state).

Other experiments proved the IR band to be due to the non-CT ^{3}LE state.[822] Time-resolved resonance Raman spectra,[821] including the study of the ^{15}N and

d_6 isotopomers of DMABN (and in the ring-deuterated DMABN-d_4[322]), in conjunction with transient absorption, helped in reassigning the triplet state of DMABN in polar solution. While Hashimoto et al., in their previous transient IR study of the triplet state of **1**, had identified the band appearing at 2040 cm^{-1} only in polar (butanol) solution and therefore assigned it to the ^{3}TICT state,[307] in the new study this band was observable in both hexane and methanol solution (at a delay time of 100 ns). From the comparison of isotopomers, the band at 1361 cm^{-1} is identified as the $C_{phenyl}-N_{amino}$ stretch vibration in the triplet state, quite similar to the ground state (1370 cm^{-1}) and not showing any strong downshift as was observed for the ^{1}ICT state (1281 cm^{-1}). From this, and from a considerable lowering of the cyano group stretch frequency (from 2210 cm^{-1} in the S_0 state to 2035 cm^{-1} in the T_1), it is concluded that the T_1 state of DMABN is of (nearly) planar structure (^1L_a-type 1,4-biradicaloid character with quinoidal ring deformation), but the resonance interaction to the amino nitrogen is weak. This state has a considerable CT character within the benzonitrile part of the molecule, with the ring (not the amino group) acting as the donor and the negative charge being localized on the cyano group.

The ^{3}CT states, prior to their observation in the singly bonded D−A compounds, were found in molecules in which the D and A entities were farther apart, separated by an insulating bridge or spacer, such as **281**−**283**.[823−825] The appropriate redox potentials of D and A were needed to shift the energy level of the ^{3}CT state below the locally excited triplets of D or A.

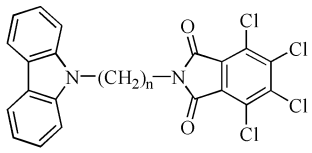

281
n = 2, 3, 4, 7

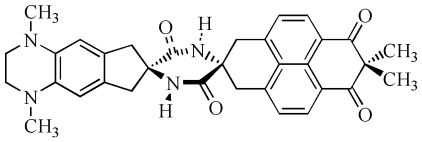

282

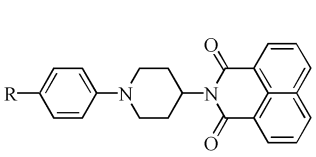

283
a: R = H
b: R = OCH_3

Studies of polymethylene-linked carbazole derivatives **281** were performed by the TRMC technique

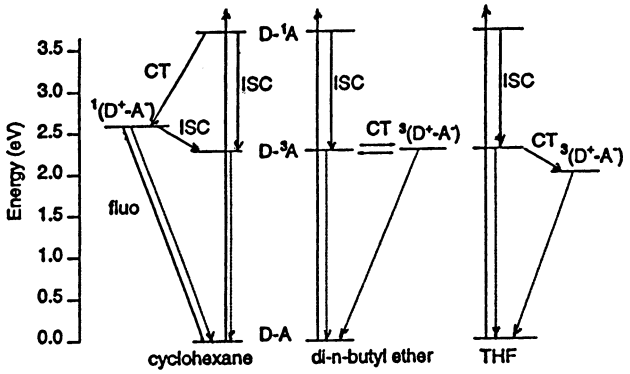

Figure 118. Energy scheme of the excited states and the deactivation processes in **283b** depending on the solvent polarity, which determines the energy of the highly polar and nearly degenerate ^{1}CT and ^{3}CT states. Reproduced with permission from ref 825. Copyright 1996 American Chemical Society.

in nonpolar and medium-polarity solvents. Highly dipolar singlet and triplet states were reported.[823] The differences in microwave conductivity signals were interpreted as resulting from different ways of ^{3}CT state population. In the case of **281** ($n = 2-4$) it occurs by ISC from the ^{1}CT state, after the electron transfer; in the case of $n = 7$ it occurs also via the local acceptor triplet state. Rough estimation of the dipole moment of the CT states resulted in $\mu \approx 10-15$ D, relatively insensitive to the length of the polymethylene bridge and to the solvent. Hence, the authors conclude a similarity of conformations in all cases, i.e., the folded conformation resulting from a harpooning (cf. section I.D) which follows the ET.

In **282**, highly effective population of the ^{3}CT state was found, $\phi_T \approx 1$. Local excitation in the acceptor unit is followed by a rapid ISC, ^{1}LE → ^{3}LE, and subsequently by electron transfer from the diaminobenzene derivative donor across the cyclic dipeptide bridge, within the triplet manifold: ^{3}LE → ^{3}CT.[824]

A nonemissive, long-lived ^{3}CT state, formed with high yield, was found in **283a**,**b**, i.e., in molecules with a smaller spatial separation between D and A than in **281** or **282**. The scheme in Figure 118 illustrates the ways of populating the ^{3}CT state, depending on the solvent polarity.[825] The transient absorption spectra were composed of the local triplet of the acceptor and of the radical ion species, in proportions depending on the solvent polarity.

In nonpolar solvents, the locally (^{3}A) excited state of **283b** is the lowest triplet state, whereas in polar solvents, the ^{3}CT state is the lowest one. In the case of **283a**, containing a weaker donor entity, both triplets appear in the transient absorption spectrum, even in strongly polar ACN. In the singlet manifold, it is the energy gap law that governs the competition between the local ISC and the CT process. The LE singlet−triplet separation is rather insensitive to solvent polarity, whereas the ^{1}LE−^{1}CT energy gap becomes very large in polar solutions (e.g., more than 1.5 eV in the Marcus' *inverted region*), and the electron transfer slows (Figure 118), which can occur only within the longer-living triplet manifold.[825]

A systematic search for the lowest triplet to be of CT nature in singly bonded D−A molecules was done

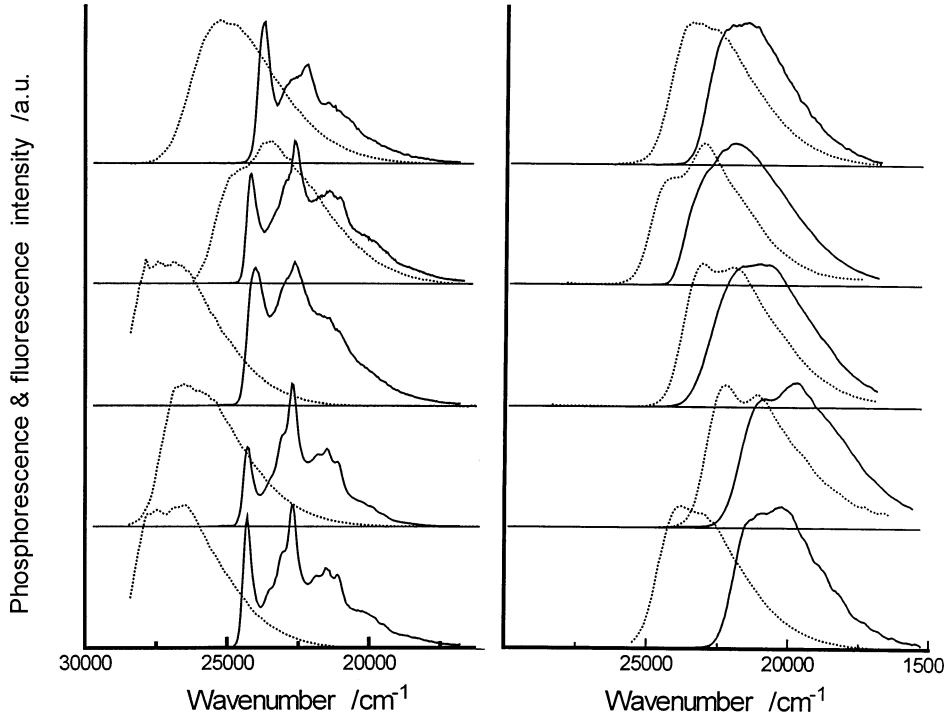

Figure 119. Luminescence spectra of **284**−**288** (left panel, from top to bottom), and (on the right panel, from the top) of **289**, **290**, **292**, **291**, and **293**. The fluorescence spectra (dashed) in *n*-hexane (left panel) or in MCH (right panel) were recorded at room temperature, and the phosphorescence spectra (solid curves) were recorded in *n*-propanol glass at 77 K. Adapted with permission from ref 812. Copyright 1996 Elsevier Science.

on the basis of the choice of appropriate redox potentials of donor and acceptor.[812] Such ^{3}CT states were reported for the *N*-dicyanobenzene derivatives of carbazole in a comparative study of a series of structurally closely related compounds, **284**−**293**.

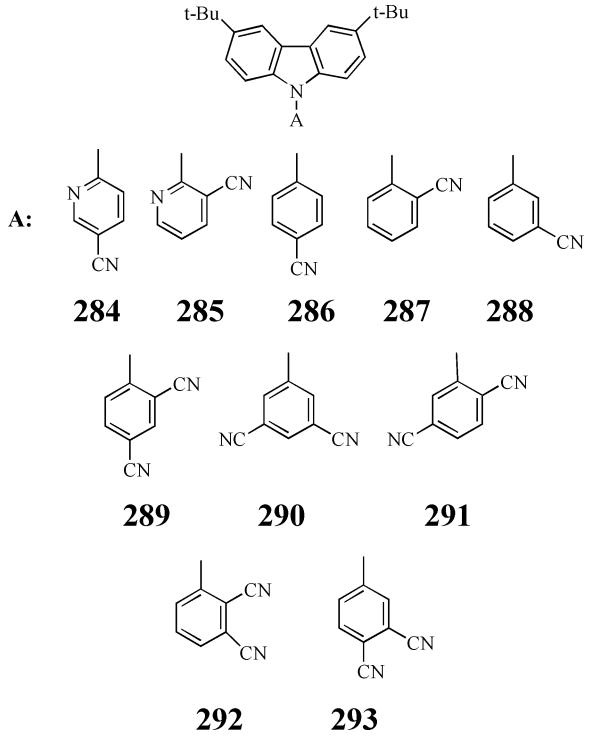

An inspection of the phosphorescence spectra (Figure 119) reveals spectacular differences between the compounds **284**−**288** and **289**−**293**. In the first group, the phosphorescence spectra resemble that of carbazole (donor π-electron system); in the second group, comprising the dicyanobenzene derivatives, the phosphorescence bands are quite different: broad and rather structureless, as is usually the case for the CT bands. In the *solid rotator* polar solvent, tetramethylene sulfone (TMS), the solvent reorientation occurs even at 77 K; the phosphorescence of **291** is noticeably red-shifted with respect to that in MCH, indicating a higher dipole moment in the emitting triplet state than in the ground state.[812,525]

A plot of the transition energy of the emissions of the compounds **284**−**293** vs the difference in redox potentials of D and A (Figure 120) demonstrates clearly that the phosphorescence of the dicyano derivatives (**289**−**293**) is emitted from the ^{3}CT state. The phosphorescence of the monocyano derivatives (**284**−**288**) is close to that of the di-*tert*-butylcarbazole (CAR); i.e., the ^{3}LE state is observed, with excitation localized in the donor unit.

At somewhat higher temperatures, a delayed CT fluorescence was observed, as the small energy gap found in the dicyano derivatives, $E(^1\text{CT}) - E(^3\text{CT}) < 1000$ cm^{-1}, promotes the intramolecular thermal repopulation of the ^{1}CT from the ^{3}CT state.

The two groups of compounds studied differ also in their phosphorescence lifetimes (4−6 s for the compounds **284**−**288**, but only 0.3−0.8 s for **289**−**293**). Analogously, the zero-field-splitting (ZFS) parameters of the triplet state, $D^* \equiv (D^2 + 3E^2)^{1/2}$, amount to 0.103−0.106 cm^{-1} in the first group and to 0.05−0.08 cm^{-1} in the second group of compounds. The low ZFS values indicate that the spin-to-spin distances are larger, clearly indicating the separation of spins (and charges) in the biradical, as opposed to the first group, typical $^3(\pi,\pi^*)$ LE states, in which

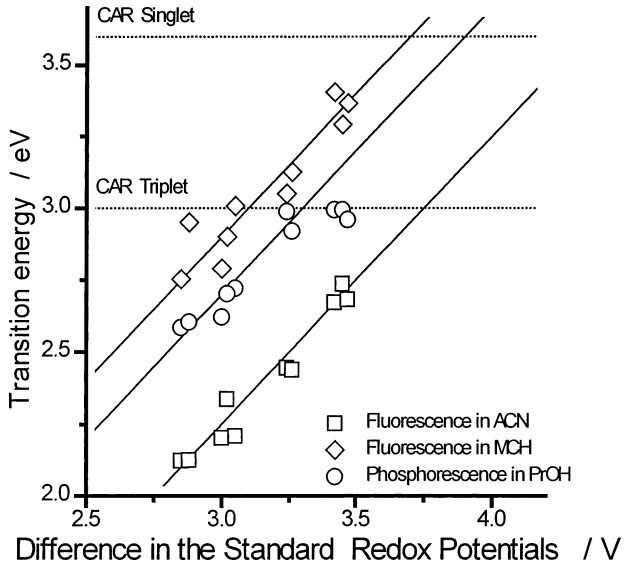

Figure 120. Emission maxima plotted vs $E^{o}_{ox}(D) - E^{o}_{red}(A)$, measured in ACN. From left to right: **291**, **293**, **292**, **289**, **290**, **285**, **284**, **288**, **287**, and **286**. The diamonds and squares refer to the room-temperature fluorescence in MCH and ACN, respectively; circles refer to the phosphorescence in PrOH at 77 K. Adapted with permission from ref 812.

both unpaired spins are localized on the same donor (carbazole) unit. The difference between the two groups of compounds is documented also by phosphorescence anisotropy measurements.[525,812]

Indirect evidence, interpreted in favor of the involvement of a ^{3}CT state in a deprotonated intermediate of DMABN, is based on the three-photon ionization of **1**.[826] Due to the complex multistep mechanism, this conclusion calls for further direct experimental testing.

Phosphorescence and ESR of a series of *N*-phenylphenothiazines, **294**−**298**, were studied to elucidate the nature of the triplet states.[827] In the molecules with a donor substituent, **294** or **295**, the triplet

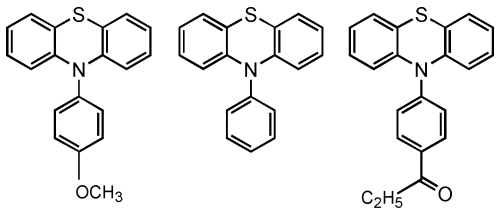

294

295

296

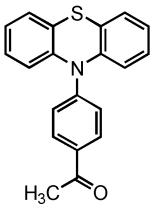

297

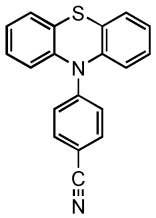

298

excitation is localized on the phenothiazine unit. In those with an acceptor substituent, **296**−**298**, the phosphorescence is similar to that of the acceptor unit (although the phenothiazine triplet is energetically lower lying), and the ZFS corresponds to a delocalization of spins. With increasing temperature (and softening of the matrix), the phenothiazine phosphorescence spectrum appears, at the cost of that observed at the lowest temperatures. The phenomena are explained by the experimentally observed folding of the phenothiazine rings in the crystal structures, whereby the phenothiazine N atom is partially conjugated to the substituent only in the case of acceptor substituents, **296**−**298**. In soft matrices, there is a structural relaxation (flattening of the phenothiazine ring), and the phosphorescence becomes similar to that in phenothiazine.[827] These results demonstrate an increasing variety in behavior and structural changes within a group of apparently closely similar D−A molecules.

The ^{3}CT state of the rigidly bridged D−A compound **299**, with fully separated charges, decays within several microseconds, as shown by the decay of transient absorption of its acceptor radical anion subunit. The singlet−triplet energy separation in these CT states is estimated to be considerable, ∼200 cm^{-1};[828] hence, the ISC process ^{1}CT → ^{3}CT is slow. Therefore, the ^{3}CT state of **299** is undetectable on direct excitation but populated by sensitization (T → T energy transfer from the benzophenone triplet).

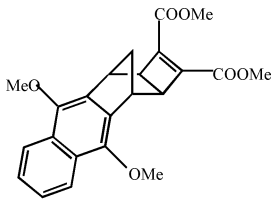

299

For the D−A molecules linked by a single bond, as in **1**, the mean distance between the separated spins is much less than that in **299**; hence, the S−T separation should be larger than that in **299**, and the ^{1}CT → ^{3}CT ISC should be still slower than that in **299**. This justifies the conviction that the ^{3}CT state is not populated from the ^{1}CT state in **1** and plays no noticeable role in the ISC of the latter leading to the ^{3}LE state.[347,829] This contradicts the tentative evidence from the time-resolved IR spectra,[307] cf. Figure 54, which has to be abandoned anyway in view of more recent experimental results.[821] The situation is different, of course, if the lowest-lying triplet is a ^{3}CT state, e.g., in the molecules **289**−**293** above.

XIII. Conclusions and Open Questions

A. General Conclusions

The structural changes which appear in the CT state along with the electron transfer are determined by the following factors:

(i) the structural changes (*i.a.*, rehybridization) connected with the localization of one excess electron in the acceptor unit, A^-, and with the deficiency of one electron in the ionized donor unit, D^+ (these changes are remarkably well predicted by the simple Walsh rules,[19] section I.B);

(ii) the Coulombic attraction of the separated opposite charges (*harpooning*) between D^+ and A^-, in all flexible molecules;

(iii) the mesomeric and other *delocalized* interactions between the component radical ions, D^+ and A^- (these interactions differ strongly for twisted and planar arrangements of the donor and acceptor moieties); and

(iv) the solute−solvent interactions, especially the solvation effects of a large dipole of a CT state.

In the broad class of molecules possessing D and A subunits which are directly connected by a formally single bond,[830] factors (iii) and (iv) seem to be usually the most important.

When comparing the different hypotheses on the structural relaxation accompanying ET in the singly bonded D−A molecules, we concentrated on three of them, the other ones being evidently discarded by ample experimental and theoretical evidence. These three hypotheses are (i) an *exciplex* formation with the solvent, (ii) a *planar* intramolecular CT state (PICT), and (iii) a *twisted* intramolecular CT state (TICT).

A flattening in the excited state of the molecules more or less twisted in their ground states (the deviation from planarity being usually due to the steric nonbonding interactions between D and A) clearly occurs in numerous cases of large aromatic donors or/and acceptors. We treat the results of the group of Kapturkiewicz on the quinoxaline derivatives **142**−**145**,[563] or those of the group of Zachariasse on the flattening of some D−A compounds,[110] as impressive proofs of such planarization. It has often been described in terms of quinoid highly dipolar structures (like **b**, Scheme 1) with the orbitals delocalized over the whole conjugated system. It is, however, rather astonishing that the spectroscopic and photophysical properties of the coplanar conformations of the molecules **142**−**145** are satisfactorily described in terms of a perturbational treatment of the orbitals of the constituent D and A units, with the frontier orbitals being to a large extent *localized* mostly either on D (HOMO) or on A (LUMO).

For the majority of the D−A compounds with *large* aromatic subunits, in particular those described in section XI, one can conclude that the internal twisting relaxation in the excited state occurs, if any, either toward larger or toward smaller twist angles, θ, with respect to the conformation in the ground state. Prediction of the direction of change of the twist angle is still far from precise, and the TICT states appear rather exceptionally in this broad group of compounds.

One recent example, in which simple methyl substituents can induce a reversal in the relaxation direction in the excited state, are the donor−acceptor biphenyls **103**−**105**.[203,333−335,507,831] The unsubstituted **103**, being somewhat twisted in the ground state as evidenced by the reduced molar absorptivity, relaxes to the planar conformation in the excited state with an emission behavior nearly identical to that of the planar model compound **104**, also in polar solvents, and connected with a large but incomplete CT. The methyl-substituted **105**, however, being considerably twisted in the ground state, relaxes toward even larger twist angles in polar solution and exhibits the characteristic features of complete decoupling (transient absorption spectra of the component radical ions and low transition moments in emission).[333,335]

On the basis of the present stage of knowledge, the TICT model seems to be especially applicable to less extended molecular systems (preferentially with only one aromatic ring), starting from the simplest one, H_2N-BH_2, known only from theory,[505] and finding its most discussed exemplification in **1**. In this exemplary case, the relaxation of the CT state by an intramolecular twist to the approximately perpendicular conformation with largely decoupled $\dot{D}^+$ and $\dot{A}^-$ units is considered to be proven by the recent time-resolved vibrational spectra and by a crucial NMR stereochemical experiment (section VIII).[517] The decoupled large dipole biradical is stabilized by solvation. One of the important patterns of this emitting state seems to be a small transition dipole moment in fluorescence, $\vec{M}_f \leq 1$ D, and its independence of the solvent (cf. Table 5).

Between these two limiting conformations, there are numerous molecules in which the two effects, stabilization by the coupling of D and A with delocalized mesomeric effects, and stabilization of the dipole by solvation (if the dipole of a TICT state is larger than that of the planar form), are energetically balanced. This results in an intermediate twist angle, $0 < \theta < 90°$.

In some families of A−D compounds, characterized by intermediate twist angles in the ground state and evidently flattening upon excitation in nonpolar media, the CT emission nevertheless becomes more forbidden with an increase of the solvent polarity, and the $\vec{M}_f$ value diminishes correspondingly. Such cases appear in the group of derivatives with anthracene or acridine as acceptors (Table 15, Figure 89). A decrease of $\vec{M}_f$ indicates a decrease in orbital overlap and an increase of CT character, meaning usually an increase of the excited-state equilibrium twist angle, θ, in polar media.[832] The question remains whether in strongly polar solvents θ corresponds to an excited-state geometry more (or less) twisted as compared to that in the ground state.

The situation has been clarified in the case of the biphenyl derivative **105**, in which two types of CT states can be present simultaneously. In the gas phase and in nonpolar solvents, the excited-state equilibrium conformation is more planar than the ground-state one (mesomeric ICT state), but it becomes more twisted in highly polar solvents (corresponding to a twisted ICT state, TICT).[333] The dipole moment has a maximum for the perpendicular geometry but is large also for nearly planar geometries. In intermediately polar solvents, dual fluorescence is observed, corresponding to the simultaneous population of both types of CT states (conformers with different twist angle and fluorescence transition moment).[333,833,834]

The k_f values seriously decrease to low values with increasing solvent polarity for a group of naphthalene derivatives, **154**−**157** (section XI.A.3).[585] In the pyrrole derivatives, a strong decrease of k_f is observed

in highly polar solvents (**164a**, **168**). The contrast of this behavior to that of the highly sterically hindered compounds **164c**, **169**, and **170** is remarkable. In this case, the k_f values are very low ($\sim 10^6$ s^{-1}) and are nearly independent of the solvent polarity (Table 17). This seems to hint at a conformation close to $\theta = 90°$ in all solvents.

Still a different behavior is found in the series of derivatives with carbazole as donor, **182** and **183**. They are characterized by very low $\bar{M}_f$ values (similar to the case of **1** or even lower, except for the *p*-CN-substituted derivatives[835]) which do not change with the polarity of the medium. The rather large ground-state twist angles, $\theta \approx 65-75°$, do not seem to change markedly in the excited state (section XI.A.7).[61,623]

The model of adiabatic ET, as applied to the cases of **26** and **111**,[550,556] deserves close attention, as it may clarify many ET phenomena in the D−A compounds — the model could be complemented by including the intramolecular coordinates.

The exciplexes with the solvent are evidently not the main cause of the dual fluorescence phenomena and of the structural changes in the CT states, but they probably contribute to the fluorescence shift in some cases. The formation of specific (perhaps stoichiometric?) solvates reappears, especially in the studies of the van der Waals complexes in supercooled molecular jets, and some aspects of this topic are discussed in sections III.A.1 and V.3.

B. Open Questions

In the case of DMABN (**1**), most evidence (especially the crucial NMR experiment[517]) supports or proves the TICT model. There are, however, several points that raise doubt or controversy. They are discussed here as open questions.

The twist angle necessary for the formation of the ICT state in derivatives of **1** is not quite clear. While the group of compounds with the amino nitrogen structurally rigidized in-plane (**20**, **29**, **55**, **56**) do not undergo any ICT reaction; this is different for **57**.[8,92,133] The case of **57** may indicate that when a steric strain prohibits the formation of the perpendicular conformation but allows an approach to it, CT emission can be observable. The twist angle of the emissive conformation (and the corresponding excited-state dipole moment) is a point open for future research.

Bandwidth. In the case of some derivatives with anthracene or acridine acceptors, $\Delta\tilde{\nu}_{1/2}$ slightly increases,[145] but on closer inspection it is seen that, e.g., in the cases of **138**, **140**, and **141**, the $\Delta\tilde{\nu}_{1/2}$ values do not change with the solvent polarity. In their more recent papers, the authors find that, in contrast to the previous conviction, the *inner* reorganization energy, λ_i, is not constant but *decreases* with growing polarity of the solvent,[524] especially in strongly sterically hindered compounds such as **140** and **141**. They interpret this as an increase in the twist angle, θ, inferring that the torsional motion (low-frequency vibration) must be associated with some high-frequency modes, especially with the A−D stretch, as this bond length and bond order should markedly change with θ.[524] This is possible in these large polycyclic aromatic systems, where only one fluorescence band is emitted. In this case, the conformation and electronic structure of the emitting CT state seems to continuously change with the changing polarity of the medium.

Excited-state CT equilibria. Depending on the solvent, the extremely fast B* → A* reactions are comparable to, or even faster than, the reorientational relaxation of the polar solvent molecules around the giant dipole formed. Therefore, the apparent thermodynamic data (ΔH^o, K_{eq}) characterizing the excited-state equilibria (section VI.A.3; Table 10), as measured from the temperature effects in *the high-temperature range*, could be affected by the nonequilibrium solvation. These data await a critical comparison with those to be determined or estimated by other, independent methods; especially promising are constructions of spectral−thermodynamic cycles involving excited-state equilibria.

Isomeric substitution effects. Strong differences between the substitutional isomers with respect to the CT (e.g., the isomers of DMABN or numerous cases in section XI) are not yet sufficiently understood.

Specific interactions. The specific effect of chlorinated solvents (cf. Figure 47) awaits further explanations.

The similarities and evident differences in the photophysical behavior of the D−A molecules with pyrrole, indole, and carbazole as donors (section XI.A.5−7; Figure 76) await an interpretation in terms of electronic and molecular structures.

XIV. List of Abbreviations and Symbols

A	absorbency; amplitude
A	electron acceptor; long-wavelength emission band in a dually fluorescent system
A*	excited state emitting the CT fluorescence
A^-	radical anion
a	Onsager radius; width of a potential step; coefficient
ABCO	azabicyclooctane
ACN	acetonitrile
ADMA	formula **26**
AM1	semiempirical quantum-chemical method
An	anthracene
ANS	(arylamino)naphthalenesulfonate (e.g., **154**−**156**)
ASE	amplified spontaneous emission
B	benzonitrile; short-wavelength ("normal") fluorescence band in a dually fluorescent system
b	coefficient
B*	primary excited state, emitting the "normal" fluorescence
BA	9,9′-bianthryl, **111**
BCN	*n*-butyronitrile
BCPPZ	*N*,*N*-bis(4-cyanophenyl)piperazine, **58**
BET	back electron transfer
BOB	di-(*n*-butyl)ether
Bu	butyl
BuCl	butyl chloride, 1-chlorobutane
BuOH (or BUOH)	butanol-1
c	coefficient
CAR	3,6-di-*tert*-butylcarbazole
CASPT2	complete active self-consistent field with perturbation correction

CASSCF	complete active space self-consistent field
CBQ	6-cyanobenzquinuclidine, **22**
CD	cyclodextrin
CDMA (or DMABN)	4-(*N*,*N*-dimethylamino)benzonitrile, **1**
CHX	cyclohexane
CI	configuration interaction
CIS	CI singles (singly excited configurations)
CISD	CI singles and doubles
CMI (or MIN)	5-cyano-*N*-methylindoline, **20**
COI	conical intersection
CT	charge transfer
CV	crystal violet, **232**
D	electron donor; Debye unit
D	diffusion coefficient
D^+	radical cation
D−A	molecule composed of electron donor and acceptor linked by a formally single bond
DANCA	formula **153**
DAPSONE	4,4′-diaminodiphenyl sulfone
DASPMI	formulas **218**−**220**; derivatives **221**−**223**
DDABN	4-(*N*,*N*-di-*n*-decylamino)benzonitrile, **40**
DEABN	4-(*N*,*N*-diethylamino)benzonitrile, **30**
DCM	CH_2Cl_2
dd	"*dot*−*dot*" configuration
DFT	density functional theory
DMAB	4-(*N*,*N*-dimethylamino)benzamide, **86**
DMABME	4-(*N*,*N*-dimethylamino)methyl benzoate, **73**
DMABN (or CDMA)	4-(*N*,*N*-dimethylamino)benzonitrile, **1**
DMABN−Crown4	formula **61**
DMABN−Crown5	formula **62**
DMF	(*N*,*N*-dimethylamino)formamide
DMSO	dimethylsulfoxide
DPrABN	4-(*N*,*N*-di-*n*-propylamino)benzonitrile, **39**
E	energy; electrode potential
EA	electron affinity
EDB	2,6-dimethyl-4-(*N*,*N*-diethylamino)benzonitrile, **41**
EE (also EOE)	diethyl ether
Et	ethyl
ET	electron transfer
EtOH (or ETOH)	ethanol
ET(30)	solvent polarity index
F	fluorescence; electric field strength
f	oscillator strength; function
FC	Franck−Condon state
FDMA	formula **28**
fwhm	full width at half-maximum, $\Delta\tilde{\nu}_{1/2}$
GTA	glycerol triacetate
HBW	half-bandwidth (the same as fwhm)
HF	Hartree−Fock method
HOMO	highest occupied molecular orbital
hp	"*hole*−*pair*" configuration
I	intensity
ICT	intramolecular charge transfer
IEOEM	integral electrooptical emission method
INDO/S	intermediate neglect differential overlap (with standard parameters)
IP	ionization potential
IVR	intramolecular vibrational redistribution
k	rate constant
k_B	Boltzmann constant
K	equilibrium constant
L_a, L_b	orbital configuration of states in Platt's nomenclature
LE	locally (primary) excited state
LIF	laser-induced fluorescence
LUMO	lowest unoccupied molecular orbital
M	optical transition moment
MABN	4-(*N*-methylamino)benzonitrile, **51**
MCH	methylcyclohexane
MDB	2,6-dimethyl-4-(*N*,*N*-dimethylamino)benzonitrile, **41**
MeOH (or MEOH)	methanol
MIM	molecules-in-molecule method
MIN (or CMI)	5-cyano-*N*-methylindoline, **20**
MMABN	3-methyl-4-(*N*,*N*-dimethylamino)benzonitrile, **16**
MMD (or TMABN)	3,5-dimethyl-4-(*N*,*N*-dimethylamino)benzonitrile, **21**
MNDO	modified neglect of diatomic differential overlap method
MRCI	multireference CI
MTHT	2-methyltetrahydrofuran
MG	malachite green, **234**
P	pyrrole
P	degree of polarization
[P]	concentration of polar cosolvent in binary solvents
PATMAN	(6-palmitoyl-2-[trimethylammoniumethyl]-methylamino)naphthalene
P4C	formula **46**
P5C (or PYRBN)	formula **23**
P6C (or PIPBN)	fomula **24**
P7C	formula **47**
P8C	formula **48**
PCILO	perturbation CI using localized orbitals
P6N	formula **49**
P6O	formula **50**
P6P	1-(4-cyanophenyl)-4-phenylpiperazine
PDB	2,6-dimethyl-4-(*N*,*N*-dipropylamino)benzonitrile, **41**
Pe	perylene
Ph	phenyl
PICT	planar intramolecular charge transfer
PIPBN	4-(*N*-piperidinyl)benzonitrile, **24**
PJT	pseudo-Jahn−Teller effect
PRODAN	6-propionyl-2-(dimethylamino)naphthalene, **152**
PYRBME	4-(*N*-pyrrolidinyl)methylbenzoate
PYRBN	4-(*N*-pyrrolidinyl)benzonitrile, **23**
q	coordinate
R, *r*	emission anisotropy; distance
REMPI	resonance-enhanced multiphoton ionization
RICT	rehybridization by intramolecular CT
S_i	*i*th singlet state
SCE	saturated calomel electrode
SCRF	self-consistent reaction field
TETRA	formula **211**
THF	tetrahydrofuran
TICT	twisted intramolecular charge transfer
TMABN (or MMD)	3,5-dimethyl-4-(*N*,*N*-dimethylamino)benzonitrile, **21**
TOL	toluene
TPE	tetraphenylethylene
TPM	triphenylmethyl dyes
TRDL	time-resolved dielectric loss (method)
TRIA	formula **209**
TRMC	time-resolved microwave conductivity (method)
V	coupling matrix elements
WICT	wagging interamolecular charge transfer

α	polarizability
β	resonance integral
$\Delta\nu_{1/2}$	bandwidth at half-maximum
ϵ	dielectric constant
ϵ_1	activation energy of emission
ϕ	phenyl
Φ, ϕ, φ	quantum yield
φ	angle
λ	Marcus' reorganization energy
μ	dipole moment
$\tilde{\nu}$	wavenumber (cm^{-1})
$\Delta\tilde{\nu}_{1/2}$	full width at half-maximum (cm^{-1})
π	orbital
θ	twist angle
σ	Hammett substituent constant; orbital
τ	period; lifetime; characteristic time ($= k^{-1}$)
τ_L	*longitudinal* relaxation time
ξ	solvent friction
Ψ	wave function

XV. Acknowledgments

The authors dedicate this work to the memory of the late Prof. Albert Weller, whom we owe inspiration to the studies of donor−acceptor systems, and many memorable discussions.

The authors express their gratitude to all those who helped us in different ways to prepare this review or discussed the topics with us, who allowed us to use their unpublished data, or who provided us with samples of the investigated compounds: Dr. J. Dobkowski, Dr. J. Herbich, Dr. A. Kapturkiewicz, Dr. J. Karpiuk, and Prof. J. Waluk (Warsaw); Prof. G. Köhler, Dr. A. Parusel, and Dr. K. Rechthaler (Vienna); Dr. K.-H. Grellmann and Dr. K. A. Zachariasse (Göttingen); Prof. J. Gębicki and Dr. M. Wolszczak (Łódź); Prof. W. Baumann and Dr. N. Detzer (Mainz); Prof. Y. Haas and Dr. S. Zilberg (Jerusalem).

We sincerely thank the following people for their helpful assistance: Mr. Y. Stepanenko, Mrs. A. Kubś, and Dr. P. Borowicz (Warsaw); Dr. I. M. Mitchell, Mrs. E. Ehlers, and Mrs. A. Rothe (Berlin).

The authors acknowledge the kind permissions to reproduce or adapt the published material from the copyright owners: Prof. E. Lippert (Figures 7 and 8); The Royal Society of Chemistry (Figures 3, 5, 9, 13, 51, and 76); the American Chemical Society (Figures 25, 29, 35, 44, 47−49, 53, 54, 69, 80, 85, 87, 89, 91, 93−97, 100, 103, 107, 108, and 118, and Scheme 8); Elsevier Science (Figures 12, 16−19, 21, 22, 26, 32, 33, 36, 39−41, 43, 52, 53, 55, 57, 60−63, 65, 70, 71, 74, 84−86, 88, 92, 102, 104−106, 114, 116, 117, 119, and 120); the Indian Academy of Sciences (Figures 6, 19, and 21); Koninklijke Nederlandse Chemische Vereniging (Figures 37 and 38); VCH Publishers (Figures 30, 34, 45, 46, and 79); The American Institute of Physics (Figures 64, 75, and 101); Acta Physica Polonica (Figure 27); Verlag der Zeitschrift für Naturforschung (Figures 31 and 84); CNRS (Figures 66, 67, 98, and 99); and Kluwer Academic Publishers (Scheme 2).

K.R. thanks the Alexander von Humboldt Foundation, DAAD, the Austrian Academy of Science, and the Polish Committee for Scientific Research (KBN), and W.R. thanks DFG, Volkswagen Foundation, DAAD, and the Fonds der Chemischen Industrie for their support in the investigations.

XVI. Supporting Information

Chart summarizing structures **1**−**299**. This material is available free of charge via the Internet at http://pubs.acs.org/cr.

XVII. References

(1) Rotkiewicz, K.; Grellmann, K. H.; Grabowski, Z. R. *Chem. Phys. Lett.* **1973**, *19*, 315; **1973**, *21*, 212 (erratum).
(2) Siemiarczuk, A.; Grabowski, Z. R.; Krówczyński, A.; Asher, M.; Ottolenghi, M. *Chem. Phys. Lett.* **1977**, *51*, 315.
(3) Grabowski, Z. R.; Rotkiewicz K.; Siemiarczuk, A. *J. Lumin.* **1979**, *18/19*, 420.
(4) Grabowski, Z. R.; Rotkiewicz, K.; Siemiarczuk, A.; Cowley, D. J.; Baumann, W. *Nouv. J. Chim.* **1979**, *3*, 443.
(5) Rettig, W. *Angew. Chem., Int. Ed. Engl.* **1986**, *25*, 971.
(6) Lippert, E.; Rettig, W.; Bonačić-Koutecký, V.; Heisel F.; Miehé, J. A. *Adv. Chem. Phys.* **1987**, *68*, 1.
(7) Visser, R. J.; Varma, C. A. G. O. *J. Chem. Soc., Faraday Trans. 2* **1980**, *76*, 453.
(8) Zachariasse, K. A.; von der Haar, T.; Hebecker, A.; Leinhos, U.; Kühnle, W. *Pure Appl. Chem.* **1993**, *65*, 1745.
(9) Sobolewski, A. L.; Domcke, W. *Chem. Phys. Lett.* **1996**, *250*, 428.
(10) Sobolewski, A. L.; Domcke, W. *Chem. Phys. Lett.* **1996**, *259*, 119.
(11) Rettig, W. In *Modern Models of Bonding and Delocalization*; Molecular Structure and Energetics 6; Liebman, J. E., Greenberg, A., Eds.; VCH Publ.: New York, 1988; p 229.
(12) Rettig W.; Baumann, W. In *Progress in Photochemistry and Photophysics*; Rabek, J. F., Ed.; CRC Press: Boca Raton, FL, 1992; Vol. VI, p 79.
(13) Rettig, W. In *Electron Transfer I*; Mattay, J., Ed.; Topics in Current Chemistry 169; Springer-Verlag: Berlin, 1994; p 253.
(14) Exceptionally, the present review contains some (reliable) private information received, and a few hitherto unpublished results from the authors' laboratories.
(15) Förster, Th. *Z. Elektrochem. Angew. Phys. Chem.* **1939**, *45*, 571.
(16) Lippert, E. *Z. Elektrochem. Ber. Bunsen-Ges. Phys. Chem.* **1957**, *61*, 962.
(17) Verhoeven, J. W. *Pure Appl. Chem.* **1990**, *62*, 1585.
(18) Rettig, W.; Haag R.; Wirz, J. *Chem. Phys. Lett.* **1991**, *180*, 216.
(19) Walsh, A. D. *J. Chem. Soc.* **1953**, 2260; (b) 2266; (c) 2288; (d) 2296; (e) 2301; (f) 2306; (g) 2318; (h) 2321; (i) 2325; (j) 2330.
(20) Walsh, A. D.; Warsop, P. A. *Trans. Faraday Soc.* **1961**, *57*, 354.
(21) Halpern, A. M.; Ondrechen, M. J.; Ziegler, L. D. *J. Am. Chem. Soc.* **1986**, *108*, 3907.
(22) Halpern, A. M. *J. Am. Chem. Soc.* **1974**, *96*, 7655.
(23) Bally, T. In *Radical Ionic Systems*; Lund, A., Shiotani, M., Eds.; Kluwer Acad. Publ.: Dordrecht, 1991; p 3.
(24) Saeva, F. D. *Top. Curr. Chem.* **1990**, *156*, 61.
(25) Qin, X. Z.; Williams, F. *J. Phys. Chem.* **1986**, *90*, 2292.
(26) Dai, S.; Wang, J. T.; Williams, F. *J. Am. Chem. Soc.* **1990**, *112*, 2837.
(27) Roth, H. D.; Schilling, M. L. M.; Wamser, C. C. *J. Am. Chem. Soc.* **1984**, *106*, 5023.
(28) Heilbronner, E.; Muszkat, K. A. *J. Am. Chem. Soc.* **1970**, *92*, 3818.
(29) Gębicki, J.; Marcinek, A.; Stradowski, C. *J. Phys. Org. Chem.* **1990**, *3*, 606.
(30) Marcinek, A.; Gębicki, J.; Płonka, A. *J. Phys. Org. Chem.* **1990**, *3*, 757.
(31) Gębicki, J.; Marcinek, A. In *General Aspects of Free Radical Chemistry*; Alfassi, Z. B., Ed.; Wiley: Chichester, 1999; p 175.
(32) Brouwer, A. M.; Zwier, J. M.; Svendsen, C.; Mortensen, O. S.; Langkilde, F. W.; Wilbrandt, R. *J. Am. Chem. Soc.* **1998**, *120*, 3748.
(33) Zwier, J. M. Electronic and Structural Consequences of Excitation and Oxidation in Cyclic Amines. Ph.D. Thesis, University of Amsterdam, 2000.
(34) Asmus, K.-D. *Acc. Chem. Res.* **1979**, *12*, 436.
(35) Rogowski, J.; Adamus, J.; Gębicki, J.; Nelsen, S. F. *J. Chem. Soc., Perkin Trans 2* **1994**, 779.
(36) Herzberg, G. *Molecular Spectra and Molecular Structure. III. Electronic Spectra and Electronic Structure of Polyatomic Molecules*; D. Van Nostrand: Princeton, NJ, 1966.
(37) Brand, J. C. D.; Williamson, D. G. In *Advances in Physical Organic Chemistry*; Gold, V., Ed.; Academic Press: New York, 1963; Vol. 1, p 365.
(38) Merer, A. J.; Mulliken, R. S. *Chem. Rev.* **1969**, *69*, 639.
(39) Douglas, J. E.; Rabinovitch, B. S.; Looney, F. S. *J. Chem. Phys.* **1955**, *23*, 315.
(40) Grabowski, Z. R.; Bylina, A. *Trans. Faraday Soc.* **1964**, *60*, 1131.

(41) Grabowski, Z. R. *Pure Appl. Chem.* **1992**, *64*, 1249.
(42) Grabowski, Z. R. *Pure Appl. Chem.* **1993**, *65*, 1751.
(43) Polanyi, M. *Atomic Reactions*; Williams & Norgate: London, 1932. The harpooning effect is in fact composed of three main stages: (i) the approach of the reactants to the region of the crossing point, (ii) the ET reaction at the crossing of the (typically uncharged) reactants, and (iii) the attraction and approach of the oppositely charged reaction products.
(44) Chandross, E. A.; Thomas, H. T. *Chem. Phys. Lett.* **1971**, *9*, 393.
(45) Weller, A. In *The Exciplex*; Gordon, M., Ware, W. R., Eds.; Academic Press: New York, 1975; p 23.
(46) Mataga, N.; Ottolenghi, M. In *Molecular Association*; Foster, R., Ed.; Academic Press: London, 1979; p 1.
(47) Mataga, N. In *Applications of Picosecond Spectroscopy to Chemistry*; Eisenthal, K. B., Ed.; D. Reidel Publ. Co.: Dordrecht, 1984; p 21.
(48) Shephard, M. J.; Paddon-Row, M. N. *J. Phys. Chem. A* **2000**, *104*, 11628.
(49) Goes, M.; de Groot, M.; Koeberg, M.; Verhoeven, J. W.; Lokan, N. R.; Shephard, M. J.; Paddon-Row, M. N. *J. Phys. Chem. A* **2002**, *106*, 2129.
(50) Beens, H.; Weller, A. In *Organic Molecular Photophysics*; Birks, J. W., Ed.; J. Wiley & Sons: London, 1975; Vol. II, Chapter 4.
(51) Weller, A.; Zachariasse, K. *Chem. Phys. Lett.* **1971**, *10*, 161.
(52) Faulkner, L. R.; Bard, A. J. In *Electroanalytical Chemistry*; Bard, A. J., Ed.; Marcel Dekker: New York, 1977; Vol. 10, p 1.
(53) Itaya, K.; Toshima, S. *Chem. Phys. Lett.* **1977**, *51*, 447.
(54) Kawai, M.; Itaya, M.; Toshima, S. *J. Phys. Chem.* **1980**, *84*, 2368.
(55) Kapturkiewicz, A.; Grabowski, Z. R.; Jasny, J. *J. Electroanal. Chem.* **1990**, *279*, 55.
(56) Kapturkiewicz, A. *J. Electroanal. Chem.* **1990**, *290*, 135; **1991**, *302*, 131.
(57) Kapturkiewicz, A. *Z. Phys. Chem. NF* **1991**, *170*, 87.
(58) Kapturkiewicz, A. *Chem. Phys.* **1992**, *166*, 259.
(59) Kapturkiewicz, A. *J. Electroanal. Chem.* **1993**, *348*, 283.
(60) Kapturkiewicz, A. *J. Electroanal. Chem.* **1994**, *372*, 101.
(61) Kapturkiewicz, A.; Herbich, J.; Karpiuk, J.; Nowacki, J. *J. Phys. Chem. A* **1997**, *101*, 2332.
(62) Called also *p*-cyano-*N*,*N*-dimethylaniline (CDMA) in numerous papers.
(63) Lippert, E.; Lüder, W.; Boos, H. In *Advances in Molecular Spectroscopy*; Mangini, A., Ed.; Pergamon Press: Oxford, 1962; p 443. The solvatochromic μ^* values are often overestimated; the error limits are due to a somewhat arbitrary choice of the Onsager radius, a_o.
(64) Lippert, E.; Lüder, W.; Moll, F.; Nägele, W.; Boos, H.; Prigge, H.; Seybold-Blankenstein, I. *Angew. Chem.* **1961**, *73*, 695.
(65) Platt's classification of the spectra and states[174] will be often used, after Lippert, as it is very useful in drawing analogies between different aromatic compounds, even if their symmetries are different.
(66) Köhler, G.; Wolschann, P.; Rotkiewicz, K. *Proc. Indian Acad. Sci. (Chem. Sci.)* **1992**, *104*, 197.
(67) Lippert, E. *Z. Naturforsch.* **1955**, *10a*, 541.
(68) Mataga, N.; Kaifu, Y.; Koizumi, M. *Bull. Chem. Soc. Jpn.* **1956**, *29*, 465.
(69) Correctly, the $\Delta f = f(\epsilon) - f(n^2)$ is applicable to the Stokes' shifts, $h\nu_{abs} - h\nu_{flu}$, or to the 0−0 transitions (eq 13). In the case of **1** and analogous excited-state reactions, the upper state in absorption is different from the emitting CT state, and the function Δf does not strictly apply to such a fluorescence, although the correlations are often satisfactory. The solvatochromic shifts of the fluorescence maxima alone, or of the absorption maxima alone, should be better correlated (under similar assumptions), with $\Delta f' = f(\epsilon) - (1/2)f(n^2)$, as in eq 14 or, not neglecting polarizability and assuming $\alpha \approx 0.5a_o^3$, as in eq 33.
(70) Grabowski, Z. R.; Rotkiewicz, K.; Rubaszewska, W.; Kirkor-Kamińska, E. *Acta Phys. Polon.* **1978**, *54A*, 767.
(71) Khalil, O. S.; Hofeldt, R. H.; McGlynn, S. P. *Chem. Phys. Lett.* **1972**, *17*, 479.
(72) Khalil, O. S.; Hofeldt, R. H.; McGlynn, S. P. *J. Lumin.* **1973**, *6*, 229.
(73) Khalil, O. S.; Hofeldt, R. H.; McGlynn, S. P. *Spectrosc. Lett.* **1973**, *6*, 147.
(74) Khalil, O. S. *Chem. Phys. Lett.* **1975**, *35*, 172.
(75) Nakashima, N.; Inoue, H.; Mataga, N.; Yamanaka, Y. *Bull. Chem. Soc. Jpn.* **1973**, *46*, 2288.
(76) Nakashima, N.; Mataga, N. *Bull. Chem. Soc. Jpn.* **1973**, *46*, 3016.
(77) Dähne, S.; Freyer, W.; Teuchner, K.; Dobkowski, J.; Grabowski, Z. R. *J. Lumin.* **1980**, *22*, 37.
(78) Dobkowski, J.; Kirkor-Kamińska, E.; Koput, J.; Siemiarczuk, A. *J. Lumin.* **1982**, *27*, 339.
(79) Rotkiewicz, K.; Rubaszewska, W. *J. Lumin.* **1984**, *29*, 329.
(80) Rotkiewicz, K.; Leismann, H.; Rettig, W. *J. Photochem. Photobiol. A: Chem.* **1989**, *49*, 347.
(81) Kosower, E. M.; Dodiuk, H. *J. Am. Chem. Soc.* **1976**, *98*, 924.
(82) Cazeau-Dubroca, C.; Peirigua, A.; Ait Lyazidi, S.; Nouchi, G. *Chem. Phys. Lett.* **1982**, *98*, 511.
(83) Cazeau-Dubroca, C.; Ait Lyazidi, S.; Nouchi, G.; Peirigua, A. *Nouv. J. Chim.* **1986**, *10*, 337.
(84) Kosower, E. M. *J. Am. Chem. Soc.* **1985**, *107*, 1114.
(85) Kosower, E. M. *Annu. Rev. Phys. Chem.* **1986**, *37*, 127.
(86) Cazeau-Dubroca, C.; Ait Lyazidi, S.; Cambou, P.; Peirigua, A.; Cazeau, Ph.; Pesquer, M. *J. Phys. Chem.* **1989**, *93*, 2347.
(87) Cazeau-Dubroca, C.; Peirigua, A.; Ben Brahim, M.; Nouchi, G.; Cazeau, Ph. *Chem. Phys. Lett.* **1989**, *157*, 393.
(88) Cazeau-Dubroca, C.; Peirigua, A.; Ben Brahim, M.; Nouchi, G.; Cazeau, Ph. *Proc. Indian Acad. Sci. (Chem. Sci.)* **1989**, *104*, 209.
(89) Cazeau-Dubroca, C.; Nouchi, G.; Ben Brahim, M.; Pesquer, M.; Gorse, D.; Cazeau, Ph. *J. Photochem. Photobiol. A: Chem.* **1994**, *80*, 125.
(90) Chandross, E. A.; Thomas, H. T. *Chem. Phys. Lett.* **1971**, *9*, 397.
(91) Chandross, E. A. In *The Exciplex*; Gordon, M., Ware, W. R., Eds.; Academic Press: New York, 1975; p 187.
(92) Chandross, E. A.; Wight, F. R. In *Contributed Papers*, VI IUPAC Symposium on Photochemistry, Aix-en-Provence, 1976; p 53.
(93) Visser, R. J.; Varma, C. A. G. O.; Konijnenberg J.; Bergwerf, P. *J. Chem. Soc., Faraday Trans. 2* **1983**, *79*, 347.
(94) Visser, R. J.; Varma, C. A. G. O.; Konijnenberg J.; Weisenborn, P. C. M. *J. Mol. Struct.* **1984**, *114*, 105.
(95) Wang, Y. *Chem. Phys. Lett.* **1985**, *116*, 286.
(96) Weisenborn, P. C. M.; Varma, C. A. G. O.; de Haas M. P.; Warman, J. M. *Chem. Phys. Lett.* **1986**, *129*, 562.
(97) Compare, however, section III.D on the fluorescence anisotropy.
(98) Leinhos, U.; Kühnle, W.; Zachariasse, K. A. *J. Phys. Chem.* **1991**, *95*, 2013.
(99) Schuddeboom, W.; Jonker, S. A.; Warman, J. M.; Leinhos, U.; Kühnle, W.; Zachariasse, K. A. *J. Phys. Chem.* **1992**, *96*, 10809.
(100) Wermuth, G.; Rettig, W.; Lippert, E. *Ber. Bunsen-Ges. Phys. Chem.* **1981**, *85*, 64.
(101) Wermuth, G. *Z. Naturforsch.* **1983**, *38a*, 641.
(102) According to Wermuth et al.,[100] the B* and A* excited states of **1** are nearly isoenergetic in hexane.
(103) Huang, K.-T.; Lombardi, J. R. *J. Chem. Phys.* **1971**, *55*, 4072.
(104) Lewis, F. D.; Holman, B., III. *J. Phys. Chem.* **1980**, *84*, 2328.
(105) Mordziński, A.; Sobolewski, A. L.; Levy, D. H. *J. Phys. Chem. A* **1997**, *101*, 8221.
(106) Sudholt, W.; Sobolewski, A. L.; Domcke, W. *Chem. Phys.* **1999**, *240*, 9.
(107) Zachariasse, K. A.; Grobys, M.; Tauer, E. *Chem. Phys. Lett.* **1997**, *274*, 372.
(108) Chattopadhyay, N.; Serpa, C.; Pereira, M. M.; de Melo, J. S.; Arnaut, L. G.; Formosinho, S. J. *J. Phys. Chem. A* **2001**, *105*, 10025. These conclusions were contradicted by Zachariasse et al. (Zachariasse, K. A.; Yoshihara, T.; Druzhinin, S. I. *J. Phys. Chem. A* **2002**, *106*, 6325), who found no evidence for the ICT state of **19**.
(109) Sakota, K.; Nishi, K.; Ohashi, K.; Sekiya, H. *Chem. Phys. Lett.* **2000**, *322*, 407.
(110) Zachariasse, K. A. *Chem. Phys. Lett.* **2000**, *320*, 8.
(111) Il'ichev, Y. V.; Kühnle, W.; Zachariasse, K. A. *J. Phys. Chem. A* **1998**, *102*, 5670.
(112) Some aspects of the PICT model were introduced in other papers by Zachariasse and his group.[107,111,133,197,201]
(113) Rettig, W. *J. Mol. Struct.* **1982**, *84*, 303.
(114) Suppan, P. *Chem. Phys. Lett.* **1986**, *128*, 160.
(115) Pilloud, D.; Suppan, P.; van Haelst, L. *Chem. Phys. Lett.* **1987**, *137*, 130.
(116) Baumann, W.; Bischof, H.; Fröhling, J. C.; Brittinger, C.; Rettig, W.; Rotkiewicz, K. *J. Photochem. Photobiol. A: Chem.* **1992**, *64*, 49. The authors remark on a possible source of error in the electrooptical emission measurements of the excited-state dipole moments. It appears in the case of vibronic mixing of states giving rise to a solvent-polarity-dependent polarization of the transition moment. Hence, some doubts appear, e.g., in the case of the dipole moment of the B* state of **1**.
(117) Kupfer, M.; Abraham, W. *J. Prakt. Chem.* **1983**, *325*, 95.
(118) Kamlet, M. J.; Abboud, J. L. M.; Taft, R. W. *Prog. Phys. Org. Chem.* **1981**, *13*, 485.
(119) Kupfer, M.; Abraham, W. *Monatsh. Chem.* **1983**, *114*, 513.
(120) Kupfer, M.; Abraham, W. *Chem. Phys. Lett.* **1985**, *122*, 300.
(121) Guo, K. R.; Kitamura, N.; Tazuke, S. *J. Phys. Chem.* **1990**, *94*, 1404.
(122) Dedonder-Lardeux, C.; Jouvet, C.; Martrenchard, D.; Solgadi, D.; McCombie, J.; Howells, B. D.; Palmer, T. F.; Subaric-Leitis, A.; Monte, C.; Rettig, W.; Zimmermann, P. *Chem. Phys.* **1995**, *191*, 271.
(123) Rettig, W.; Dedonder-Lardeux, C.; Jouvet, C.; Martrenchard-Barra, S.; Szrifiger, P.; Krim, L.; Castano, F. *J. Chim. Phys.* **1995**, *92*, 465.
(124) Krauss, O.; Lommatzsch, U.; Lahmann, C.; Brutschy, B.; Rettig, W.; Herbich, J. *Phys. Chem. Chem. Phys.* **2001**, *3*, 74.
(125) Köhler, G.; Rechthaler, K.; Rotkiewicz, K.; Rettig, W. *Chem. Phys.* **1996**, *207*, 85.
(126) Grabowski, Z. R.; Dobkowski, J. *Pure Appl. Chem.* **1983**, *55*, 245.
(127) Liptay, W. *Z. Naturforsch.* **1965**, *20a*, 1441.

(128) This is a simplistic view. The clusters 1:*r* of the same size *r* can correspond to different cluster isomers which can be reactive or nonreactive. This does not change the conclusion, however.
(129) Rettig, W.; Lippert, E. *J. Mol. Struct.* **1980**, *80*, 17.
(130) Rotkiewicz, K.; Grabowski, Z. R.; Krówczyński, A.; Kühnle, W. *J. Lumin.* **1976**, *12/13*, 877. In this paper, a hint is given for a possible role of the Rydberg state in the ICT phenomena, in connection with the photophysics of other *tertiary* amines. This line was not continued, but it may revive in view of the studies of photoionizations (e.g., ref 465) that are now in course (Sobolewski, A. L., private communication, 2003).
(131) Rettig, W.; Rotkiewicz, K.; Rubaszewska, W. *Spectrochim. Acta* **1984**, *40A*, 241.
(132) Rotkiewicz, K.; Rubaszewska, W. *Chem. Phys. Lett.* **1980**, *70*, 444.
(133) Zachariasse, K. A.; Grobys, M.; von der Haar, Th.; Hebecker, A.; Il'ichev, Yu. V.; Jiang, Y.-B.; Morawski, O.; Kühnle, W. *J. Photochem. Photobiol. A: Chem.* **1996**, *102*, 59; **1998**, *115*, 259 (erratum).
(134) Okada, T.; Uesugi, M.; Köhler, G.; Rechthaler, K.; Rotkiewicz, K.; Rettig, W.; Grabner, G. *Chem. Phys.* **1999**, *241*, 327.
(135) Rotkiewicz, K.; Rubaszewska, W. *J. Lumin.* **1982**, *27*, 221. (Cf. the corrigendum.[394])
(136) Bischof, H.; Baumann, W.; Detzer, N.; Rotkiewicz, K. *Chem. Phys. Lett.* **1985**, *116*, 180.
(137) Rettig, W.; Braun, D.; Suppan, P.; Vauthey, E.; Rotkiewicz, K.; Luboradzki, R.; Suwińska, K. *J. Phys. Chem.* **1993**, *97*, 13500.
(138) Kobayashi, T.; Futakami, M.; Kajimoto, O. *Chem. Phys. Lett.* **1987**, *141*, 450.
(139) Rotkiewicz, K.; Herbich, J.; Pérez Salgado, F.; Rettig, W. *Proc. Indian Acad. Sci. (Chem. Sci.)* **1992**, *104*, 105.
(140) The term *pretwisted* denotes throughout this review the mutually markedly non-coplanar conformation of D and A in the ground state of a D−A molecule, irrespective of the conformational changes upon excitation.
(141) For such *delocalized* excitation, however, generally — even in this review — the paradoxical term *local* excitation (LE) is traditionally used, in opposition to the CT state.
(142) Grabowski, Z. R. In *Supramolecular Photochemistry*; Balzani, V., Ed.; D. Reidel Publ.: Dordrecht, 1987; p 319.
(143) Grabowski, Z. R. *Electrochim. Acta* **1968**, *13*, 1218.
(144) Marcus, R. A. *J. Phys. Chem.* **1989**, *93*, 3078.
(145) Herbich, J.; Kapturkiewicz, A. *Chem. Phys.* **1993**, *170*, 221.
(146) It is also possible that the interconnecting C−N bond elongates with solvent polarity; the corresponding force constant would then decrease (and the dipole moment would increase). This reminds us of the flexible exciplexes, in which the initial ET structure is much more extended in polar solvents.
(147) Weisenborn, P. C. M.; Huizer, A. H.; Varma, C. A. G. O. *Chem. Phys.* **1988**, *126*, 425.
(148) Köhler, G.; Rotkiewicz, K. *Spectrochim. Acta* **1986**, *42 A*, 1127.
(149) de Lange, M. C. C.; Thorn Leeson, D.; van Kuijk, K. A. B.; Huizer, A. H.; Varma, C. A. G. O. *Chem. Phys.* **1993**, *174*, 425.
(150) Except under specific conditions, at excitation considerably above the onset of absorption (see Figure 17 and the related text).
(151) Stevens, B.; Ban, M. I. *Trans. Faraday Soc.* **1964**, *60*, 1515.
(152) Hamill, W. H. In *Radical Ions*; Kaiser, E. T., Kevan, L., Eds.; Wiley: New York, 1968; p 321.
(153) Rotkiewicz, K.; Köhler, G. *J. Lumin.* **1987**, *37*, 219.
(154) Bangal, P. R.; Chakravorti, S. *Photochem. Photobiol. A: Chem.* **1998**, *116*, 47.
(155) Karpiuk, J.; Grabowski, Z. R.; De Schryver, F. C. *Proc. Indian Acad. Sci. (Chem. Sci.)* **1992**, *104*, 133.
(156) Karpiuk, J. Photophysical and Photochemical Processes in Lactones of Some Rhodamines. Ph.D. Thesis, Institute of Physical Chemistry, Polish Academy of Sciences, Warsaw 1996.
(157) Karpiuk, J.; Grabowski, Z. R.; De Schryver, F. C. *J. Phys. Chem.* **1994**, *98*, 3247.
(158) Liptay, W. In *Excited States*; Lim, E. C., Ed.; Academic Press: New York 1974; p 129.
(159) Baumann, W.; Bischof, H. *J. Mol. Struct.* **1982**, *84*, 181.
(160) Suppan, P. *J. Chem. Soc., Faraday Trans. 2* **1981**, *77*, 1553.
(161) Kawski, A. *Asian J. Spectrosc.* **1997**, *1*, 27.
(162) Fessenden, R. W.; Hitachi, A. *J. Phys. Chem.* **1987**, *91*, 3456.
(163) Haas, M. P. de; Warman, J. M. *Chem. Phys.* **1982**, *73*, 35.
(164) Bulliard, C.; Allan, M.; Wirtz, G.; Haselbach, E.; Zachariasse, K. A.; Detzer, N.; Grimme, S. *J. Phys. Chem. A* **1999**, *103*, 7766.
(165) Brittinger, C.; Maiti, A. K.; Baumann, W.; Detzer, N. *Z. Naturforsch.* **1990**, *45a*, 883. For a possible source of errors, see ref 116.
(166) Heine, A.; Herbst-Irmer, R.; Stalke, D.; Kühnle, W.; Zachariasse, K. A. *Acta Crystallogr. Sect. B: Struct. Sci.* **1994**, *50*, 363.
(167) Serrano-Andrés, L.; Merchán, M.; Roos, B. O.; Lindh, R. *J. Am. Chem. Soc.* **1995**, *117*, 3189.
(168) Rettig, W.; Marschner, F. *Nouv. J. Chim.* **1990**, *14*, 819.
(169) DMABN and most of its *not pretwisted* derivatives do not emit the CT fluorescence in nonpolar solvents.
(170) Demeter, A.; Druzhinin, S.; George, M.; Haselbach, E.; Roulin, J.-L.; Zachariasse, K. A. *Chem. Phys. Lett.* **2000**, *323*, 351.
(171) Rettig, W. *J. Lumin.* **1980**, *26*, 21.
(172) Van der Auweraer, M.; Grabowski, Z. R.; Rettig, W. *J. Phys. Chem.* **1991**, *95*, 2083.
(173) There is an exception in the case of **16**: the transition moment is 1.25 D in *n*-hexane, 0.70 in EtOH, and 0.73 in MeOH. **16** exhibits only a single fluorescence band, of CT character, but the dipole moment of the emitting state is not constant: $\mu^* =$ 11.7 D in heptane but 15.5 D in polar solvents.[116] Obviously, in a nonpolar solvent there is some vibronic mixing of the CT state with the nearby $^1\pi,\pi^*$ state. The state mixing is facilitated by the low symmetry (C_s) of the molecule. In polar solvents, the energy gap between these states increases.
(174) Platt, J. R. *J. Chem. Phys.* **1949**, *17*, 484.
(175) Hammett, L. P. *Physical Organic Chemistry*; McGraw-Hill: New York, 1940; p 186
(176) Jaffé, H. H. *Chem. Rev.* **1953**, *53*, 191.
(177) The Hammett substituent constants[175] are taken from the tables: [176] σ_p^* or σ_p (except the substituents $-NH_3^+$ and $-NMe_3^+$, which negligibly affect the spectra; their $\sigma_{eff} \approx 0$). For the monosubstituted benzenes, $f(\sigma) = |\sigma|$; for the D,A *p*-disubstituted, $f(\sigma) = \sigma_A + |\sigma_D|$. Spectral correlations with Hammett constants σ are very rough and have no rational basis.
(178) Grabowski, Z. R. *Proceedings of the Polarographic Conference;* PWN: Warsaw, 1956; p 323.
(179) Hochstrasser, R. M.; Marzacco, C. A. In *Molecular Luminescence*; Lim, E. C., Ed.; W. A. Benjamin: New York, 1969; p 631.
(180) Gregory, A. R.; Siebrand, W.; Zgierski, M. Z. *J. Chem. Phys.* **1976**, *64*, 3145.
(181) Wermuth, G.; Rettig, W. *J. Phys. Chem.* **1984**, *88*, 2729.
(182) Measured by P. Nikolov, in Warsaw.
(183) Jabłoński, A. *Bull. Acad. Polon. Sci., Ser. Sci. Math. Astron. Phys.* **1960**, 8, 259.
(184) Wermuth, G. *Z. Naturforsch.* **1983**, *38a*, 368.
(185) Rettig, W.; Wermuth, G.; Lippert, E. *Ber. Bunsen-Ges. Phys. Chem.* **1979**, *83*, 692.
(186) Lippert, E.; Rettig, W. *J. Mol. Struct.* **1978**, *45*, 373.
(187) Kawski, A.; Piszczek, G. *Z. Naturforsch.* **1997**, *52a*, 409.
(188) Rotkiewicz, K. *Spectrochim. Acta* **1986**, *42A*, 575.
(189) Fisz, J. J.; van Hoek, A. *Chem. Phys. Lett.* **1997**, *270*, 432.
(190) Köhler, G.; Rechthaler, K.; Grabner, G.; Luboradzki, R.; Suwińska, K.; Rotkiewicz, K. *J. Phys. Chem. A* **1997**, *101*, 8518.
(191) Baumann, W.; Nagy, Z.; Reis, H.; Detzer, N. *Chem. Phys. Lett.* **1994**, *224*, 517.
(192) Rettig, W. *J. Phys. Chem.* **1982**, *86*, 1970.
(193) The large blue shift of F_A is caused by a considerable change of the polarity function of the solvent with the temperature rise by 160 K.
(194) This view assumes that the twist angular range covered by the CT reaction is similar for those compounds. If pretwisting effects are operative for the longer-chain compounds such as **40**, similar to the cyclic compounds **23** and **24**, the rate for the CT reaction can be faster, as is observed, although the actual angular diffusion is slower. A theoretical model that is able to simulate this behavior is described in the kinetics section (section VI.E). There is, however, no evidence for any *pretwist* in most of these compounds.
(195) Druzhinin, S. I.; Demeter, A.; Zachariasse, K. A. *Chem. Phys. Lett.* **2001**, *347*, 421.
(196) Daum, R.; Druzhinin, S.; Ernst, D.; Rupp, L.; Schroeder, J.; Zachariasse, K. A. *Chem. Phys. Lett.* **2001**, *341*, 272.
(197) Haar, T. von der; Hebecker, A.; Il'ichev, Y.; Jiang, Y. B.; Kühnle, W.; Zachariasse, K. A. *Recl. Trav. Chim. Pays-Bas* **1995**, *114*, 430.
(198) Dobkowski, J.; Grabowski, Z. R.; Jasny, J.; Zieliński, Z. *Acta Phys. Polon.* **1995**, *A88*, 455.
(199) Gorse, A. D.; Pesquer, M. *J. Phys. Chem.* **1995**, *99*, 4039.
(200) Broo, A.; Zerner, M. C. *Chem. Phys. Lett.* **1994**, *227*, 551.
(201) Zachariasse, K. A.; Grobys, M.; von der Haar, Th.; Hebecker, A.; Il'ichev, Yu. V.; Morawski, O.; Rückert, I.; Kühnle, W. *J. Photochem. Photobiol A: Chem.* **1997**, *105*, 373.
(202) Rettig, W.; Zietz, B. *Chem. Phys. Lett.* **2000**, *317*, 187.
(203) Rettig, W.; Maus, M. In *Conformational Analysis of Molecules in Excited States*; Waluk, J., Ed.; Wiley VCH: New York, 2000; p 1.
(204) Rettig, W.; Kharlanov, V.; Maus, M. *Chem. Phys. Lett.* **2000**, *318*, 173.
(205) Rettig, W.; Rurack, K.; Sczepan M. In *New Trends in Fluorescence Spectroscopy. Applications to Chemical and Life Sciences*; Valeur, B., Brochon, J. C., Eds.; Springer-Verlag: Berlin, 2001; p 125.
(206) Parusel, A. B. J.; Köhler, G. *Int. J. Quantum Chem.* **2001**, *84*, 149.
(207) Parusel, A. B. J. *Chem. Phys. Lett.* **2001**, *340*, 531.
(208) The directly measured electrochemical irreversible oxidation potentials of aliphatic amines correlate, however, well with the *adiabatic* — sp^3 amines to sp^2 radical ions — ionization potentials, although the slope differs from unity (Jacques, P.; Burget, D.; Allonas, X. *New J. Chem.* **1996**, *20*, 933). The most interesting distinction between the n-donors (such as aliphatic amines)

and π-donors (such as anthracene in bianthryl) was discussed extensively in the papers by Jacques et al. with respect to its effect on the ET kinetics, due to the sterical and ET distance differences (Jacques, P.; Allonas, X. *Chem. Phys. Lett.* **1995**, *233*, 533). In the case of the TICT emission energies, however, the distinction — though similar — is between the donors which markedly change their structure if ionized (especially aliphatic amines, with the charge localized on the N atom in the ion) and those in which the ionization does not involve large structural changes (as in anthracene, where the charge in its ion is delocalized over the π-electronic system).

(209) Rettig, W.; Gleiter, R. *J. Phys. Chem.* **1985**, *89*, 4676.

(210) The reported decay kinetics of **20** were interpreted in terms of an excited-state reaction, leading to the formation of a partial CT state.[98] This interpretation was later abandoned.[197]

(211) Rotkiewicz, K.; Rettig, W. *J. Lumin.* **1992**, *54*, 221.

(212) Theoretical calculations[213] indicate also the barrier height as the cause of the slow rate of the CT reaction in **51**.

(213) Gedeck, P. Experimentelle und theoretische Untersuchungen zum Elektronentransfer in verknüpften Donor−Akzeptor Systemen. Ph.D. Thesis, University Erlangen-Nürnberg, 1996.

(214) Rückert, I.; Hebecker, A.; Parusel, A. B. J.; Zachariasse, K. A. *Z. Phys. Chem.* **2000**, *214*, 1597.

(215) Druzhinin, S. I.; Jiang, Y. B.; Demeter, A.; Zachariasse, K. A. *Phys. Chem. Chem. Phys.* **2001**, *3*, 5213.

(216) Aue, D. H.; Well, H. M.; Bower, M. T. *J. Am. Chem. Soc.* **1976**, *98*, 311.

(217) de Lange, M. C. C.; Thorn Leeson, D.; van Kuijk, K. A. B.; Huizer, A. H.; Varma, C. A. G. O. *Chem. Phys.* **1993**, *177*, 243.

(218) Jonker, S. A.; Warman, J. M. *Chem. Phys. Lett.* **1991**, *185*, 36.

(219) Gourdon, A.; Launay, J.-P.; Bujoli-Doeuff, M.; Heisel, F.; Miehé, J. A.; Amouyal, E.; Boillot, M.-L. *J. Photochem. Photobiol. A: Chem.* **1993**, *71*, 13.

(220) Launay, J. P. In *Molecular Electronics—Science and Technology*; Aviram, A., Ed.; Engineering Foundation: New York, 1989; p 237.

(221) Launay, J. P.; Sowińska, M.; Leydier, L.; Gourdon, A.; Amouyal, E.; Boillot, M.-L.; Heisel, F.; Miehé, J. A. *Chem. Phys. Lett.* **1989**, *160*, 89.

(222) Warman, J. M.; Schuddeboom, W.; Jonker, S. A.; de Haas, M. P.; Paddon-Row, M. N.; Zachariasse, K. A.; Launay, J.-P. *Chem. Phys. Lett.* **1993**, *210*, 397.

(223) Choi, L.-S.; Collins, G. E. *Chem. Commun.* **1998**, 893.

(224) Van der Auweraer, M.; Vannerem, A.; De Schryver, F. C. *J. Mol. Struct.* **1982**, *84*, 343.

(225) Létard, J. F.; Delmond, S.; Lapouyade, R.; Braun, D.; Rettig, W.; Kreissler, M. *Recl. Trav. Chim. Pays-Bas* **1995**, *114*, 517.

(226) Grabowski, Z. R. *J. Lumin.* **1981**, *24/25*, 559.

(227) The stability constants can be evaluated for the excited states on the basis of the *generalized Förster cycle*.[226]

(228) Rettig, W.; Bliss, B.; Dirnberger, K. *Chem. Phys. Lett.* **1999**, *305*, 8.

(229) Warren, J. A.; Bernstein, E. R.; Seeman, J. I. *J. Chem. Phys.* **1988**, *88*, 871.

(230) Shang, Q.-Y.; Bernstein, E. R. *J. Chem. Phys.* **1992**, *97*, 60.

(231) Rettig, W.; Vogel, M.; Lippert E.; Otto, H. *Chem. Phys.* **1986**, *108*, 381.

(232) Gedeck, P.; Schneider, S. *J. Photochem. Photobiol. A: Chem.* **1999**, *121*, 7.

(233) Rotkiewicz, K, Rettig, W.; Detzer, N.; Rothe, A. *Phys. Chem. Chem. Phys.* **2003**, *5*, 998.

(234) Lin, L. R.; Jiang, Y. B. *Sci. China, Ser. B—Chemistry* **2000**, *43*, 295.

(235) Cowley, D. J.; Peoples, A. H. *J. Chem. Soc., Chem. Commun.* **1977**, 352.

(236) Siemiarczuk, A.; Koput, J.; Pohorille, A. *Z. Naturforsch.* **1982**, *37a*, 598.

(237) Kirkor-Kamińska, E.; Rotkiewicz, K.; Grabowska, A. *Chem. Phys. Lett.* **1978**, *58*, 379.

(238) Purkayastha, P.; Bhattacharyya, P. K.; Bera, S. C.; Bhattacharyya, P. K.; Chattopadhyay, N. *Phys. Chem. Chem. Phys.* **1999** *1*, 3253.

(239) In a recent paper,[238] the authors found with optoacoustic measurements the ISC of **11** to be highly efficient in nonpolar solvents, opposite to the case in polar solvents. The same conclusions were reported earlier.[77,78]

(240) Kallir, A. J.; Suter, G. W.; Wild, U. P. *J. Phys. Chem.* **1987**, *91*, 60.

(241) Dubroca, C.; Lozano, P. *Chem. Phys. Lett.* **1974**, *24*, 49.

(242) Dobkowski, J.; Herbich, J.; Waluk, J.; Koput, J.; Kühnle, W. *J. Lumin.* **1989**, *44*, 149.

(243) Grabowski, Z. R.; Dobkowski, J. *SPIE Proc.* **1992**, *1711 (High-Performance Optical Spectrometry)*, 111. See also: Dobkowski, J.; Karpiuk, J. In *Kinetyka Nieklasyczna* (*Nonclassical Kinetics*, in Polish): Institute of Physical Chemistry, Polish Academy of Sciences: Warsaw, 1989; p 102.

(244) Grabowski, Z. R.; Dobkowski, J.; Kühnle, W. *J. Mol. Struct.* **1984**, *114*, 93.

(245) Dobkowski, J.; Grabowski, Z. R.; Heumann, E.; Kechinashvili, D.; Kozankiewicz, B.; Kühnle, W.; Sepioł, J. In *Proceedings of the International Symposium on Molecular Photophysics: "Half a Century of the Jabłoński Diagram"*; Institute of Physics, N. Copernicus University: Toruń, 1986; p 81.

(246) Rullière, C.; Grabowski, Z. R.; Dobkowski, J. *Chem. Phys. Lett.* **1987**, *137*, 408.

(247) Marguet, S.; Mialocq, J. C.; Millie, P.; Berthier, G.; Momicchioli, F. *Chem. Phys.* **1992**, *160*, 265.

(248) Sun, Y.-P.; Bunker, C. E. *J. Chem. Soc., Chem. Commun.* **1994**, 5.

(249) Sun, Y.-P.; Bunker, C. E. *J. Photochem. Photobiol. A: Chem.* **1994**, *80*, 445.

(250) Howell, R.; Jones, A. C.; Taylor, A. G.; Phillips, D. *Chem. Phys. Lett.* **1989**, *163*, 282.

(251) Visser, R. J.; Weisenborn, P. C. M.; Varma, C. A. G. O. *Chem. Phys. Lett.* **1985**, *113*, 330.

(252) Hrnjez, B. J.; Yazdi, P. T.; Fox, M. A.; Johnston, K. P. *J. Am. Chem. Soc.* **1989**, *111*, 1915.

(253) Revill, J. A. T.; Brown, R. G. *Chem. Phys. Lett.* **1992**, *188*, 433.

(254) At very low concentrations, an adsorption of the solute on walls of the cell should be taken into account and checked. Its operation may result in an apparent nonlinearity of the signal vs nominal concentration plots.

(255) Zhen, Z.; Tung, C.-H. *Chem. Phys. Lett.* **1991**, *180*, 211.

(256) Tazuke, S.; Hayashi, R.; Frank, C. W. *Chem. Phys. Lett.* **1987**, *135*, 123.

(257) Tazuke, S.; Guo, R. K. *Macromolecules* **1990**, *23*. 719.

(258) Al-Hassan, K. A.; Rettig, W. *Chem. Phys. Lett.* **1987**, *126*, 273.

(259) Al-Hassan, K. A.; Meetani, M. A.; Said, Z. F. M. *J. Fluoresc.* **1998**, *8*, 93.

(260) Rettig, W.; Fritz, R.; Springer, J. In *Photochemical Processes in Organized Molecular Systems*; Honda, K., Ed.; Elsevier Sci. Publ.: Amsterdam, 1998; p 61.

(261) Paczkowski, J.; Neckers, D. C. *Macromolecules* **1991**, *24*, 3013.

(262) Gormin, D.; Kasha, M. *Chem. Phys. Lett.* **1988**, *153*, 574.

(263) Heldt, J.; Gormin, D.; Kasha, M. *Chem. Phys.* **1989**, *136*, 321.

(264) Chou, P.-T.; Martinez, M. L.; Cooper, W. C. *Chem. Phys. Lett.* **1992**, *198*, 188.

(265) Smagowicz, J.; Wierzchowski, K. L. *J. Lumin.* **1976**, *14*, 9.

(266) Kawski, A. *Acta Phys. Polon.* **1966**, *29*, 507.

(267) Herbich, J.; Waluk, J. *Chem. Phys.* **1994**, *188*, 247.

(268) Herbich, J.; Grabowski, Z. R.; Wójtowicz, H.; Golankiewicz, K. *J. Phys. Chem.* **1989**, *93*, 3439.

(269) Almog, J.; Meyer, A. Y.; Shanan-Atidi, H. J. *J. Chem. Soc., Perkin Trans. 2* **1972**, 451.

(270) Herbich, J.; Karpiuk, J.; Grabowski, Z. R.; Tamai N.; Yoshihara, K. *J. Lumin.* **1992**, *54*, 165.

(271) Herbich, J.; Salgado, F. P.; Rettschnick, R. P. H.; Grabowski, Z. R.; Wójtowicz, H. *J. Phys. Chem.* **1991**, *95*, 3491.

(272) Herbich, J.; Salgado, F. P.; Karpiuk, J. *Proc. Indian Acad. Sci. (Chem. Sci.)* **1992**, *104*, 117.

(273) Bangal, P. R.; Chakravorti, S.; Mustafa, G. *Photochem. Photobiol. A: Chem.* **1998**, *113*, 35.

(274) Mishina, S.; Takayanagi, M.; Nakata, M.; Otsuki, J.; Araki, K. *J. Photochem. Photobiol. A: Chem.* **2001**, *141*, 153. Recently, the behavior of the pyridines **83** and its 3-methyl and 3,5-dimethyl derivatives is reported in more detail. **83** emits a typical dual fluorescence, whereas the compounds with a sterically hindered dimethylamino group emit only one CT fluorescence band. The dipole moments of the emitting CT states were found for these molecules to be 11−13.6 D (Szydłowska, I.; Kyrychenko, A.; Nowacki, J.; Herbich, J. *Phys. Chem. Chem. Phys.* **2003**, *5*, 1032).

(275) Braun, D.; Rettig, W.; Delmond, S.; Létard, J.-F.; Lapouyade, R. *J. Phys. Chem. A* **1997**, *101*, 6836.

(276) If the amide acceptor group contains an aromatic moiety linked to the nitrogen, then a new CT relaxation channel becomes accessible, twisting around the nitrogen−carbonyl bond. The prototype of this series of compounds is benzanilide. This type of relaxation has been investigated recently in a study using several bridged model compounds and comparison to quantum-chemical calculations: Lewis, F. D.; Liu, W. *J. Phys. Chem. A* **2002**, *106*, 1976 and references therein.

(277) Delmond, S.; Létard, J.-F.; Lapouyade, R.; Rettig, W. *BESSY Yearbook* **1996**, 461. See also: Delmond, S.; Létard, J.-F.; Lapouyade, R.; Mathevet, R.; Jonusauskas, G.; Rullière, C. *New J. Chem.* **1996**, *20*, 861.

(278) Malval, J.-P.; Lapouyade, R. *Helv. Chim. Acta* **2001**, *84*, 2439.

(279) Hamasaki, K.; Ikeda, H.; Nakamura, A.; Ueno, A.; Toda, F.; Suzuki, I.; Osa, T. *J. Am. Chem. Soc.* **1993**, *115*, 5035.

(280) Hamasaki, K.; Ueno, A.; Toda, F.; Suzuki, I.; Osa, T. *Bull. Chem. Soc. Jpn.* **1994**, *67*, 516.

(281) Sinha, H. K.; Yates, K. *J. Chem. Phys.* **1990**, *93*, 7085.

(282) Sinha, H. K.; Yates, K. *Can. J. Chem.* **1991**, *69*, 550.

(283) Mataga, N.; Okada, T.; Masuhara, H.; Nakashima, N.; Sakata Y.; Misumi, S. *J. Lumin.* **1976**, *12/13*, 159.

(284) Nagakura, S. In *Excited States*; Lim, E. C., Ed.; Academic Press: New York, 1975; Vol. 2, p 322.

(285) Mataga, N.; Miyasaka, H.; Asahi, T.; Ojima, S.; Okada, T. In *Ultrafast Phenomena VI*; Yajima, T., Yoshihara, K., Harris, C. B., Shionoya, S., Eds.; Springer-Verlag: Berlin-Heidelberg, 1988; p 511.
(286) Salem, L. *Acc. Chem. Res.* **1979**, *12*, 87.
(287) Bonačić-Koutecký, V.; Koutecký, J.; Michl, J. *Angew. Chem., Int. Ed. Engl.* **1987**, *26*, 170.
(288) Schilling C. L.; Hilinski, E. F. *J. Am. Chem. Soc.* **1988**, *110*, 2296.
(289) Hoytink, G. J.; Weiland, W. P. *Recl. Trav. Chim. Pays-Bas* **1958**, *76*, 836.
(290) Tahara, T.; Hamaguchi, H. *Chem. Phys. Lett.* **1994**, *217*, 369.
(291) Morais, J.; Ma, J.; Zimmt, M. B. *J. Phys. Chem.* **1991**, *95*, 3887.
(292) Hilinski, E. F., private communication, 1988.
(293) Okada, T.; Mataga, N.; Baumann, W. *J. Phys. Chem.* **1987**, *91*, 760.
(294) Ishitani, A.; Nagakura, S. *Theor. Chim. Acta* **1966**, *4*, 236.
(295) It is, however, reported that the benzonitrile radical anion, $PhCN^-$, in THF solution exhibits three absorption maxima, at 380, 490 (main), and 750 (weak) nm.[294] The difference in the spectra of the radical anion reported by these and other authors[296] may be due to the ion pairing in the low-polarity solvent (THF), which usually markedly affects the spectra.
(296) Chutny, B.; Swallow, A. J. *Trans. Faraday Soc.* **1970**, *66*, 2847.
(297) Shida, T.; Nosaka, Y.; Kato, T. *J. Phys. Chem.* **1978**, *82*, 695.
(298) Shida, T.; Iwata S.; Imamura, M. *J. Phys. Chem.* **1974**, *78*, 741.
(299) Beckett, A.; Osborne, A. D.; Porter, G. *Trans. Faraday Soc.* **1964**, *60*, 873.
(300) Earlier, Porter et al. reported for $PhCHO^-$ $\lambda \approx 445$ nm, and for $PhC(O^-)CH_3$ $\lambda \approx 450$ nm in alkaline ethanolic−aqueous solutions.[299]
(301) Miertuš, S.; Kysel', O. *Chem. Phys.* **1977**, *21*, 27.
(302) Zahradník R.; Polák, R. *Elements of Quantum Chemistry*; Plenum Press: New York-London, 1980.
(303) Grabowski, Z. R.; Kemula, W. *Abh. Deutsch. Akad. Wiss. Berlin, Kl. Chem., Geol., Biol.* **1964**, *1*, 377.
(304) Liptay, W. *Z. Naturforsch.* **1966**, *21a*, 1605.
(305) One can apply here, with due modifications, the treatment of the electric field effect on the *neutral* molecules, e.g., in the classical papers of Liptay,[127,304] or include the solvent interaction into the Hamiltonian, as was done for some radical ions, e.g. ref 301.
(306) CarGrabnerter, H. V.; McClelland, B. J.; Warhurst, E. *Trans. Faraday Soc.* **1960**, *56*, 455.
(307) Hashimoto, M.; Hamaguchi, H. *J. Phys. Chem.* **1995**, *99*, 7875.
(308) Chudoba, C.; Kummrow, A.; Dreyer, J.; Stenger, J.; Nibbering, E. T. J.; Elsaesser, E.; Zachariasse, K. A. *Chem. Phys. Lett.* **1999**, *309*, 357.
(309) Changenet, P.; Plaza, P.; Martin, M. M.; Meyer, Y. H. *J. Phys. Chem. A* **1997**, *101*, 8186.
(310) Dreyer, J.; Kummrow, A. *J. Am. Chem. Soc.* **2000**, *122*, 2577.
(311) Kummrow, A.; Dreyer, J.; Chudoba, C.; Stenger, J.; Nibbering, E. T. J.; Elsaesser, Th. *J. Chinese Chem. Soc.* **2000**, *47*, 721.
(312) Okamoto, H. *J. Phys. Chem. A* **2000**, *104*, 4182.
(313) Okamoto, H. *Chem. Phys. Lett.* **1998**, *283*, 33.
(314) Huppert, D.; Rand, S. D.; Rentzepis, P. M.; Barbara, P. F.; Struve, W. S.; Grabowski, Z. R. *J. Chem. Phys.* **1981**, *75*, 5714.
(315) Rotkiewicz, K.; Grabowski, Z. R.; Jasny, J. *Chem. Phys. Lett.* **1975**, *34*, 55.
(316) Takagi, Y.; Sumitani, M.; Yoshihara, K. *Rev. Sci. Instrum.* **1981**, *52*, 1003.
(317) Okamoto, H.; Inishi, H.; Nakamura, Y.; Kohtani, S.; Nakagaki, R. *Chem. Phys.* **2000**, *260*, 193.
(318) Okamoto, H.; Inishi, H.; Nakamura, Y.; Kohtani, S.; Nakagaki, R. *J. Phys. Chem. A* **2001**, *105*, 4182. In a recent paper, Okamoto et al. stated the single bond character not concluding about the structure of the ICT state of **1**, in view of inconsistencies between the calculated and observed vibrational bands (Okamoto, H.; Kinoshita, M.; Kohtani, S.; Nakagaki, R.; Zachariasse, K. A. *Bull. Chem. Soc. Jpn.* **2002**. *75*, 957).
(319) Okamoto, H., private communication, March 2001.
(320) Kwok, W. M.; Ma, C.; Phillips, D.; Matousek, P.; Parker, A. W.; Towrie, M. *J. Phys. Chem. A* **2000**, *104*, 4188.
(321) Kwok, W. M.; Ma, C.; Matousek, P.; Parker, A. W.; Phillips, D.; Toner, W. T.; Towrie, M. *Chem. Phys. Lett.* **2000**, *322*, 395.
(322) Ma, C.; Kwok, W. M.; Matousek, P.; Parker, A. W.; Phillips, D.; Toner, W. T.; Towrie, M. *J. Photochem. Photobiol. A: Chem.* **2001**, *142*, 177. In a most recent publication (Kwok, W. M.; Ma, C.; George, M. W.; Grills, D. C.; Matousek, P.; Parker, A. W.; Phillips, D.; Toner, W. T.; Towrie, M. *Phys. Chem. Chem. Phys.* **2003**, *5*, 1043), DMABN is compared to its twisted model compound TMABN, and the results (cyano mode of the CT state is similar in frequency to the benzonitrile radical anion) are in favor of the electronically decoupled TICT model.
(323) Techert, S.; Schotte, F.; Wulff, M. *Phys. Rev. Lett.* **2001**, *86*, 2030.
(324) In the crystal, the excited molecule neighbors other molecules of DMABN, and after structural relaxations in the lattice, at the reported very high density of excitation, the little-known interactions of two excited molecules (annihilation of excitons) may lead to unexpected products.
(325) Cazeau-Dubroca, C.; Peirigua, A.; Ait-Lyazidi, S.; Nouchi, G.; Cazeau P.; Lapouyade, R. *Chem. Phys. Lett.* **1986**, *124*, 110.
(326) Wang, Y.; Eisenthal, K. B. *J. Chem. Phys.* **1982**, *77*, 6076.
(327) Declémy, A.; Rullière, C.; Kottis, Ph. *Chem. Phys. Lett.* **1983**, *101*, 401.
(328) Hagopian, S.; Singer, L. A. *J. Am. Chem. Soc.* **1985**, *107*, 1874.
(329) In EtOH + H_2O (1:1), the rate of quenching by the H^+ ions, $k_q \approx 7 \times 10^8$ M^{-1} s^{-1}, is less than the diffusion limit.[328] At the same room temperature, the dissociation rate of the primary excited **98*** was $k_{-H} \approx 3 \times 10^7$ s^{-1}.
(330) Förster, Th. *Chem. Phys. Lett.* **1972**, *17*, 309.
(331) Tsutsumi, K.; Shizuka, H. *Chem. Phys. Lett.* **1977**, *52*, 485.
(332) Tobita, S.; Shizuka, H. *Chem. Phys. Lett.* **1980**, *75*, 140.
(333) Maus, M.; Rettig, W.; Bonafoux, D.; Lapouyade, R. *J. Phys. Chem. A* **1999**, *103*, 3388.
(334) Rettig, W.; Maus, M.; Lapouyade, R. *Ber. Bunsen-Ges. Phys. Chem.* **1996**, *100*, 2091.
(335) Maus, M.; Rettig, W.; Jonusauskas, G.; Lapouyade, R.; Rullière, C. *J. Phys. Chem. A* **1998**, *102*, 7393.
(336) Förster, Th. *Z. Elektrochem.* **1950**, *54*, 42; 531.
(337) Shizuka, H.; Ogiwara, T.; Kimura, E. *J. Phys. Chem.* **1985**, *89*, 4302.
(338) Förster, Th. *Chem. Phys. Lett.* **1972**, *17*, 309.
(339) Shizuka, H.; Tobita, S. *J. Am. Chem. Soc.* **1982**, *104*, 6919.
(340) Shizuka, H.; Tsutsumi, K. *Bull. Chem. Soc. Jpn.* **1983**, *56*, 629.
(341) The same effect operates in other aromatic amines, preventing the attainment of a protolytic equilibrium. Most anilinium and *N,N*-dialkylanilinium cations, including the protonated form of **1**, are very strong acids ($pK^* \approx -5$ to -9, as follows from the Förster cycle[336,435]) in their excited states *thermodynamically*, dissociate slowly, and do not *kinetically* reach the equilibrium during their excited-state lifetimes.[328,337] In the reverse proton transfer to the excited amine, another reaction occurs: a proton is attached to a different basicity center in the aromatic ring.[328,338−340]
(342) Köhler, G. *Chem. Phys. Lett.* **1986**, *126*, 260.
(343) Köhler, G. *J. Photochem.* **1986**, *35*, 189.
(344) Rechthaler, K. Dissertation, University Vienna, 1996.
(345) Grellmann, K. H.; Rotkiewicz, K. *Abstracts*, International Conference on Luminescence, Leningrad, 1972; p 224.
(346) Rotkiewicz, K. *2nd Polish Luminescence Conference; A. Luminescence of Organic Substances*; Institute of Physics, N. Copernicus University: Toruń, 1974; p 123.
(347) Köhler, G.; Grabner, G.; Rotkiewicz, K. *Chem. Phys.* **1993**, *173*, 275.
(348) Siebrand, W. *J. Chem. Phys.* **1967**, *47*, 2411.
(349) Siebrand, W. *J. Chem. Phys.* **1971**, *55*, 5843.
(350) Förster, Th. *Fluoreszenz Organischer Verbindungen*; Vandenhoeck & Ruprecht: Göttingen, 1951; Chapter X.
(351) Kołos, R.; Grabowski, Z. R. *J. Mol. Struct.* **1982**, *84*, 251.
(352) Pearson, R. G. *J. Am. Chem. Soc.* **1963**, *85*, 3533.
(353) Pearson, R. G. *Chem. Ber.* **1967**, *3*, 103.
(354) Pearson, R. G. *J. Chem. Educ.* **1968**, *45*, 643.
(355) Rotkiewicz, K.; Köhler, G.; Grabowski, Z. R. *Experimental and Theoretical Aspects of Excited-State Electron Transfer and Related Phenomena*, International Conference, Pułtusk, Poland, 1992; p 49.
(356) In concentrated aqueous electrolyte solutions, the negative curvature of the Stern−Volmer plots can be caused by several factors, inter alia, by the changes in the structure of liquid H_2O, partial freezing of the rotations, and thus slowing the quenching by water molecules, and increasing the intensity of the F_A fluorescence.
(357) Kasha, M. *Faraday Soc. Discuss.* **1950**, *9*, 14.
(358) Rettig, W.; Zander, M. *Chem. Phys. Lett.* **1982**, *87*, 229.
(359) Jivan, J. L. H.; Soumillon, J. Ph. *J. Photochem. Photobiol. A: Chem.* **1992**, *64*, 145.
(360) Soumillon, J. P. *Top. Curr. Chem.* **1993**, *168*, 93.
(361) Rehm, D.; Weller, A. *Isr. J. Chem.* **1970**, *8*, 259.
(362) Schopf, G.; Rettig, W.; Bendig, J. *J. Photochem. Photobiol. A: Chem.* **1994**, *84*, 33.
(363) Rettig, W.; Zander, M. *Z. Naturforsch.* **1984**, *39a*, 41.
(364) Shizuka, H.; Ishii, Y.; Morita, T. *Chem. Phys. Lett.* **1977**, *51*, 40.
(365) Mac, M.; Najbar, J.; Wirz, J. *Chem. Phys. Lett.* **1994**, *235*, 187.
(366) Mac, M.; Najbar, J.; Wirz, J. *J. Photochem. Photobiol. A: Chem.* **1995**, *88*, 93.
(367) Sowińska, M.; Launay, J.-P.; Mugnier, J.; Pouget, J.; Valeur, B. *J. Photochem.* **1987**, *37*, 69.
(368) Perkins, T. A.; Poureau, D. B.; Netzel, T. L.; Schanze, K. S. *J. Am. Chem. Soc.* **1989**, *93*, 4511.
(369) Levy, A.; Avnir, D.; Ottolenghi, M. *Chem. Phys. Lett.* **1985**, *121*, 233.
(370) For example, on the silica gel or modified or derivatized silicas, there occurs the B* → A* process, indicating the polarity conditions at the surface.[369]
(371) Rettig, W.; Lapouyade, R. In *Probe Design and Chemical Sensing*; Topics in Fluorescence Spectroscopy, Vol. 4; Lakowicz, J. R., Ed.; Plenum Press: New York 1994; p 109.

(372) Kundu, S.; Maity, S.; Bera, S. C.; Chattopadhyay, N. *J. Mol. Struct.* **1997**, *405*, 231.
(373) Cox, G. S.; Hauptmann, P. J.; Turro, N. J. *Photochem. Photobiol.* **1984**, *39*, 597.
(374) The authors misleadingly use in their paper the abbreviation LE for the *long-wavelength emission*, F_A.
(375) Monti, S.; Marconi, G.; Manoli, F.; Bortolus, P.; Mayer, B.; Grabner, G.; Koehler, G.; Boszczyk, W.; Rotkiewicz, K. *Phys. Chem. Chem. Phys.* **2003**, *5*, 1019. (b) Monti, S.; Marconi, G.; Manoli, F.; Bortolus, P.; Mayer, B.; Grabner, G.; Koehler, G.; Boszczyk, W.; Rotkiewicz, K. *Photochem. Photobiol. Sci.* **2003**, *2*, 203.
(376) Nag, A.; Bhattacharyya, K. *Chem. Phys. Lett.* **1988**, *151*, 474.
(377) Bhattacharyya, K.; Chowdhury, M. *Chem. Rev.* **1993**, *93*, 507.
(378) Al-Hassan, K. A.; Klein, U. K. A.; Suwaiyan, A. *Chem. Phys. Lett.* **1993**, *212*, 581.
(379) Al-Hassan, K. A. *Chem. Phys. Lett.* **1994**, *227*, 527.
(380) Kundu, S.; Chattopadhyay, N. *J. Mol. Struct.* **1995**, *344*, 151.
(381) Al-Hassan, K. A.; Suwaiyan, A.; Klein, U. K. A. *Arab. J. Sci. Eng.* **1997**, *22*, 45.
(382) Matsushita, Y.; Hikida, T. *Chem. Phys. Lett.* **1998**, *290*, 349.
(383) Nag, A.; Dutta, R.; Chattopadhyay, N.; Bhattacharyya, K. *Chem. Phys. Lett.* **1989**, *187*, 83.
(384) El Baraka, M.; García, R.; Quiñones, E. *J. Photochem. Photobiol. A: Chem.* **1994**, *79*, 181.
(385) Kundu, S.; Chattopadhyay, N. *J. Photochem. Photobiol. A: Chem.* **1995**, *88*, 105.
(386) Feliciano, C. E.; Quiñones, E. *J. Photochem. Photobiol. A: Chem.* **1999**, *120*, 23.
(387) Nag, A.; Bhattacharyya, K. *J. Chem. Soc., Faraday Trans.* **1990**, *86*, 53.
(388) Nakamura, A.; Sato, S.; Hamasaki, K.; Ueno, A.; Toda, F. *J. Phys. Chem.* **1995**, *99*, 10952.
(389) A heterodimer is the 1:1 complex of **1** + CD, associated with a complex — also 1:1 — of another chemical species with CD.
(390) Pozuelo, J.; Nakamura, A.; Mendicuti, F. *J. Inclusion Phenom. Macrocycl. Chem.* **1999**, *35*, 467.
(391) Al-Hassan, K. A.; Azumi, T.; Rettig, W. *Chem. Phys. Lett.* **1993**, *206*, 25.
(392) Kundu, S.; Bera, S. C.; Chattopadhyay, N. *Ind. J. Chem. A* **1998**, *37*, 102. Similarly, the properties of the 1:1 complex of **72** are ascribed to the structure with the $-NR_2$ group inside the cavity of α- *resp.* β-CD (Jiang, Y.-B. *J. Photochem. Photobiol. A: Chem.* **1995**,*88*, 109).
(393) Banu, H. S.; Pitchumani, K.; Srinivasan, C. *J. Photochem. Photobiol. A: Chem.* **2000**, *131*, 101.
(394) An apparent difference in the spectral positions of the gas-phase absorption spectrum of **21** in two papers[135,138] results from an obvious misprint on the wavenumber scale in Figure 1 of the first paper:[135] instead of 30×10^3 and 32×10^3 cm^{-1}, the numbers should be 32×10^3 and 36×10^3 cm^{-1}.
(395) Peng, L. W.; Dantus, M.; Zewail, A. H.; Kemnitz, K.; Hicks, J. M.; Eisenthal, K. B. *J. Phys. Chem.* **1987**, *91*, 6162.
(396) Sun, Y.-P.; Fox, M. A.; Johnston, K. P. *J. Am. Chem. Soc.* **1992**, *114*, 1187.
(397) Kajimoto, O.; Nayuki, T.; Kobayashi, T. *Chem. Phys. Lett.* **1993**, 209, 357.
(398) Subaric-Leitis, A.; Monte, Ch.; Roggan, A.; Rettig, W.; Zimmermann, P.; Heinze, J. *J. Chem. Phys.* **1990**, *93*, 4543.
(399) Monte, C.; Roggan, A.; Subaric-Leitis, A.; Rettig, W.; Zimmermann, P. *J. Chem. Phys.* **1993**, *98*, 2580.
(400) Kobayashi, T.; Futakami M.; Kajimoto, O. *Chem. Phys. Lett.* **1986**, *130*, 63.
(401) Kajimoto, O.; Yokoyama, H.; Ooshima, Y.; Endo, Y. *Chem. Phys. Lett.* **1991**, *179*, 455.
(402) Kajimoto, O. In *Dynamics of Excited Molecules*; Kuchitsu, K., Ed.; Studies in Physical and Theoretical Chemistry; Elsevier Science: Amsterdam, 1994; p 363.
(403) Scholes, G. D.; Phillips, D.; Gould, I. R. *Chem. Phys. Lett.* **1997**, *266*, 521.
(404) Polimeno, A.; Barbon, A.; Nordio, P. L.; Rettig, W. *J. Phys. Chem.* **1994**, *98*, 12158.
(405) Grassian, V. H.; Warren, J. A.; Bernstein, E. R.; Secor, H. V. *J. Chem. Phys.* **1989**, *90*, 3994. Comment: Gordon, R. D. *J. Chem. Phys.* **1990**, *93*, 6908. Reply to the Comment: Bernstein, E. R.; Grassian, V. H.; Warren, J. A. *J. Chem. Phys.* **1990**, *93*, 6910.
(406) Gorse, A. D.; Pesquer, M. *J. Mol Struct. (THEOCHEM)* **1993**, *281*, 21.
(407) Kato, S.; Amatatsu, Y. *J. Chem. Phys.* **1990**, *92*, 7241.
(408) August, J.; Palmer, T. F.; Simons, J. P.; Jouvet, C.; Rettig, W. *Chem. Phys. Lett.* **1988**, *145*, 273.
(409) Gibson, E. M.; Jones, A. C.; Phillips, D. *Chem. Phys. Lett.* **1987**, *136*, 454.
(410) Gibson, E. M.; Jones, A. C.; Phillips, D. *Chem. Phys. Lett.* **1988**, *146*, 270.
(411) Howells, B. D.; McCombie, J.; Palmer, T. F.; Simons, J. P.; Walters, A. *J. Chem. Soc., Faraday Trans.* **1992**, *88*, 2587.
(412) Howells, B. D.; McCombie, J.; Palmer, T. F.; Simons, J. P.; Walters, A. *J. Chem. Soc., Faraday Trans.* **1992**, *88*, 2595.
(413) Howells, B. D.; McCombie, J.; Palmer, T. F.; Simons, J. P.; Walters, A. *J. Chem. Soc., Faraday Trans.* **1992**, *88*, 2603.
(414) Howell, R.; Petek, J.; Phillips, D.; Yoshihara, K. *Chem. Phys. Lett.* **1991**, *183*, 249.
(415) Howell, R.; Phillips, D.; Petek, H.; Yoshihara, K. *Chem. Phys.* **1994**, *188*, 303.
(416) Phillips, D. *J. Photochem. Photobiol. A: Chem.* **1997**, *105*, 307.
(417) Lommatzsch, U.; Gerlach, A.; Lahmann, C.; Brutschy, B. *J. Phys. Chem. A* **1998**, *102*, 6421.
(418) Nakashima, N.; Inoue, H.; Mataga, N.; Yamanaka, Y. *Bull. Chem. Soc. Jpn.* **1973**, *46*, 2288.
(419) Fuss, W.; Pushpa, K. K.; Rettig, W.; Schmid, W. E.; Trushin, S. A. *Photochem. Photobiol. Sci.* **2002**, *1*, 255.
(420) Phillips, D.; Howell, R.; Taylor, A. G. *Proc. Indian Acad. Sci. (Chem. Sci.)* **1992**, *104*, 153.
(421) Weersink, R. A.; Wallace, S. C. *J. Phys. Chem.* **1994**, *98*, 10710.
(422) Kobayashi, T.; Futakami M.; Kajimoto, O. *Chem. Phys. Lett.* **1986**, *130*, 63.
(423) Herbich, J.; Brutschy, B. In *Electron Transfer in Chemistry*; Balzani, V., Ed.; Wiley-VCH: Weinheim-New York, 2001; Vol. 4, p 697.
(424) Sobolewski, A. L.; Sudholt, W.; Domcke, W. *J. Phys. Chem. A* **1998**, *102*, 2716.
(425) Howells, B. D.; Martinez, M. T.; Palmer, T. F.; Simons, J. P.; Walters, A. *J. Chem. Soc., Faraday Trans.* **1990**, *86*, 1949.
(426) Grégoire, G.; Dimicoli, I.; Mons, M.; Dedonder-Lardeux, C.; Jouvet, C.; Martrenchard, S.; Solgadi, D. *J. Phys. Chem. A* **1998**, *102*, 7896.
(427) Bliss, B.; Lommatzsch, U.; Monte, C.; Rettig, W.; Brutschy, B. *Chem. Phys.* **2000**, *254*, 407.
(428) Yu, H.; Joslin, E.; Zain, S. M.; Rzepa, H.; Phillips, D. *Chem. Phys.* **1993**, *178*, 483.
(429) Yu, H.; Joslin, E.; Crystall, B.; Smith, T.; Sinclair, W.; Phillips, D. *J. Phys. Chem.* **1993**, *97*, 8146.
(430) Hepworth, P. A.; McCombie, J.; Simons, J. P.; Pfanstiel, J. F.; Ribblett, J. W.; Pratt, D. W. *Chem. Phys. Lett.* **1996**, *249*, 341.
(431) Berden, G.; van Rooy, J.; Meerts, W. L.; Zachariasse, K. A. *Chem. Phys. Lett.* **1997**, *278*, 373.
(432) Helm, R. M.; Vogel, H.-P.; Neusser, H. J. *Chem. Phys. Lett.* **1997**, *270*, 285.
(433) Sinclair, W. E.; Pratt, D. W. *J. Chem. Phys.* **1996**, *105*, 7942.
(434) The effect of temperature can also be indirect, changing the polarity of the solvent. The polarity of the fluid solvents *increases* with lowering temperature. This in turn influences the rates, especially the internal conversion (charge recombination), contributing thus to k_A.
(435) Grabowski Z. R.; Grabowska A. *Z. Phys. Chem., N.F.* **1976**, *101*, 197; **1977**, *105*, 112 (erratum).
(436) Struve, W. S.; Rentzepis, P. M.; Jortner, J. *J. Chem. Phys.* **1973**, *59*, 5014.
(437) Huppert, D.; Kanety, H.; Kosower, E. M. *Chem. Phys. Lett.* **1981**, *84*, 48.
(438) Wang, Y.; McAuliffe, M.; Novak, F.; Eisenthal, K. B. *J. Phys. Chem.* **1981**, *85*, 3736.
(439) Struve, W. S.; Rentzepis, P. M. *J. Chem. Phys.* **1974**, *60*, 1533.
(440) Horng, M. L.; Gardecki, A.; Papazyan, A.; Maroncelli, M. *J. Phys. Chem.* **1995**, *99*, 17311.
(441) The longitudinal relaxation time, $\tau_L = \tau_D(\epsilon_\infty/\epsilon_0)$, describes the dipolar relaxation in the field of a constant *charge*, e.g., of a newly formed large dipole, whereby the Debye relaxation time, τ_D, corresponds to the relaxation at a constant *field strength*.[443] ϵ_0 is the static dielectric permittivity, and ϵ_∞ is the permittivity at $\nu \rightarrow \infty$, $\epsilon_\infty \approx n^2$. Another measure of the solvent relaxation time is the *average solvation time*, τ_S, as determined from the time-resolved solvatochromic shift of the fluorescence bands.[440]
(442) Kosower, E. M.; Huppert, D. *Chem. Phys. Lett.* **1983**, *96*, 433.
(443) Mozumder, A. *J. Chem. Phys.* **1969**, *50*, 3153; 3162.
(444) Simon, J. D. *Acc. Chem. Res.* **1988**, *21*, 128.
(445) Förster Th. *Pure Appl. Chem.* **1970**, *24*, 443.
(446) Turro, N. J.; McVey, J.; Ramamurthy V.; Lechtken, P. *Angew. Chem.* **1979**, *91*, 597.
(447) If the emission of the product is strongly forbidden; emission from the reaction path may initially be more intense than that from the potential minimum of the product; the *fluorescence rise* of the product in such cases would be faster than that of its *population* (Grabowski, Z. R.; Dobkowski, J.; Rullière, C. *ICL'93 Technical Digest*; University of Connecticut: Storrs, CT, 1993; p 99). Therefore, in doubtful cases it is advisable to take for comparison the rise time of the transient absorption, which can reflect the population rise more exactly than the fluorescence intensity.
(448) Birks, J. B. *Photophysics of Aromatic Molecules*; Wiley-Interscience: London, 1970.
(449) Birks, J. B. *Nouv. J. Chim.* **1977**, *1*, 455.
(450) Hicks, J.; Vandersall, M.; Babarogic, Z.; Eisenthal, K. B. *Chem. Phys. Lett.* **1985**, *116*, 18.
(451) Hicks, J. M.; Vandersall, M. T.; Sitzmann E. V.; Eisenthal, K. B. *Chem. Phys. Lett.* **1987**, *135*, 413.
(452) Heisel, F.; Miehé, J. A. *Chem. Phys.* **1985**, *98*, 233.

(453) Meech, S. R.; Phillips, D. *Chem. Phys. Lett.* **1985**, *116*, 262; *J. Chem. Soc., Faraday Trans. 2* **1987**, *83*, 1941. The complex kinetics of the fluorescence of **1** in the mixed solvents CHX + EtOH is ascribed to the existence of more than two excited chemical species in the ICT reaction.
(454) Braun, D.; Rettig, W. *Chem. Phys.* **1994**, *180*, 231.
(455) Rettig, W. *Ber. Bunsen-Ges. Phys. Chem.* **1991**, *95*, 259.
(456) Rettig, W. In *Dynamics and Mechanisms of Photoinduced Electron Transfer and Related Phenomena*; Mataga, N., Okada, T., Masuhara, H., Eds.; Elsevier Science Publ.: Amsterdam, 1992; p 57.
(457) Rettig, W.; Wermuth, G. *J. Photochem.* **1985**, *28*, 351.
(458) Heisel, F.; Miehé, J. A.; Martinho, J. M. G. *Chem. Phys.* **1985**, *98*, 243.
(459) Rettig, W.; Fritz, R.; Braun, D. *J. Phys. Chem. A* **1997**, *101*, 6830.
(460) Grobys, M.; Zachariasse, K. A. *J. Inf. Recording* **1998**, *24*, 405.
(461) Bagchi, B. *Chem. Phys. Lett.* **1987**, *135*, 558.
(462) Bagchi, B.; Fleming, G. R. *J. Phys. Chem.* **1990**, *94*, 9.
(463) Bagchi, B.; Fleming, G. R.; Oxtoby, D. W. *J. Chem. Phys.* **1983**, *78*, 7375.
(464) Braun, D.; Rettig, W. *Chem. Phys. Lett.* **1997**, *268*, 110.
(465) Köhler, G.; Getoff, N.; Rotkiewicz, K.; Grabowski, Z. R. *J. Photochem.* **1985**, *28*, 537.
(466) Bernardi, F.; Olivucci, M.; Robb, M. A. *Chem. Soc. Rev.* **1996**, *25*, 1321.
(467) Changenet, P.; Plaza, P.; Martin, M. M.; Meyer, Y. H. *J. Phys. Chem. A* **1997**, *101*, 8186.
(468) Sumi, H.; Marcus, R. A. *J. Chem. Phys.* **1986**, *84*, 4894.
(469) Nadler, W.; Marcus, R. A. *J. Chem. Phys.* **1987**, *86*, 3906.
(470) Heitele, H. *Angew. Chem.* **1993**, *105*, 378.
(471) Su, S. G.; Simon, J. D. *J. Chem. Phys.* **1988**, *89*, 908.
(472) Schenter, G. K.; Duke, C. B. *Chem. Phys. Lett.* **1991**, *176*, 563.
(473) Fonseca, T.; Kim, H. J.; Hynes, J. T. *J. Mol. Liq.* **1994**, *60*, 161.
(474) Fonseca, T.; Kim, H. J.; Hynes, J. T. *J. Photochem. Photobiol. A: Chem.* **1994**, *82*, 67.
(475) Giacometti, G.; Moro, G. J.; Nordio, P. L.; Polimeno, A. *J. Mol. Liq.* **1989**, *42*, 19.
(476) Moro, G. J.; Nordio, P. L.; Polimeno, A. *Mol. Phys.* **1989**, *68*, 1131.
(477) Nordio, P. L.; Polimeno, A.; Barbon, A. *Polish J. Chem.* **1993**, *67*, 8.
(478) Saielli, G.; Braun, D.; Polimeno, A.; Nordio, P. L. *Chem. Phys. Lett.* **1996**, *257*, 381.
(479) Braun, D.; Nordio, P. L.; Polimeno, A.; Saielli, G. *Chem. Phys.* **1996**, *208*, 127.
(480) Kim, H. J.; Hynes, J. T. *J. Photochem. Photobiol. A: Chem.* **1997**, *105*, 337.
(481) Nordio, P. L.; Polimeno, A.; Saielli, G. *J. Photochem. Photobiol. A: Chem.* **1997**, *105*, 269.
(482) Dorairaj, S.; Kim, H. J. *J. Phys. Chem. A* **2002**, *106*, 2322.
(483) Nordio, P. L.; Polimeno, A. *Mol. Phys.* **1996**, *88*, 315.
(484) Rettig, W.; Bonačić-Koutecký, V. *Chem. Phys. Lett.* **1979**, *62*, 115.
(485) Lipiński, J.; Chojnacki, H.; Grabowski, Z. R.; Rotkiewicz, K. *Chem. Phys. Lett.* **1980**, *70*, 449.
(486) Majumdar, D.; Sen, R.; Bhattacharyya, K.; Bhattacharyya, S. P. *J. Phys. Chem.* **1991**, *95*, 4324.
(487) Soujanya, T.; Saroja G.; Samanta, A. *Chem. Phys. Lett.* **1995**, *236*, 503.
(488) Broo, A.; Zerner, M. C. *Theor. Chim. Acta (Berlin)* **1995**, *90*, 383.
(489) Gedeck, P.; Schneider, S. *J. Photochem. Photobiol. A: Chem.* **1997**, *105*, 165.
(490) Hayashi, S.; Ando, K.; Kato, S. *J. Phys. Chem.* **1995**, *99*, 955.
(491) Sudholt, W.; Staib, A.; Sobolewski, A. L.; Domcke, W. *Phys. Chem. Chem. Phys.* **2000**, *2*, 4341.
(492) Ando, K.; Kato, S. *J. Chem. Phys.* **1991**, *95*, 5966.
(493) Scholes, G. D.; Fournier, T.; Parker, A. W.; Phillips, D. *J. Chem. Phys.* **1999**, *111*, 5999.
(494) Lommatzsch, U.; Brutschy, B. *Chem. Phys.* **1998**, *234*, 35.
(495) Jameson, G. B.; Sheikh-Ali, B. M.; Weiss, R. G. *Acta Crystallogr., Sect. B: Struct. Sci.* **1994**, *50*, 703.
(496) Sobolewski, A. L.; Domcke, W. *J. Photochem. Photobiol. A: Chem.* **1997**, *105*, 325.
(497) Parusel, A. B. J.; Köhler, G.; Grimme, S. *J. Phys. Chem. A* **1998**, *102*, 6297.
(498) Bergamasco, S.; Calzaferri, G.; Hädener, K. *J. Photochem. Photobiol. A: Chem.* **1992**, *66*, 327.
(499) Calzaferri, G.; Rytz, R. *J. Phys. Chem.* **1995**, *99*, 12141.
(500) Parusel, A. B. J.; Köhler, G.; Nooijen, M. *J. Phys. Chem. A* **1999**, *103*, 4056.
(501) Cammi, R.; Menucci, B.; Tomasi, J. *J. Phys. Chem. A* **2000**, *104*, 5631.
(502) This finding may be of importance in interpreting the uncertainties as to the Onsager radius in cases when bulky uncharged groups increase the molecular volume; for the treatment of the point dipole situated eccentrically in the Onsager cavity, see the appendix to ref 61.
(503) Parusel, A. B. J.; Rettig, W.; Sudholt, W. *J. Phys. Chem. A* **2002**, *106*, 804.
(504) Zilberg, S.; Haas, Y. *J. Phys. Chem. A* **2002**, *106*, 1.
(505) Bonačić-Koutecký, V.; Michl, J. *J. Am. Chem. Soc.* **1985**, *107*, 1765.
(506) Klock, A. M.; Rettig, W. *Polish J. Chem.* **1993**, *67*, 1375.
(507) Maus, M.; Rettig, W.; Lapouyade, R. *J. Inf. Recording* **1996**, *22*, 451.
(508) Lapouyade, R.; Czeschka, C.; Majenz, W.; Rettig, W.; Gilabert, E.; Rullière, C. *J. Phys. Chem.* **1992**, *96*, 9643.
(509) Dobkowski, J.; Rettig, W.; Paeplow, B.; Koch, K.; Müllen, K. H.; Lapouyade, R.; Grabowski, Z. R. *New J. Chem.* **1994**, *18*, 525.
(510) Herbich, J.; Kapturkiewicz, A. *Chem. Phys.* **1991**, *158*, 143.
(511) Bixon, M.; Jortner, J.; Verhoeven, J. W. *J. Am. Chem. Soc.* **1994**, *116*, 7349.
(512) Verhoeven, J. W.; Scherer, T.; Wegewijs, B.; Hermant, R. M.; Jortner, J.; Bixon, M.; Depaemelaere, S.; De Schryver, F. C. *Recl. Trav. Chim.* **1995**, *114*, 443.
(513) Gould, I. R.; Young, R. H.; Mueller, L. J.; Albrecht, A. C.; Farid, S. *J. Am. Chem. Soc.* **1994**, *116*, 8188.
(514) Kwok, W. M.; Ma, C.; Matousek, P.; Parker, A. W.; Phillips, D.; Toner, W. T.; Towrie, M.; Umpathy, S. *J. Phys. Chem. A* **2001**, *105*, 984.
(515) Ma, C.; Kwok, W. M.; Matousek, P.; Parker, A. W.; Phillips, D.; Toner, W. T.; Towrie, M. *J. Phys. Chem. A* **2001**, *105*, 4648.
(516) Okamoto, H.; Kinoshita, M. *J. Phys. Chem. A* **2002**, *106*, 3485.
(517) Dobkowski, J.; Wójcik, J.; Koźmiński, W.; Kołos, R.; Waluk, J.; Michl, J. *J. Am. Chem. Soc.* **2002**, *124*, 2407.
(518) **22** emits a forbidden CT band, which disagrees with the state-interaction model: for this compound, with a large energy gap between the two low-lying π,π^* states, ^1L_b and ^1L_a (0.8−0.9 eV[164]), the state interaction should be very weak. The lowest excited singlet state seems in reality to be the n,π^* (CT) state, strongly mixed with the π,π^* states.
(519) The theory developed by Beens and Weller[50] is derived for the sandwich exciplexes; it is, however, fairly general and easily applicable to the D−A molecules.
(520) Mulliken, R. S. *J. Am. Chem. Soc.* **1950**, *72*, 600.
(521) Murrell, J. N. *Q. Rev.* **1961**, *15*, 191.
(522) Murrell, J. N. *The Theory of Electronic Spectra of Organic Molecules*; Methuen: London, 1963.
(523) Longuet-Higgins, H. C.; Murrell, J. N. *Proc. Phys. Soc.* **1955**, *A68*, 601.
(524) Herbich, J.; Kapturkiewicz, A. *J. Am. Chem. Soc.* **1998**, *120*, 1014.
(525) Herbich, J. Photoinduced Intramolecular Electron Transfer in Donor−Acceptor Molecules. Structural & Environmental Aspects. Habilitation thesis, Institute of Physical Chemistry, Polish Academy of Sciences, Warsaw, 1998.
(526) Dogonadze, R. R.; Kuznetsov, A. M.; Marsagishvili, T. A. *Electrochim. Acta* **1980**, *25*, 1.
(527) Gould, I. R.; Noukakis, D.; Gomez-Jahn, L.; Young, R. H.; Goodman, J. L.; Farid, S. *Chem. Phys.* **1993**, *176*, 439.
(528) Jortner, J.; Bixon, M. *J. Photochem. Photobiol. A: Chem.* **1992**, *64*, 145.
(529) Cortés, J.; Heitele, H.; Jortner, J. *J. Phys. Chem.* **1994**, *98*, 2527.
(530) Kapturkiewicz, A. Electrochemical Generation of Excited States. Habilitation thesis, Institute of Physical Chemistry, Polish Academy of Sciences, Warsaw, 1992.
(531) Marcus, R. A. *J. Chem. Phys.* **1965**, *43*, 2654.
(532) The transition moments are calculated from the absorption (eq 30) or from the emission band: eq 17, or $M_f^2 = 3h\phi_f/64n^3\pi^4\tau_f\langle\tilde{\nu}_f^3\rangle$.
(533) Grabowski, Z. R.; Rotkiewicz, K.; Sadlej, A. J. *Proceedings of the International Conference on Luminescence*; Akademiai Kiado: Budapest, 1966; p 310.
(534) Rotkiewicz, K.; Grabowski, Z. R. *Trans. Faraday Soc.* **1969**, *91*, 6863.
(535) Dey, J.; Warner, I. M. *J. Phys. Chem. A* **1997**, *101*, 4872.
(536) Moreover, the compound is very easily oxidizable by atmospheric oxygen; no attention seems to have been paid to this in the cited work.
(537) Muralidharan, S.; Yates, K. *Chem. Phys. Lett.* **1992**, *192*, 571.
(538) Druzhinin, S.; Demeter, A.; Niebuer, M.; Tauer, E.; Zachariasse, K. A. *Res. Chem. Intermed.* **1999**, *25*, 531.
(539) Lee, S.; Arita, K.; Kajimoto, O. *Chem. Phys. Lett.* **1997**, *265*, 579.
(540) Okada, T.; Fujita, T.; Kubota, M.; Masaki, S.; Mataga, N.; Ide, R.; Sakata, Y.; Misumi, S. *Chem. Phys. Lett.* **1972**, *14*, 563.
(541) Okada, T.; Fujita T.; Mataga, N. *Z. Phys. Chem. N.F.* **1976**, *101*, 57.
(542) Kajimoto, O.; Hayami, S.; Shizuka, H. *Chem. Phys. Lett.* **1991**, *177*, 219.
(543) Okada, T.; Kawai, M.; Ikemachi, T.; Mataga, N.; Sakata Y.; Misumi, S.; Shionoya, S. *J. Phys. Chem.* **1984**, *88*, 1976.
(544) A simple thermodynamic estimate assuming a center-to-center ET between the aromatic rings (resulting in $\mu^* = 20.6$ D) and using the solvent polarity function, eq 3, resulted in a fluorescence maximum of 2.06 eV for **26** in ACN; the experimental value is 2.07 eV. [126]
(545) Baumann, W.; Petzke, F.; Loosen, K.-D. *Z. Naturforsch.* **1979**, *34a*, 1070.
(546) Baumann, W.; Schwager, B.; Detzer, N.; Okada T.; Mataga, N. *J. Phys. Chem.* **1988**, *92*, 3742.

(547) Mataga, N.; Okada, T.; Yamamoto, N. *Chem. Phys. Lett.* **1967**, *1*, 119.
(548) Siemiarczuk, A.; Ware, W. R. *J. Phys. Chem.* **1987**, *91*, 3677.
(549) Huppert, D.; Rentzepis, P. M. *J. Phys. Chem.* **1988**, *92*, 5466.
(550) Tominaga, K.; Walker, G. C.; Jarzęba, W.; Barbara, P. F. *J. Phys. Chem.* **1991**, *95*, 10475.
(551) Detzer, N.; Baumann, W.; Fröhling, J.-C.; Brittinger, C. *Z. Naturforsch.* **1987**, *42a*, 395.
(552) Okada, T.; Mataga, N.; Baumann, W.; Siemiarczuk, A. *J. Phys. Chem.* **1987**, *91*, 4490.
(553) Baumann, W.; Schwager, B.; Detzer, N.; Okada T.; Mataga, N. *Bull. Chem. Soc. Jpn.* **1987**, *60*, 4245.
(554) Okada, T. *Proc. Indian Acad. Sci. (Chem. Sci.)* **1992**, *104*, 173.
(555) Rollison, A. M.; Drickamer, H. G. *J. Chem. Phys.* **1980**, *73*, 5981.
(556) Tominaga, K.; Walker, G. C.; Kang, T. J.; Barbara, P. F.; Fonseca, T. *J. Phys. Chem.* **1991**, *95*, 10485.
(557) Siemiarczuk, A. *Chem. Phys. Lett.* **1984**, *110*, 437.
(558) Menzel, R.; Windsor, M. W. *Chem. Phys. Lett.* **1991**, *184*, 6.
(559) Reduced absorption band is defined as $\epsilon(\nu)/\nu$ plotted vs ν; a reduced emission band means $I_f(\nu)n^3$ plotted against ν.
(560) Martin, M. M.; Plaza, P.; Changenet-Barret, P.; Siemiarczuk, A. *J. Phys. Chem. A* **2002**, *106*, 2351.
(561) Herbich, J.; Dobkowski, J.; Rullière, C.; Nowacki, J. *J. Lumin.* **1989**, *44*, 87.
(562) Kindly synthesized electrochemically by A. Kapturkiewicz.
(563) Czerwieniec, R.; Herbich, J.; Kapturkiewicz, A.; Nowacki, J. *Chem. Phys. Lett.* **2000**, *325*, 589.
(564) Meech, S. R.; O'Connor, D. V.; Phillips, D.; Lee, A. *J. Chem. Soc., Faraday Trans. 2* **1983**, *79*, 1563.
(565) Röckert, I.; Demeter, A.; Morawski, O,; Kühnle, W.; Tauer, E.; Zachariasse, K. A. *J. Phys. Chem. A* **1999**, *103*, 1958. Suzuki, K.; Demeter, A.; Kûhnle, W.; Tauer, E.; Zachariasse, K. A.: Tobita, S.; Shizuka, H. *Phys. Chem. Chem. Phys* **2000**, *2*, 981.
(566) Nowak, W.; Rettig, W. *J. Mol. Struct. (THEOCHEM)* **1993**, *283*, 1.
(567) Parusel, A. B. J.; Nowak, W.; Grimme, S.; Köhler, G. *J. Phys. Chem. A* **1998**, *102*, 7149.
(568) Ayuk, A. A.; Rettig, W.; Lippert, E. *Ber. Bunsen-Ges. Phys. Chem.* **1981**, *85*, 553.
(569) Lippert, E.; Ayuk, A. A.; Rettig, W.; Wermuth, G. *J. Photochem.* **1981**, *17*, 237.
(570) Ayuk, A. A. *J. Mol. Struct.* **1982**, *84*, 169.
(571) Weber, G.; Farris, F. J. *Biochemistry* **1979**, *18*, 3075.
(572) Cowley, D. J. *Nature* **1986**, *319*, 14.
(573) MacGregor, R. B.; Weber, G. *Nature* **1986**, *319*, 70.
(574) Hutterer, R.; Parusel, A. B. J.; Hof, M. *J. Fluoresc.* **1998**, *8*, 389.
(575) Parasassi, T.; Krasnowska, E. K.; Bagatolli, L.; Gratton, E. *J. Fluoresc.* **1998**, *8*, 365.
(576) Nowak, W.; Adamczak, P.; Balter, A.; Sygula, J. *J. Mol. Struct. (THEOCHEM)* **1986**, *39*, 13.
(577) Lakowicz, J. R.; Balter, A. *Biophys. Chem.* **1982**, *16*, 117; 223.
(578) Heisel, F.; Miehé, J. A.; Szemik, A. W. *Chem. Phys. Lett.* **1987**, *138*, 321.
(579) Parusel, A. B. J.; Schneider, F. W.; Köhler, G. *J. Mol. Struct. (THEOCHEM)* **1997**, *398/399*, 341.
(580) Catalan, J.; Perez, P.; Laynez, J.; Blanco, F. G. *J. Fluoresc.* **1991**, *1*, 215.
(581) Baumann, W.; Nagy, Z.; Maiti, A. K.; Reis, H.; Rodrigues, S. V.; Detzer, N. In *Dynamics and Mechanism of Photoinduced Transfer and Related Phenomena*; Mataga, N., Okada T., Masuhara, H., Eds.; Elsevier Sci. Publ.: Amsterdam, 1992; p 211.
(582) Bunker, C. E.; Bowen, T. L.; Sun, Y.-P. *Photochem. Photobiol.* **1993**, *58*, 499.
(583) Parusel, A. B. J. Quantum Mechanical Studies: Intramolecular Charge Transfer in Organic Donor−Acceptor Systems. Ph. D. Thesis, University of Vienna, 1998; p 225.
(584) Samanta, A.; Fessenden, R. W. *J. Phys. Chem. A* **2000**, *104*, 8972.
(585) Kosower, E. M.; Dodiuk, H. *J. Am. Chem. Soc.* **1978**, *100*, 4173.
(586) Kosower, E. M.; Dodiuk, H.; Kanety, H. *J. Am. Chem. Soc.* **1978**, *100*, 4179.
(587) Lakowicz, J. R. *Principles of Fluorescence Spectroscopy*; Plenum Press: New York, 1983; Chapter 7.
(588) Kosower, E. M. *Acc. Chem. Res.* **1982**, *15*, 259.
(589) Kosower, E. M.; Kanety, H. *J. Am. Chem. Soc.* **1983**, *105*, 6236.
(590) Huppert, D.; Kanety, H.; Kosower, E. M. *Faraday Discuss. Chem. Soc.* **1982**, *74*, 161.
(591) Huppert, D.; Ittah, V.; Kosower, E. M. *Chem. Phys. Lett.* **1988**, *144*, 15.
(592) Kanety, H.; Kosower, E. M. *J. Phys. Chem.* **1982**, *86*, 3776.
(593) Dodiuk, H.; Kosower, E. M. *Chem. Phys. Lett.* **1975**, *34*, 253.
(594) Kosower, E. M.; Kanety, H.; Dodiuk, H.; Striker, G.; Jovin, T.; Boni, H.; Huppert, D. *J. Phys. Chem.* **1983**, *87*, 2479.
(595) Kosower et al. use for the ^{1}LE the symbols $S_{1,np}$ (np for nonplanar) and $S_{1,ct}$ for the ^{1}CT state. Additionally, they distinguish the $S_{1,ct(U)}$ and $S_{1,ct(C)}$ for unconjugated *resp.* conjugated, whereby the conjugation is meant between the central amino N atom and the phenyl ring.
(596) Paczkowski, J.; Neckers, D. C. *Macromolecules* **1992**, *25*, 548.
(597) Albinsson, B. J. *J. Am. Chem. Soc.* **1997**, *119*, 6369.
(598) Andréasson, J.; Holmén, A.; Albinsson, B. *J. Phys. Chem. B* **1999**, *103*, 9782.
(599) Parusel, A. B. J.; Rettig, W.; Rotkiewicz K. *J. Phys. Chem. A* **2002**, *106*, 2293.
(600) Wilson, R. W.; Callis, P. R. *Photochem. Photobiol.* **1980**, *31*, 323.
(601) Parusel, A. B. J.; Szczepanik, B.; Rotkiewicz, K. *Book of Abstracts*, 18th IUPAC Symposium on Photochemistry, Dresden, 2000; p 519.
(602) The (only) fluorescence band B of, e.g., **20** or **114**, is also strongly quenched at room temperature by the protic solvents, especially by H_2O.[125,211]
(603) In alcohols, the intensity of the CT band depends also on the quenching by the proton donors (like in section IV.C.1).
(604) Fluorescence of **164a** and **168** in hexane possesses a structured component,[605] interpreted as dual emission from LE and CT.
(605) Cornelissen-Gude, C.; Rettig, W. *J. Phys. Chem. A* **1998**, *102*, 7754.
(606) Rettig, W.; Marschner, F. *Nouv. J. Chim.* **1983**, *7*, 425.
(607) Okuyama, K.; Numata, Y.; Odawara, S.; Suzuka, I. *J. Chem. Phys.* **1998**, *109*, 7185.
(608) Proppe, B.; Merchàn, M.; Serrano-Andrés, L. *J. Phys. Chem. A* **2000**, *104*, 1608.
(609) Parusel, A. B. J. *Phys. Chem. Chem. Phys.* **2000**, *2*, 5545.
(610) Sarkar, A.; Chakravorti, S. *Chem. Phys. Lett.* **1995**, *235*, 195.
(611) Suzuka, I.; Odawara, S.; Numata, Y.; Okuyama, K.; Kozawa, M. *Book of Abstracts*, 17th IUPAC Symposium on Photochemistry, Sitges, Spain, 1998; p 75.
(612) Cornelissen-Gude, C.; Rettig, W. *J. Phys. Chem. A* **1999**, *103*, 4371.
(613) Weedon, A. In *Advances in Photochemistry*; Neckers, D. C., Volman, D. H., von Bûnau, G., Eds.; J. Wiley & Sons: New York, 1997; Vol. 22, p 229.
(614) Disanayaka, B. W.; Weedon, A. C. *Can. J. Chem.* **1990**, *68*, 1685.
(615) Weedon, A. C.; Wong, D. F. *J. Photochem. Photobiol. A: Chem.* **1991**, *61*, 27.
(616) Disanayaka, B. W.; Weedon, A. C. *Can. J. Chem.* **1987**, *65*, 245.
(617) Zander, M. *Z. Naturforsch.* **1969**, *24a*, 251.
(618) Zander, M. *Z. Naturforsch.* **1970**, *25a*, 440.
(619) Schneider, F.; Zander, M. *Ber. Bunsen-Ges. Phys. Chem.* **1971**, *75*, 887.
(620) Evers, F.; Giraud-Girard, J.; Grimme, S.; Manz, J.; Monte, C.; Oppel, M.; Rettig, W.; Saalfrank, P.; Zimmermann, P. *J. Phys. Chem. A* **2001**, *105*, 2911.
(621) Jurczok, M.; Plaza, P.; Martin, M. M.; Meyer, Y. H.; Rettig, W. *Chem. Phys.* **2000**, *253*, 339.
(622) Jurczok, M.; Plaza, P.; Rettig, W.; Martin, M. M. *Chem. Phys.* **2000**, *256*, 137.
(623) Kapturkiewicz, A.; Nowacki, J. *J. Phys. Chem. A* **1999**, *103*, 8145.
(624) If the torsional motion toward perpendicularity were responsible for the remaining reorganization energy $\delta\lambda_o$ (∼0.08−0.10 eV, i.e., very small as compared to the λ_o values, and found as the intercept of the plot of the latter vs the solvent polarity function), it should also be polarity dependent, increasing with the solvent polarity. As the potential energy minimum (or minima) around $\theta = 90°$ can be shallow, the interpretation is somewhat arbitrary. The relaxation within such shallow minima cannot be found by this method ($\delta\lambda_o$ dependence on solvent polarity being hidden both in the slope λ_o vs $f(\epsilon,n)$ and in the imprecise value of its intercept. The forbidden character of the radiative transition in fluorescence, growing with the solvent polarity (diminishing k_f and M_f values for most of these compounds, see Table 14) seems to be the strongest evidence for the conformational changes.
(625) Demeter, A.; Bérces, T.; Zachariasse, K. A. *J. Phys. Chem. A* **2001**, *105* 4611.
(626) Rotkiewicz, K.; Rechthaler, K.; Puchała, A.; Rasała, D.; Styrcz, S.; Köhler, G. *J. Photochem. Photobiol. A: Chem.* **1996**, *98*, 15.
(627) Parusel, A. B. J.; Schamschule, R.; Köhler, G. *J. Comput. Chem.* **1998**, *19*, 1584.
(628) Parusel, A. B. J.; Schamschule, R.; Köhler, G. *Ber. Bunsen-Ges. Phys. Chem.* **1997**, *101*, 1836.
(629) Miyasaka, H.; Itaya, A.; Rotkiewicz, K.; Rechthaler, K. *Chem. Phys. Lett.* **1999**, *307*, 121.
(630) Parusel, A. B. J.; Rechthaler, K.; Piorun, D.; Danel, A.; Khatchatryan, K.; Rotkiewicz, K.; Köhler, G. *J. Fluoresc.* **1998**, *8*, 375.
(631) Rechthaler, K.; Rotkiewicz, K.; Danel, A.; Tomasik, P.; Khatchatryan, K.; Köhler, G. *J. Fluoresc.* **1997**, *7*, 301.
(632) Schneider, F.; Lippert, E. *Ber. Bunsen-Ges. Phys. Chem.* **1968**, *72*, 1155.
(633) Schneider, F. Elektronenspektren und π-Elektronenstruktur von 9,9′-Dianthryl und verwandten Verbindungen. Ph.D. Thesis, Techn. Univ. Berlin 1969.
(634) Schneider, F.; Lippert, E. *Ber. Bunsen-Ges. Phys. Chem.* **1970**, *74*, 624.
(635) In the simplest approximation, the excitonic splitting is $V \approx |\mathbf{M}_{G,A^*}|^2 \cos\alpha/R^3$, where α is the angle between the transition dipoles and R the distance between their centers.[673] The transition moments being parallel here, one can expect that the excitonic interaction of the two aryl moieties should be rather independent of their mutual twist angle. Thus, the calculated

red shift vs anthracene is 1100 cm^{-1}, while that found experimentally in the molecular jet is 910 cm^{-1}.[645]
(636) Beens, H.; Weller, A. *Chem. Phys. Lett.* **1969**, *3*, 666.
(637) Zachariasse, K. A., private communication, 1976.
(638) Zachariasse, K. A. *XIIIth European Congress on Molecular Spectroscopy*, Wrocław, 1977.
(639) Zachariasse, K. A.; Busse, R. *NATO Adv. Study Inst. on Excited States in Biochemistry and Biology*, Acireale, 1984.
(640) Zachariasse, K. A. *Trends Photochem. Photobiol.* **1994**, *3*, 211.
(641) Zander, M.; Rettig, W. *Chem. Phys. Lett.* **1984**, *110*, 602.
(642) Ionic dissociation of benzoic acid in H_2O corresponds to $T\Delta S_o \approx -0.25$ eV; the formation of larger ions from the neutrals, in polar organic solvents, corresponds to $T\Delta S_o \approx -0.15$ or -0.1 eV.[176]
(643) Rettig, W.; Zander, M. *Ber. Bunsen-Ges. Phys. Chem.* **1983**, *87*, 1143.
(644) Yamasaki, K.; Arita, K.; Kajimoto, O. *Chem. Phys. Lett.* **1986**, *123*, 277.
(645) Khundkar, L. R.; Zewail, A. H. *J. Chem. Phys.* **1986**, *84*, 1302.
(646) Wortmann, R.; Elich, K.; Lebus, S.; Liptay, W. *J. Chem. Phys.* **1991**, *95*, 6371.
(647) Wortmann, R.; Lebus, S.; Elich, K.; Assar, S.; Detzer, N.; Liptay, W. *Chem. Phys. Lett.* **1992**, *198*, 220.
(648) Elich, K.; Kitazawa, M.; Okada, T.; Wortmann, R. *J. Phys. Chem. A* **1997**, *101*, 2010.
(649) Kajimoto, O.; Yamasaki, K.; Arita, K. *Chem. Phys. Lett.* **1986**, *125*, 184.
(650) Ishida, T.; Fujimura, Y.; Fujiwara, T.; Kajimoto, O. *Chem. Phys. Lett.* **1998**, *288*, 433.
(651) Tanaka, K.; Honma, K. *J. Phys. Chem. A* **2002**, *106*, 1926.
(652) Mataga, N.; Yao, H.; Okada T.; Rettig, W. *J. Phys. Chem.* **1989**, *93*, 3383.
(653) Fritz, R. Temperatur- und druckabhängige Untersuchungen zur Bestimmung des freien Volumens in niedermolekularen organischen Gläsern und Polymeren mittels adiabatischer Photoreaktionen fluoreszierender Sondenmoleküle. Ph.D. Thesis, Techn. Univ. Berlin, 1993 (Köster Verlag: Berlin, 1994; ISBN 3-929937-57-3).
(654) Grabner, G.; Rechthaler, K.; Köhler, G. *J. Phys. Chem. A* **1998**, *102*, 689.
(655) Kang, T. J.; Kahlow, M. A.; Giser, D.; Swallen, S.; Nagarajan, V.; Jarzeba, W.; Barbara, P. F. *J. Phys. Chem.* **1988**, *92*, 6800.
(656) Barbara, P. F.; Nagarajan, V. In *Ultrafast Phenomena V*; Fleming, G. R., Siegman, A. E., Eds.; Springer Verlag: Berlin, 1986; p 299.
(657) Jurczok, M.; Gustavsson, T.; Mialocq, J.-C.; Rettig, W. *Chem. Phys. Lett.* **2001**, *344*, 357.
(658) Anthon, D. W.; Clark, J. H. *J. Phys. Chem.* **1987**, *91*, 3530.
(659) Nakashima, N.; Murakawa M.; Mataga, N. *Bull. Chem. Soc. Jpn.* **1976**, *49*, 854.
(660) Hoshino, M.; Kimura. K.; Imamura, M. *Chem. Phys. Lett.* **1973**, *20*, 193.
(661) Lueck, H.; Windsor, M. W.; Rettig, W. *J. Phys. Chem.* **1990**, *94*, 4550.
(662) Lueck, H.; Windsor, M. W.; Rettig, W. *J. Lumin.* **1991**, *48*−*49*, 425.
(663) Mataga, N.; Nishikawa, S.; Okada, T. *Chem. Phys. Lett.* **1996**, *257*, 327.
(664) Piet, J. J.; Schuddeboom, W.; Wegewijs, B. R.; Grozema, F. C.; Warman, J. M. *J. Am. Chem. Soc.* **2001**, *123*, 5337.
(665) Tsuboi, Y.; Kumagai, T.; Shimizu, M.; Itaya, A.; Schweitzer, G.; De Schryver, F. C.; Asahi, T.; Masuhara, H.; Miyasaka, H. *J. Phys. Chem. A* **2002**, *106*, 2067.
(666) Fujiwara, T.; Fujimura, Y.; Kajimoto, O. *J. Chem. Phys.* **2000**, *113*, 11109.
(667) Fujiwara, F.; Egashira, K.; Ohshima, Y.; Kajimoto, O. *Phys. Chem. Chem. Phys.* **2000**, *2*, 1365.
(668) Monte, C.; Rettig, W.; Baumgarten, M.; Yüksel, T., unpublished results.
(669) Jurczok, M.; Rettig, W.; Yüksel, T.; Baumgarten, M., unpublished results.
(670) Grellmann, K. H.; Watkins, A. R. *Chem. Phys. Lett.* **1971**, *9*, 439.
(671) Vauthey, E.; Suppan, P.; Haselbach, E.; Davidson, R. S. *Helv. Chim. Acta* **1986**, *69*, 430.
(672) Koch, K. H.; Müllen, K. *Chem. Ber.* **1991**, *124*, 2091.
(673) Förster, Th. *Pure Appl. Chem.* **1962**, *4*, 121.
(674) Weller, A. In *Supramolecular Photochemistry*; Balzani, V., Ed.; D. Reidel Publ.: Dordrecht, 1987; p 343. ET precedes the formation of an exciplex in less polar media, or of the free solvated ions in polar solvents. The latter case occurs here with Pe.
(675) Herndon, W. C. *J. Am. Chem. Soc.* **1990**, *112*, 4546.
(676) Waluk, J.; Fetzer, J.; Hamrock, S. J.; Michl, J. *J. Phys. Chem.* **1991**, *95*, 8660.
(677) Thulstrup, E. W.; Spanget-Larsen, J.; Waluk, J. *Theor. Chim. Acta* **1994**, *89*, 301.
(678) Marczyk, J.; Waluk, J.; Fetzer, J. *Acta Phys. Polon. A* **1995**, *88*, 295.
(679) Szubiakowski, J.; Balter, A.; Nowak, W.; Kowalczyk, A.; Wiśniewski, K.; Wierzbowska, M. *Chem. Phys. Lett.* **1996**, *208*, 283.
(680) Bunte, R.; Gundermann, K. D.; Leitich, J.; Polanski, O. E.; Zander, M. *Chem. Ber.* **1986**, *119*, 1683.
(681) Baumgarten, M.; Gherghel, L.; Friedrich, J.; Jurczok, M.; Rettig, W. *J. Phys. Chem. A* **2000**, *104*, 1130.
(682) Stolarczyk, L. Z.; Piela, L. *Chem. Phys.* **1984**, *85*, 451.
(683) Rettig, W. *Appl. Phys.* **1988**, *B 45*, 145.
(684) Jurczok, M.; Fritz, R.; Rettig, W.; Baumgarten, M. *International Symposium of the Volkswagen-Stiftung on "Intra- and Intermolecular Electron Transfer"*, Berlin, 1996; poster 23.
(685) Fritz, R.; Rettig, W.; Nishiyama, K.; Okada, T.; Müller, U.; Müllen, K. *J. Phys. Chem. A* **1997**, *101*, 2796.
(686) Nishiyama, K.; Honda, T.; Reis, H.; Müller, U.; Müllen, K.; Baumann, W.; Okada, T. *J. Phys. Chem. A* **1998**, *102*, 2934.
(687) Piet, J. J.; Warman, J. M.; Baumgarten, M.; Müllen, K. *J. Phys. Chem. A* **2002**, *106*, 2318.
(688) Ephardt, H.; Fromherz, P. *J. Phys. Chem.* **1989**, *93*, 7717.
(689) Ephardt, H.; Fromherz, P. *J. Phys. Chem.* **1991**, *95*, 6792.
(690) Fromherz, P.; Heilemann, A. *J. Phys. Chem.* **1992**, *96*, 6964.
(691) Ephardt, H.; Fromherz, P. *J. Phys. Chem.* **1993**, *97*, 4540.
(692) Röcker, C.; Heilemann, A.; Fromherz, P. *J. Phys. Chem.* **1996**, *100*, 12172.
(693) Kakitani, T.; Mataga, N. *J. Phys. Chem.* **1986**, *90*, 993.
(694) Tachiya, M. *J. Phys. Chem.* **1993**, 97, 5911.
(695) Strehmel, B.; Rettig, W. *J. Biomed. Opt.* **1996**, *1*, 98.
(696) Strehmel, B.; Seifert, H.; Rettig W. *J. Phys. Chem. B* **1997**, *101*, 2232.
(697) van der Meer, M. J.; Zhang, H.; Rettig, W.; Glasbeek, M. *Chem. Phys. Lett.* **2000**, *320*, 673.
(698) Sczepan, M.; Rettig, W.; Tolmachev, A. I.; Kurdyukov, V. V. *Phys. Chem. Chem. Phys.* **2001**, *3*, 3555.
(699) Bingemann, D.; Ernsting, N. P. *J. Chem. Phys.* **1995**, *102*, 2691.
(700) Jonkman, A. M.; van der Meulen, P.; Zhang, H.; Glasbeek, M. *Chem. Phys. Lett.* **1996**, *256*, 21.
(701) Lewis, G. N.; Calvin, M. *Chem. Rev.* **1939**, *25*, 273.
(702) Hofer, L. J. E.; Grabenstetter, R. J.; Wiig, E. O. *J. Am. Chem. Soc.* **1950**, *72*, 203.
(703) Sczepan, M.; Rettig, W.; Bricks, Y. L.; Slominski, J. L.; Tolmachev, A. I. *J. Photochem. Photobiol. A: Chem.* **1999**, *124*, 75.
(704) Gilabert, E.; Lapouyade, R.; Rullière, C. *Chem. Phys. Lett.* **1988**, *262*, 145.
(705) Gilabert, E.; Lapouyade, R.; Rullière, C. *Chem. Phys. Lett.* **1991**, *185*, 82.
(706) Létard, J. F.; Lapouyade R.; Rettig, W. *J. Am. Chem. Soc.* **1993**, *115*, 2441.
(707) Viallet, J.-M.; Dupuy, F.; Lapouyade, R.; Rullière, C. *Chem. Phys. Lett.* **1994**, *222*, 571.
(708) Abraham, E.; Oberlé, J.; Jonusauskas, G.; Lapouyade, R.; Rullière, C. *Chem. Phys.* **1997**, *214*, 409.
(709) Recently, a new interpretation has been published for the "dual fluorescence" observed in **225** under high-intensity laser excitation: the two bands are only apparent and are due to the effect of the reabsorption of the central spectral part of the fluorescence by the strongly populated S_1 excited state.[710] For a clear-cut answer regarding the multiple fluorescence of **225**−**227**, time-resolved experiments with lower-intensity light sources should therefore be compared. This[710] seems similar to the apparently dual emission of some coumarins (section XI.D.1) under high excitation intensity,[770−772] which results from the transient absorption dividing the emission band.[773]
(710) Kovalenko, S. A.; Schanz, R.; Senyushkina, T. A.; Ernsting, N. P. *Phys. Chem. Chem. Phys.* **2002**, *4*, 703.
(711) Michl, J.; Bonačić-Koutecký, V. *Electronic Aspects of Organic Photochemistry*; J. Wiley & Sons: New York, 1990.
(712) Garavelli, M.; Vreven, T.; Celani, P.; Bernardi, F.; Robb, M. A.; Olivucci, M. *J. Am. Chem. Soc.* **1998**, *120*, 1285.
(713) Sanchez-Galvez, A.; Hunt, P.; Robb, M. A.; Olivucci, M.; Vreven, T.; Schlegel, H. B. *J. Am. Chem. Soc.* **2000**, *122*, 2911.
(714) Rettig, W.; Majenz, W. *Chem. Phys. Lett.* **1989**, *154*, 335. The more recent literature on **225** is very controversial. There are several papers in which multiple states have been evidenced for **225** and related compounds, and at least as many papers saying that they cannot evidence that. The situation is not at its end; further experiments are necessary. For some relevant recent references in this context, see: Il'ichev, Yu. V.; Kühnle, W.; Zachariasse, K. A. *Chem. Phys.* **1996**, *211*, 441. Il'ichev, Yu. V.; Zachariasse, K. A. *Ber. Bunsen-Ges. Phys. Chem.* **1997**, *101*, 625. Pines, D.; Pines, E.; Rettig W. *J. Phys. Chem. A* **2003**, *107*, 236. See also ref 710.
(715) Rettig, W.; Majenz, W.; Lapouyade R.; Haucke, G. *J. Photochem. Photobiol. A: Chem.* **1992**, *62*, 415.
(716) Dähne, S.; Leupold, D. *Angew. Chem.* **1966**, *78*, 1029.
(717) Dähne, S. *Science* **1978**, *199*, 1163.
(718) Dähne, S. *Prog. Phys. Org. Chem.* **1985**, *15*, 1.
(719) Fromherz, P.; Dambacher, K. H.; Ephardt, H.; Lambacher, A.; Müller, C. O.; Neigl, R.; Schaden, H.; Schenk, O.; Vetter, T. *Ber. Bunsen-Ges. Phys. Chem.* **1991**, *95*, 1333.
(720) Fromherz, P.; Schaden, H.; Vetter, T. *Neurosci. Lett.* **1991**, *129*, 77.

(721) Loew, L. M.; Scully, S.; Simpson, L.; Waggoner, A. S. *Nature* **1979**, *281*, 497.
(722) Loew, M. L.; Simpson, L. L. *Biophys. J.* **1981**, *34*, 353.
(723) Fluhler, E.; Burnham, V. G.; Loew, L. M. *Biochemistry* **1985**, *24*, 5749.
(724) Grinvald, A.; Fine, I.; Farber, I. C.; Hildesheim, R. *Biophys. J.* **1983**, *39*, 301.
(725) Förster, Th.; Hoffmann, G. *Z. Phys. Chem., N.F.* **1971**, *75*, 63.
(726) Hoffmann, G. *Z. Phys. Chem., N.F.* **1970**, *71*, 132.
(727) Hoffmann, G.; Schönbucher, A.; Steidl, H. *Z. Naturforsch.* **1973**, *28a*, 1136−1139.
(728) Schönbucher, A. Blitzlichtspektroskopische Untersuchung ûber strahlungslose Desaktivierungsprozesse an Triphenylmethanfarbstoffen. Ph.D. Thesis, Stuttgart, 1973.
(729) Vogel, M.; Rettig, W. *Ber. Bunsen-Ges. Phys. Chem.* **1985**, *89*, 962.
(730) Vogel, M.; Rettig, W. *Ber. Bunsen-Ges. Phys. Chem.* **1987**, *91*, 1241.
(731) Plaza, P.; Dai Hung, N.; Martin, M. M.; Meyer, Y. H.; Vogel, M.; Rettig, W. *Chem. Phys.* **1992**, *168*, 365.
(732) Posch, H. E.; Leiner, M. J. P.; Wolfbeis, O. S. *Fresenius Z. Anal. Chem.* **1989**, *334*, 162.
(733) Whitaker, J. E.; Haugland, R. P.; Prendergast, F. G. *Anal. Biochem.* **1991**, *194*, 330.
(734) Hirsch, M. D.; Mahr, H. *Chem. Phys. Lett.* **1979**, *60*, 299.
(735) Cremers, C. A.; Windsor, M. W. *Chem. Phys. Lett.* **1980**, *71*, 27.
(736) Doust, T. *Chem. Phys. Lett.* **1983**, *96*, 522.
(737) Martin, M. M.; Breheret, E.; Nes, F.; Meyer, Y. H. *Chem. Phys.* **1989**, *130*, 279.
(738) Martin, M. M.; Plaza, P.; Dai Hung, N.; Meyer, Y. H. In *Ultrafast Phenomena VII*; Harris, C. B., Ippen, E. P., Mourou, G. A., Zewail, A. H., Eds.; Springer Series in Chemical Physics 53; Springer: Berlin 1990; p 504.
(739) Martin, M. M.; Plaza, P.; Meyer, Y. H. *Chem. Phys.* **1991**, *153*, 297.
(740) Martin, M. M.; Plaza, P.; Meyer, Y. H. *J. Phys. Chem.* **1991**, *95*, 9310.
(741) Martin, M. M.; Plaza, P.; Changenet, P.; Meyer, Y. H. *J. Photochem. Photobiol. A: Chem.* **1997**, *105*, 197.
(742) Jurczok, M.; Plaza, P.; Martin, M. M.; Rettig, W. *J. Phys. Chem. A* **1999**, *103*, 3372.
(743) Ben-Amotz, D.; Harris, C. B. *Chem. Phys. Lett.* **1985**, *119*, 305.
(744) Ben-Amotz, D.; Harris C. B. *J. Chem. Phys.* **1987**, *86*, 4856.
(745) Holzwarth, A.; Rettig, W., unpublished results.
(746) Sundström, V.; Gillbro, T.; Bergström, H. *Chem. Phys.* **1982**, *73*, 439.
(747) Sundström, V.; Gillbro, T. *J. Chem. Phys.* **1984**, *81*, 3463.
(748) Bonačić-Koutecký, V.; Köhler, J.; Michl, J. *Chem. Phys. Lett.* **1984**, *104*, 440.
(749) Oster, G.; Nishijima, N. J. *J. Am. Chem. Soc.* **1956**, *78*, 1581.
(750) Fritz, R.; Rettig, W., unpublished results.
(751) In protic solvents. In *aprotic* polar solvents, Rhodamine 101 in the *zwitterionic* form is also quenched with increasing temperature.[156,157,794] Derivatives with an esterified acid group are expected not to show such behavior.
(752) Karstens, T.; Kobs, K. *J. Phys. Chem.* **1980**, *84*, 1871.
(753) Vogel, M.; Rettig, W.; Sens, R.; Drexhage, K. H. *Chem. Phys. Lett.* **1988**, *147*, 452.
(754) Vogel, M.; Rettig, W.; Sens, R.; Drexhage, K. H. *Chem. Phys. Lett.* **1988**, *147*, 461.
(755) For rhodamines with a −COOH group which can populate their *zwitterionic* forms, another important quenching channel opens: the temperature- and polarity-dependent ISC, populating the triplet state of the zwitterionic form of the dye (triplet state is practically not populated from the lowest excited singlet of the *ionic* dye).[157,790] This quenching pathway can be avoided by using the ester derivative of the dyes.
(756) Czerney, P.; Graness, G.; Birckner, E.; Vollmer, F.; Rettig, W. *J. Photochem. Photobiol. A: Chem.* **1995**, *89*, 31.
(757) Momicchioli, F.; Baraldi, I.; Carnevali, A.; Caselli, M.; Ponterini, G. *Coord. Chem. Rev.* **1993**, *125*, 301.
(758) Haucke, G.; Czerney, P.; Steen, D.; Rettig W.; Hartmann, H. *Ber. Bunsen-Ges. Phys. Chem.* **1993**, *97*, 561.
(759) Vollmer, F.; Rettig, W.; Birckner, E.; Haucke, G.; Czerney P. *J. Inf. Record. Mater.* **1994**, *21*, 497.
(760) Lahmadi, F.; Valat, P.; Kossanyi, J. *New J. Chem.* **1995**, *19*, 965.
(761) Lahmadi, F.; Valat, P.; Simalty, M.; Kossanyi, J. *Res. Chem. Intermed.* **1995**, *21*, 807.
(762) Kharlanov, V. A.; Rettig, W.; Knyazhansky, M. I.; Makarova N. *J. Photochem. Photobiol. A: Chem.* **1997**, *103*, 45.
(763) Lampre, I.; Marguet, S.; Markovitsi, D.; Delysse, S.; Nunzi, J. M. *Chem. Phys. Lett.* **1997**, *272*, 496.
(764) Markovitsi, D.; Sigal, H.; Ecoffet, C.; Millie, P.; Charra, F.; Fiorini, C.; Nunzi, J. M.; Strzelecka, H.; Veber, M. *Chem. Phys.* **1994**, *182*, 69.
(765) Manoj, N.; Gopidas, K. R. *Chem. Phys. Lett.* **1997**, *267*, 567.
(766) Kharlanov, V. A.; Knyazhansky, M. I.; Rettig, W. *J. Mol. Struct.* **1996**, *380*, 113.
(767) Grabowska, A.; Pakuła, B.; Sepioł, J. *Nouv. J. Chim.* **1979**, *3*, 287.
(768) Waluk, J.; Grabowska, A.; Lipiński, J. *Chem. Phys. Lett.* **1980**, *70*, 175.
(769) Jones, G., II; Farahat, M. S.; Greenfield, S. R.; Gosztola, D. J.; Wasielewski, M. R. *Chem. Phys. Lett.* **1994**, *229*, 40.
(770) Masilamani, V.; Chandrasekar, V.; Sivaram, B. M.; Sivasankaran, B.; Natarajan, S. *Opt. Commun.* **1986**, *59*, 203.
(771) Masilamani, V.; Natarajan, S.; Natarajan, P. *Opt. Commun.* **1987**, *62*, 389.
(772) Ramalingam, A.; Palanisamy, P. K.; Masilamani, V.; Sivaram, B. M. *J. Photochem. Photobiol. A: Chem.* **1989**, *49*, 89.
(773) Sepioł, J., private communication, 1989.
(774) Yip, R. W.; Wen, Y. X. *J. Photochem. Photobiol. A: Chem.* **1990**, *54*, 263.
(775) Yip, R. W.; Wen, Y. X. *Can. J. Chem.* **1991**, *69*, 1413.
(776) Jones, G., II; Jackson, W. R.; Halpern, A. M. *Chem. Phys. Lett.* **1980**, *72*, 391.
(777) Jones, G., II; Jackson, W. R.; Kanoktanaporn, S.; Halpern, A. M. *Opt. Commun.* **1980**, *33*, 315.
(778) Nemkovich, N. A.; Reis, H.; Baumann, W. *J. Lumin.* **1997**, 71, 255.
(779) Aaron, J.-J.; Buna, M.; Parkanyi, C.; Antonious, M. S.; Tine, A.; Cisse, L. *J. Fluoresc.* **1995**, *5*, 337.
(780) Suppan, P. *Chem. Phys. Lett.* **1983**, *94*, 272.
(781) Rechthaler, K.; Köhler, G. *Chem. Phys.* **1994**, *189*, 99.
(782) Samanta, A.; Fessenden, R. W. *J. Phys. Chem. A* **2000**, *104*, 8577.
(783) Nag, A.; Chakrabarty, T.; Bhattacharyya, K. *J. Phys. Chem.* **1990**, *94*, 4203.
(784) Nag, A.; Bhattacharyya, K. *Chem. Phys. Lett.* **1990**, *169*, 12.
(785) Corrie, J. E. T.; Munasinghe, V. R. N.; Rettig, W. *J. Heterocycl. Chem.* **2000**, *37*, 1447.
(786) Rettig, W.; Klock, A. *Can. J. Chem.* **1986**, *63*, 1649.
(787) Jones, G., II; Jackson, W. R.; Choi, C. Y.; Bergmark, W. R. *J. Phys. Chem.* **1985**, *89*, 294.
(788) In very numerous cases, in different structural groups of compounds, the *nonfluorescent TICT states* are postulated in the literature often with insufficient evidence. We mention them only in the case of coumarins, as an example.
(789) Arbeloa, T. L.; Arbeloa, T. L.; Estévez, M. J. T.; Arbeloa, I. L. *J. Lumin.* **1994**, *59*, 369.
(790) Klein, U.K.A.; Hafner, F. W. *Chem. Phys. Lett.* **1976**, *43*, 141.
(791) Grigoryeva, T. M.; Ivanov, V. L.; Nizamov, N.; Kuzmin, M. G. *Dokl. Akad. Nauk SSSR* **1977**, *232*, 1108.
(792) Grigoryeva, T. M.; Ivanov, V. I.; Kuzmin, M. G. *Dokl. Akad. Nauk SSSR* **1978**, *238*, 603.
(793) Vlaskin, V. I.; Gorlenko, A. J.; Melnichuk, S. V.; Nizamov, N.; Tikhomirov, S. A.; Tolstorozhev, G. B. *Dokl. Akad. Nauk SSSR* **1988**, *302*, 1141.
(794) Karpiuk, J. *J. Lumin.* **1994**, *60/61*, 474.
(795) Along with this CT emission, in strongly polar solvents the lactones undergo an adiabatic ring-opening, thus forming the *excited* rhodamine dye in its zwitterionic form (two highly different fluorescence bands appear). The mechanism of the lactone ring-opening is beyond the present review. The fluorescence yield of the zwitterionic dye increases with solvent polarity, while that of the lactone decreases. In alcohols as solvents, the lactone emission is totally quenched, and only the dye fluorescence appears with a high quantum yield.[157,790]
(796) Karpiuk, J. *Book of Abstracts*, 18th IUPAC Symposium on Photochemistry, Dresden, 2000; p 335.
(797) In the case of **265**, the processes are more complex. There appear subsequently two CT emissions: one localized within the acceptor unit, then another, corresponding to the CT between the two subunits of the spiro system.[796]
(798) These molecules undergo, in the excited state, an opening of their acceptor ring, to form extended conjugated π-electronic systems of the colored photochromic products.
(799) Häupl, T.; Zimmermann, T.; Hermann, R.; Brede, O. *Chem. Phys. Lett.* **1998**, *291*, 215.
(800) Kosower, E. M.; Dodiuk, H. *Chem. Phys. Lett.* **1974**, *26*, 545.
(801) Kapelle, S.; Rettig, W. *J. Inf. Recording* **1996**, *23*, 187.
(802) Kapelle, S. Ph.D. Thesis, Humboldt University, Berlin, 1998.
(803) Kapelle, S.; Rettig, W.; Lapouyade, R. *Chem. Phys. Lett.* **2001**, *348*, 416.
(804) Kapelle, S.; Rettig, W.; Lapouyade, R. *Photophys. Photobiol. Sci.* **2002**, *1*, 492.
(805) Rettig, W.; Chandross, E. A. *J. Am. Chem. Soc.* **1985**, *107*, 5617.
(806) Malval, J. P.; Lapouyade, R.; Rettig, W., unpublished results.
(807) Nalva, H. S., Ed. *Handbook of Organic Conductive Molecules and Polymers*; J. Wiley & Sons: New York, 1997.
(808) Vogel, M.; Rettig, W.; Heimbach, P. *J. Photochem. Photobiol. A* **1991**, *61*, 65.
(809) Changenet, P.; Plaza, P.; Martin, M. M.; Meyer, Y. H.; Rettig, W. In *Fast Elementary Processes in Chemical and Biological Systems*; Tramer, A., Ed.; AIP Press: Woodbury, NY, 1996; Vol. 364, p 363.
(810) Changenet, P.; Plaza, P.; Martin, M. M.; Meyer, Y. H.; Rettig, W. *J. Chim. Phys.* **1996**, *93*, 1697.

(811) Changenet, P.; Plaza, P.; Martin, M. M.; Meyer, Y. H.; Rettig, W. *Chem. Phys.* **1997**, *221*, 311.
(812) Herbich, J.; Kapturkiewicz, A.; Nowacki, J. *Chem. Phys. Lett.* **1996**, *262*, 633.
(813) Rotkiewicz, K., unpublished results.
(814) Cowley, D. J.; Pasha, I. *J. Chem. Soc., Perkin Trans. 2* **1983**, 1139.
(815) The $T_n \leftarrow T_1$ absorption spectra of the carbonyl derivatives **11**[245,814] and **44**[198] in fluid polar solvents are definitely different from the $S_n \leftarrow S_1$ absorption of the corresponding ^{1}TICT states.
(816) Chattopadhyay, N.; Rommens, J.; Van der Auweraer, M.; De Schryver, F. C. *Chem. Phys. Lett.* **1997**, *264*, 265.
(817) Chattopadhyay, N.; Van der Auweraer, M.; De Schryver, F. C. *Chem. Phys. Lett.* **1997**, *279*, 303.
(818) Rotkiewicz, K.; Komorowski, S. *Abstracts*, Annual Meeting of the Polish Chemistry Society, Bydgoszcz, 1987; p 155.
(819) An opposite statement[486,377] resulted from a wrong interpretation of the early data[2] indicating an absence of solvent effect on k_{ISC} in the case of **26**.
(820) Avouris, P.; Gelbart, W. M.; El-Sayed, M. A. *Chem. Rev.* **1977**, *77*, 793.
(821) A noticeable red shift of the T−T absorption spectra of **1**, as well as some contribution of biexponential decay of this transient, in polar solvents, was interpreted as support for the existence of a ^{3}TICT state, this time in equilibrium with a more stable ^{3}LE state (Chattopadhyay, N.; Serpa, C.; Arnaut, L. G.; Formosinho, J. *Helv. Chim. Acta* **2002**, *85*, 19). It is, however, difficult to find in the reported spectra any trace of a CT-state absorption spectrum, characterized by the benzonitrile radical anion bands. On the other hand, the singlet−triplet splitting of the TICT state, probably close to that of the *intimate* radical ion pairs, should be due to the exchange interactions being, at these small (one bond) distances, markedly stronger than the hyperfine interactions. The lack of a magnetic field effect, up to 0.05 T, on the phosphorescence yield of **21** (Rotkiewicz, K.; Grabowski, Z. R., unpublished results) suggests that the ISC route probably avoids the ^{3}TICT state.
(822) Ma, C.; Kwok, W. M.; Matousek, P.; Parker, A. W.; Phillips, D.; Toner, W. T.; Towrie, M. *J. Phys. Chem. A* **2001**, *105*, 4648.
(823) Smit, K. J.; Warman, J. M. *J. Lumin.* **1988**, *42*, 149.
(824) Anglos, D.; Bindra, V.; Kuki, A. *J. Chem. Soc., Chem. Commun.* **1994**, *2*, 213.
(825) van Dijk, S. I.; Groen, C. P.; Hartl, F.; Brouwer, A. M.; Verhoeven, J. W. *J. Am. Chem. Soc.* **1996**, *118*, 8425.
(826) Goez, M.; Zubarev, V. *Angew. Chem.* **2001**, *113*, 2948; *Angew. Chem., Int. Ed. Engl.* **2001**, *113*, 2867.
(827) Borowicz, P.; Herbich, J.; Kapturkiewicz, A.; Anulewicz-Ostrowska, R.; Nowacki, J.; Grampp, G. *Phys. Chem. Chem. Phys.* **2000**, *2*, 4275.
(828) Hviid, L.; Brouwer, A. M.; Paddon-Row, M. N.; Verhoeven, J. W. *Chem. Phys. Chem.* **2001**, 232.
(829) With a possible exception of **1** and derivatives adsorbed on surfaces, see: Günther, R.; Oelkrug, D.; Rettig, W. *J. Phys. Chem.* **1993**, *97*, 8512.
(830) In some cases, the reacting groups, D and A, are identical, e.g., in the symmetric biaryls **111**, **198**−**202**.
(831) Maus, M. Photoinduced Intramolecular Charge Transfer in Donor−Acceptor Biaryls and Resulting Applicational Aspects Regarding Fluorescent Probes and Solar Energy Conversion. Ph.D. Thesis, Humboldt University, Berlin, 1998.
(832) Lowering of the orbital overlap may also result from the growing D···A distance or from the symmetry, as it frequently occurs in the inter- or intramolecular exciplexes.[41,172]
(833) Maus, M.; Rettig, W. *Phys. Chem. Chem. Phys.* **2001**, *3*, 5430.
(834) Maus, M.; Rettig, W. *J. Phys. Chem. A.* **2002**, *106*, 2104.
(835) Rather high transition moments in the case of the para derivatives of **182**−**185** ($M_f \approx 2$ D) are related to the LCAO coefficient, C_{LUMO}, of the acceptor subunits, with the largest value of all positions in the ring (in accord with the analysis of the hyperfine structure of the ESR spectra of the radical anion of benzonitrile). This, in view of the eqs 32, determines the matrix element of electronic coupling of the CT and the ground state.[61,623]

CR940745L